A MATHEMATICAL STUDY FOR THE DYNAMICS OF SPACETIME, INFLATION AND ACCELERATING UNIVERSE

BY

Muhammad Zahid Mughal

REGISTRATION # 18034209369

PhD

Department of Mathematics

University of Gujrat

Session 2018-21

Muhammad Zahid Mughal PhD 2018 – 21

A MATHEMATICAL STUDY FOR THE DYNAMICS OF SPACETIME, INFLATION AND ACCELERATING UNIVERSE

A Thesis Submitted in Partial Fulfillment of the Requirements for the Award of Degree of

PhD

In

Mathematics

BY

Muhammad Zahid Mughal

REGISTRATION # 18034209369

Department of Mathematics

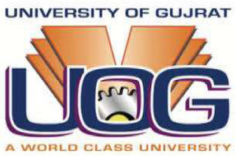

University of Gujrat

Session 2018-21

ACKNOWLEDGEMENT

The Almighty Sustainer, veritably I acknowledge Him the foremost. It is He, to Whom existence en masse owes through the manifestation of His names and attributes weaving thereout the warp and woof of the phenomenal world as the fabric of spacetime. Verily it is He, Who occasions the creatio ex nihilo and nurtures the sprawling diversity of life and cosmological phenomena which we perceive through unfolding the consciousness embedded into stratification of Spatio-temporal dimensions.

Afterward, I am extremely grateful to my supervisor, Prof. Dr. Iftikhar Ahmad who accorded me the freedom to go after my inherent interests and encouraged me during hard times. He is a man of profound erudition with a background in relativity and cosmology. I have to thank him, especially for his altruistic and incessant support towards the completion of this dissertation. He not only stimulated me considerably during the learning period but also his enlightening comments and remarks on various facets of this thesis were indeed very precious and meritorious. I am particularly grateful to him for drawing my attention to the shortcomings of certain topics, and for the fruitful discussions on some abstruse aspects of the dissertation. In the course of this research work, whenever I succumb to ennui and felt destitute of courage, enthusiasm, and verve, his words reinvigorated me to move forward. He remained and is, indeed, a perpetual source of inspiration. It would have been difficult, methinks, to achieve creative feats of my potentialities without him. I am ever indebted to him and seek his benediction to succeed in life.

Thanks are also due to the teachers in the Department of Mathematics who exerted a lot in making us learn maximally during course work and proved a constant source of knowledge and motivation. I feel indebted to Dr. Jamshed Ahmad, Dr. Azad Husain, and Dr. Shahida Bashir for their sincere efforts to instruct impressively during teaching and indoctrinating the students. They invested all they can into ensuring that the students are challenged to grow and take on whatever discipline of knowledge is chosen might be specialized. I pay my special tribute to Dr. Zaffar Iqbal whose teaching style, magnanimity, and eagerness to learn students in their utmost capacity are always influential. My heartfelt appreciation is also due to Dr. Shafaq Naz and the coordinator Ph.D. Program Dr. Sadia Noureen for committing to making time available for help at the earliest. My acknowledgments would be incomplete without thanking and expressing gratitude to the rest of the faculty members and clerical staff in the Department of Mathematics who deserve gratefulness in one way or the other.

I would like to express my unaffected gratitude to Hira Ilyas, Ph.D., and Zirwa Khan for their help and cooperation in the development of a code and drafting some figures, and

for the affectionate attitude, they showed. My special thanks are due to Mirza Faisal Shafique for rendering help in the typesetting of the manuscript at its various stages and for the drafting of many of the figures.

I would like to thank University fellows especially Tahir Nawaz Cheema, Sayyid Ali Asghar, Sharafat Ali, and Amir Rizwan who remained a constant source of help and a hospitable company. We usually used to sit for dispelling the pressure of Ph.D. studies and to reinstate ourselves by having had tea in a congenial environment of the University canteens. Friends and well-wishers outside the University circle with whom relevant discussions and consultations are carried out time and again could not be ignored. Muhammad Shafique Malik, lecturer of Physics in Govt. Graduate College(B) Satellite Town Gujranwala deserves special thanks in this regard. He remained and is a perpetual source of discussion and consultation on Physics topics. I owe him a lot for his cordial welcome ever.

I also feel indebted to my mother and elder brothers who occasioned me the circumstances leading to pursue my Ph.D. studies in physical and mathematical cosmology.

(Muhammad Zahid Mughal)

DEDICATION

Dear Professor Albert Einstein (the late),

The modern view of looking at the physical world is maximally under an obligation to you and is gleaning from your scientific thoughts incessantly to the present day. You stand par excellence in mathematical aesthetics. I have been receiving inspiration from your theories especially those related to the structure of spacetime and gravitation for the last fifteen years. This thesis is my humble scientific effort which I supplicate to dedicate it, to the ingenuity of your radical thoughts which completely revolutionized the modern physics as an expression of gratitude. Submitting optimistically, you will not mind it from a mediocre apprentice.

.

(Muhammad Zahid Mughal)

DECLARATION

I, Muhammad Zahid Mughal s/o Muhammad Tufail Mirza, roll # $18026109-001$, PhD Mathematics scholar, Department of Mathematics, Faculty of Science, University of Gujrat Pakistan, hereby solemnly declare that this thesis titled "A Mathematical Study for the Dynamics of Spacetime, Inflation and Accelerating Universe" is based on genuine work and has not yet been submitted or published elsewhere. Furthermore, I shall not use this thesis for obtaining any other degree from this University or any other Institute.

I also understand that if evidence of plagiarism is found in this thesis at any stage, even after the award of the degree, the degree may be canceled and revoked by the University.

(Muhammad Zahid Mughal)

It is certified that Muhammad Zahid Mughal s/o Muhammad Tufail Mirza, roll # $18026109-001$, PhD Mathematics scholar, Department of Mathematics, Faculty of Science, University of Gujrat Pakistan worked under my supervision and the above stated declaration is true to the best of my knowledge.

Dr. Iftikhar Ahmad
Professor,
Department of Mathematics,
University of Gujrat Pakistan.
Email: dr.iftikhar@uog.edu.pk
Dated:_____

THESIS COMPLETION CERTIFICATE

It is certified that this thesis titled "A Mathematical Study for the Dynamics of Space-time, Inflation and Accelerating Universe" submitted by Muhammad Zahid Mughal s/o Muhammad Tufail Mirza, roll # 18026109-001, PhD Mathematics scholar, Department of Mathematics, Faculty of Science, University of Gujrat Pakistan is evaluated and acceptance is made for the award of degree "Doctor of Philosophy (PhD)" in Mathematics by the following members of the Thesis / Dissertation Viva Voce Examination Committee.

The evaluation report is available in the Directorate of Advanced Studies and Research Board of the University.

Dr. Muhammad Mushtaq
Professor,
Chairperson, Department of Mathematics,
University of Engineering & Technology,
Lahore, Pakistan.
Email: mmushtaq@uet.edu.pk

Dr. Iftikhar Ahmad
Professor,
Department of Mathematics,
University of Gujrat Pakistan.
Email: dr.iftikhar@uog.edu.pk

Dr. Iftikhar Ahmad
Professor,
Chairperson, Department of Mathematics,
University of Gujrat Pakistan.
Email: dr.iftikhar@uog.edu.pk
Office Dispatch #: UOG/MATH/CH/22/
Date:_____

CERTIFICATE OF PLAGIARISM

It is certified that PhD Thesis titled "A Mathematical Study for the Dynamics of Space-time, Inflation and Accelerating Universe" by Muhammad Zahid Mughal has been examined by us. We undertake the following:

- Thesis has significant new work/knowledge as compared to already published or under consideration to be published elsewhere. No sentence, equation, diagram, table, paragraph, or section has been copied verbatim from previous work unless it is placed under quotation marks and duely referenced.
- The work presented is original and own work of the author (i.e. there is no plagiarism). No ideas, processes, results, or words of others have been presented as Author own work.
- There is no fabrication of data or results which have been compiled/analyzed.
- There is no falsification by manipulating research materials, equipment, or processes, or changing or omitting data or results such that the research is not accurately represented in the research record.
- The thesis has been checked using TURNITIN (copy of originality report attached) and found within the limits as per HEC plagiarism Policy and instructions issued from time to time.
- While generating the Turnitin report, nothing has been excluded from Abstract to Conclusions parts of the thesis.

Muhammad Zahid Mughal
Reg. No. 18034209369,
Department of Mathematics,
University of Gujrat Pakistan.
Email: 18026109-001@uog.edu.pk

Dr. Iftikhar Ahmad
Professor,
Department of Mathematics,
University of Gujrat Pakistan.
Email: dr.iftikhar@uog.edu.pk

TABLE OF CONTENTS

LIST OF FIGURES

CONTENTS **PAGE**

LIST OF TABLES

CONTENTS **PAGE**

LIST OF APPENDICES

CONTENTS **PAGE**

ABSTRACT

This thesis discusses the dynamics of spacetime by describing inherent properties connected to the structural geometry of it as the universe evolves. The accelerated cosmic expansion of spacetime takes place twice, first in the very early universe just after the big bang and prior to the radiation era and secondly starting in the late universe following the matter era i.e., inflation and dark energy eras respectively which constitute significant dynamical properties of spacetime. These two epochs may turn out to be decisive in describing the beginning and ultimate fate of the universe. Inflation has become a widely accepted paradigm and is now believed to be irrefutable and is backed by ever-increasing observational evidence. It was proposed to have occurred in the early universe to solve flatness and homogeneity problems faced by standard big bang cosmology. However, now it has transformed into a fascinating paradigm for the beginning of the universe that describes how it evolves after nucleation from a nothingness-like state. On the other hand, dark energy accounting for two-thirds of the cosmic budget came up with the observation-based discovery of the accelerated expansion of the late time universe.

For the inflationary universe, the study of the spectrum of curvature perturbation is carried out by considering multifield inflation and using small field potential. We investigate the effect of the number of e-folds N, slow-roll parameters ϵ_V, η_V, and spectral index n_s which carry significant information about the multi-field inflationary universe as it evolves cosmologically. Sasaki-Stewart formalism is used to determine these observables assuming that isocurvature perturbations can be neglected during early cosmic evolution. The analysis is carried out by observing the impact of increasing the number of e-folds on the power spectrum through the spectral index and its impact on the observable parameters of the slow-roll inflationary phase. It is also observed that the spectrum of multifield inflation is effectively different than its corresponding single-field inflation. The field values and their masses impact the results effectively at the time of horizon-crossing.

Afterward, we investigate a Nflationary phase diagram that illustrates its phase transitions with a multifield polynomial potential. The gradual vanishing of the inflationary phase during the slow-roll phase of the Nflation model has been demonstrated for a large number of fields in the case when there are voluminous N phase transitions occurring

in it. A phase diagram for Nflation model illustrates its phase transitions for a multifield potential $\Lambda_j^4\left(\frac{\phi_j}{\mu_j}\right)^p$. We use Marčenko-Pastur law to find the likely distribution of different mass scales of the fields. Further, the study for the conditions of entropy is carried out in the form of a bound that conforms to the number of e-folds $\mathcal{N}$ and the number of fields N. These drive the Nflationary phase and are mostly responsible for the phenomena taking place in it. We investigate in addition, that all the de Sitter entropy in the neighborhood of the critical point is concentrated around it and is largely condensed in the number of fields N for the potential under consideration.

The time-independent Schrödinger equation conforming to the Wheeler DeWitt equation is briefly explored for modeling the quantized behavior of the universe during its early phase of evolution. We solve it numerically for a single scalar field in flat spacetime with FLRW metric using artificial neural networks (ANN) and observe how it governs the early universe as it evolves through the inflationary phase following the big bang to later classical phase. To construct a continuous neural network mapping, the explicit Runge-Kutta method is used as the target parameter to generate the datasets. In order to determine the solution datasets for different scenarios, the processes of training, testing and validation are employed to take advantage of these processes in the learning of neural network models based upon the backpropagation technique of Levenberg-Marquardt.

To study the accelerating universe in the context of general relativity, we explore both sectors, gravitational and matter sectors of the Einstein field equation. At first, by modifying the matter sector a multi-field model of dark energy is investigated to drive the late-time accelerated expansion. On considering two multiple scalar fields, tachyon, and phantom tachyon, analysis of the autonomous dynamical system in phase space is carried out using the inverse square potentials suitable for such models. Calculating critical points and their eigenvalues, stability analysis is performed. It is observed that stable critical points are satisfied by power-law solutions. Equation of state changes from $w \geq -1$ to $w < -1$ that is about phantom divide which is decisive in evolutionary phases of the universe in these models.

Moreover, we also study cosmological dynamics of the late time accelerating universe through modifying the geometry of spacetime that is the gravitational sector. This can effectively be modified through $f(R)$ gravity, which offers a viable candidacy for the late time cosmic phenomenology. We investigate a viable $f(R)$ model and choose the Einstein frame to analyze the cosmic dynamics through the dynamical system approach. The results through stability analysis show that our universe is currently undergoing accelerated expansion regardless of the existence of dark energy.

CHAPTER-01

INTRODUCTION

This thesis consists of four chapters written and presented juxtapositionally, namely Introduction, Literature Review, Methodology, and Results and Discussions respectively. The first chapter of the introduction introduces the fundamentals of inflationary cosmology and later developments concerned with the accelerating universe. It further furnishes an introduction to the problems taken into consideration in the thesis and is composed of six sections, each of which comprises the introduction for the corresponding section accommodated in the subsequent chapters namely Literature Review, Methodology, and Results and Discussions respectively. To begin with, in section 1.1, we discuss the geometric structure of spacetime as brought forth by the theory of general relativity, and the rudimentary definitions with basics of cosmology are covered in addition.

1.1 On the Cosmological Dynamics of Spacetime and Basics of Cosmology

With the advent of general theory of relativity in 1916, spacetime was itself transformed into one of the four fundamental interactions of the universe, and the geometrical structure attached to it was considered to demonstrate gravity in a dynamical way (Einstein, 1922). The force of gravity was replaced by the curvature of spacetime that is mirrored through the geometric structure of metric tensor $g_{\mu\nu}$, the fundamental tensor. Consequently, the paradigm of spacetime became an integral part of the cosmic fabric and proved a dynamical medium where the whole phenomenal world exists. Any solution of the field equations of general relativity entails a certain structural geometry of spacetime or just a spacetime that represents a universe itself, therefore determining a solution of the field equations amounts to coming across a specific model of the universe.

Cosmology studies the universe as a whole i.e. in its totality (V. Mukhanov, 2005) encompassing its beginning in spacetime or as spacetime itself, its evolution over time, and its eventual fate. It is important to mention that the universe is not merely a random and accidental heap of material stuff piled up haphazardly and distributed over a void irregularly, rather it forms a single organic whole, parts of which evolve symmetrically and proportionally depending on one another and perform their functions in unison with one another. The history of cosmology dates back to ancient Greeks,

Babylonians, Indians, and Iranians with its roots at that time in philosophy and religion. Before the era of modern scientific cosmology dawns, it has been nurtured in the womb of Abrahamic religions especially Judaism, Christianity, and Islam. Cosmology as a modern science begins with the surfacing of general relativity when Einstein himself first put it to use for formulating a cosmological model of the universe mathematically. The model brought about a dynamic universe, however, it was rendered to be static by adding a fudge factor known as cosmological constant, as there was no cosmological evidence of its contraction or expansion at that time (Einstein, 1986). Einstein's static model was afterward proved to be inconsistent with the cosmological observations and was discarded; however, its formulation as the first mathematical model based on the field equations of general relativity laid the foundation stone for the inception of relativistic cosmology to emerge as one of modern sciences.

Cosmology takes into account the largest structure or scale of spacetime that is the causally connected and maximally symmetric patch of the cosmological fabric from the perspective of its origin, evolution, and eventual futuristic fate. It gives the universe a mathematical description as large as the cosmological observational parameters reveal and accordingly and consequently allow. The modern relativistic cosmology was established on general relativity which brought forth the big bang model by extrapolating the cosmic expansion backward in time. The big bang model was, however, marred with some inward problems related coherently to it, which were removed by introducing an exponentially expanding phase in the very early universe to be known as inflation.

When the energy density of the matter and radiation is removed in Einstein's static model retaining the positive cosmological constant that plays a very important role in making the universe appear static in time, the de Sitter model results. De Sitter's model presented in 1917 was proposed just after Einstein presented his static and closed model of the universe. Resorting to Mach's principle, Einstein was of the view that it is merely the matter density in the universe that is the cause of inertia and gravitation. For investigating the status of Einstein's belief, de Sitter posed the 2nd model devoid of matter density, however retaining the cosmological constant that was introduced by Einstein to halt the cosmic phenomena from expanding. The de Sitter model is the maximally symmetric solution of Einstein's field equations with vanishing matter density. The geometrical structure of spacetime of the de Sitter model is comparatively more complicated than that of Einstein's static model. The characteristic of the de Sitter model is that it predicts a redshift despite containing neither matter density nor

radiation, however, its geometry was proved to be accelerating (De Sitter, 1916). De Sitter universe corresponds to the specific case that is related to one of the very early solutions of Einstein's Field Equations (EFE). The importance of the de Sitter model was not recognized until the introduction of inflation in the late 20th century as the actual universe must be considered as a local set of perturbations in the geometry of de Sitter having validity at large. De Sitter geometry represents Euclidean space with a metric that depends on time. It was found that the inflation could be de Sitter geometry in general or quasi-de Sitter geometry which has an innate impact on the evolution of the geometry of FLRW spacetimes. It further bears its relation with the late-time accelerated expansion of the universe and to the dynamic geometry of the spacetime intrinsically which is cohered with it. The de Sitter universe represents the inflationary phase of the universe with slightly broken time translational symmetry.

Alexander Friedmann predicted theoretically the possibility of the dynamic universe, the one which can expand, contract, or even could be born out of a singularity i.e., it could nucleate from literal nothingness as Alexander Vilenkin has suggested (A. Friedmann, 1924, 1999; Vilenkin, 1982). Later on, George Lemaitre, unaware of Friedmann's work at that time, reached independently the same conclusion. His findings were motivated, however by semi-observational working. Later in 1931, he also proposed a theory of the primeval atom which came to be known afterward, as the big bang theory by Fred Hoyle accidentally during a radio speech (Lemaître, 1927; Lemaitre, 2013). Edwin Hubble first in 1927 proved the existence of other galaxies besides the Milky Way and afterward in 1929 discovered on the basis of observational evidence that the universe was indeed expanding (Hubble, 2013). This was actually discovering what Friedmann already had predicted theoretically in 1922 (S. Hawking, 2009). The discovery of observation-based cosmic expansion was a radical breakthrough in the purview of relativistic cosmology that bore far-reaching influence upon evolving field of cosmological studies. In the late 1940s, George Gamow (1904–1968) who had been a student of Friedmann and his collaborators, Ralph Alpher (1921–2007) and Robert Herman (1914–1997), independently worked on Friedmann's and Lemaître's hypothesis and transformed it into a model of the early universe. They made a supposition about the initial state of the universe as comprising of a very hot, compressed mixture of nucleons and photons, thereby introducing the big bang model on the basis of comparatively strong shreds of evidence. They, however, did not associate a particular name with their findings in connection

with the early state of the universe. Based on this model they were successful in calculating the amount of helium in the universe, nonetheless, unfortunately, there was no authentic observational evidence available through which their calculations could be compared and verified (ALPHER & Herman, 1988).

The standard relativistic model of cosmology underpinning the big bang theory could not explain the global structure of the universe and the origin of matter in it. On the other hand, the distribution of matter in it homogeneously on large scales and the spatial flatness also remained enigmatic. The big bang model just made an assumption concerning these enigmatic issues, nonetheless could not solve them. In the framework of effective field theory, the aspects of nonsingular cosmology are explored by Yong Cai et al. It is shown that the effective field theory can assist in providing the clarification about the origin of no-go-theorem and helps to resolve this theorem (Y. Cai, Wan, Li, Qiu, & Piao, 2017).

The inflationary era was proposed in the standard model of cosmology which propounds the big bang theory of the creation of the universe. Inflation solves the problems encountered in the big bang cosmology. Gliner, in 1965, hypothesized an era of exponential expansion for the universe earlier than any significant inflationary model surfaced (Gliner, 1966). It was found that the scalar fields are dynamic existing in nature, and in 1972 it was proposed that during phase transitions the energy density of the universe as a scalar field changes (Kirzhnits & Linde, 1972). Andrei Linde, in 1974, realized that scalar fields can play an important role in describing the phases of the very early universe. He speculated that the energy density of a scalar field can play the role of vacuum energy dubbed as a cosmological constant (A. D. Linde, 1974).

In 1978, Englert, Brout, and Gunzig (Brout, Englert, & Gunzig, 1978) forwarded a proposal of the "fireball" hypothesis attempting to resolve the primordial singularity problem. They based their investigations on the entropy contained in the universe and approached the issue of the early evolution of the universe by introducing particle production in it. They inquired deep down into it and on the basis of their hypothesis inferred that a universe undergoing a quantum mechanical effect would itself appear in a state of negative pressure and would be subject to a phase of exponential expansion. A work was mentioned by Linde in his review article (A. D. Linde, 1979) where he sought, in collaboration with Chibisov, to develop a cosmological model based upon the facts known in connection with the scalar fields. Considering the supercooled vacuum

as a self-contained source for entropy, they tried to bring about the exponential expansion of the universe to be concerned with it. They, however, discovered instantly that the universe becomes very inhomogeneous after the bubble wall collisions take place. Slightly before Alan Guth's original proposal of inflation surfaced, Alexei Starobinsky in 1980 proposed a model of inflation on the base of a conformal anomaly in quantum gravity. His proposal was presented in the framework of general relativity where slight modification of the equations of general relativity in the matter sector was proposed and quantum corrections were employed to it in order to have a phase of the early universe. Starobinsky's model can be considered as the first model of inflation which has semi-realistic nature and evades from the graceful exit problem. (Starobinsky, 1980; Müller, Ricciardone, Starobinsky, & Toporensky, 2018). It was hardly concerned with the problems of homogeneity and isotropy which occur in the relativistic cosmological model of the big bang. His model, as he himself accentuated, can be considered the extreme opposite of chaos in Misner's model. The model is found to agree with cosmological observations with slight deviations from recent measurements. Tensor perturbations that represent gravitational waves have also been predicted in Starobinsky's model with a flat spectrum.

Alan Guth employed the dynamics of a scalar field and with a clear physical motivation presented an inflationary model (Guth, 1981) in 1981 on the basis of supercooling theory during the cosmological phase transitions occur and the universe expands in a supercooled false vacuum state. A false vacuum is a metastable state containing a huge energy density without the existence of any field or particle in it so that when the universe expands from this heavy nothingness state its energy density does not change and the empty space remains empty such that the inflationary phase occurs in a false vacuum state (A. D. Linde, 1984b). The duration of the inflationary phase in Guth's original scenario is too short to be capable of resolving any problem, although it was proposed to solve the big bang problems, instead, the universe becomes very inhomogeneous consequently which leads to the graceful exit problem (S. W. Hawking, Moss, & Stewart, 1982; Guth & Weinberg, 1983). The problem prevents the universe from evolving to later classical stages and is inherently existing in the originally proposed version of Guth.

The graceful exit problem was addressed independently by Linde, Steinhardt, and Albrecht (A. D. Linde, 1982a; Albrecht, Steinhardt, Turner, & Wilczek, 1982; Allahverdi, Brandenberger, Cyr-Racine, & Mazumdar, 2010; A. Linde, 1982; A. D. Linde, 1982c,

1982b; Albrecht & Steinhardt, 1982), where they introduced a phase of slow-roll inflation at the end of the normal inflationary phase all inclusively known as new inflation. The resolution of the problem was sought by constructing a new inflationary paradigm where inflation can have its inception either in an unstable state at the top of the effective potential or in a state of a false vacuum. In this scenario, the dynamics of the scalar field are such that it rolls gradually down to the lowest of its effective potential. It is of great importance to note that the shifting away of the scalar field from the state of false vacuum to other later states has remarkable consequences. When the scalar field rolls slowly towards its lowest, that is so-called slow-roll inflation, it gives rise to the generation of density perturbations which seed the cosmic structure formation of the universe (S. W. Hawking, 1982; Starobinsky, 1982; Guth & Pi, 1982). It was observed that the production of density perturbations during the phase of slow-roll inflation is inversely proportional to the motion of the scalar field (Kachru et al., 2003; V. F. Mukhanov & Chibisov, 1981). The basic difference between the new inflationary scenario and that of the old one is that the advantageous portion of the inflation in the new inflation scenario, which is responsible for the large-scale homogeneity and global flatness of the universe, does not take place in the false vacuum state, where the scalar field vanishes. This means that the new inflation could explain why our universe was so large only if it was very large initially and contained many particles from the very beginning.

The course of the 20th century has presented many challenges to standard cosmology. In the framework of the standard model, in addition to inflation, another breakthrough came forth in 1998 when the observation-based accelerated expansion of the universe was discovered (Perlmutter, Aldering, et al., 1999; Perlmutter, Turner, & White, 1999; Riess et al., 1998). Before this discovery, it was, however, thought that in the perspective of all known forms of matter and energy that obey the strong energy condition $\rho + 3p > 0$, the expansion of the universe would slow down over time. This was a natural consequence of Friedmann's equations that play a central role in the evolution of the universe. From the 2nd Friedmann's equation $\frac{\ddot{a}}{a} = -\frac{4\pi G}{3}(\rho + 3p)$ that have to absolutely dictate the cosmic acceleration phenomenon, the universe must be undergoing deceleration characterized by the deceleration parameter $q_0 = -\frac{a\ddot{a}}{\dot{a}^2}$; however, astoundingly the value of the deceleration parameter was observationally determined to be less than zero i.e. $q_0 < 0$, meaning that the expansion of the universe is accelerating rather to be decelerating. The discovery of the accelerated expansion has won the Noble Prize of 2011 in Physics in favor of its discoverers namely Saul Perlmutter, Brian Shmidt, and Adam G. Riess. In

order to explain the cause of the accelerated expansion, an exotic form of energy density was hypothetically introduced that is usually known as dark energy. The name "dark energy" was first used by D. Huterer and M. S. Turner in their 1999 paper (Huterer & Turner, 1999). On the basis of observational data, the present budget of the universe is contributed about 70% by dark energy, 26% dark matter, and 4% ordinary baryon matter where the dark side of the universe is prevalent and sits patiently in a camouflaged hide. Based on it, dark energy constitutes two-thirds whereas the matter in its baryonic and dark form amounts to one-third of the total cosmic species. It is significant to remark that dark energy is substantially effective on the largest scales of intra-galaxies and does not affect gravitationally bound local systems such as the solar system, or local distances between planets or stars. There exist a large number of proposed models to explain the origin and nature of dark energy. Many independent observations lend support to the existence of dark energy such as discovery of cosmic background radiation (CMB) radiation, supernovae of Type Ia (SN, Ia), Baryonic acoustic oscillation (BAO), etc. Dark energy, today constitutes a very significant subject of standard cosmology in the wake of observational data by providing information about its basic nature, however, its exact nature remains unknown to the present day, for reviews see the references (Nojiri & Odintsov, 2007; SAMI, 2009; Bamba, Capozziello, Nojiri, & Odintsov, 2012; Nojiri, Odintsov, & Oikonomou, 2017b).

The layout of this ongoing Section 1.1 is as follows: Section 1.1.1 begins with describing relativistic cosmology with some discussion on its underlying principles. The basics of general relativity with cosmological principle and Weyl's principle are discussed briefly in its subsections . The standard model of cosmology is discussed in Section 1.1.2 with thirteen subsections underlying it . We carry out a reviewal study of the standard model of cosmology by investigating the geometric structure of spacetime related to it in the framework of general relativity. In these subsections, possible geometries concerned with the standard FLRW universe are also discussed, in addition to the derivation of Friedmann equations. The consequences based on Friedmann's equations about cosmic evolution are its part as well, ending in the discussion of cosmological problems faced by the standard model. In Section 1.1.3, we embark on inflation and discuss its dynamics in scalar field perspective. It is observed that how the proposal of exponential expansion in the early universe logically solves the cosmological problems. It comprises five subsections investigating the dynamics of slow-roll inflation and its related definitions. Further, four indices are added in the end to elaborate on some relevant topics. In

Appendix-03, the structure of space, time, and spacetime is reviewed as it is described in relativity and prerelativity perspectives.

1.1.1 Relativistic Cosmology

Albert Einstein himself applied general relativity to the largest scale of spacetime (Einstein, 1986) and presented the very first relativistic model of the universe laying the foundations of modern theoretical cosmology. The model was later on called as Einstein world or universe. For this purpose, Einstein modified his field equations by proposing an inherent energy density known as cosmological constant Λ in the geometrical structure of spacetime itself that provides repulsive gravity to keep the universe from expanding. Relativistic cosmology was, however founded on three fundamental principles

1. Cosmological principle;
2. Weyl's principle;
3. General relativity.

These are illustrated in the following subsections.

1.1.1.1 Cosmological Principle

The cosmological principle states that on sufficiently large scale, the universe is homogenous and isotropic at any time. Therefore, it is the same for all observers and has similar properties on larger scales. It is the generalization of Copernican Principle which incorporates two aspects of uniformity that is homogeneity and isotropy and almost all the standard cosmological models of the spacetime underpin it explicitly or implicitly. Homogeneity means location independence, i.e., all places in the universe at galactic scales are indistinguishable. Isotropy gives direction independence, i.e., in whatever direction we look in the universe it appears the same. Certainly, the isotropy connotes homogeneity, however this is not true vice versa. It has two forms:

1. Cosmological principle with respect to spatial invariance;
2. Cosmological principle with respect to temporal invariance.

In spatial invariance, we suppose the invariance of space with respect to translational and rotational properties known as homogeneity and isotropy, respectively, and the principle

may be regarded as cosmological principle. Under both the invariant properties the space remains isomorphic. Temporal invariance in cosmological principle, on the other hand leads to a static universe that does not change with time and exists from a time without beginning. It deprives cosmic evolution from a free will. A perfect cosmological principle incorporates temporal homogeneity and isotropy which was employed by the steady state theory of the eternal universe and was not supported by the observations and was therefore disfavored. Slight time translation symmetry breakage leads to the universe to evolve in the present form. For a local observer the principle might not be satisfied as the Earth and the solar system are not homogeneous and isotropic since the matter clumps together to form objects like planets, stars, galaxies with voids of vacuum-like in between them but on the larger scales of about MP ¿ 1000 Pc the universe obeys the cosmological principle. The uniformity of CMB radiation in all directions (homogeneity and isotropy) provides the confirmatory proof of the cosmological principle.

1.1.1.2 Weyl's Principle

Weyl's principle helps us consider the universal stuff as consisting of a fluid, the particles of which are constituted by galaxies. Therefore, what we name "the universe" is just cosmic fluid. In the cosmological spacetime, the world lines of the fundamental observers form a smooth bundle of time-like geodesics which would never meet except in the past singularity from where the universe emerged or at the future singularity if it would happen. The fundamental observers are those who comove with the cosmic fluid. The world lines of galaxies as fluid particles are always and everywhere orthogonal to the family of spatial hypersurfaces. The postulate was presented by Hermann Weyl (1885–1955) in 1923 which is essentially about the nature of matter in the universe (Scholz, 2001). He regarded the material content of the universe in the form of fluid whose constituent particles make a substratum in the cosmic fluid.

It means that in the substratum of spacetime it allows us to consider the structure of the universe as fluid. The Weyl principle introduces further symmetry in the structure of spacetime described by the metric tensor by considering the galaxies as test particles and postulates that the geodesics on which these galaxies move do not intersect. It states that the world lines of galaxies considered as "test particles" form a 3-bundle of non-intersecting geodesics orthogonal to a series of spacelike hypersurfaces.

1.1.1.3 General Relativity

General relativity played a key role in establishing the cosmic expansion and provided clues and imprints for later developments to crop up related to accelerated cosmological expansion in the very and late early universe. General relativity provides the best existing theory of gravitation on cosmological scales and models it as structured into the geometric structure of spacetime. In Appendix-03, the structure of spacetime is reviewed as described by classical and relativistic mechanics. It would be convenient to have a retrospective look into the basics of general relativity whose role has been very fundamental to the modern cosmology. Therefore, we briefly review the structure of the theory specifically in connection with the geometrical structure of spacetime in it. General relativity in its core describes that gravity is the geometry of four-dimensional spacetime manifested through its curvature. It is a theory of spacetime and gravitation that are the very basic components of the universe. Einstein's journey towards general relativity in order to introduce gravity in his previous theory sought the fascinating geometry of the structure of spacetime, such that gravity as a field force disappeared and was assimilated in the very geometric structure of spacetime. In constructing the framework of new theory, Einstein was influenced and governed by Mach's principle, which states that it is a priori existence and distribution of matter which determines the geometry of spacetime, and in the absence of it, there shall be no geometric structure of a spacetime in the universe. Therefore, there will be no inertial properties in an, otherwise, empty universe. In general, relativity gravitation and inertia are essentially indistinguishable. The metric tensor $g_{\mu\nu}$ describes the effect of both combinedly, and it is arbitrary to ask which one contributes its effect more and which less, therefore to call it with a single name is suitable either inertia or gravitation (De Sitter, 1916). In general relativity gravitation, inertia and the geometry of spacetime are coalesced into a single entity represented by a symmetric tensor of second rank $g_{\mu\nu}$ which owes its existence due to presence and distribution of matter which is represented by an other symmetric tensor $T_{\mu\nu}$ known as energy-momentum tensor. The metric tensor $g_{\mu\nu}$ is the fundamental object of study in general relativity and takes into consideration all the causal and geometrical structure of spacetime. General relativity underlies five fundamental principles connotated by it implicitly or explicitly manner (D'Inverno & Harvey, 1993):

1. The principle of general covariance

The laws of physical phenomena are same both for inertial and non-inertial frames of reference and it establishes equivalence between all observers. Consequently, it requires the covariant formulation of physical laws, which is accomplished using the coordinate-independent language of tensors.

2. The principle of equivalence between gravitation and inertia
   In general relativity, gravitation and inertia are not essentially different entities. The fundamental tensor $g_{\mu\nu}$ assimilates both, however with arbitrary ratio. The weak and strong forms of equivalence principle give the coupling of gravitational field to everything and everything moves in it without dependence on its mass and composition respectively. The principle of equivalence allows to construct a coordinate system in which gravitational effects can be made to disappear.

3. The Mach's principle
   Mach's principle is about ontological property of being. It describes that it is the distribution of matter that specifies cosmic geometry and in the otherwise condition, there would exist no geometry.

4. The principle of minimal gravitational coupling
   This principle explicates how one could make a shift from special covariance to general covariance. It describes that the unnecessary terms should be avoided being added in Riemann's curvature tensor.

5. The principle of correspondence
   It describes that general relativity must concur with special relativity and Newton's law of gravitation for the absence and the weak field limit of gravitational field respectively. It is also known as the principle of consistency.

The principle of general covariance and equivalence principles are explicitly implied whereas the rest of three are implicitly assumed in the formulation of general relativity. Furthermore, in explaining Mach's principle, Einstein was impelled to tacitly assume the essence of cosmological principle. The principle of equivalence and the principle of general covariance lie at the heart of general relativity and are concomitantly implied. The principle of general covariance can be derived from the equivalence principle. In the light of the principle of general covariance, the theory requires that the laws of physics might be formulated in a coordinate-independent style. The coordinate-independence requires the replacement of partial derivatives by covariant derivatives which further introduces the connection coefficients $\Gamma^{\lambda}_{\mu\nu}$ as the 2nd kind of Christoffel symbols. The

presence of the gravitational field demands existence of metric tensor $g_{\mu\nu}$ and the affine connection $\Gamma^{\rho}_{\mu\nu}$. All the geometric structure of the curved spacetime is based on the existence of these tensor and nontensors respectively (Weinberg, 1972; P. J. E. Peebles & Peebles, 1993; D'Inverno & Harvey, 1993). The field equations of general relativity read as $G_{\mu\nu} = 8\pi T_{\mu\nu}$, where $G_{\mu\nu} = R_{\mu\nu} - \frac{1}{2}g_{\mu\nu}R$ is the Einstein tensor and is expressed in terms of Ricci tensor $R_{\mu\nu}$, metric tensor $g_{\mu\nu}$, and Ricci scalar R, whereas $T_{\mu\nu}$ is the energy momentum tensor standing for whatever is existing physically or as effect therein coherently associated with physical objects or within physical objects. The spacetime continuum of general relativity is postulated as a 4-dimensional Lorentzian manifold (M, g), where M denotes the Manifold and g is metric defined over it. The geometry of a spacetime is encoded in its metric which has a geodesic structure, though complex and frequently solved numerically for a specific bunch of geodesics. These geodesics specify the physical properties of the geometry of spacetime which are interpreted by drawing graphically in a certain spacelike volume. In general relativity, the geometry of spacetime is itself gravity and is described through dynamic structure of spacetime in its framework. The interaction between spacetime and the content it contains taken together form what we manifestly call cosmological phenomenon of which the causally connected patch is what makes our observable universe. General relativity thus models the universe as something whose warp and woof is woven by spacetime itself. This formulates that the universe is not more than dynamics of spacetime. John Archibald Wheeler has described general relativity in a single sentence "Matter tells spacetime how to curve and spacetime tells the matter how to move" (Thorne, Misner, & Wheeler, 2000). The presence of matter occasions the geometry of spacetime as the geodesic fabric which governs other matter. General relativity thus transforms gravitation from being a force to being it a property of spacetime, so that gravity does remain a force but curvature of the geometric structure of spacetime. Einstein worked out a relation between matter–energy content of the universe and its gravitating effects in the form of geometry of spacetime. He employed the language of tensors to describe it. The invariant interval between two events separated infinitesimally with coordinates (t, x, y, z) and $(t + dt, x + dx, y + dy, z + dz)$ has been defined according to special relativity

$$ds^2 = \eta_{\mu\nu}dx^{\mu}dx^{\nu} \tag{1.1.1}$$

which defines a Lorentz invariant Minkowski flat spacetime whose spacetime geometry is encoded in $\eta_{\mu\nu}$. Under the change of coordinates ds^2 remains invariant and is spacelike for $ds^2 < 0$, timelike for $ds^2 > 0$ and light-like for $ds^2 = 0$. Material bodies travel on

time-like geodesics whereas the rays of light follow the light-like geodesics. The light rays i.e. photon path is described by $ds = 0$ and the baryonic matter following a path between two events comes out for which

$$\int ds = 0 \tag{1.1.2}$$

i.e., it generates stationary values and conforms to the shortest distance between two points to be a straight line which means that there are no external forces to set their path deviated. General relativity was based on five basic principles as explained earlier which are incorporated into it in explicit form or implicit form, namely, equivalence principle, relativity principle, Mach's principle, and Correspondence principle. Tensors are geometric objects defined on a manifold M, which remain invariant under the change of coordinates. It is composed of a set of quantities which are called its components, therefore it is the generalization of a vector which means that it has more than three components. They represent mathematical entities that conform to certain laws of transformations. The properties of components of a tensor do not depend on a coordinate system that is used to describe the tensors. The transformation laws of a tensor relate its components to two different coordinate systems. The mathematical representation of a tensor is displayed usually by considering a boldface alphabetical letter like A, B, T, P, etc. with an index or a set of indices in the form of superscripts or subscripts or both in mixed form. These superscripts and subscripts in the case of a tensor are called contravariant and covariant indices. Contravariant indices of a tensor are used to give the meaning of contravariant components of it like A^{μ}, $A^{\mu\nu}$, $A^{\mu\nu\xi\cdots\cdots}$. Covariant indices of a tensor are used to signify the meaning of contravariant components of it like A_{μ}, $A_{\mu\nu}$, $A_{\mu\nu\xi\cdots\cdots}$. The indices of both types namely contravariant and covariant are used to specify the components of a mixed tensor like A^{ν}_{μ}, $A^{\nu}_{\mu\xi}$, $A^{\nu\sigma}_{\mu}$, $A^{\nu\sigma\cdots}_{\mu\xi\upsilon\cdots}$. A mixed tensor is a tensor that has contravariant as well as covariant components. The number of indices appearing in the symbol representing a certain type of a tensor is known as its rank. The appearing indices in the symbol representing a tensor can be contravariant or covariant or both types of indices in it. The order of a tensor is the same thing as rank, only the name differs. The number of components of a tensor is related to its rank or order and the dimensions of the space in which the is being described. In n-dimensional space, a tensor of rank, say, k will have a number of components equal to the number of components of a tensor in n-dimensional space is equivalent to $n^k = (number\ of\ dimensions\ of\ space)^{rank}$. However, the spacetime of general relativity is pseudo-Riemannian having four dimensions, three spatial and one temporal. Coordinate

patches are necessarily considered to map the whole of the spacetime. Each point-event of a coordinate patch in the four-dimensional pseudo-Riemannian spacetime is labeled by a general coordinate system, which conventionally runs over 0, 1, 2, and 3, where 0 stands for time and the rest for space coordinates. An inertial or otherwise frame of reference characterized by a coordinate system can be attached to every point event of the spacetime and coordinate transformations between any two coordinate systems can be found. These can be written as

$$\begin{aligned} A'_{\mu} &= \frac{\partial x^{\nu}}{\partial x'^{\mu}} A_{\nu} \\ B'^{\mu} &= \frac{\partial x'^{\mu}}{\partial x^{\nu}} B^{\nu} \\ A'^{\mu}_{\nu} &= \frac{\partial x'^{\mu}}{\partial x^{\zeta}} \frac{\partial x^{\sigma}}{\partial x'^{\nu}} A^{\zeta}_{\sigma} \end{aligned} \tag{1.1.3}$$

while switching to Riemannian geometry for non-Euclidean spaces ordinary partial differentiation is generalized to covariant differentiation and is defined using a semi-colon ; as

$$\begin{aligned} B_{\nu;\mu} &= \partial_{,\mu} B_{\nu} - \Gamma^{\sigma}_{\nu\mu} B_{\sigma} \\ B^{\nu}{}_{;\mu} &= \partial_{,\mu} B^{\nu} + \Gamma^{\nu}_{\mu\sigma} B^{\sigma} \end{aligned} \tag{1.1.4}$$

where comma , denotes an ordinary partial differentiation with respect to the corresponding variable and ; signifies covariant differentiation. In the covariant differentiation, indices can also be raised or lowered with the help of metric tensor, however on differentiating it covariantly, we see it vanishes, i.e., $g_{\mu\nu;\alpha} = 0$. The interval between infinitesimally separated events x^{μ} and $x^{\mu} + dx^{\mu}$ is given by

$$ds^2 = g_{\mu\nu} dx^{\mu} dx^{\nu} \tag{1.1.5}$$

The corresponding contravariant tensor of $g_{\mu\nu}$ is given by $g^{\mu\nu}$ and they result in Kronecker delta. Moreover, indices can be lowered or raised using the metric tensor in either form as

$$\begin{aligned} g_{\mu\nu} g^{\mu\zeta} &= \delta^{\zeta}_{\nu} \\ g_{\mu\nu} B^{\nu} &= B_{\mu} \\ g^{\mu\nu} B_{\nu} &= B^{\mu} \end{aligned} \tag{1.1.6}$$

In general relativity, all the geometry of curved spacetime is contained in the second-rank symmetric tensor $g_{\mu\nu}$ known as fundamental or metric tensor and is the function of four coordinates $g_{\mu\nu} = g_{\mu\nu}(x_0, x_1, x_2, x_3)$ and $g_{\mu\nu}$ encodes all the information about gravitational field induced by presence of matter. It governs the other matter as a response mimicking the role of gravitational potential similar to that of Newtonian gravity

so that the paths remain no more straight, and the action in Eq. (1.1.2) determines the path of a free particle known as geodesic

$$\frac{d^2x^\mu}{ds^2} + \Gamma^\mu_{\nu\zeta}\frac{dx^\nu}{ds}\frac{dx^\zeta}{ds} = 0 \tag{1.1.7}$$

where

$$\Gamma^\mu_{\nu\zeta} = g^{\mu\lambda}\Gamma_{\nu\zeta\lambda} = \frac{1}{2}g^{\mu\lambda}\left(\frac{\partial g_{\nu\lambda}}{\partial x^\zeta} + \frac{\partial g_{\zeta\lambda}}{\partial x^\nu} + \frac{\partial g_{\nu\zeta}}{\partial x^\lambda}\right) \tag{1.1.8}$$

are the Christoffel symbols which through the geodesic equation specify the world lines of free particles. The "acceleration due to gravity" in Newtonian gravitation law is described by these symbols in Einstein's picture of gravity as the geometric properties of spacetime encoding the similar information. Locally these symbols vanish in the inertial frame of reference in free fall and under coordinate transformation from x^μ and x'^μ do not constitute components of a tensor and therefore do not represent a tensor.

$$\Gamma'^\sigma_{\mu\nu} = \frac{\partial x'^\sigma}{\partial x^\lambda}\frac{\partial x^\zeta}{\partial x'^\mu}\frac{\partial x^\rho}{\partial x'^\nu}\Gamma^\lambda_{\zeta\rho} + \frac{\partial^2 x^\zeta}{\partial x'^\mu \partial x'^\nu}\frac{\partial x'^\sigma}{\partial x^\zeta} \tag{1.1.9}$$

The Riemann tensor is defined as

$$R^\sigma_{\mu\nu\lambda} = \frac{\partial}{\partial x^\nu}\Gamma^\sigma_{\mu\lambda} - \frac{\partial}{\partial x^\lambda}\Gamma^\sigma_{\mu\nu} + \Gamma^n_{\mu\lambda}\Gamma^\sigma_{n\nu} - \Gamma^n_{\mu\nu}\Gamma^\sigma_{n\lambda} \tag{1.1.10}$$

It has symmetry properties and satisfies the following Bianchi identity:

$$R^\sigma_{\mu\nu\lambda;\zeta} + R^\sigma_{\mu\zeta\nu;\lambda} + R^\sigma_{\mu\lambda\zeta;\nu} = 0 \tag{1.1.11}$$

The Ricci tensor is obtained from Riemann tensor contracting

$$R_{\mu\nu} = g_{\lambda\sigma}R^\sigma_{\mu\nu\lambda} = \frac{\partial}{\partial x^\nu}\Gamma^\sigma_{\mu\lambda} - \frac{\partial}{\partial x^\lambda}\Gamma^\sigma_{\mu\nu} + \Gamma^n_{\mu\lambda}\Gamma^\sigma_{n\nu} - \Gamma^n_{\mu\nu}\Gamma^\sigma_{n\lambda} \tag{1.1.12}$$

Another expression of Ricci tensor is written in the form given below when determinant of the metric tensor $g_{\mu\nu}$ is envisaged as a matrix and denoted by g

$$R_{\mu\nu} = \Gamma^\lambda_{\mu\nu,\lambda} - \left(\ln\sqrt{-g}\right)_{,\mu\nu} + \left(\ln\sqrt{-g}\right)_{,\lambda}\Gamma^\lambda_{\mu\nu} - \Gamma^\lambda_{\pi\mu}\Gamma^\pi_{\lambda\nu} \tag{1.1.13}$$

The Ricci scalar or scalar curvature is described as

$$R = g^{\mu\nu}R_{\mu\nu} \tag{1.1.14}$$

contraction of the Bianchi Identity in Eq. (1.1.11) gives

$$R_{\mu\nu} - \frac{1}{2}g_{\mu\nu}R \tag{1.1.15}$$

which is the Einstein tensor. Now we can write basic equations of general relativity

$$R_{\mu\nu} - \frac{1}{2}g_{\mu\nu}R = 8\pi T_{\mu\nu} \tag{1.1.16}$$

or

$$G_{\mu\nu} = 8\pi T_{\mu\nu} \tag{1.1.17}$$

$$G_{\mu\nu} \propto T_{\mu\nu} \tag{1.1.18}$$

These are written with cosmological constant also. From Eq. (1.1.17)

$$G_{\mu\nu} + \Lambda g_{\mu\nu} = 8\pi T_{\mu\nu} \tag{1.1.19}$$

The energy-momentum tensor $T_{\mu\nu}$ is the source term for the metric tensor $g_{\mu\nu}$ which for a most general matter-energy fluid that is consistent with the assumption of homogeneity and isotropy represents a perfect fluid and has the form

$$T_{\mu\nu} = (\rho + p)\, u_\mu u_\nu - p g_{\mu\nu} \tag{1.1.20}$$

where $u^\mu = (1, 0, 0, 0)$ is the four velocity in a comoving frame of reference and

$$T_{\mu\nu} = \begin{pmatrix} \rho & 0 & 0 & 0 \\ 0 & p & 0 & 0 \\ 0 & 0 & p & 0 \\ 0 & 0 & 0 & p \end{pmatrix} \tag{1.1.21}$$

1.1.2 The Standard Model of Cosmology

The standard model in cosmology has been established on the most general homogeneous and isotropic spacetime. The standard model that propounds the hot big bang model of the universe is known as Friedmann–Lemaitre–Robertson–Walker (FLRW) line element which reads as in the Cartesian coordinates

$$ds^2 = -dt^2 + dx^2 + dy^2 + dz^2 \tag{1.1.22}$$

or in spherical coordinates, we have

$$\begin{aligned} ds^2 = g = g_{\mu\nu} dx^\mu dx^\nu = -dt^2 \\ + a(t)^2 \left(\frac{1}{1 - kr^2} dr^2 + r^2 d\theta^2 + r^2 \sin^2\theta d\phi^2 \right) \end{aligned} \tag{1.1.23}$$

The predictions for the quantitative behavior of the expanding universe is enunciated suitably by the metric tensor and the scale factor as a function of time, i.e., $a(t)$ describes the scale of coordinate grid interrelating the coordinate distance with physical distance, i.e., in a smooth and homogeneously expanding universe.

1.1.2.1 Geometric Properties of the FLRW Line Element

From the line element in Eq. (1.1.23), as the time flows only in one direction and the space obeys the cosmological principle, therefore we are allowed to separate the metric in temporal and spatial parts. To understand the four dimensional spacetime geometry of FLRW universe we begin with the geometry of spatial part of the line element that is

$$a(t)^2 \left(\frac{1}{1-kr^2} dr^2 + r^2 d\theta^2 + r^2 \sin^2\theta d\phi^2 \right) \tag{1.1.24}$$

This is the spatial part of the metric in Eq. (1.1.23) and is characterized by the scale factor $a(t)$, which is the explicit function of time and 2nd curvature of the space k. These parameters are obviously determined by the self-gravitating properties of the matter–energy content in the universe. The spatial part of the metric incorporates cosmological principle implying homogeneity and isotropy which provides the kinematics for the geometry of space(spacetime) while we will observe afterwards that Einstein equations provide the dynamics into it through supplying the scale factor $a\,(t)$.

1.1.2.2 Comoving Coordinates and Peculiar Velocities

The coordinates (r, θ, ϕ) form the cosmological rest frame and are known as comoving coordinates. They can be considered constant because the particles remain at rest in these coordinates. The peculiar velocity is the motion of the particles with respect to the comoving coordinates. The peculiar velocities of the galaxies and the supernovae are ignored in cosmology on cosmological scales in the expanding spacetime. The galaxies are envisaged to constitute the fundamental particles of which the cosmic fluid is considered to consist of altogether. As $p\,(a) \propto \frac{1}{a(t)}$, therefore momentum in expanding spacetime is red-shifted and freely moving particles come to rest in comoving coordinates. The physical distance between two points is calculated as the scale factor $a\,(t)$ times the coordinate distance i.e. it is the product of coordinate distance and the cosmic scale factor. The expression inside the bracket(parenthesis) without the scale factor $a\,(t)$ is solely kinematical statement of the geometry of space(spacetime) and demonstrates a hypersurface as it is embedded in four-dimensional geometry of spacetime

$$\frac{1}{1-kr^2} dr^2 + r^2 d\theta^2 + r^2 \sin^2\theta d\phi^2 \tag{1.1.25}$$

and represents the line element of the three-dimensional space with hidden symmetry of being homogeneous and isotropic. It represents three geometries for the corresponding

three values of the curvature term k. The expression multiplied by the scale factor $a(t)$, however indicates an expanding space embedded in a four-dimensional spacetime.

1.1.2.3 The Geometry of Spherical World

For $k = +1$, the hypersurface is

$$\frac{1}{1-r^2}dr^2 + r^2 d\theta^2 + r^2 \sin^2\theta d\phi^2 \tag{1.1.26}$$

and represents a three dimensional sphere embedded in a four dimensional Euclidean space. This space is finite and closed.

1.1.2.4 The Geometry of Hyperbolic World

For $k = -1$, the hypersurface is

$$\frac{1}{1+r^2}dr^2 + r^2 d\theta^2 + r^2 \sin^2\theta d\phi^2 \tag{1.1.27}$$

and demonstrates a three-dimensional hypersphere or hyperbola embedded in a four-dimensional pseud-Euclidean space. This space is open and infinite.

1.1.2.5 The Geometry of Euclidean World

For $k = 0$, the hypersurface is

$$dr^2 + r^2 d\theta^2 + r^2 \sin^2\theta d\phi^2 \tag{1.1.28}$$

and shows a three-dimensional Euclidean flat space. This space is also infinite and open.

1.1.2.6 Friedmann Equations for Cosmological Evolution

Now, using the Einstein field equations, we set to derive the Friedmann's Equations that describe the evolution of the universe by relating the large-scale geometrical characteristics of spacetime to the large-scale distribution of matter–energy and momentum in it. We determine the following Einstein Field Equations for the metric in Eq. (1.1.23)

$$\begin{aligned}
3\left[\left(\tfrac{\dot{a}}{a}\right)^2 + \tfrac{k}{a^2}\right] &= 8\pi G\rho \\
g_{11}\left[2\tfrac{\ddot{a}}{a} + \left(\tfrac{\dot{a}}{a}\right)^2 + \tfrac{k}{a^2}\right] &= -8\pi G p \\
g_{22}\left[2\tfrac{\ddot{a}}{a} + \left(\tfrac{\dot{a}}{a}\right)^2 + \tfrac{k}{a^2}\right] &= -8\pi G p \\
g_{33}\left[2\tfrac{\ddot{a}}{a} + \left(\tfrac{\dot{a}}{a}\right)^2 + \tfrac{k}{a^2}\right] &= -8\pi G p
\end{aligned} \tag{1.1.29}$$

In the first place we derive these equations without incorporating cosmological constant. From Eq. (1.1.29), we can write

$$3\left[\left(\frac{\dot{a}}{a}\right)^2+\frac{k}{a^2}\right]=8\pi G\rho \tag{1.1.30}$$

$$2\frac{\ddot{a}}{a}+\left(\frac{\dot{a}}{a}\right)^2+\frac{k}{a^2}=-8\pi Gp \tag{1.1.31}$$

For other two components expressed in Eq. (1.1.29) the 2nd and 3rd components repeat, therefore we will write only one time from the three components. From Eqs. (1.1.30) and (1.1.31), we derive the Friedmann's Equations and another equation for the conservation of cosmic matter stuff that is how energy density, pressure and cosmic expansion rate interdependently evolve. For this purpose, substituting Eq. (1.1.30) in Eq. (1.1.31) and performing simplification, we get

$$\frac{\ddot{a}}{a}=-\frac{4\pi G}{3}\left(\rho+3p\right) \tag{1.1.32}$$

and from Eq. (1.1.30) which is the time-time component of the Einstein Equations.

$$\left(\frac{\dot{a}}{a}\right)^2+\frac{k}{a^2}=\frac{8\pi G}{3}\rho \tag{1.1.33}$$

for

$$\frac{\dot{a}}{a}=H \tag{1.1.34}$$

which is Hubble parameter and gives expansion rate. The above Eq. (1.1.34) can be written as

$$H^2+\frac{k}{a^2}=\frac{8\pi G}{3}\rho \tag{1.1.35}$$

differentiating Eq. (1.1.34) with respect to time 't'

$$\partial_t H=\partial_t\left(\frac{\dot{a}}{a}\right) \tag{1.1.36}$$

we obtain

$$\dot{H}=\frac{\ddot{a}}{a}-H^2 \tag{1.1.37}$$

which gives

$$\dot{H}+H^2=\frac{\ddot{a}}{a} \tag{1.1.38}$$

Therefore, that Eq. (1.1.32) takes the form in terms of Hubble parameter.

$$\dot{H}+H^2=-\frac{4\pi G}{3}\left(\rho+3p\right) \tag{1.1.39}$$

we can also find

$$\dot{H}=-\frac{4\pi G}{3}\left(\rho+3p\right)-H^2 \tag{1.1.40}$$

From Eq. (1.1.35) $H^2 = \frac{8\pi G}{3}\rho$ with $k = 0$, for flat universe substituting it in Eq. (1.1.40) above

$$\dot{H} = -\frac{4\pi G}{3}(\rho + 3p) - \frac{8\pi G}{3}\rho \tag{1.1.41}$$

which results in

$$\partial_t H = -4\pi G(\rho + p) \tag{1.1.42}$$

Now, differentiating Eq. (1.1.30) with respect to time after shifting the factor 3 on the right side, we have

$$\frac{\dot{a}}{a}\left[2\frac{\ddot{a}}{a} - 2\left(\frac{\dot{a}}{a}\right)^2 - 2\frac{k}{a^2}\right] = \frac{8\pi G}{3}\dot{\rho} \tag{1.1.43}$$

subtracting now Eq. (1.1.30) from Eq. (1.1.31), we obtain

$$2\frac{\ddot{a}}{a} - 2\left(\frac{\dot{a}}{a}\right)^2 - 2\frac{k}{a^2} = -8\pi G(\rho + p) \tag{1.1.44}$$

substituting Eq. (1.1.44) in Eq. (1.1.43), after simplification we have

$$\dot{\rho} + 3\frac{\dot{a}}{a}(\rho + p) = 0 \tag{1.1.45}$$

The cosmological principle compels us to consider a fluid in which inhomogeneities will be considered smoothed out and evolution of the universe shall be considered in the form of perfect fluid characterized by energy density ρ and isotropic pressure p and are contributed by all types of whatever exists and constitutes the universe. Further we consider that the pressure of the fluid depends only on the density neglecting its impact on the cosmic volume and the temperature, i.e., $p = p(\rho)$ which defines a barotropic fluid. In addition, pressure and density bear a linear relationship

$$p \propto \rho \Rightarrow p = w\rho \tag{1.1.46}$$

where $w = \frac{p}{\rho}$ is a dimensionless constant known as equation of state parameter. Substituting Eq. (1.1.46) in Eq. (1.1.45), we have another form of energy conservation for the equation of state parameter w,

$$\frac{\dot{\rho}}{\rho} + 3\frac{\dot{a}}{a}(1 + w) = 0 \tag{1.1.47}$$

Now, Eqs. (1.1.32), (1.1.33), and Eq. (1.1.45) represent two Friedmann's Equations, namely, acceleration and evolution equations, and the equation of conservation, respectively. According to this equation, the evolution of all kinds of matter is determined by the conservation of energy and momentum.

We have to incorporate dark matter and dark energy in the matter–energy content due to the significance of their role in current accelerated expansion and the present

Minkowskian flat geometry of the universe. Therefore, their role is however unavoidable in the evolution of the universe. The solution of FLRW line element gives the Friedman's equations using Einstein field equations with cosmological constant Λ written usually in the form

$$G_{\mu\nu} + \Lambda g_{\mu\nu} = 8\pi T_{\mu\nu} \tag{1.1.48}$$

and Friedmann's equations with cosmological constant Λ can be worked out

$$\frac{\dot{a}^2}{a^2} + \frac{k}{a^2} = \frac{8\pi G}{3}\rho + \frac{\Lambda}{3} \tag{1.1.49}$$

$$\frac{\ddot{a}}{a} = -\frac{4\pi G}{3}(\rho + 3p) + \frac{\Lambda}{3} \tag{1.1.50}$$

The equation of energy conservation can also be calculated from these Friedman equations in the presence of cosmological constant Λ. Multiplying Eq. (1.1.49) with $3a^2$, differentiating it with respect to time and then dividing by $\dot{a}$, we have

$$6\ddot{a} = 8\pi G a\left(2\rho + \frac{a}{\dot{a}}\dot{\rho}\right) + 2\Lambda a \tag{1.1.51}$$

dividing Eq. (1.1.51) by a.

$$6\frac{\ddot{a}}{a} = 8\pi G\left(2\rho + \frac{a}{\dot{a}}\dot{\rho}\right) + 2\Lambda \tag{1.1.52}$$

Substituting now the 2nd Friedman Equation from Eq. (1.1.50) in it, we have

$$6\left(-\frac{4\pi G}{3}(\rho + 3p) + \frac{\Lambda}{3}\right) = 8\pi G\left(2\rho + \frac{a}{\dot{a}}\dot{\rho}\right) + 2\Lambda \tag{1.1.53}$$

after simplification, we obtain Eq. (1.1.45) again. In order to get the relation between energy density ρ, scale factor a and equation of state parameter $w = \frac{p}{\rho}$ we solve Eq. (1.1.45)

$$\dot{\rho} = -3\frac{\dot{a}}{a}(\rho + p) = -3\frac{\dot{a}}{a}\rho\left(1 + \frac{p}{\rho}\right) \tag{1.1.54}$$

$$\Rightarrow \frac{\dot{\rho}}{\rho} = -3\frac{\dot{a}}{a}(1 + w) \tag{1.1.55}$$

where $\frac{p}{\rho} = w$. Integrating Eq. (1.1.55)

$$\int \frac{1}{\rho} d\rho = -3(1 + w)\int \frac{1}{a} da \tag{1.1.56}$$

which gives

$$\rho = a^{-3(1+w)} \tag{1.1.57}$$

Now from 1st Friedmann equation, after simplification and performing integration, we find

$$a = t^{\frac{2}{3(1+w)}} \tag{1.1.58}$$

For $w = -1,\ 0,\ \frac{1}{3}$, we find pressure, energy density and scale factor characterizing the expansion of the universe which demonstrates three phases of the universe namely vacuum dominated, radiation dominated and matter dominated, respectively.

1.1.2.7 Vacuum Domination (Λ-Dominated Era)

For $w = -1$

$$\rho = a^{-3(1+w)} = a^0 \tag{1.1.59}$$

and

$$a = t^{\frac{2}{3(1-1)}} = t^{\infty} \tag{1.1.60}$$

1.1.2.8 Radiation Domination

For $w = \frac{1}{3}$

$$\rho = a^{-3\left(1+\frac{1}{3}\right)} = a^{-4} \tag{1.1.61}$$

and

$$a = t^{\frac{2}{3\left(1+\frac{1}{3}\right)}} = t^{\frac{1}{2}} \tag{1.1.62}$$

1.1.2.9 Matter Domination

For $w = 0$

$$\rho = a^{-3(1+0)} = a^{-3} \tag{1.1.63}$$

and

$$a = t^{\frac{2}{3(1+0)}} = t^{\frac{2}{3}} \tag{1.1.64}$$

1.1.2.10 Critical Density (ρ_c) and Density Parameter (Ω)

Now, considering the cosmic evolution equation that is the first Friedman Eq. (1.1.33) in the presence of cosmological constant $\Lambda = 0$ and $H = \partial_t \ln a$, we relate the curvature of spacetime k and the expansion characterized by the scale factor $a(t)$ to the energy density $\rho(t)$ of the universe and find the expression for the critical density required to keep the current rate of the expansion.

$$H^2 = \frac{8\pi G}{3}\rho - \frac{k}{a^2} \tag{1.1.65}$$

For critical density ρ_c the curvature of spacetime geometry k must vanish, so that Eq. (1.1.65) reduces to the form

$$H^2 = \frac{8\pi G}{3}\rho \tag{1.1.66}$$

where we obtain the expression for critical density

$$\rho = \rho_c = \frac{3H^2}{8\pi G} \tag{1.1.67}$$

From Eq. (1.1.65) dividing both sides by H^2 and rearranging

$$1 = \frac{8\pi G}{3H^2}\rho - \frac{k}{a^2H^2} = \frac{\rho}{\left(\frac{3H^2}{8\pi G}\right)} - \frac{k}{a^2H^2} \tag{1.1.68}$$

where $\frac{3H^2}{8\pi G} = \rho_c$, therefore Eq. (1.1.68) becomes

$$1 = \frac{\rho}{\rho_c} - \frac{k}{a^2H^2} = \Omega - \frac{k}{a^2H^2} \tag{1.1.69}$$

$$\Rightarrow \Omega - 1 = \frac{k}{a^2H^2} \tag{1.1.70}$$

where $\Omega = \frac{\rho}{\rho_c}$ is the density parameter and we can predict in terms of it about the geometry of universe. The local geometry of the universe is investigated by this parameter by observing whether the relative density is smaller than unity, greater than or equal to it. In the Figure-1.1 given below, all three geometries are illustrated based on the unity value of density parameter Ω. Three possible geometries spherical, hyperbolic and Euclidean emerge as the density parameter allows for shifting away, shifting towards unity and having equivalent value to it respectively.

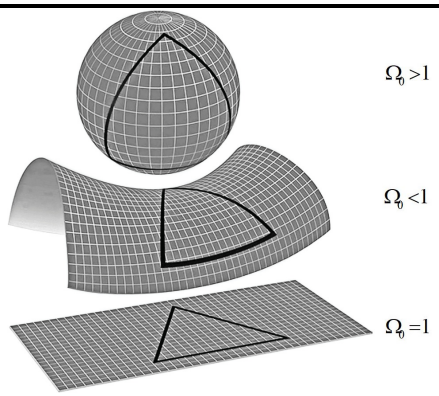

Figure– 1.1: Three spatial geometries: spherical geometry correspnds to $\Omega_0 > 1$ and hyperbolic geometry corresponds to $\Omega_0 < 1$ whereas $\Omega_0 = 1$ represents flat geometry

Now, Eq. (1.1.70) can also be derived from Eq. (1.1.65) in an alternative style. Writing now Eq. (1.1.65) by multiplying and dividing the 1st term on the right side with ρ_c

$$H^2 = \frac{8\pi G\rho}{3}\frac{\rho_c}{\rho_c} - \frac{k}{a^2} \tag{1.1.71}$$

Using the density parameter $\Omega = \frac{\rho}{\rho_c}$, in Eq. (1.1.71) we can write

$$H^2 = \frac{8\pi G}{3}\rho_c\Omega - \frac{k}{a^2} \tag{1.1.72}$$

Now, from the critical density expression in Eq. (1.1.67),

$$\begin{aligned} &\Rightarrow \tfrac{3}{8\pi G} = \tfrac{\rho_c}{H^2} \\ &\Rightarrow \tfrac{8\pi G}{3} = \tfrac{H^2}{\rho_c} \end{aligned} \tag{1.1.73}$$

substituting the 2nd part in Eq. (1.1.73) in Eq. (1.1.72) and using the density parameter, we get

$$H^2 = H^2\Omega - \frac{k}{a^2} \tag{1.1.74}$$

which gives the following form similar to Eq. (1.1.70)

$$\Omega - 1 = \frac{k}{a^2H^2} \tag{1.1.75}$$

Now,

$$\Omega = \frac{\rho}{\rho_c} \tag{1.1.76}$$

is considered decisive in describing the evolution of the universe. The present value of it is denoted by Ω_0 and it gives following three geometries of the universe

$$\Omega_0 > 1 \tag{1.1.77}$$

a closed universe implying the universe with spherical geometry

$$\Omega_0 < 1 \tag{1.1.78}$$

an open universe implying the universe with hyperbolic geometry and

$$\Omega_0 = 1 \tag{1.1.79}$$

a flat universe implying the universe with Euclidean or Minkowskian geometry. The present value of critical density can be calculated with present value of Hubble constant H_0, gravitational constant G and π.

$$\begin{aligned} \rho_{c,0} &= \tfrac{3H_0^2}{8\pi G} \\ &= \tfrac{3(73.8)^2}{8(3.14)\left(6.67\times10^{-11}\right)} \\ &= 1.1 \times 10^{-5}h^2 \end{aligned} \tag{1.1.80}$$

where the scaled Hubble parameter h is defined by $H = 100$ hkm s^{-1} Mpc^{-1}
and
$H^{-1} = 9.778$ h^{-1} Gyr $H^{-1} = 2998\,$h^{-1} Mpc.

1.1.2.11 Particle Horizon

When the scale factor $a(t)$ is multiplied with the co-moving coordinates we get the proper distance. In cosmology, causality is one directional since we just receive photons from the outer world that serves to be self-sufficient approach. The horizon or horizon distance of the universe is defined as the maximum distance that light could have traveled to our reference, i.e., Earth as the time after the beginning of the universe when for the first time it became exposed to electromagnetic radiation (Kolb & Turner, 2018), thus horizon represents the causal distance in the universe.

$$d_H(t) = a(t) \int_0^t \frac{dt'}{a(t')} \tag{1.1.81}$$

such that $d_H(t) \sim H^{-1}(t)$ Particle horizon is defined to be the distance traveled by a photon from the time of big bang up to a certain later time, t. Particle horizon puts limits on communication from the deep inward past.

1.1.2.12 Event Horizon

An event horizon defines such a set of points from which light signals sent at some given time will never be received by an observer in the future. It sets limits on the horizon distance and on communication to the future so that as long as it exists, the size of the causal patch of the universe will be finite.

1.1.2.13 Deceleration Parameter (q_0)

A Taylor series is a series expansion of a function about a given point. We require here a one dimensional Taylor series which is the expansion of a real function $f(x)$ about a point $x = a$ and is given by

$$\begin{aligned} f(t) = f(x)|_{x=a} = f(a) + f'(a)(x-a) + \tfrac{f''(a)}{2!}(x-a)^2 \\ + \tfrac{f'''(a)}{3!}(x-a)^3 + \cdots + \tfrac{f^n(a)}{n!}(x-a)^n + \cdots \end{aligned} \tag{1.1.82}$$

We take the function $f(x) = a(t)$ which is scale factor and find its Taylor series expansion about the present time $t = t_0$

$$\begin{aligned} a(t) = a(t)|_{t=t_0} = a(t_0) + \dot{a}(t_0)(t-t_0) + \tfrac{\ddot{a}(t_0)}{2!}(t-t_0)^2 \\ + \tfrac{(t_0)}{3!}(t-t_0)^3 + \cdots + \tfrac{a^n(t_0)}{n!}(t-t_0)^n + \cdots \end{aligned} \tag{1.1.83}$$

dividing Eq. (1.1.83) by $a(t_0)$ throughout, we have

$$\begin{aligned} \tfrac{a(t)}{a(t_0)} = \tfrac{a(t_0)}{a(t_0)} + \tfrac{\dot{a}(t_0)}{a(t_0)}(t-t_0) + \tfrac{1}{2}\tfrac{\ddot{a}(t_0)}{a(t_0)}(t-t_0)^2 \\ + \tfrac{1}{6}\tfrac{(t_0)}{a(t_0)}(t-t_0)^3 + \cdots + \tfrac{1}{n!}\tfrac{a^n(t_0)}{a(t_0)}(t-t_0)^n + \cdots \end{aligned} \tag{1.1.84}$$

on ignoring the higher terms, we have the following surviving expression

$$\frac{a\left(t\right)}{a\left(t_0\right)} = 1 + \frac{\dot{a}\left(t_0\right)}{a\left(t_0\right)}\left(t - t_0\right) + \frac{1}{2}\frac{\ddot{a}\left(t_0\right)}{a\left(t_0\right)}(t - t_0)^2 \tag{1.1.85}$$

multiplying and dividing now by $\dot{a}\left(t\right)$ with 3rd term of Eq. (1.1.85) on the right hand side:

$$\frac{a\left(t\right)}{a\left(t_0\right)} = 1 + \frac{\dot{a}\left(t_0\right)}{a\left(t_0\right)}\left(t - t_0\right) + \frac{1}{2}\frac{\dot{a}\left(t_0\right)}{a\left(t\right)}\frac{\ddot{a}\left(t_0\right)}{\dot{a}\left(t_0\right)}(t - t_0)^2 \tag{1.1.86}$$

Multiplying again the 3rd term on the right hand side of Eq. (1.1.86) with $\frac{\dot{a}(t_0)}{a(t_0)}$ and its reciprocal $\frac{a(t_0)}{\dot{a}(t_0)}$, we have

$$\frac{a\left(t\right)}{a\left(t_0\right)} = 1 + \frac{\dot{a}\left(t_0\right)}{a\left(t_0\right)}\left(t - t_0\right) + \frac{1}{2}\left(\frac{\dot{a}\left(t_0\right)}{a\left(t_0\right)} \times \frac{a\left(t_0\right)}{\dot{a}\left(t_0\right)}\right)\frac{\dot{a}\left(t_0\right)}{a\left(t\right)}\frac{\ddot{a}\left(t_0\right)}{\dot{a}\left(t_0\right)}(t - t_0)^2 \tag{1.1.87}$$

Putting for $\frac{\dot{a}(t_0)}{a(t_0)} = H_0$, the present value of Hubble parameter and $\frac{a(t_0)\ddot{a}(t_0)}{[\dot{a}(t_0)]^2} = -q_0$, Eq. (1.1.87) reduces to the following:

$$\frac{a\left(t\right)}{a\left(t_0\right)} = 1 + H_0\left(t - t_0\right) + \frac{1}{2}H_0^2\left(-q_0\right)\left(t - t_0\right)^2 \tag{1.1.88}$$

where

$$q_0 = -\frac{a\left(t_0\right)\ddot{a}\left(t_0\right)}{\left[\dot{a}\left(t_0\right)\right]^2} = -\frac{\ddot{a}\left(t_0\right)}{\dot{a}\left(t_0\right)}H_0^{-1} = -\frac{\ddot{a}\left(t_0\right)}{a\left(t_0\right)}H_0^{-2} \tag{1.1.89}$$

is called the deceleration parameter. It tells us that greater the value of q_0, the faster will be speed of deceleration. It can be further related with the acceleration equation

$$\frac{\ddot{a}\left(t\right)}{a\left(t\right)} = -\frac{4\pi G}{3}\left(\rho + 3p\right) \tag{1.1.90}$$

Putting Eq. (1.1.90) in Eq. (1.1.89)

$$q_0 = -\left(-\frac{4\pi G}{3}\left(\rho + 3p\right)\right)H_0^{-2} \tag{1.1.91}$$

with $p = 0$ for a universe having matter domination and present energy density $\rho = \rho_0$ with dividing and multiplying by 2, we possess

$$q_0 = \frac{1}{2}\frac{8\pi G}{3H_0^2}\rho_0 \tag{1.1.92}$$

Now, as the critical density is given by $\rho_c = \frac{3H_0^2}{8\pi G}$ from the 1st Friedmann equation. Therefore Eq. (1.1.92) takes the form

$$q_0 = \frac{1}{2}\left(\frac{1}{\rho_c}\right)\rho_0 = \frac{1}{2}\frac{\rho_0}{\rho_c} = \frac{1}{2}\Omega_0 \tag{1.1.93}$$

The measurement of deceleration parameter q_0 determines how much bigger the universe was in earlier times. The explorations conducted on redshift measures of supernovae of Type $SNIa$ to measure the value of q_0 has shown astoundingly that $q_0 < 0$ at the

present which means that the expansion of the universe is accelerating rather than to be decelerating which affirms that the concept of dark energy must be acknowledged altogether. The accelerated expansion of the universe corresponds to $q_0 < 0$, whereas $q_0 > 0$ corresponds decelerated expansion. It is interesting to notice that for all of these components we have $H > 0$, i.e., an increasing scale factor which gives the expansion rate of the universe. Moreover, to get a better understanding of the properties of each species, it is useful to introduce the deceleration parameter q_0 as

$$\begin{aligned} q_0 &= -\frac{\ddot{a}\dot{a}}{\dot{a}^2} \\ &= -\frac{\ddot{a}}{\dot{a}}\frac{a}{\dot{a}} \\ &= -\frac{\ddot{a}}{\dot{a}}H^{-1} \end{aligned} \tag{1.1.94}$$

such that for both matter-dominated or radiation-dominated universe the expansion is decelerating. It is also interesting to notice that components with $w < -\frac{1}{3}$ give an accelerated expansion. The standard model of cosmology ensues big bang model to the origin of cosmological evolution, however it encounters some issues like flatness problem, horizon problem and monopole problem etc intrinsically related to it. Introduction of inflation in its very early evolution nonetheless, solves these altogether.

1.1.3 Introduction to Cosmic Inflation

Inflation is the period of superluminally accelerated expansion of the universe taking place sometime in the very early history of the universe. It is now a widely accepted paradigm which is described as the monumental outgrowth gushing out during the tiniest fraction of the first second between (10^{-36}–10^{-32}) s. Inflation maintains that just after the occurrence of the big bang, exponential stretching of spacetime geometry took place, i.e., becoming twice in size again and again at least about (60–70) times over before slowing down. Alexei Strobinsky approached the exponentially expanding phase in the early universe by modifying Einstein Field Equations whereas Alan Guth approached the scenario in the realm of particle physics proposing a new picture of the time elapsed in the very small fraction of the first second in the 1980. He suggested that the universe spent its earliest moments growing exponentially faster than it does today. There is a large number of inflation models in hand today but every model has its own limitations to draw the true picture of what happened actually in the early universe.

As the theory of inflation is recognized today, it has myriad models describing inflationary phase in the early universe. From among the heap of these competing models which differ slightly from one to the other, no model can claim a complete and all-embracing

prospectus of what happened actually in the universe so that the fast expansion of or in spacetime takes place. All the energy density that can be adhered to the early exponentially expanding phase of the universe was in the very fabric of spacetime itself despite ti being in the form of radiation or particles. The early accelerating phase can be now best described with de Sitter model with slightly broken time symmetry.

With the creation of spacetime that purports to be the earliest patch of the universe that comes to being would be stretched apart in an incredibly small time span of the order of a tiniest fraction of first second to such a colossally larger size that its geometry and topology would be hardly indiscernible from Euclidean geometry. It will logically ensue similar initial conditions for the energy density to be dispersed at every point in the fabric of spacetime and the same will be the condition of temperature in this early phase. That's why the quantum fluctuations which seed in later times the structure formation in the universe impart the uniform temperature to all parts of the universe thereby resolving the homogeneity problem of the universe. This is because all the quantum fluctuations which cause the observable universe were once causally connected in the deep past of the universe. It might have attained a highest temperature which was within or lesser than the limits of Planck scale (10^{19} GeV). The energy scale mentioned earlier when the inflation comes to an end and transforms into the uniform, very hot, largely dense that is a cooling and expanding state we ascribe to the hot big bang. This will take place for a universe inflating from a lower entropy state to an entropy state at higher level in the panorama of the hot big bang, where the entropy would carry on to get larger as it happens in our observed universe. The point of time in the earliest where the universe can be viewed approximately and hardly as classical is known as the Planck Era. It is thought that prior to this era the universe might be described as the hitherto unsuspected theory of certain quantum nature like quantum gravity etc. This era corresponds to $E_P \sim 10^{19}\,\mathrm{GeV} > E > E_{GUT} \sim 10^{15}\,\mathrm{GeV}$ and the energies, temperature and times of particles are $E_P \sim 10^{19}\,\mathrm{GeV}$, $T_P \sim 10^{32}\,\mathrm{K}$, $t_P \sim 10^{-43}\,\mathrm{s}$, respectively. Grand unified theories describe that at high energies as described above the Electroweak and strong force are unified into a single force and that these interactions bring the particles present into thermal equilibrium Electroweak Era corresponds to phase transitions that occur through spontaneous symmetry breaking (SSB) which can be characterized by the acquisition of certain non-zero values by scalar parameters known as Higgs fields. Until the Higgs field has zero values, symmetry remains observable and spontaneously breaks at the moment the Higgs field becomes non-zero. The idea of phase transitions in the

very early universe suggests the existence of the scalar fields and provides the motivation for considering their effect on the expansion of the universe. The power spectrum of CMB radiation is calculated by measuring the magnitude of temperature variations versus the angular size of hot and cold spots. In order to understand the nature of CMB radiation, the spectrum of a perfect blackbody is utilized which is briefly discussed in Appendix-04. During these measurements, a series of peaks with different strengths and frequencies are determined which conforms to the predictions of inflation theory which confirms that all sound waves were indeed produced at the same moment by inflation. It is believed that inflation might have given rise to sound waves-the waves traveling in the primordial vacuum-like medium with different frequencies after the big bang at 10^{-35} s starting in phase and would have been oscillating in radiation era for 380,000 years. Now, in the acoustic oscillations of the early universe, these must be measurable as power spectrum similar to that of measuring the sound spectrum of a musical instrument. we see how inflationary period is obtained in the perspective of particle physics where a negative pressure is achieved for it to take place. Friedmann solved EFE with $\Lambda = 0$, so

$$\frac{\dot{a}^2}{a^2} + \frac{k}{a^2} = \frac{8\pi G}{3}\rho \tag{1.1.95}$$

$$\frac{\ddot{a}}{a} = -\frac{4\pi G}{3}(\rho + 3p) \tag{1.1.96}$$

Eq. (1.1.96) is known as acceleration equation. The inflationary period, as its definition implies, is the acceleratingly expanding phase of the universe in a very small fraction of first second, as the expansion is characterized by the scale factor a; therefore, we have such an era as

$$\ddot{a} > 0 \tag{1.1.97}$$

thus Inflationary era

$$\Leftrightarrow \ddot{a} > 0 \tag{1.1.98}$$

dividing both sides of Eq. (1.1.98) by scale factor a

$$\frac{\ddot{a}}{a} > 0 \tag{1.1.99}$$

which is the left hand side of Eq. (1.1.96) and Eq. (1.1.99) altogether and imposes the condition on the right hand side of Eq. (1.1.96)

$$\begin{aligned} &-\tfrac{4\pi G}{3}(\rho + 3p) > 0 \\ &\Rightarrow \rho + 3p < 0 \\ &\Rightarrow p < -\tfrac{1}{3}\rho \\ &\Rightarrow \rho > -3p \end{aligned} \tag{1.1.100}$$

For the inflation to occur and set the universe in an accelerating phase, we require the matter to possess an equation of state with negative pressure. The possibility of this negative pressure p which is less than negative of one-third of density is in perspective of symmetry breaking in modern models of particle physics. From

$$\frac{\dot{a}^2}{a^2} + \frac{k}{a^2} = \frac{8\pi G}{3}\rho \tag{1.1.101}$$

$$\dot{a}^2 = \frac{8\pi G}{3}\rho a^2 - k \tag{1.1.102}$$

For $\ddot{a} > o$, the scale factor shall increase faster than $a\,(t) \propto t$ and the term $\frac{8\pi G}{3}\rho a^2$ shall increase during this accelerated era such that the curvature term k will become negligibly small and shall vanish. Inflationary era is also defined by considering the shrinking of Hubble Sphere (Schrödinger, 1985) due to its direct linkage to the horizon problem and because it provides a fundamental role in producing of quantum fluctuations. The shrinking Hubble Sphere is defined as

$$\frac{d\left[(aH)^{-1}\right]}{dt} < 0 \tag{1.1.103}$$

and

$$\frac{d\left[(aH)^{-1}\right]}{dt} = \frac{d\left[\left(a\frac{\dot{a}}{a}\right)^{-1}\right]}{dt} = \frac{d\left[(\dot{a})^{-1}\right]}{dt} = -\frac{\ddot{a}}{a^2} \tag{1.1.104}$$

$$-\frac{\ddot{a}}{a^2} < 0 \tag{1.1.105}$$

which will imply accelerated expansion

$$\ddot{a} > 0 \tag{1.1.106}$$

At $t = 0$, the scale factor a characterizing expansion of the universe comes out to be of a specific value. In Eq. (1.1.101), when $\rho = \rho_\phi$ is of very larger value and the scale factor a dominates over the curvature term k, then we have

$$\left(\frac{\dot{a}}{a}\right)^2 = H^2 = \frac{8\pi G}{3}\rho_\phi \tag{1.1.107}$$

$$a = a_0 e^{Ht} \tag{1.1.108}$$

de Sitter line element is given by

$$ds^2 = -dt^2 + e^{2Ht}\left(dx^2 + dy^2 + dz^2\right) \tag{1.1.109}$$

inflation has to terminate and H is constant, meaning that the de Sitter phase cannot give perfect inflationary era, however for $\frac{\dot{H}}{H^2}$, it would compensate. It would be interesting here to note that Z. G. Lie and Y.S. Piao have shown that the universe we observe today may have emerged from a de Sitter background without having the requirement of a large tunneling in potential and with low energy scale (Liu & Piao, 2013).

1.1.3.1 The Conditions under Which the Inflation Occurs

Shrinking Hubble sphere has been considered as basic definition of inflationary era due to its direct connection to the horizon problem and with mechanism of quantum fluctuation generations (Baumann, 2009, 2018b, 2018a, 2012). differentiating the comoving Hubble radius $(aH)^{-1}$ with respect to time we find the acceleratedly expanding Hubble sphere

$$\partial_t (aH)^{-1} = -\frac{\ddot{a}}{\dot{a}^2} \tag{1.1.110}$$

We see that $-\frac{\ddot{a}}{\dot{a}^2} < 0$, multiplying the inequality by -1 and simplifying, we have

$$\ddot{a} > 0 \tag{1.1.111}$$

which means that shrinking comoving Hubble sphere $(aH)^{-1}$ points toward accelerated expansion $\ddot{a} > 0$. As Hubble sphere H remains nearly constant, in order to understand the meaning of nearly constant we see how its slow roll variation takes place, so taking H as variable

$$\partial_t \left(\frac{1}{aH}\right) = -\frac{\dot{a}H + a\dot{H}}{(aH)^2} = -\frac{1}{a}\left(1 + \frac{\dot{H}}{H^2}\right) \tag{1.1.112}$$

where $\frac{\dot{H}}{H^2} = -\varepsilon$ known as slow roll parameter. It can be inferred that $\frac{\dot{H}}{H^2} < 0$ implies shrinking Hubble sphere.

1.1.3.2 Slow Roll Inflation—The Cosmological Dynamics of Scalar Field

Elementary particles in modern physics are represented by quantum fields and oscillations of these fields are translated as particles. Scalar fields represent spin zero particles in field theories and look like vacuum states because they have same quantum numbers as vacuum. The matter with negative pressure $\rho = -p$ represents physical vacuum-like state where the quantum fluctuations of all types of physical fields exist. These fluctuations can be considered as waves of all possible wavelengths related with physical fields, i.e., wavy physical fields moving freely in all directions. The negative pressure violates the strong energy condition which is necessary for the inflation to occur. To keep things simpler a single scalar field namely inflaton $\phi = \phi(x,t)$ is considered present in the very early universe, as the value of the scalar field depends upon position x in space which assigns potential energy to each field value. It is also dynamical due to being function of time t and has kinetic energy as well, i.e., energy density $\rho(\phi)$ associated with the inflaton ϕ is $\rho(\phi) = \rho_p + \rho_k$. The ratio of the potential and kinetic energy terms of $\phi = \phi(x,t)$, decides the evolution of the universe. The Lagrangian of the scalar inflaton

field ϕ is expressed as the energy difference between its kinetic and potential terms, that is

$$\mathcal{L} = \frac{1}{2}\left(g_{\mu\nu}\partial^2\phi - V(\phi)\right) \tag{1.1.113}$$

It is assumed that the background of FLRW universe has been sourced by energy-momentum associated with the inflaton that dominates the universe in the beginning. We shall observe under what conditions this causes accelerated expansion of the FLRW universe.

$$S = \int d^4x\sqrt{-g}\mathcal{L} = \int d^4x\sqrt{-g}\left[\frac{1}{2}\left(g_{\mu\nu}\partial^2\phi - V(\phi)\right)\right] \tag{1.1.114}$$

The energy-momentum tensor of the inflaton field is given as

$$T_{\mu\nu} = \partial_\mu\phi\partial_\nu\phi - g_{\mu\nu}\mathcal{L} \tag{1.1.115}$$

or

$$T_{\mu\nu} = \partial_\mu\phi\partial_\nu\phi - g_{\mu\nu}\left(\mathcal{L}\right) \tag{1.1.116}$$

which for $\mu = 0$, $\nu = 0$ results as

$$T_{00} = \frac{1}{2}\dot{\phi}^2 + \frac{1}{2a^2}\nabla^2\phi + V(\phi) \tag{1.1.117}$$

and for $\mu = \nu = j$

$$T_{jj} = \frac{1}{2}\dot{\phi}^2 - \frac{1}{6a^2}\nabla^2\phi - V(\phi) \tag{1.1.118}$$

The gradient term vanishes, in the otherwise condition, the pressure gained is much less than the required value to impart impetus for inflation to take place, therefore we obtain the following values for energy density and pressure

$$\rho_\phi = T_{00} = \frac{1}{2}\dot{\phi}^2 + V(\phi) \tag{1.1.119}$$

and

$$p_\phi = T_{jj} = \frac{1}{2}\dot{\phi}^2 - V(\phi) \tag{1.1.120}$$

The condition $V(\phi) >> \dot{\phi}^2$ corresponds to the negative pressure condition $\rho_\phi = -p_\phi$ which means that the potential (vacuum) energy of the inflaton derives inflation. Now using Euler–Lagrange equations

$$\partial^\mu\frac{\delta\left(\sqrt{-g}\mathcal{L}\right)}{\delta\partial^\mu\phi} - \frac{\delta\left(\sqrt{-g}\mathcal{L}\right)}{\delta\phi} = 0 \tag{1.1.121}$$

we can find equation for inflaton field that comes to be

$$\ddot{\phi} + 3\frac{\dot{a}}{a}\dot{\phi} - \frac{1}{a^2(t)}\nabla^2\phi + V_{,\phi}(\phi) = 0 \tag{1.1.122}$$

It can also be computed from the energy density and the pressure terms as given in Eq. (1.1.119) and Eq. (1.1.120) respectively by substituting in the equation of energy conservation i.e.,

$$\frac{d\rho}{dt} + 3H\left(\rho + p\right) = 0 \tag{1.1.123}$$

Eq. (1.1.123) in terms of inflation field ϕ

$$\frac{d\rho_\phi}{dt} + 3H\left(\rho_\phi + p_\phi\right) = 0 \tag{1.1.124}$$

By substituting Eq. (1.1.119) and Eq. (1.1.120) in Eq. (1.1.124), we have

$$\frac{d\left(\frac{1}{2}\dot{\phi}^2 + V(\phi)\right)}{dt} + 3H\left(\frac{1}{2}\dot{\phi}^2 + V(\phi) + \frac{1}{2}\dot{\phi}^2 - V(\phi)\right) = 0 \tag{1.1.125}$$

$$\left(\ddot{\phi} + V'(\phi) + 3H\dot{\phi}\right)\dot{\phi} = 0 \tag{1.1.126}$$

$$\ddot{\phi} + V'(\phi) + 3H\dot{\phi} = 0 \tag{1.1.127}$$

where $V'(\phi) = \frac{dV(\phi)}{d\phi}$ and the term $3H\dot{\phi}$ is known as friction term and offers friction to the inflaton field when it rolls down ($\dot{\phi}$) its potential during expansion of the universe $H = \frac{\dot{a}}{a}$.

1.1.3.3 Conditions of the Slow Roll Inflation

According to the big bang model, that is, the currently accepted model, the universe is about 14 billion years old. At the point of existence the curvature of spacetime was very large or equivalently can be described in other words that space was largely warped and curved where only quantum effects can prevail and the question of time to exist is likely to become absurd. From this state how the very brief era of exponential expansion can be had is fulfilled by assumption of scalar field which take the responsibility of such state mentioned. We know from the 2nd Friedmann's equation which is acceleration equation

$$\frac{\ddot{a}}{a} = -\frac{4\pi G}{3}\left(\rho_\phi + 3p_\phi\right) \tag{1.1.128}$$

For $\ddot{a} > 0$

$$\rho_\phi + 3p_\phi < 0 \Rightarrow p_\phi < \frac{1}{3}\rho_\phi \tag{1.1.129}$$

From Eq. (1.1.119) and Eq. (1.1.120), on substituting for p_ϕ and ρ_ϕ in Eq. (1.1.129), it can be had

$$\left(\frac{1}{2}\dot{\phi}^2 - V(\phi)\right) < -\frac{1}{3}\left(\frac{1}{2}\dot{\phi}^2 + V(\phi)\right) \tag{1.1.130}$$

solving the inequality and keeping in mind that $\dot{\phi}$ is a squared term, we have

$$\dot{\phi}^2 << V(\phi) \tag{1.1.131}$$

which means that the inflaton field is slowly rolling down its potential. Differentiating Eq. (1.1.131) with respect to time, we have

$$\ddot{\phi} < \frac{1}{2}V'(\phi) \tag{1.1.132}$$

Now, from Eq. (1.1.127), we obtain

$$\ddot{\phi} + V'(\phi) = -3H\dot{\phi} \tag{1.1.133}$$

We neglect the acceleration providing term $\ddot{\phi} = \frac{d^2\phi}{dt^2}$ as the inflaton field has to roll now slowly to escape from graceful exit problem in inflation i.e., it is decelerating, so we write

$$V'(\phi) = -3H\dot{\phi} \tag{1.1.134}$$

plugging Eq. (1.1.134) into Eq. (1.1.132), it gives

$$\ddot{\phi} < \frac{1}{2}(-3H\dot{\phi}) \tag{1.1.135}$$

On neglecting the constant factor, it gives

$$\ddot{\phi} << 3H\dot{\phi} \tag{1.1.136}$$

differentiating now Eq. (1.1.134) with respect to time,

$$3\left(\dot{H}\dot{\phi} + H\ddot{\phi}\right) = -V''(\phi)\dot{\phi} \tag{1.1.137}$$

As H remains constant during inflation, therefore $\dot{H}$ vanishes and we have

$$\ddot{\phi} = -\frac{V''(\phi)\dot{\phi}}{3H} \tag{1.1.138}$$

Putting Eq. (1.1.138) in Eq. (1.1.136), we obtain

$$-\frac{V''(\phi)\dot{\phi}}{3H} << 3H\dot{\phi} \tag{1.1.139}$$

It gives

$$V''(\phi) << H^2 \tag{1.1.140}$$

1.1.3.4 Cosmological Parameters for the Slow Roll Inflation

Two slow roll parameters ε and η are defined in terms of Hubble parameter H as well as potential V which quantify slow roll inflation.

$$\varepsilon_H = -\frac{\dot{H}}{H^2} \tag{1.1.141}$$

Using the relation $a(t) \propto e^{-N} \Rightarrow N = \ln a$, it can also be expressed in the form

$$\varepsilon_H = -\frac{d\left(\ln H\right)}{dN} \tag{1.1.142}$$

where N is the number of e-folds and 2nd is defined as

$$\eta_H = -\frac{1}{2}\frac{\ddot{H}}{\dot{H}H} \tag{1.1.143}$$

From 1st Friedmann equation

$$\left(\frac{\dot{a}}{a}\right)^2 - \frac{k}{a^2} = \frac{8\pi G}{3}\rho \tag{1.1.144}$$

For $\rho = \rho_\phi$ and from Eq. (1.1.119) $\rho_\phi = \frac{1}{2}\dot{\phi}^2 + V(\phi)$, as during inflation $V\left(\phi\right) >> \dot{\phi}^2$, so that $\rho_\phi = V(\phi)$ also curvature term k is negligibly small, so that Eq. (1.1.144) takes the form as expressed beneath

$$H^2 = \frac{8\pi G}{3}V\left(\phi\right) \tag{1.1.145}$$

differentiating Eq. (1.1.145) with respect to time and simplifying

$$\dot{H} = \frac{4\pi G}{3H}V'\left(\phi\right)\left(\dot{\phi}\right) \tag{1.1.146}$$

and from Eq. (1.1.134) substituting in Eq. (1.1.146), we have

$$\dot{H} = -4\pi G\left(\dot{\phi}^2\right) \tag{1.1.147}$$

substituting above in Eq. (1.1.141), we have

$$\varepsilon_H = -\frac{\dot{H}}{H^2} = -\frac{-4\pi G\left(\dot{\phi}^2\right)}{H^2} = \frac{4\pi G}{H^2}\dot{\phi}^2 \tag{1.1.148}$$

again from Eq. (1.1.134), we have

$$\dot{\phi} = -\frac{V'(\phi)}{3H} \tag{1.1.149}$$

squaring

$$\dot{\phi}^2 = -\frac{V'^2(\phi)}{9H^2} \tag{1.1.150}$$

substituting in Eq. (1.1.148)

$$\varepsilon_H = \frac{4\pi G}{H^2}\left(-\frac{V'^2(\phi)}{9H^2}\right) = \frac{4\pi G V'^2(\phi)}{9(H^2)^2} \tag{1.1.151}$$

From Eq. (1.1.145) putting for H^2

$$\varepsilon_V = \frac{4\pi G V'^2(\phi)}{9\left(\frac{8\pi G}{3}V(\phi)\right)^2} = \frac{1}{16\pi G}\left(\frac{V'(\phi)}{V(\phi)}\right)^2 = \frac{M_{pl}^2}{2}\left(\frac{V'(\phi)}{V(\phi)}\right)^2 \tag{1.1.152}$$

η_H can also be expressed as

$$\eta_H = -\frac{\ddot{\phi}}{H\dot{\phi}} \tag{1.1.153}$$

$$\eta_V = \frac{1}{8\pi G}\left(\frac{V''(\phi)}{V(\phi)}\right) = M_{pl}^2\left(\frac{V''(\phi)}{V(\phi)}\right) \tag{1.1.154}$$

From Eq. (1.1.145) $H^2 = \frac{8\pi G}{3}V(\phi)$, which gives $8\pi G V(\phi) = 3H^2$ substituting above in Eq. (1.1.154), we have

$$\eta_V = \frac{V''(\phi)}{3H^2} \tag{1.1.155}$$

1.1.3.5 Number of e-Folds

It is usual practice to have the inflation quantified and the quantity which does this is called number of e-fold denoted by N before the inflation ends. As the time goes by N goes on decreasing and becomes zero when inflation ends. It is counted or measured backwards in time from the end of inflation which means that $N = 0$ at the end of inflation grows to maximal value towards the beginning of inflation. It measures the number of times the space grows during inflationary period. The amount of e-folds necessarily required to resolve the big bang problems of Horizon, Flatness, Monopole, Entropy, etc. is $N \sim 60$–75 depending upon the different models and on the reasonable estimation of the observational parameters. To find the number of e-folds between beginning and end of inflation we know that during inflation the scale factor evolves as

$$a(t) = a(t_0)\, e^{Ht} \tag{1.1.156}$$

or

$$a(t) = a(t_0)\, e^{H(t-t_i)} \tag{1.1.157}$$

The factor Ht constitute the number of e-folds denoted by N, i.e.,

$$N = Ht \tag{1.1.158}$$

differentiating Eq. (1.1.158) with respect to time

$$\frac{dN}{dt} = H = \partial_t \ln a \tag{1.1.159}$$

$$N = \int_{t_i}^{t_f} H dt = \int_{t_i}^{t_f} \frac{\dot{a}}{a} dt = \ln\left(\frac{a_{t_f}}{a_{t_i}}\right) \tag{1.1.160}$$

Further, the relation between Hubble parameter H and the number of e-folds N can be written. we have derived earlier the evolution equation for inflaton field that reads

$$\ddot{\phi} + 3H\dot{\phi} + V_{,\phi} = 0 \tag{1.1.161}$$

During slow roll inflation $\ddot{\phi} = 0$, so that Eq. (1.1.161) becomes

$$3H\dot{\phi} + V_{,\phi} = 0 \tag{1.1.162}$$

$$3H\dot{\phi} = -V_{,\phi} \tag{1.1.163}$$

Moreover, during slow roll the Friedmann's 1st equation evolves as with $k = 0$ and $\rho = V(\phi) + \frac{1}{2}\dot{\phi}^2$

$$H^2 = \frac{8\pi G}{3}\left(V(\phi) + \frac{1}{2}\dot{\phi}^2\right) \tag{1.1.164}$$

During slow roll of the inflaton field down to its potential $\left(\dot{\phi}\right)^2 << V(\phi)$ and only $\dot{\phi}$ works, thus Eq. (1.1.164) becomes

$$H^2 = \frac{8\pi G}{3} V(\phi) \tag{1.1.165}$$

Dividing Eq. (1.1.163) by Eq. (1.1.165)

$$\frac{\dot{\phi}}{H} = -\frac{V_{,\phi}}{8\pi G V(\phi)} \tag{1.1.166}$$

Now, from Eq. (1.1.158), we can write because $t = t_f - t_i$, so $t = \int_{t_i}^{t_f} dt$ and with dividing and multiplying by $d\phi$

$$N = Ht = \int_{t_i}^{t_f} H dt = \int_{t_i}^{t_f} H \frac{dt}{d\phi} d\phi \tag{1.1.167}$$

where $\dot{\phi} = \frac{d\phi}{dt}$, Eq. (1.1.167) takes the form

$$N = \int_{\phi_i}^{\phi_f} \frac{H}{\dot{\phi}} d\phi \tag{1.1.168}$$

substituting from Eq. (1.1.166) after inverting

$$N = \int_{\phi_i}^{\phi_f} \left(-\frac{8\pi G V(\phi)}{V_{,\phi}}\right) d\phi = -8\pi G \int_{\phi_i}^{\phi_f} \frac{V(\phi)}{V_{,\phi}} d\phi \tag{1.1.169}$$

or

$$N = 8\pi G \int_{\phi_f}^{\phi_i} \frac{V(\phi)}{V_{,\phi}} d\phi \tag{1.1.170}$$

Thus number of e-folds can be found in terms of potential of the inflaton field. Further slow roll parameter ε_H can be described in terms of number of e-fold N, we know

$$\varepsilon_H = -\frac{\dot{H}}{H^2} = -\frac{1}{H^2}\frac{dH}{dt} = -\frac{1}{H^2}\frac{dH}{dN}\frac{dN}{dt} \tag{1.1.171}$$

$$\varepsilon_H = -\frac{1}{H^2}\frac{d\ln N}{dt} \tag{1.1.172}$$

The paradigm of inflation as the exponential expansion occurring in a tiny fraction of very first second of the cosmic evolution after big bang resolves satisfactorily the problems of flatness, horizon and monopole formation.

1.2 Multifield Inflationary Universe and Spectrum of Curvature Perturbation

Inflation as a phase of exponential cosmological expansion was introduced in the standard big bang model accepted as the origin of the observable universe being implied by the standard FLRW model of cosmology in order to extirpate cosmic conundrums faced by it. It resolved enigmatic issues encountered in the standard model of cosmology. It sets the initial conditions on one hand and explains the growth of cosmic structure on the other hand. There is a large number of inflationary models proposed with single as well as with multiple scalar fields. The inflationary models with more than one light field are referred to as multifield models. Obtaining the inflationary era in multi-field models with two or more fields has comparatively more perspectives, however, the possibly less predictive power of observables (A. D. Linde, 1984a; Starobinsky, 1980; L. A. Kofman & Linde, 1987; Silk & Turner, 1987). A notable difference between single field and multifield models is their sensitivity to respond to the initial conditions. Multi-field models increase the characterization and features of the adiabatic spectrum by creating isocurvature or entropy perturbations that have an impact on anisotropies of the CMB (A. D. Linde, 1984a; L. A. Kofman & Linde, 1987; L. Kofman & Pogosyan, 1988; Lesgourgues, 2000; Polarski & Starobinsky, 1994; Gordon, Wands, Bassett, & Maartens, 2000). The Generation of density perturbations in some multi-field models is treated in such a way as if to decouple it from the dynamics of the inflationary era.

At the end of inflation in a multi-field scenario, primordial density perturbations can be created on account of the inhomogeneous phase of reheating or modulated hybrid inflation if decaying of dark energy turns out to be sensitive to the local values of multi-fields except for inflaton (Dvali, Gruzinov, & Zaldarriaga, 2004; L. Kofman, 2003; Bernardeau, Kofman, & Uzan, 2004). The Curvaton inflation on the other hand traverses its path averse to it (A. Linde & Mukhanov, 1997; Lyth & Wands, 2002; Moroi & Takahashi, 2001) where at some time after inflation a weakly coupled field produces primordial

density perturbations during its decay into radiation. Isocurvature density perturbations are also a relict from the curvaton scenario but the abundance of it differs from thermal equilibrium abundance at the time when curvaton decays (Lyth, Ungarelli, & Wands, 2003). The realization of inflation can also be availed through multi-field scenarios comprising of the double and hybrid models as well. Inflationary theory (Guth, 1981; A. D. Linde, 1982a; Albrecht & Steinhardt, 1982) resolves the flatness, homogeneity, and monopole problems in a very natural way and predicts almost scale-invariant density perturbations, that are found to be consistent with present observational data.

Cosmic inflationary models propound that the early universe underwent an incipient phase of accelerated expansion driven by the dynamics of single, double, or more scalar field fields (Bassett, Tsujikawa, & Wands, 2006; Guth & Kaiser, 2005; Lyth & Liddle, 2009; Baumann, 2009; Guth, Kaiser, & Nomura, 2014; A. Linde, 2015). Inflation also takes the responsibility of seeding all structure formation of the universe we observe today in the form of quantum fluctuations accompanying it in the very tiny fraction of the first second. Quantum fluctuations (Taylor & Berera, 2000; Lyth & Riotto, 1999) are considered to intertwine with the exponential expansion but were frozen in Hubble radius while crossing it and when once inflation comes to end they stretch to cosmological scales and grow out to the present universe (Riotto, 2002).

Inflationary dynamics are backed up by the contribution of generic entropic perturbations to the adiabatic one. In single-field models of inflation, adiabatic perturbations are produced whereas in the multi-field models of inflation, both types of perturbations namely entropic and adiabatic are generated,altogether (Man, 2018). Inflation has, thus become the dominant paradigm for understanding the features of our observable universe. However, single-field inflationary models generally have some fine-tuning problems on the parametric scales, such as the mass and the coupling of the fields, and the value of the fields also, which renders it difficult to realize in a high energy theory realistically.

The working out of remaining part of the problem is organized in the following style: In section 2.2 of chapter 2, the literature in connection with the problem is reviewed whereas the methodology is developed for finding out the expressions for the number of e-folds and spectral index by making use of the formalism as developed by Sasaki and Stewart in section 3.2 of chapter 3. Section 3.2, incorporates subsection 3.2.1 where at first we discuss the validation and justification of the potential under consideration and determine analytically two observables, number of e-folds N and spectral index n_s

corresponding to the value of p. Two significant cases for $p > 2$ and $p = +2, -2$ are taken into consideration to solve analytically. This is accomplished in subsequent subsections 3.2.1.1, 3.2.1.2 and 3.2.1.3 of this section. In section 4.2 of chapter 4, the results and consequences are presented alongside the explanatory and argumentative discussion with summarizing and concluding remarks. It is observed that as the value of p is negative, it is satisfactorily accepted for the considered potential, however positive values lead to the absurd results for a range of number of e-folds and spectral index. For different values of p, we infer the predictions about the number of e-folds and spectral index. However, assigning a value of -2, it gives suitably interpretable results. We have also used Marčenko-Pastur law for the distribution of a large number of scalar fields. The results are tabulated and plotted graphically with remarks on these plots that describe how the relationship is developed for the determined cosmological observables.

1.3 An Nflationary Phase Diagram with Multifield Polynomial Potential

The dynamics of the early universe is explained in the framework of widely accepted Inflationary paradigm, however the microphysical nature of the universe prior to the inflationary era of subPlanckian regime is not completely understood yet. Inflationary cosmology is now about forty years old science where the inflation is recognized with de Sitter phase with slight change in time translational symmetry. Inflation has been very successful so far to account for the observational data. The recent measurements of cosmological parameters imply the convincing evidence that the early universe underwent through de Sitter phase (Aghanim et al., 2020). The theory of inflation was introduced by Alexei Starobinsky, Alan Guth, and was amended by Andrei Linde, Paul Steinhardt and Andreas Albrecht in the '80s of the 20th century (Starobinskii, 1979; Starobinsky, 1980; Guth, 1981; A. D. Linde, 1982c, 1982b, 1982a; A. Linde, 1982; Albrecht & Steinhardt, 1982; S. W. Hawking et al., 1982; Guth & Weinberg, 1983). The simplest models of inflation involve one scalar field, however beyond the standard model in particle physics, in SUGRA, quantum gravity, and in string theories the presence of more than one scalar field is predicted (A. Linde, 1991, 1994). Therefore, consideration of multifield models makes an appropriate choice.

The concept of Nflation based on multiple fields was introduced by Dimopoulos in 2005. He was motivated from phase transitions in particle physics. In this model of inflation, a large number of uncoupled scalar fields are considered to give assistance to each other to derive an inflationary phase. The motivation behind Nflation model was found in the

vacua solutions of string theory and in the mechanism of assisted inflation, where hundreds to thousands of scalar fields can approximately be involved (Dimopoulos, Kachru, McGreevy, & Wacker, 2008). A significant aspect of Nflation is that it does not require sub-Planckian initial conditions to be imposed on scalar fields such as inflaton to resolve the horizon problem. The outcomes from the theory of random matrix are used to calculate the spectrum of masses of the scalar field inflatons in this model and are found to correspond with results from the Marčenko-Pastur law (Easther & McAllister, 2006). The current data shows complete compatibility with Nflationary cosmological parameters like spectral index, tensor to scalar ratio, and non-Gaussianity etc. The Nflation model gives almost similar values of the observables to that of measured by single field models.

The subsequent work scheme in relation to the problem under consideration is organized in the following way: In section 2.3 of chapter 2, latest relevant literature whatever possible in connection with the problem is reviewed in order to come to know the retrospective work rendered regarding the problem. Section 3.3 of chapter 3 is concerned with developing the methodology in order to work out the problem. It consists of subsections 3.3.1 and 3.3.2, where first is concerned with determining the values of the field ϕ by calculating all the changes occurring in it and second discussed the case of different mass scale distribution using Marčenko-Pastur law. we find that the result of values for the fields converge to a single point to be known as critical point which separates between the boundary of slow roll and eternal inflations. The plot for the phase transition diagram of Nflationary phase for the considered multifield potential is drawn here. The distribution of mass-scale factors using Marčenko-Pastur law has been carried out in 3.3.2 where the graphical representation is also displayed to observe the behaviors of these mass scales. In section 4.3, with three subsections 4.3.1, 4.3.2 and 4.3.3 of chapter 4, the results and consequences are presented in relation to the problem. We carry out the study for finding out a bound numerically which mimics the role of a condition on entropy. Moreover, we work out its relationship with the number of fields N that take part in driving the Nflationary phase and its relation to the number of e-folds $\mathcal{N}$ for this model. Subsection 4.3.2 is devoted to the findings related with primordial density perturbations in Nflation, whereas in subsection 4.3.3, we summarize our findings with a discussion of concluding remarks.

We mention here a few precautions for the conventions adopted with regard to this problem of Nflation that is, the letter N is used here to denote the number of fields

rather than e-folding number, whereas the letter $\mathcal{N}$ denotes the number of e-folds and the letter S is reserved to stand for entropy.

1.4 Time Independent Schrödinger Equation Conforming to Wheeler-DeWitt Equation for the Evolution of Early Universe

The development of quantum mechanics and the discovery of expansion of the universe, both occur almost simultaneously. Quantum mechanics comes into play with the regime of cosmology in the context of early universe that comes forth as a result of the big bang implied by the expansion. In 1923, de Broglie hypothesized that all material particles, in addition to radiation might also possess wave-like properties $\lambda = \frac{\hbar}{p}$, $\vec{k} = \frac{\vec{p}}{\hbar}$, ensuing that the nature universally exhibits wave-particle duality (de Broglie, 1925). Afterwards in 1927, Heisenberg proposed the uncertainty principle $\Delta x \Delta p_x \geq \hbar$ which arises from wave-particle duality (W. Heisenberg, n.d.; Wheeler & Zurek, 1983). On the other hand, Bohr's 1928 complementarity principle describes that wave and particle aspects of physical systems are complementary to each other and are required for the complete description of the nature (Bohr, 1928, 1961). Pursuing the idea of matter waves due to de Broglie, Ervin Schrödinger in 1925 formulated wave mechanics, in addition to the earlier formulated matrix mechanics, and later in 1926 he proved that the both are equivalent (Valentini et al., 1992; Schrodinger, 1926; Schrödinger, 1926). His ambitious aim was not less than a unification of the wave mechanics and general theory of relativity; atomic physics and cosmology together would provide an explanation of the discrete structure of matter and elucidate the nature of matter waves (Rüger, 1988).

Quantum mechanics gives a consistent description of matter on the microscopic scales. In classical physics, generally second order partial differential equations are used to describe the laws of motion for particles as well as for waves. Schrödinger equation serves the same purpose in quantum mechanics on the microscopic level (Bransden & Joachain, n.d.). For a particle with mass m, momentum $p \rightarrow -i\hbar\nabla$, kinetic energy operator $-\frac{\hbar^2}{2m}\nabla^2$ and potential energy operator $-\nabla V(r,t)$, the Hamiltonian H of the system is defined as the total energy of a classical system which is the sum of its kinetic and potential energies described as a function of momentum and coordinates that is $H = T + V = -\frac{\hbar^2}{2m}\nabla^2 + V(r,t)$. However, in quantum mechanics total energy cannot be expressed as the sum of these two due to the uncertainty principle, therefore it is measured as a single entity known as wave function $\Psi = \Psi(x_\mu, t)$. Therefore Schrödinger equation is described as $i\hbar\frac{\partial\Psi}{\partial t} = H\Psi$, where $i = \sqrt{-1}$ makes the equation to give

periodic solutions despite being its 1st order in time contrary to the classical physics. It is a linear and 1st order with respect to time and homogeneous wave equation. The Schrödinger equation constitutes the 5th postulate of quantum mechanics and is the basic equation of quantum theory which describes the dynamics of a quantum mechanical system consisting of single particle or as large as the universe itself as a whole. The dependent variable $\Psi = \Psi(x_\mu, t)$ is complex entity called state or wave function and plays the role of probability amplitude. The probability $p(x_\mu, t)$ of determining a particle or physical system at a particular point within the volume V about the point with coordinates x_μ at time t is proportional to $p(x_\mu, t) \propto |\Psi(x_\mu, t)|^2$. It comes in two forms time-dependent Schrödinger wave equation since wave function generally behaves like a wave where the time appears explicitly and describes how the wave function of a particle evolves in time. The solution obtained from time-dependent Schrödinger equation describes the dynamics of a particle in the form of wave function in quantum mechanics in some sense similar to Newton's 2nd law $F = ma$ provides the position of a particle in classical physics. The 2nd type of Schrödinger equation is time-independent, where time dependence is relaxed and it describes, in addition to other things, the allowed level of energies for the particles. These two forms, however are not independent and separate equations rather the time-independent equation can be derived readily from the time-dependent equation.

The Wheeler-DeWitt equation was developed by John Archibald Wheeler (1911-2008) and Bryce DeWitt (1923-2004) in the late 1960s to describe the universe based on the application of quantum theory (Wheeler, 1957; DeWitt, 1967c, 1967b, 1967a). Since that time to the present there is a lot of work engendered due to this equation for the evolution of the universe. The equation is believed to describe the universe quantum mechanically by combining general relativity and quantum mechanics and corresponds to the zero-point energy Schrödinger time-independent equation as the quantum fields are independent of time. Both types of fields gravitational and non-gravitational like scalar fields may be constituent parts of the Hamiltonian in this case. The scale factor, scalar fields and their respective conjugate momenta play the role of dynamical variables for the presence of these fields in the Hamiltonian. DeWitt introduced canonically a quantum theory of gravity which, in addition, to his other work leads to quantum cosmology and the results emphasize to describe the gravitationally bound system of universe as a whole a single quantum state and therefore can be described by a wave function (Misner, 1969; Vilenkin, 1982, 1984, 1983; Hartle & Hawking, 1983; S. W. Hawking, 1984; Atkatz &

Pagels, 1982; Halliwell & Hawking, 1985; Vilenkin, 1986, 1988, 1994).

A wave function describing a classical system behaves like a wave. A spacelike surface is used to predict by the wave function and the classical notion of the system is captured quantum mechanically as a state in a moment of time. The wave function is a functional of three dimensional space and matter fields and the Wheeler-DeWitt theory satisfies it (Bojowald, 2011; Kiefer, 2006; Esposito, 2011). DeWitt equation is analogous to a zero-energy Schrödinger equation of which the Hamiltonian could contain the gravitational field as well as nongravitational fields, as for example, scalar fields. If these fields are present in the Hamiltonian, the dynamical variables are the scale factor and the scalar field as well as their respective conjugate momenta. Quantum fields are independent of time.

The layout for carrying out the subsequent numerical study concerning the problem undertaken in this section 1.4 of the thesis is designed as follows: In section 2.4 of chapter 2, related literature whatever possible be in connection with the problem is reviewed in order to familiarize the retrospective work previously rendered concerning the problem. In section 3.4 and its subsection 3.4.1, the formulation of the problem statement is presented mathematically where the Wheeler-DeWitt equation and the time-independent Schrödinger equation are utilized by using a quantization technique. The Wheeler-DeWitt equation reduces to the time-independent Schrödinger equation with zero energy function which is solved numerically for the evolution of early universe phenomenon which takes place quantum mechanically. By assigning the different values to the parameters, we discuss different cases. Section 4.4 with subsections 4.4.1, 4.4.2, is devoted to the results derived from the numerical solution of the problem. Further simulations as graphical display of the results and discussions are presented to explain the results and tables. In subsection 4.4.1 the results generated with the help of our proposed ANN-LMB solver are come up with describing thoroughly in both numerical as well graphical fashion. The subsection 4.4.2 consists of the conclusions and the remarks summarising the results with conclusion.

1.5 Accelerating Universe Driven by Multifield Tachyon-Quintom Dark Energy

At present, the universe is undergoing accelerated expansion cosmologically as the astrophysical and cosmological observational data within past 20 years from type Ia supernovae (SNe) and other sources confirm it (Riess et al., 1998; Perlmutter, Aldering, et al., 1999; Riess et al., 2001; Tonry et al., 2003; Astier & Pain, 2012; Yang & Gong, 2020; Riess, 2020; Rubin & Heitlauf, 2020; Tegmark et al., 2004; Sherwin et al., 2011; Tu, Hu, & Wang, 2019). Spatial curvature being negligibly small $\Omega_K = 0.001 \pm 0.002$ ascribes a spatially flat (Euclidean) geometry to the observable universe (Aghanim et al., 2020, 2021). The accelerated expansion is thought either due to the presence of some exotic form of matter with negative pressure ($\rho = -p$) dubbed as dark energy that necessitates to modify $T_{\mu\nu}$-the RHS of Einstein Field Equation (EFE) or is explained in the framework of $f(R)$ gravity theories that modify LHS of EFE (Yoo & Watanabe, 2012; Bamba et al., 2012; Ruiz-Lapuente, 2010; M. Li, Li, Wang, & Wang, 2011; Novosyadlyj, Pelykh, Shtanov, & Zhuk, 2015; Wei & Zhang, 2008; Faraoni & Capozziello, 2011).

The equation of state (EoS) parameter $w = \frac{p}{\rho}$ characterizing the dark energy has recent observational constraint to be -1.03 ± 0.03 (Aghanim et al., 2020) that favours dynamical dark energy models to a certain extent (C.-J. Feng, Zhai, & Li, 2020; Zhao et al., 2017; Y.-C. Zhang et al., 2017). It describes the nature of dark energy and determines whether the universe will end as a time-reversed process of the big bang (big crunch) or will expand forever (big freeze). The energy-momentum tensor $T_{\mu\nu}$ in EFE representing the energy density of normal baryonic matter in the universe and succumbs to failure in order to be responsible for the cosmic accelerated expansion on the base of observational evidence (Zhao et al., 2007; Copeland, Sami, & Tsujikawa, 2006).

The cosmological constant Λ, when it is treated as one of the candidates for dark energy, as Einstein predicted (Einstein, 1986; Zeldovich, 1965; Bertotti, Balbinot, Bergia, & Messina, 1990), it encounters the problems of accounting for the extremely fine tuned value related to it at one hand and an extraordinarily small value on the other hand. Due to this the status of Λ does not possess amenability and remains unacceptable, however different proposals to suitably tackle these issues are presented (Armendariz-Picon, Mukhanov, & Steinhardt, 2000; P. J. E. Peebles & Ratra, 2003; Kang, Zhang, Jun, & Zong, 2020; J.-J. Zhang, Lee, & Geng, 2019; P. Peebles & Ratra, 1988; Demirtas, Kim, McAllister, Moritz, & Rios-Tascon, 2021).

A scalar field in the perspective of particle physics or particle cosmology is considered to play a crucial role in spontaneous symmetry breaking (SSB). In these disciplines, they are used to stand for particles of zero spin. They are characterized with specific feature of transforming as an entity or quantity having scalar nature under the transformations of coordinates and evolve as function of time only in a universe that satisfies cosmological principle as implied by general relativity. A very known example of such scalar field is Higgs field which is responsible for symmetry breaking of the electroweak force. Similarly, they are considered as well associated with symmetry breaking such as those of supersymmetry and Grand Unified Theories (GUTs).

The plan to work out the subsequent part of the solution to the problem under consideration is designed in the following way: In section 2.5 of chapter 2, we review the latest relevant literature whatever be possible in relation to the problem for knowing the retrospective work performed in regard to the problem. Section 3.5 of chapter 3 with subsection 3.5.1 is involved with developing the methodology in order to work out the problem. It is devoted to the development of the mathematical machinery for the model. It presents the development of autonomous dynamical system that plays a significant role in investigating and understanding the behavior of such models. We draw plots for evolutionary phases between the multifield scalars and the parameters of the EoS w and dark energy Ω_{DE} as a function of the number of e-folds N. The results and discussion is presented in section 4.5 and its subsections 4.5.1 and 4.5.2, where we perform the analysis of the data and study the stability of the critical points inferring the future evolutionary development of the universe. In the end, a summary with concluding remarks is described in 4.5.2.

1.6 Accelerating Universe in the Framework of $f(R)$ Modified Gravity

The late-time accelerated expansion of the universe poses one of the major challenges to present-day cosmology. The observational data acquired in 1998 by distance measurements of Type Ia Supernovae (SNe Ia) led to the discovery of expansion rate ($H = \partial_t a$) of the universe to be accelerating (Riess et al., 1998; Perlmutter, Aldering, et al., 1999; Riess et al., 2001). The discovery won the 2011 Nobel prize and since that time it is taken prima facie evidence that the universe is undergoing accelerated expansion (Perlmutter, Schmidt, & Riess, 2011; Straumann & Zürich, 2012; Massó, 2012). This unexpected and bizarre behavior was thought due to an exotic form of energy density called dark energy (Huterer & Turner, 1999). Dark energy posits one of the most challenging problems

in cosmology and as well in other relevant disciplines. It possesses immense negative pressure $p = -\rho$ as its defining feature which by nullifying the gravitational interaction causes the rate of cosmic expansion to accelerate (Perlmutter, Turner, & White, 1999). It constitutes almost two-third of the critical density $\rho_c = 3(M_p H_0)^2$ with negligibly small curvature term $\frac{k}{a^2}$ making the universe to have spatially flat i.e., $\Omega_0 \simeq 1$ geometry (Euclidean). From the recent astrophysical and cosmological observational data the density parameters constituting the energy budget of the universe are constrained to be $\Omega_m = 0.315 \pm 0.007$, $\Omega_\Lambda = 0.6889 \pm 0.0056$ (Aghanim et al., 2020; Di Valentino, Melchiorri, & Silk, 2020; Ivanov, Simonović, & Zaldarriaga, 2020). The recent observational data accumulated from multifarious sources approve the compelling evidence in favor of the late time accelerated expansion (To et al., 2021; Benisty & Staicova, 2021; Mazumdar, Mohanty, & Parashari, 2021; Mohayaee, Rameez, & Sarkar, 2021). The simplest candidate to account for the effects of dark energy is considered a positive cosmological constant Λ satisfying the negative pressure $p = -\rho$.

In the framework of general relativity, the standard model of cosmology is accepted with big bang ($t = 0$) as the beginning of the universe (Lemaître, 1931; Kragh & Lambert, 2007; A. A. Friedmann, 2014). Inflation, an early time phase of accelerated expansion taking place just after the big bang, was proposed in 1980 to resolve the cosmological problems faced by the standard big bang model (Starobinsky, 1980; Guth, 1981; Sato, 1981; Kazanas, 1980). Dark energy as a hypothetical cause behind the late accelerated expansion emerged as part of the standard model at the end of the 20th century (Huterer & Turner, 1999). A widely accepted parameterization of the standard big bang cosmology is a six-parameter model known as ΛCDM, which is the best fit of data for recent observations, however, with some challenges being faced in the recent times (Perivolaropoulos & Skara, 2021; Sola, 2016; Turner, 2018; Scannapieco, White, Springel, & Tissera, 2009). The cosmological constant Λ represents dark energy, CDM stands for cold dark matter and 3rd element is the ordinary matter known as baryon matter density. The general theory of relativity as a classical theory cannot be extrapolated back in time beyond $10^{-2}s$ and therefore gives a description of classical cosmology and describes basically the evolution of radiation and matter-dominated eras. On the other hand, the inflationary phase is proposed to have occurred in the early universe prior to the radiation-dominated epoch somewhere in time after the Planck era 10^{-43}s of the big bang to some time between 10^{-32}s and 10^{-35}s which requires the quantum description of cosmology (Guth et al., 2014; Smeenk, 2005; Earman & Mosterin, 1999).

On the other hand, the cosmological accelerated expansion is conjectured established on observational evidence to have commenced since the universe crossed the threshold of the matter-dominated era and got into the Λ-dominated era approximately four billion years earlier. The Λ-domination i.e., dark energy dominated epoch requires new Physics as well. Therefore, to incorporate the early time acceleration i.e., inflation, and the late time acceleration of expansion i.e., dark energy into its framework, it needs modification in it (Ishak, 2019; Spaans, 2013; Carroll, 2004).

These two epochs of accelerated expansion require some exotic form of matter with negative pressure $p < 0$ and could not be justified and explained by the presence of normal matter represented by $T_{\mu\nu}$ with pressure $p \geq 0$. For this purpose, both the gravitational sector i.e., geometry of spacetime, and the matter sector i.e., source term respectively in the equation of general relativity $G_{\mu\nu} = 8\pi T_{\mu\nu}$ are open to modifications which introduce a semiclassical mechanism in the theory (Ye & Piao, 2019; Mughal & Ahmad, 2021; Berti et al., 2015; L. Heisenberg, 2019). Einstein has himself felt the need to modify general relativity at different times: "The theory is based on a separation of the concepts of the gravitational field and matter. While this may be a valid approximation for weak fields, it may presumably be quite inadequate for very high densities of matter. One may not, therefore, assume the validity of the equations for very high densities and it is just possible that in a unified theory there would be no such singularity" (Einstein, 1986, 1950). In the light of considerations mentioned above, general relativity needs to be modified and might not be the final theory of gravitation and the structure of spacetime, despite the remarkable success it has achieved.

The layout of the work plan for the remaining part of the problem is laid out as follows: Section 2.6 of chapter 2 is devoted to review the literature about the problem in order to know historical progress and for finding out the research gap. In Section 3.6 and its subsections, In order to utilize and construct the methods, we review the cosmological dynamics briefly as is described in the context of $f(R)$ modified gravity i.e., Einstein field equation for modified gravity, modified Friedmann equations assuming a spatially flat, isotropic and homogeneous FLRW spacetime. Moreover, construction of the autonomous system with the help of defined dimensionless parameters, finding out the critical points valid for any $m(r)$ and their eigenvalues is the part of this section. Effective Equation of state (EoS) parameter w_{eff} and dark energy EoS w_{DE} parameter are described as well in the methodological section. Section 4.6 with its subsections discuss the results for the problem under consideration by investigating a particular model selected for

study. By using the first and the second derivatives of $f(R)$, the variables m and r are calculated which help out in determining the geometric curve $m(r)$. Critical points, their eigenvalues, and other related parameters are calculated in this section for the autonomous dynamical system. The study of stability analysis for the system is carried out in this section where properties of the eigenvalues and the effective EoS play an important role with regard to the stability analysis. At the end of section 4.6, we give a comprehensive and illustrative discussion on the results with the prospect of some future work. The section also describes a summary with concluding remarks.

CHAPTER-02

REVIEW OF LITERATURE

A considerable attention is focussed in order to carry out the analysis of the proposed problems mathematically due to their extensive applications in various fields of life and different physical phenomena. The detailed literature is reviewed here for the proposed problems in the following sections.

2.1 On the Cosmological Dynamics of Spacetime and Basics of Cosmology

This section is retained for keeping the order of corresponding sections as it is related with introduction section1.1. Therefore, it has no important analytical or numerical results.

2.2 Multifield Inflationary Universe and Spectrum of Curvature Perturbation

On the other hand, when many fields were taken into account, it was found that they can work in coordination with one another to drive a period of inflation with the help of assisted inflation mechanism proposed by Liddle et al. (Liddle, Mazumdar, & Schunck, 1998), although neither of these fields has the ability to sustain the inflationary era separately. The multi-field inflationary models diminish the difficulties encountered by single-field inflationary models and thus can be regarded as an attractive implementation of inflation. The evolution of the universe faces problems when we use a single tachyonic field to derive inflation because in this case, a larger anisotropy is likely to generate. Y.S. Piao et al. studied a model of assisted inflation (Piao, Cai, Zhang, & Zhang, 2002) by taking multi-tachyon fields to derive inflationary period. The spectrum of curvature perturbations of multi-field inflation with a small field potential was studied (Ashoorioon, Krause, & Turzynski, 2009) by I. Ahmad et al. They put to use the Sasaki-Stewart formalism and reached the results which were obtained with the assumption that isocurvature i.e., entropy perturbations can, nonetheless, be neglected. Y.S. Piao investigated that (Piao, 2009) primordial density perturbations can be possibly generated by taking into account the sufficient number of e-folds and with making the

use of decaying speed of sound in a deceleratedly expanding phase of the universe.

R.G. Cai et al. investigated the entropy perturbations in Nflation and computed the entropy corrections to the power spectrum of curvature perturbations (R.-G. Cai, Hu, & Piao, 2009) by finding out a transfer coefficient analytically. He described a correlation function between entropic and curvature perturbations for this purpose. The mechanism of relating the power spectrum to the slow-roll parameters is described in the reference (Stewart & Lyth, 1993; Lieb & Yngvason, 1999) with a detailed account presented there. The evolutionary background equations for the process of driving primordial power spectrum (Wolfson & Brustein, 2018) are given by $\dot{H} = -\frac{\dot{\phi}^2}{2}$ and $\ddot{\phi} = -3H\dot{\phi} - V_{,\phi}(\phi)$.

Avgoustidis et al. investigated (Avgoustidis et al., 2012) the importance of slow-roll corrections in multi-field inflationary models when the evolution of cosmological perturbations in the form of quantum fluctuations takes place. They studied the evolution of curvature and isocurvature perturbations to the next-order in the regime of slow-roll inflation. Cosmological observables are sensitive during the time of reheating phase in multi-field inflationary models. A study was carried out by S.C. Hotinli et al. to examine (Hotinli et al., 2018) the observables during this phase by devising a method that permits the semi-analytic treatment of the effect of perturbative reheating on cosmological perturbations using the technique of sudden decay approximation. They further showed that the rate at which the scalar fields decay into radiation affects the tensor to the scalar ratio "r" and scalar spectral index "n_s". A method was presented by J. Frazer (Frazer, 2014) for deriving an analytical expression of the density function of cosmological observables in multi-field models of inflation using semi-separable potentials. Frazer found that the sharp peak of the density function is very faintly sensitive to the distribution of initial conditions which means inflationary models of multi-field may possess a density function for observables that is peaked sharply.

The dynamics of the exact multi-field scenarios have been investigated in the classical style in the ref. (Clesse, 2011) for the case of the hybrid inflationary model. K. Asadi et al. investigated a multi-field model with two fields to study its reheat phase in order to have some constraints in the parametric space. They found the number of e-folds and the temperature during this era of reheating phase of their model (Asadi & Nozari, 2019). A class of multi-field models based on those fields that decay or get stabilized in a staggered style during inflation was explored by D. Battefeld et al. (Battefeld & Battefeld, 2009). They observed that fields remain flat before marching towards a steep downfall in assisted inflation and when these fields face such a decrease their decay rate

is measured dynamically and transfer of energy takes place to the other degrees of freedom. A further decrease in potential energy caused by decay of the fields contributes to the observables such as spectral index and tensor to scalar ratio. The number of e-folds is bounded for the acceleratedly expanding universe that emerges out from the de Sitter epoch asymptotically (Banks & Fischler, 2003) and multi-field model of dark energy is investigated.

This paper has the purpose of studying the inflationary models with multi-fields in the vista of their number of e-folds, the slow roll parameters, and the spectral indices. The multi-field inflationary models possess some remarkably interesting signatures which single field models digress and have more perspective for the observational evidence which provides motivation to study these models theoretically. The study of inflationary phase driven combinedly by multifields usually by axions sparsely spaced is of great interest. The curvature perturbations are an inflationary relic that seed the structure formation specifically. The investigations of the spectrum of these perturbations in multifield inflation are carried out enormously. For the case of equal and unequal masses by considering the suitable initial conditions these are investigated (Alabidi & Lyth, 2006; Mughal & Ahmad, 2021; Urakawa & Tanaka, 2009, 2009; Easther & McAllister, 2006; Kim & Liddle, 2006; R.-G. Cai, Guo, & Wang, 2015). When we use power-law potential for multifields the spectrum for these perturbations comes out to be redder than it is when a single scalar field is employed (Piao, 2006; Gong, 2007; Olsson, 2007; Thomas & Ward, 2007; Kim & Liddle, 2006, 2007). Spontaneous symmetry breaking naturally gives rise to the small field models with multifields where the fields usually begin with unstable equilibrium about the origin and roll down towards a stable minimum.

2.3 An Nflationary Phase Diagram with Multifield Polynomial Potential

It was investigated based on the vacua solutions in string theory that a large number of axion fields can drive an inflationary phase. These fields working together with following the mechanism of assisted inflation do not violate the Planck scale. (Liddle et al., 1998). A large number of fields with different mass-scales was predicted to possibly participate, see Refs. (Kanti & Olive, 1999; Kaloper & Liddle, 2000). The dynamics of Nflation as studied by Dimopoulos et al. in his pioneering model, it was supposed that all the fields will slow roll together starting with Planck scale values. The Nflation model was generalized for all possible distribution of masses using the outcomes of random matrix theory soon after it (Easther & McAllister, 2006).

Density perturbations in Nflation model are predicted similar to that of single massive scalar field. The study of its dynamics and perturbations was carried out by S.A. Kim et al. (2006). They investigated numerically the random initial conditions to predict tensor to scalar ratio and density perturbations. It was observed that tensor to scalar ratio and scalar spectral index depend completely on the number of e-folds and the parameters of the model respectively. It was further explored that the tensor to scalar ratio is independent of the number of fields driving inflation, masses of the fields and their initial conditions with conclusion that it matches with single field massive inflation (Kim & Liddle, 2006). Nflation model in the framework of IIB compactifications as a large volume scenario was also proposed. The pairwise occurrence of geometric moduli with axion fields play an important role in the development of Nflationary scenario. To construct Nflation model in the perspective of string theory it is necessary to stabilize these moduli (Cicoli, Dutta, & Maharana, 2014).

The multifield axion Nflation can be explored with cosine potential to study its properties. Investigating density perturbations in this model it was found how this is affected when a quadratic potential is used. The tensor to scalar ratio and scalar spectral index tend to lower values, however showing compatibility. A bispectrum non-Gaussianity parameter f_{NL} was calculated whose values for axion decay constant range from 10 to 100 from moderate to larger slightly less than Planck scale respectively (Kim, Liddle, & Seery, 2010). Pole Nflation is also proposed with a large number of open string moduli like D_3-brains in which each brain covers comparatively short distance due to unified motion of it and produces the attractor inflationary phase. The theoretical study for the dynamics of pole Nflation gives the possibility of working together of many fields like inflaton scalars. To embed pole Nflation in the framework of IIB string theoretical set-up using Calabi-Yau manifolds is also investigated (Dias, Frazer, Retolaza, Scalisi, & Westphal, 2019).

The large field models of Nflation are also possible where each field has value of sub-Planckian order i.e., $\sim\leq 10^{-43}s$. The realization of the model is achieved by generalizing the chaotic single-field inflation in the perspective of supergravity (Das & Dutta, 2014). The findings of the scalar spectral index and tensor to scalar ratio match with the predictions of chaotic inflation. The entropy perturbations in Nflation model can be calculated by entropy corrections to the power spectrum of the curvature perturbations P_ζ using δN formalism (R.-G. Cai et al., 2009). A transfer coefficient T^2_{RS} is found analytically for this purpose that develops a correlation function between entropy and

curvature perturbations. When the inflation ends the coefficient is $T_{RS}^2 \sim O(1)$ and both adiabatic and entropy perturbations are of the same order. This also poses that the entropy perturbations can not be ignored. Non-Gaussianities in Nflation can be calculated where the potentials separable, quadratic and Marčenko-Pastur distribution law gives the masses of the fields (Battefeld & Battefeld, 2007; Bartolo, Matarrese, & Riotto, 2002; Bernardeau & Uzan, 2002). A non-linearity parameter f_{NL} is significant which describes the measure of bispectrum by estimating those parameters which define the bispecrums and trispectrums as well for the phase of horizon crossing. The occurrence of larger non-Gaussianities for the fields growing comparatively faster is expected. The contribution of each field can be estimated in this model.

Multiple scalar fields working altogether for the multifield phantom power law can be considered to discuss various features of multifield inflation. We can study such models to find values of parameters with constraints on observables with data from BAO, H_0, and CMB (Ahmad, 2012; Adshead, Easther, & Lim, 2009; Gott & Slepian, 2011). It is interesting feature of Nflation model that the slow roll phase gradually disappears on increasing the number of fields against the square of the ratio of Planck mass M_p to the average of field masses in phase diagram (Ahmad, Piao, & Qiao, 2008, 2009). This ratio can be implemented to find a bound on the entropy of Nflationary phase. The entropy in Nflationary phase can be matched with the entropy of event horizon of a black hole. The two cases bear very close similarity and can be understood with the help of one another. We consider a multifield potential and plot the phase transition diagram for it. We consider first the equal field masses case and afterwards using Marčenko-Pastur law find all likely distribution of field masses. We investigate that de Sitter (dS) entropy is saturated by the number of fields near the critical point. It is viable to study a bound as a condition on entropy related with the number of fields and the number of e-folds.

2.4 Time Independent Schrödinger Equation Conforming to Wheeler-DeWitt Equation for the Evolution of Early Universe

By reducing the Friedmann-Einstein dynamical equations into Schrödinger equation a model of the oscillating universe can be constructed where bounded eigensolutions represent oscillating solutions. Taking into account the cosmic expansion, it can be shown that large scale periodic structure can be traced out when amplitudes and correlation lengths of galaxies are considered (Capozziello, Feoli, & Lambiase, 2000). The evolution of collisionless matter under the influence of gravity can be proposed as a Schrödinger

field obeying the coupled Schrödinger and Poisson equations (Widrow & Kaiser, 1993). The time-independent Schrödinger like equation can be derived form the equation of motion for a single scalar field which drive inflationary phase in FLRW standard cosmology with flat spacetime geometry. The one dimensional bound state solutions produce one exact solution at the lowest for Friedmann equations of standard cosmology (Barbosa-Cendejas & Reyes, 2009). In the recent era artificial neural network are frequently used almost in all disciplines of science (Yalcin & Pekcan, 2020; Bijari, Zare, Veisi, & Bobarshad, 2018). In order to determine numerical solutions for wave equation there exists a voluminous number of analytical methods for example Range-Kutta methods with different orders, Tunneling Probability, WKB Approximation, Euler method and Crank-Nicholson Method with their implicit and explicit forms respectively etc. (Fujiwara, Higuchi, Hosoya, Mishima, & Siino, 1991; Louko & Ruback, 1991; Halliwell & Louko, 1990; Oliveira-Neto, 1998; Fujiwara, Ishihara, & Kodama, 1993; Bouhmadi-Lopez & Moniz, 2005; Moss & Wright, 1984; Gotay & Demaret, 1983; Monerat, Silva, Oliveira-Neto, Ferreira Filho, & Lemos, 2006).

The boundary conditions on the wave functions can describe how the atomic particles tunnel through the potential energy barriers. The tunneling probability for de Sitter universe has been investigated by using numerical approximation. For this purpose, quantization is utilized by considering a radiation-dominated FLRW universe in the presence of positive cosmological constant which leads to the Wheeler-DeWitt equation. For a potential barrier the scale factor as it emerges in the equation, results in the form of Schrödinger equation. The numerical solution can be determined for the resulting Schrödinger equation from Wheeler-DeWitt equation by finding tunneling probability to achieve inflation through de Sitter universe asymptotically for the mean energy of the wave function in the initial state. For some stable constant value of the mean energy of the wave function in initial state, the tunneling probability grows in the presence of cosmological constant. (de Barros et al., 2007). The use of Matlab and C++ language is made for utilizing different methods to numerically inquire into the Schrödinger equation. Employing an effective algorithm of programming language the numerical solution of Schrodinger equation can be sought in one and two dimensions with considering many different cases. Morefully these can both be used for the comparison of results with the use of 4rth order Runge-Kutta method. Such a numerical solution turns out to be of immense interest from the perspective of both physically and pedagogically (Jørgensen, Cardozo, & Thibierge, 2011).

Wheeler DeWitt equation can also be numerically solved for one dimensional Schrödinger equation with vanishing effect of the potential. The equation is solved numerically with positive cosmological constant for the investigation of a universe coming forth form quantum state. Matter field, however are not taken into account in this model which was considered in the Hartle-Hawking no boundary context. Here the interpretation is rendered in terms of internal and external space expansion and using anthropic principle it can be shown that the external space expands and the internal one behaves in the opposite (Ochiai & Sato, 2000).

Our motivation is the attractive numerical solutions of the Schrödinger equation for the evolution of the early universe. Wheeler-DeWitt equation reduces to time-independent Schrödinger equation with zero-energy on the right hand side. There is an increasing trend to use numerical methods to solve partial differential equations and ordinary differential equations with the help of code development in the Matlab. for this purpose feed forward artificial neural network is used for investigating the Schrödinger equation (Amato et al., 2013; Palani, 2010) for a universe with negligible effect of cosmological constant. The FLRW metric is used for minisuper space model of the universe where we reach at Schrödinger equation by the derivation of Wheeler-DeWitt equation and its quantization. The use of local stochastic solvers, active set algorithm (ASA) (Shawagfeh, 1993; Fukushima & Tseng, 2002), interior point algorithm (IPA) (Adler, Resende, Veiga, & Karmarkar, 1989; Lee & Swaminathan, 2005) and sequential quadratic programming (SQP) is made (Raja, 2014). The number of datasets that are to be trained play a very important and key role in determining the predictive quality of artificial neural network as the frequent studies show the evidence. In order to run the mentioned solvers to generate the numerical results the use of Matlab is benefitted. The Levenberg-Marquardt Algorithm(LMA) is used in this paper which is a iterative technique employed to furnish solutions numerically in order to minimize some non-linear functions. As a technique of optimization it is used to solve the large scale non-linear least square problems. This technique can shuffle between Gradient descent method and Gauss-Newton Algorithm depending upon the closeness of current result to local minima and the nature of the result (Lourakis & Argyros, 2005). Backpropagation refers to the mechanism in which the error computed at the output layer of the ANN is transmitted into the hidden layer where all the computations are performed.

- A naive and robust application based on stochastic and computing is developed to investigate the dynamics of the early universe by solving the Schrödinger equation

numerically.

- A framework for computations is efficiently laid out for the Wheeler-DeWitt equation by taking advantage from the structural artificial neural network with the use of algorithm of Levenberg-Marquardt backpropagation.

- The dynamics of the problem is impressively explored by the technique considered for the distinct scenarios on the basis of changing the values of involved parameters and their corresponding cases are developed to illustrate the evolution, dynamics and the related versions.

- Verification and Validating of the considered strategy are endorsed on exact analysis in the sense of accuracy assessments, the studies regression and histograms carried out for the developing system introduced in frequent illustrations graphically and numerically.

2.5 Accelerating Universe Driven by Multifield Tachyon-Quintom Dark Energy

Scalar fields can atone for the fine-tuning and coincidence problems pertaining to Λ and might restitute, as well to the insufficiency of the energy-momentum tensor $T_{\mu\nu}$. To investigate the properties of dark energy, there is a large number of dynamical scalar field models like quintessence, K-essence, phantom, quintom, tachyon, phantom tachyon etc. discussed in the literature, see Refs. (Amendola & Tsujikawa, 2010; Frieman, Turner, & Huterer, 2008; Sahni & Starobinsky, 2006; M. Li et al., 2011; Sami, 2007; Yoo & Watanabe, 2012; Rong-Gen, 2007; Bahamonde et al., 2018; M. Li, Li, Wang, & Wang, 2013). Quintessence is a scalar field minimally coupled to gravity and evolves dynamically with a canonical kinetic energy term in its Lagrangian $\mathcal{L}$ and has EoS parameter $w > -1$, see Refs.(Oks, 2021; Ratra & Peebles, 1988; Steinhardt, 2003; Guo, Ohta, & Zhang, 2005, 2007; Qi, Zhang, & Liu, 2016; Hughes, 2019; Zlatev, Wang, & Steinhardt, 1999; Barreiro, Copeland, & Nunes, 2000). K-essence arises from a non-canonical kinetic energy term, see Refs. (Barreiro et al., 2000; Chiba, Okabe, & Yamaguchi, 2000; Armendariz-Picon et al., 2000; Armendariz-Picon, Damour, & Mukhanov, 1999; S. Li & Liddle, 2012; S. D. Odintsov & Oikonomou, 2019; Armendariz-Picon, Mukhanov, & Steinhardt, 2001; Rendall, 2006; Rong-Jia & Xiang-Ting, 2009; Sur & Das, 2009; Scherrer, 2004; González-Dıaz, 2004). All the models with negative kinetic energy term can

be considered its subcases. On the other hand Phantom has non-canonical kinetic energy term in its Lagrangian $\mathcal{L}$ and has EoS parameter $w < -1$. Introduction of negative energies is, however a significant issue in these fields, see Refs. (Sami & Toporensky, 2004; Cline, Jeon, & Moore, 2004; Sami, Toporensky, Tretjakov, & Tsujikawa, 2005; Vikman, 2005; Kujat, Scherrer, & Sen, 2006; Wen-Fu, Zheng-Wei, & Bin, 2010; Caldwell, Kamionkowski, & Weinberg, 2003; Hu, 2005; Carroll, Hoffman, & Trodden, 2003; Guo & Zhang, 2005; Ludwick, 2017; Caldwell et al., 2003; González-Díaz, 2003; Fang, Tu, Huang, & Shu, 2016; Scherrer, 2005).

Neither quintessence nor phantom individually is able to cross over -1, however the unified model developed from the two, known as quintom, see Refs. (Štefančić, 2005; B. Feng, Wang, & Zhang, 2005; Riess et al., 2004) fulfils the requirement. In quintom models EoS parameter w transitions from $w > -1$ to $w < -1$ as the constraint on dark energy favors it mildly, see Refs. (Guo, Piao, Zhang, & Zhang, 2005; X.-F. Zhang, Li, Piao, & Zhang, 2006; Y.-F. Cai, Li, Lu, et al., 2007; B. Feng, Li, Piao, & Zhang, 2006; Guo, Piao, Zhang, & Zhang, 2006; Y.-F. Cai, Li, Piao, & Zhang, 2007; Y.-F. Cai, Qiu, Zhang, Piao, & Li, 2007; Mishra & Chakraborty, 2018; Panpanich, Burikham, Ponglertsakul, & Tannukij, 2021). Recently a model is proposed to resolve Hubble tension using quintom dark energy (Panpanich et al., 2021). In its earliest emergence, tachyon field surfaced in string theory and was used in cosmology afterwards to drive inflationary phase in the early universe, see Refs. (Mazumdar, Panda, & Perez-Lorenzana, 2001; Piao et al., 2002; Sami, Chingangbam, & Qureshi, 2002; Guo, Piao, Cai, & Zhang, 2003; L. Kofman & Linde, 2002; Fairbairn & Tytgat, 2002; X.-z. Li, Liu, & Hao, 2002; Sen, 2005). The governing equation for tachyon can be worked out from equation of relativistic mass in special relativity

$$m = \frac{m_0}{\sqrt{(-1)\,\frac{v^2}{c^2} - 1}} = \frac{m_0}{\sqrt{(-1)}} \frac{1}{\sqrt{\frac{v^2}{c^2} - 1}} \tag{2.5.1}$$

Multiplying both sides by c^2

$$mc^2 = \frac{m_0 c^2}{\sqrt{(-1)\,\frac{v^2}{c^2} - 1}} = \frac{m_0}{\sqrt{(-1)}} \frac{c^2}{\sqrt{\frac{v^2}{c^2} - 1}} \tag{2.5.2}$$

From mass-energy equivalence relation $E = mc^2$

$$E_{Tach} = \frac{c^2 \xi}{\sqrt{\frac{v^2}{c^2} - 1}} \tag{2.5.3}$$

where

$$\xi = \frac{m_0}{\sqrt{(-1)}} \tag{2.5.4}$$

Eq. (2.5.2) is the dictating energy equation of the motion of tachyon and describes it in terms of energy. From Eq. (2.5.3) we see that the energy of the tachyon will be negative i.e. imaginary for the mass being real whereas if the mass becomes negative i.e. imaginary, then energy of the tachyon will turn out to be real. It is important to note that it has not been until now possible to produce such a particle in the laboratory and its existence could not be proven experimentally to this day. It stood up for the candidate of dark energy after the expansion was proven to be accelerating, see Refs. (Padmanabhan, 2002; Gibbons, 2002; Hao & Li, 2002; Gibbons, 2003; Novosyadlyj, 2013; Abramo & Finelli, 2003; Bagla, Jassal, & Padmanabhan, 2003; Gorini, Kamenshchik, Moschella, & Pasquier, 2004; Sami, Chingangbam, & Qureshi, 2004; Calcagni & Liddle, 2006; Copeland, Garousi, Sami, & Tsujikawa, 2005; Shao, Gui, & Wang, 2007; Shao & Gui, 2008; Martins & Moucherek, 2016; Singh, Sangwan, & Jassal, 2019; Shi, Piao, & Qiao, 2009; Frolov, Kofman, & Starobinsky, 2002; Feinstein, 2002; Aguirregabiria & Lazkoz, 2004; Guo & Zhang, 2004). It is, nonetheless, significant to note that tachyonic dark energy models require fine tuning larger than quintessence models. Tachyon field with negative kinetic energy term represents its phantom version, see Refs. (Hao & Li, 2003; Sheykhi, Movahed, & Ebrahimi, 2012) with EoS parameter $w < -1$ as the data mildly favours it. The Lagrangian density $\mathcal{L}$ for tachyon field and its phantom version is written as $\mathcal{L} = -V(\phi)\sqrt{1+\varepsilon g^{\mu\nu}\partial_\mu\partial^\nu}$ where $\varepsilon = +1$ is for tachyon and $\varepsilon = -1$ for phantom tachyon.

Although, recent data-fit gives specific trend to EoS w, however it does not determine exactly whether the dark energy is quintessence, phantom, quintom or tachyon. Tachyon models can effectively illustrate the dark energy and have efficient viability. A quintom version of tachyon field was investigated in Ref. (Shi et al., 2009), where two scalar fields namely tachyon and phantom-tachyon represent dark energy that drive the late time accelerated expansion. These scalar fields easily allow EoS parameter to change from $w > -1$ to $w < -1$ that is it crosses phantom divide. Theoretically, It is possible that the dark energy consists of more than one scalar field. This allows one to consider N scalar fields by adapting to the Lagrangian $\mathcal{L}$ for N scalar fields $\mathcal{L}_{\xi_1,.....\xi_N}$. Being motivated by the interesting prospects of tachyon-quintom dark energy, we consider a multi-field model incorporating tachyon and phantom tachyon fields to explain the late time acceleration within the context of flat FLRW spacetime in the background. Using inverse square potentials we study the dynamics of the model in phase space.

Further, the value attached to the cosmological constant Λ for dark energy is in conflict with the predicted value in the context of quantum field theory treated as vacuum energy (Padmanabhan, 2003; Sahni & Starobinsky, 2000; Sola, 2013; Volovik, 2005; Weinberg, 2001) and must be theoretically remedied. At the earliest, to derive inflation in the very early universe, the quantum corrections to energy-momentum tensor $T_{\mu\nu}$ are well known in the community of cosmologists (Starobinsky, 1980). Further, to meet this purpose, the modifications rendered in the matter sector $T_{\mu\nu}$ with the addition of time-varying canonical and non-canonical scalar fields are famously known as quintessence and k-essence respectively. In addition to these, there are scalar fields originating from these with slightly different cosmological aspects and with some other proposals. See for reviews (Copeland et al., 2006; Y.-C. Zhang et al., 2017; Bamba et al., 2012; Bahamonde et al., 2018; Yoo & Watanabe, 2012).

The modification in the gravitational sector is studied under extended theories of gravity (ETGs) resting on extensions and corrections of general relativity. In ETGs, either geometry is non-minimally coupled to some scalar field, or there arise derivatives of the metric higher than second-order which constitute scalar-tensor and higher-order curvature theories of gravity respectively (Faraoni & Capozziello, 2011). The latter approach is largely discussed in the literature where higher-order derivatives of the metric are obtained to explain the early time and the late time accelerated expansion of the universe. The significant point of these theories is that they do not bother to modify the matter sector by proposing any exotic form, instead, by modifying the geometry of spacetime these accommodate both phenomena of the early time accelerated expansion and the late time accelerated expansion inclusively. One of these is the simplest case of $f(R)$ gravity, where the Lagrangian density $\mathcal{L}$ is the arbitrary non-linear function f of the Ricci scalar invariant R (Buchdahl, 1970; Brejzman, Gurovich, & Sokolov, 1970; Bergmann, 1968; Ruzmaikina & Ruzmaikin, 1970; De Felice & Tsujikawa, 2010). $f(R)$ gravity models offer very interesting astrophysical and cosmological applications without exotic matter. This feature renders the gravity-modified models very attractive.

In general relativity, Ricci scalar R in the Lagrangian $\mathcal{L}$ of Einstein-Hilbert action yields the second-order equations of motion that describe the curvature of spacetime geometry as the source of gravity, however, the modified gravity equations consist of higher-order derivative terms e.g. R^2, $R\Box R$ and $R\Box^2 R$ in the Lagrangian $\mathcal{L}$ produce 4th, 6th and 8th

order equations of motion respectively (Ruzmaikina & Ruzmaikin, 1970; Amendola et al., 1993; Gottlober, Schmidt, & Starobinsky, 1990; Mayer & Schmidt, 1993). However, any term with 2nd order derivative is consistent with a scalar field, therefore 4th, 6th and 8th order derivative terms are equivalent to gravity-induced by Lagrangian density $\mathcal{L}$ in Einstein-Hilbert action i.e., R in addition to one, two, and three scalar fields respectively. It means that the extra degrees of freedom in $f(R)$ can be treated as a scalar field. This helps us in expressing the effective energy-momentum tensor modified form and the corresponding dynamics can be accordingly described. This is how the Jordan frame is rendered equivalent to Einstein frame (Gottlober et al., 1990; Schmidt, 1990; Capozziello, Carloni, & Troisi, 2003). The Jordan frame includes a scalar field that is non minimally coupled to gravity through Ricci scalar R. The case of $f(R)$ in the Lagrangian $\mathcal{L}$ of Einstein-Hilbert action produces 4th order equations of motion. In general, there are three approaches in the context of $f(R)$ gravity, we can derive modified field equations for it. In the first approach, the action is varied with respect to the metric tensor $g_{\mu\nu}$ and the affine connection $\Gamma^{\gamma}_{\alpha\beta}$ depends upon it. This approach is known as standard metric formalism. In the 2nd approach, introduced by Einstein himself (Faraoni & Capozziello, 2011; Einstein, 1925; Capozziello, De Laurentis, & Faraoni, 2009), however, known after Palatini as Palatini formalism, the torsion-free affine connection $\Gamma^{\gamma}_{\alpha\beta}$ is independent of the metric tensor $g_{\mu\nu}$, therefore both, the metric tensor $g_{\mu\nu}$ and the affine connection $\Gamma^{\gamma}_{\alpha\beta}$ are dealt as independent variables and the action is varied with respect to both. In the Palatini formalism, it is assumed that matter action is independent of the affine connection, however when this assumption is relaxed, we get a third approach known as metric-affine $f(R)$ (Capozziello et al., 2009; Clifton, Ferreira, Padilla, & Skordis, 2012; Nojiri et al., 2017b; Sotiriou, 2006; Sotiriou & Liberati, 2007; Ferraro, 2012). Theories of Palatini and the standard metric $f(R)$ are equivalent to Scalar-tensor theories where the role of $f_{,R}$ derivative as Brans-Dicke scalar is central. It means that in Brans-Dicke theories the vanishing of parameter makes the $f(R)$ models equivalent to Scalar-Tensor theories. We will use here the standard metric formalism in the Jordan frame without requiring it to convert back to the Einstein frame. To understand deep down into the theory of $f(R)$ and its applications one can find fascinating and detailed literature in the following and the references therein (Nojiri & Odintsov, 2007; Sotiriou & Faraoni, 2010; Starobinsky, 2007; S. D. Odintsov & Oikonomou, 2020; Nojiri, Odintsov, & Oikonomou, 2017a; S. Odintsov & Oikonomou, 2019; Nojiri & Odintsov, 2011; S. Odintsov & Oikonomou, 2018; Capozziello, Mantica, & Molinari, 2019; Capozziello & De Laurentis, 2011; Capozziello, Nojiri, & Odintsov,

2018; Bamba et al., 2012; Mughal, Ahmad, & García Guirao, 2021; Bekov, Myrzakulov, Myrzakulov, & Sáez-Chillón Gómez, 2020; Nojiri & Odintsov, 2006; Bamba & Odintsov, 2015; Vasilev, Bouhmadi-López, & Martín-Moruno, 2021; Amendola & Tsujikawa, 2010; Capozziello & De Laurentis, 2015).

The models with Lagrangian density $\mathcal{L} = \sqrt{-g}\left(R + \frac{1}{R}\right)$, in their action, were ruled out because they do not fulfill the constraints in the solar system i.e., local gravity constraints were violated which make these models non-viable. In fact, in the beginning, inverse Ricci scalar invariant term $\frac{1}{R}$ was added to the Lagrangian density $\mathcal{L}$ in the Einstein-Hilbert action with a view that as long as the universe expands, the added inverse term might dominate and cause the late-time acceleration. However, it was shown that adding a term $\sqrt{-g}R^n$, where $n > 1$ in Einstein-Hilbert action leads to the modification of cosmology in the early universe where de Sitter era can be achieved. On the other hand, for $n < 0$, it gives self-accelerating vacuum solutions in the late universe which can explain the accelerated expansion. Similarly, an earlier presented model having Lagrangian density $\mathcal{L} = \sqrt{-g}\left(R + \frac{R^2}{6M^2}\right)$ does not show viability for the late time cosmological behavior of accelerated expansion of the universe, whereas for the early time accelerated expansion i.e., inflation it is viable (Amendola, Gannouji, Polarski, & Tsujikawa, 2007).

In perspective of this problem, we try to understand the late-time accelerated expansion of the universe and seek its explanation through carrying out study of a viable $f(R)$ model following the dynamical system approach. The stability of the cosmic structure as a dynamical system with its accelerated expansion is sought by analyzing it. In the cosmological context, there is a growing concern with $f(R)$ modified gravity models due to their simplicity, novel features, and viability. The study of these models for the late time accelerated expansion by autonomous dynamical system approach is a very robust technique which is applied frequently (Amendola et al., 2007; Shah & Samanta, 2019). In particular, by constructing a dynamical system of partial differential equations that is autonomous, we perform a stability analysis of the system through critical points and their eigenvalues and find the related parameters describing the densities of matter and effective dark energy, etc. The plots for the eigenvalues are drawn which throw light graphically on the late time behavior of the universe through the stability of the points and eigenvalues. The aspects we discuss are extremely relevant to the late time acceleration in the $f(R)$ perspective in connection with equation of state (EoS) parameter w.

CHAPTER-03

RESEARCH METHODOLOGY

3.1 On the Cosmological Dynamics of Spacetime and Basics of Cosmology

This section is retained for keeping the order of corresponding sections as it is related with introduction section1.1. Therefore, it does not contain any significant analytical and numerical results.

3.2 Multifield Inflationary Universe and Spectrum of Curvature Perturbation

We consider a small field potential consisting of multifield scalars and study its inflationary dynamics analytically as the universe evolves in its earliest phases. Afterward, we calculate the spectrum of curvature perturbation by assigning suitable values to the parameter p.

3.2.1 Driving Multifield Inflation due to Small Field Potential and the Spectrum of Curvature Perturbation

3.2.1.1 Validation and Justification of the Multifield Potential

We consider the following potential for investigation the problem

$$\sum_i V_i(\phi_i) = \sum_i \Lambda_i \left[1 - \left(\frac{\phi_i}{\mu_i}\right)^{-p}\right] \tag{3.2.1}$$

The subscript "i" in the potential stands for the ith field and for the entities related to it. In addition, Λ_i is the mass scale and μ_i is a parameter and these describe the height and tilt of the potential of the ith field respectively. It has p and μ_i as free parameters. The potential given in Eq. (3.2.1) is the multifield version of the brane inflationary potential $V(\phi) = \Lambda\left(1 - \left(\frac{\phi}{\mu}\right)^{-p}\right)$ used in brane model of inflation. In brane model, the inflation is proposed to engender by motion of branes in the extra dimensions. The effective Lagrangian $\mathcal{L}$ for such a system comes out to be $\mathcal{L} = -\frac{1}{2}(\partial_t\phi)^2 - \frac{2T_3 r_o^4}{r_{UV}^4}\left(1 - \frac{T_3^2 r_o^4}{N\phi^4}\right)$ where T_3 is the tension of a light brane, r is related to the distance between two branes. Other parameters are similarly defined for the system. The effective lagrangian for the brane

inflation can be worked out to have the form of the potential expressed in Eq. (3.2.1) for the case $i = 1$ with an arbitrary value of p (Martin, Ringeval, & Vennin, 2014). For $i = 1$, it is studied frequently in the literature e.g. see the Ref. (Martin et al., 2014) and the references furnished therein in the corresponding section. The potential can be considered a generalized version of the small field models of inflation as discussed in the references (Martin et al., 2014; Freese, Frieman, & Olinto, 1990; Knox & Olinto, 1993; Kinney & Mahanthappa, 1996; Covi, 2001; Tzirakis & Kinney, 2007; Kawasaki & Yamaguchi, 2002) for the negative values of p. Various potentials bearing resemblance to such models in many aspects are also used in the reference (Kinney & Riotto, 1999, 1998; Boubekeur & Lyth, 2005). When plotted it demonstrates an increasing function of the field, therefore the inflation field advances from the right direction to the left. The field would disappear for $\phi = \mu$ or $\frac{\phi}{\mu} = 1$ and it might, therefore work in the domain $\frac{\phi}{\mu} > 1$. The study of this model, hence should be carried out only in the region lying in the limit $\frac{\phi}{\mu} > 1$. In addition, the brane inflation conforms to the condition $\frac{\mu}{M_{pl}} << 1$ and occurs under it. Below in Figure-3.1 drawn on the same lines as given in Reference (Martin et al., 2014), the potential and its logarithm are plotted for $i = 1$ and $p = 2$. The dynamics

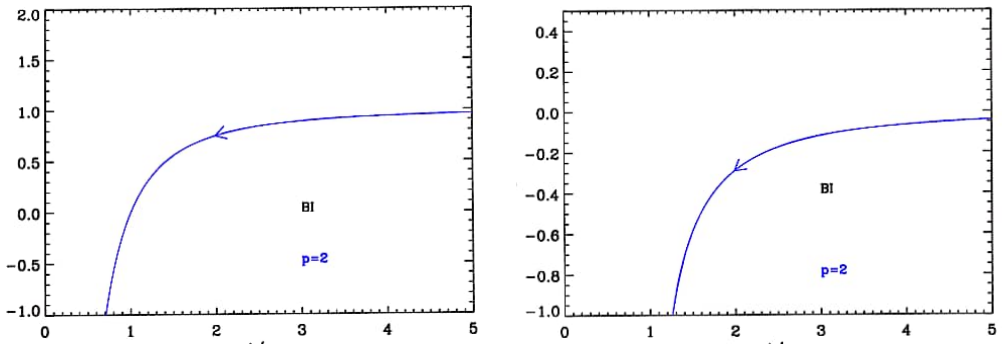

(a) **(b)**

Figure– 3.1: Plot of the potential of brane inflationary scenario, it depicts potential plot at the left and its logarithm at the right as a function of $\frac{\phi}{\mu}$ for $p = 2$

in the background of a multifield model of inflation can be realized and understood by describing in terms of dimensionless slow roll parameters ε, $\eta_{\|}$ and $\eta_{\perp}$ similar to the situation of a single field models, however the second slow roll parameter η is required to modify in the scenario due multifield inflation likely to be confronted with eta problem. The parameter ε is the first slow roll parameter and $\eta_{\|}$ and $\eta_{\perp}$ give the slow roll rate of

the fields along and perpendicular direction of the motion of the fields. The parameter $\eta_\perp$ gives the turn rate of the fields along the perpendicular direction of motion. The slow roll would last as long as $\varepsilon << 1$ and $\left|\eta_\parallel\right| << 1$, whereas the parameter $\eta_\perp$ gives the turn rate of the fields perpendicular to the motion of the fields. Comparatively larger value of $\eta_\perp$ may pose interesting phenomena to the multifield scenario, however it does not imply that it will necessarily violate the slow roll conditions and will destroy it altogether as is described for multifield inflation. It is also manifest from the slow roll parameters defined for multifield inflation that Hubble parameter H and the field derivative $\partial_t\phi$ would grow gradually. We can discuss two cases that make enough sense for the constraints applied on p.

3.2.1.2 Analytical Analysis For the Case Related to $p > 2$

Let us we consider the potential that is usually used for driving the inflationary phase in brane cosmology with $p > 2$. This potential was found to be relevant and useful in a large number of multifaceted physical situations (Cervantes-Cota & Dehnen, 1995; Gong, 2006; Lazarides & Vamvasakis, 2007; Bauer & Demir, 2011; Barvinsky, 2011; Kallosh & Linde, 2010). It is also important to note that this model is sometimes considered as a realistic version of small field inflation with adapting the value of p = 2. The potential we consider here is with $-p$. This is the profile representing small field inflation and can be regarded as a lowest order of Taylor series expansion of an arbitrary potential about the origin of maxima and minima of it. A generalized version of this potential is given in Eq. (3.2.1) with uncoupled fields. The slow roll potential parameters are given $\varepsilon_V = \frac{1}{2}\sum_i \left(\frac{pM_p}{\frac{\phi_i}{\mu_i^2}\left[\left(\frac{\phi_i}{\mu_i}\right)^p - 1\right]} \right)^2$ and $\eta_V = -\frac{p(p+1)}{3H^2}\sum_i \frac{\Lambda_i}{\mu_i}\left(\frac{\phi_i}{\mu_i}\right)^{-(p+2)}$. The equation of motion of the scalar field ϕ_i when it slow-rolls, is

$$\ddot{\phi}_i + 3H\dot{\phi}_i + V_i'\left(\phi_i\right) = 0 \tag{3.2.2}$$

with $\ddot{\phi}_i \approx 0$ during slow-roll phase, we have from above

$$\dot{\phi}_i = -\frac{V'_i\left(\phi_i\right)}{3H} \tag{3.2.3}$$

now for the number of e-folds using above we have

$$N = \int_{t_i}^{t_f} H dt = -M_p^{-2}\sum_i \int_{\phi_i^s}^{\phi_i^e} \frac{V_i}{V_i'} d\phi_i \tag{3.2.4}$$

here ϕ_i^s represents the point of time when the corresponding perturbations crosses the horizon and ϕ_i^e, the upper limit in the integral corresponds to the phase when the

inflationary phase terminates. It is notable, however that $\phi_i^s < \phi_i^e$ in general. For further evaluation of the Eq. (3.2.4), we have from Eq. (3.2.1)

$$\sum_i V'_i(\phi_i) = \sum_i \frac{\Lambda_i}{\mu_i}\left(\frac{\phi_i}{\mu_i}\right)^{-(p+1)} = p\sum_i \frac{\Lambda_i}{\mu_i}\left(\frac{\phi_i}{\mu_i}\right)^{-(p+1)} \tag{3.2.5}$$

further,

$$\frac{\sum_i V_i(\phi_i)}{\sum_i V'_i(\phi_i)} = \frac{V_i}{V_i'} = \frac{\sum_i \Lambda_i\left[1-\left(\frac{\phi_i}{\mu_i}\right)^{-p}\right]}{\sum_i \frac{\Lambda_i}{\mu_i} p\left(\frac{\phi_i}{\mu_i}\right)^{-(p+1)}} \tag{3.2.6}$$

which simplifies to

$$\frac{V_i}{V_i'} = \frac{1}{p}\left(-\phi_i + \frac{{\phi_i}^{p+1}}{\mu_i^p}\right) \tag{3.2.7}$$

substituting Eq. (3.2.7) into Eq. (3.2.4) gives

$$N = \frac{1}{pM_p^2}\sum_i \begin{bmatrix} \frac{1}{\mu_i^p(p+2)}\left((\phi_i^s)^{p+2} - (\phi_i^e)^{p+2}\right) \\ -0.5\left((\phi_i^e)^2 - (\phi_i^s)^2\right) \end{bmatrix} \tag{3.2.8}$$

For the small field inflation it turns out that the value of μ_i is less than the Planck mass M_p i.e., $\mu_i \leq M_p$ and the inflation comes to end for $\phi_i^e \leq \mu_i$. This causes the quadratic terms i.e., $(\phi_i^s)^2$ and $(\phi_i^e)^2$ to disappear due to $\phi_i^s \leq \phi_i^e \leq M_p$. From Eq. (3.2.8)

$$N = \sum_i \begin{bmatrix} \frac{1}{\mu_i^p p(p+2)}\left(\left(\frac{\phi_i^s}{M_p}\right)^{p+2} - \left(\frac{\phi_i^e}{M_p}\right)^{p+2}\right) \\ -\frac{0.5}{p}\left(\left(\frac{\phi_i^e}{M_p}\right)^2 - \left(\frac{\phi_i^s}{M_p}\right)^2\right) \end{bmatrix} \tag{3.2.9}$$

or

$$N = \frac{1}{p\,(p+2)\,\mu_i^p}\sum_i \left(\left(\frac{\phi_i^s}{M_p}\right)^{p+2} - \left(\frac{\phi_i^e}{M_p}\right)^{p+2}\right) \tag{3.2.10}$$

which is simplified further to

$$N = \frac{\mu_i^2}{p\,(p+2)\,M_p^2}\sum_i \left[\frac{\phi_i^s}{\mu_i}\left(1-\left(\frac{\phi_i^s}{\phi_i^e}\right)\right)\right]^{p+2} \tag{3.2.11}$$

If we approximate the expression $1-\left(\frac{\phi_i^s}{\phi_i^e}\right)^{p+2}$ to unity, we are left with

$$N = \frac{1}{p\,(p+2)\,M_p^2}\sum_i \mu_i^2\left(\frac{\mu_i}{\phi_i^s}\right)^{-(p+2)} \tag{3.2.12}$$

Curvature perturbations as well as isocurvature perturbations both exist in multifield inflation models, however to keep the things simpler it is considered here that the during the slow-roll isocurvature are suppressed and can be neglected. For the remaining perturbations which are due to the curvature only can be suitably tackled by the mechanism developed by the formalism by Sasaki and Stewart (Langlois, 1999; Gordon et al., 2000; Amendola, Gordon, Wands, & Sasaki, 2002; Byrnes & Wands, 2006; Bassett

et al., 2006; Sasaki & Tanaka, 1998; Sasaki & Stewart, 1996; Polarski & Starobinsky, 1994). The expression for spectral index $n_s - 1$ according to this formalism is given as

$$n_s - 1 = \left[\sum_i \left(\frac{V'_i}{V_i} \right)^2 + 2 \sum_i \left(\frac{V'_i}{V_i} \right)^{-2} - 2 \sum_i \frac{1}{V_i} \frac{\sum_i \left(\frac{V_i}{V'_i} \right)^2 V''}{\sum_j \left(\frac{V_j}{V'_j} \right)^2} \right] M_p^2 \tag{3.2.13}$$

In Eq. (3.2.12), we replace $\frac{\mu_i}{\phi_i^s}$ by ω_i i.e.,

$$\frac{\mu_i}{\phi_i^s} \simeq \omega_i \tag{3.2.14}$$

then Eq. (3.2.12) can be re-expressed in the form

$$N = \frac{1}{p\,(p+2)\,M_p^2} \sum_i \mu_i^2 \omega_i^{-(p+2)} \tag{3.2.15}$$

Now, we substitute from Eq. (3.2.15)

$$\sum_i \mu_i^2 \omega_i^{-(p+2)} = B_1 \tag{3.2.16}$$

then Eq. (3.2.15) is

$$N = \frac{1}{p\,(p+2)\,M_p^2} B_1 \tag{3.2.17}$$

The reduced Planck mass M_p can be expressed in terms of newly defined constant B_1

$$M_p^2 = \frac{B_1}{p\,(p+2)} \frac{1}{N} \tag{3.2.18}$$

Now, we calculate all three terms in the Sasaki-Stewart formalism. For this from Eq. (3.2.1) squaring both sides, we

$$V^2 = \sum_i \left(V_i\left(\phi_i\right) \right)^2 = \sum_i \Lambda_i^2 \left[1 + \left(\frac{\phi_i}{\mu_i} \right)^{-2p} - 2 \left(\frac{\phi_i}{\mu_i} \right)^{-p} \right] \tag{3.2.19}$$

neglecting the 2nd and 3rd terms, we have

$$V^2 = \sum_i \left(V_i\left(\phi_i\right) \right)^2 = \sum_i \Lambda_i^2 \tag{3.2.20}$$

Let we put

$$\sum_i \Lambda_i = B_2 \tag{3.2.21}$$

then Eq. (3.2.20) takes the form

$$V^2 = \sum_i \left(V_i\left(\phi_i\right) \right)^2 = B_2^2 \tag{3.2.22}$$

Now, from Eq. (3.2.5) squaring both sides and making use of the Eq. (3.2.14), we obtain the form

$$\sum_i \left(V_i' \right)^2 = p^2 \sum_i \frac{\Lambda_i^2}{\mu_i^2} \frac{1}{\omega_i^{-2(p+1)}} \tag{3.2.23}$$

Let us take the expression

$$\sum_i \frac{\Lambda_i^2}{\mu_i^2} \frac{1}{\omega_i^{-2(p+1)}} = B_3 \tag{3.2.24}$$

then Eq. (3.2.23) becomes

$$\sum_i \left(V_i'\right)^2 = p^2 B_3 \tag{3.2.25}$$

Now, from Eq. (3.2.6), the simplification after squaring both sides and using from Eq. (3.2.14) gives

$$\sum_i \left(\frac{V_i(\phi_i)}{V'_i(\phi_i)}\right)^2 = \frac{1}{p^2} \sum_i \left(\phi_i^2 + \phi_i^2 \left(\frac{\mu_i}{\phi_i}\right)^{-2p} - 2\phi_i^2 \left(\frac{\mu_i}{\phi_i}\right)^{-p}\right) \tag{3.2.26}$$

Using the definition from Eq. (3.2.14) in above Eq. (3.2.26), we obtain

$$\sum_i \left(\frac{V_i(\phi_i)}{V'_i(\phi_i)}\right)^2 = \frac{\phi_i^2}{p^2} \sum_i \left(1 + \omega_i^{-2p} - 2\omega_i^{-2p}\right) \tag{3.2.27}$$

absorbing ϕ_i^2 into the definition of ω_i as given in Eq. (3.2.14). After simplification we obtain

$$\sum_i \left(\frac{V_i(\phi_i)}{V'_i(\phi_i)}\right)^2 = \frac{1}{p^2} \sum_i \left(\omega_i^{-2} + \omega_i^{-2(p+1)} - 2\omega_i^{-4}\right)\mu_i^2 \tag{3.2.28}$$

Let us take

$$\sum_i \left(\omega_i^{-2} + \omega_i^{-2(p+1)} - 2\omega_i^{-4}\right)\mu_i^2 = B_4 \tag{3.2.29}$$

now Eq. (3.2.29) takes the form using above defined constant

$$\sum_i \left(\frac{V_i(\phi_i)}{V'_i(\phi_i)}\right)^2 = \frac{1}{p^2} B_4 \tag{3.2.30}$$

Eq. (3.2.5) now, gives on differentiating once again

$$\sum_i V_i''(\phi_i) = -p\,(p+1) \sum_i \frac{\Lambda_i}{\mu_i^2} \left(\frac{\phi_i}{\mu_i}\right)^{-(p+2)} \tag{3.2.31}$$

use of Eq. (3.2.14) gives

$$\sum_i V_i''(\phi_i) = -p\,(p+1) \sum_i \frac{\Lambda_i}{(\omega_i)^{-(p+2)}\mu_i^2} \tag{3.2.32}$$

By working out the product of Eq. (3.2.26) and Eq. (3.2.31) and using Eq. (3.2.14), we get

$$\sum_i \left(\frac{V_i(\phi_i)}{V'_i(\phi_i)}\right)^2 V_i''(\phi_i) = -\frac{p+1}{p} \sum_i \Lambda_i \left(\omega_i^p + \omega_i^{-p} - 2\right) \tag{3.2.33}$$

Let we substitute

$$\sum_i \Lambda_i \left(\omega_i^p + \omega_i^{-p} - 2\right) = B_5 \tag{3.2.34}$$

then, Eq. (3.2.33) becomes

$$\sum_i \left(\frac{V_i(\phi_i)}{V'_i(\phi_i)}\right)^2 V_i''(\phi_i) = -\frac{p+1}{p} B_5 \tag{3.2.35}$$

with

$$\sum_i \left(\frac{V_i(\phi_i)}{V'_i(\phi_i)}\right)^2 = \sum_i \left(\frac{V_j(\phi_j)}{V'_j(\phi_j)}\right)^2 \tag{3.2.36}$$

we substitute from Eqs. (3.2.18), (3.2.20)-(3.2.22), (3.2.25), (3.2.30) and (3.2.35) in Eq. (3.2.13),

$$n_s - 1 = \left[\frac{p^2 B_3}{B_2^2} - 2\frac{1}{\left(B_4/p^2\right)} + 2\frac{1}{B_2}\frac{\left(-\frac{p+1}{p}B_5\right)}{\left(B_4/p^2\right)}\right]\left(\frac{B_1}{p\,(p+1)}\frac{1}{N}\right) \tag{3.2.37}$$

on simplification, it gives

$$\begin{aligned} n_s - 1 = &-\tfrac{p}{p+2}\tfrac{1}{N}\left(\tfrac{B_1 B_3}{B_2^2}\right) - 2\left(\tfrac{p}{p+2}\right)\tfrac{1}{N}\left(\tfrac{B_1}{B_4}\right) \\ &-2\left(\tfrac{p+1}{p+2}\right)\tfrac{1}{N}\left(\tfrac{B_1 B_5}{B_2 B_4}\right) \end{aligned} \tag{3.2.38}$$

By multiplying and dividing the 1st and 2nd terms in the above expression with $p+1$ and on simplifying, we obtain

$$n_s - 1 = -2\frac{(p+1)}{p+2}\frac{1}{N}\left(\frac{1}{2}\frac{p}{p+2}\frac{B_1 B_3}{B_2^2} + \frac{p}{p+1}\frac{B_1}{B_4} + \frac{B_1 B_5}{B_2 B_4}\right) \tag{3.2.39}$$

In Eq. (3.2.39) on the right hand side, the 1st and 2nd terms inside the parenthesis vanish due to $\omega_i^{-np\pm n} \simeq 0$, the remaining part is

$$n_s - 1 = -2\frac{(p+1)}{p+2}\frac{1}{N}\left(\frac{B_1 B_5}{B_2 B_4}\right) \tag{3.2.40}$$

we further mould the above equation in suitable form by adding and subtracting 1 on the right hand side within parenthesis

$$n_s - 1 = -2\frac{(p+1)}{p+2}\frac{1}{N}\left(\frac{B_1 B_5}{B_2 B_4} + 1 - 1\right) \tag{3.2.41}$$

or

$$n_s - 1 = -2\frac{(p+1)}{p+2}\frac{1}{N}\left(1 + \frac{B_1 B_5 - B_2 B_4}{B_2 B_4}\right) \tag{3.2.42}$$

Let we replace

$$\frac{B_1 B_5 - B_2 B_4}{B_2 B_4} = R\,(\omega_i) \tag{3.2.43}$$

then Eq. (3.2.42) has the form

$$n_s - 1 = -2\frac{(p+1)}{p+2}\frac{1}{N}\left(1 + R\,(\omega_i)\right) \tag{3.2.44}$$

For $R\,(\omega_i) \simeq 0$, Eq. (3.2.44) serves to calculate the spectral index for a single scalar field. However, the term $R\,(\omega_i)$ adds up in for the case when we are considering multifields.

Therefore, it is important to determine this factor. We will use the definitions of involved constants to find out the approximate value of the $R(\omega_i)$ for larger values of p than 2. From Eqs. (3.2.16), (3.2.21), (3.2.29) and (3.2.34) substituting for the constants B_1, B_2, B_4, B_5 in Eq. (3.2.43) to determine $R(\omega_i)$

$$R(\omega_i) = \sum_i \frac{2\left(\omega_i^p - \omega_i^2\right)\omega_i^p}{\omega_i^{2(p+1)} - 2\omega_i^{2p} + \omega_i^2} \tag{3.2.45}$$

From Eq. (3.2.32), we have the expression for ω_i^p with considering $\sum_i V_i''(\phi_i) = V_i''(\phi_i) = m_i^2$, we have

$$\omega_i^p = -\frac{1}{p(p+1)} \frac{\mu_i^2 m_i^2}{\Lambda_i \omega_i^2} \tag{3.2.46}$$

using the value of ω_i^p in Eq. (3.2.45), we get

$$R(\omega_i) = \sum_i \frac{2\left(\mu_i^2 m_i^2 + \omega_i^4 \Lambda_i p(p+1)\right)}{\mu_i^2 m_i^2\left(\omega_i^2 - 1\right) - \omega_i^4 \Lambda_i p(p+1)} \tag{3.2.47}$$

The expression of $R(\omega_i)$ as found in above Eq. (3.2.47) is due to consideration of multiple fields rather than using a single field. Eq. (3.2.44) becomes now

$$n_s - 1 = -2\frac{(p+1)}{p+2}\frac{1}{N}\left(1 + \sum_i \frac{2\left(\mu_i^2 m_i^2 + \omega_i^4 \Lambda_i p(p+1)\right)}{\mu_i^2 m_i^2\left(\omega_i^2 - 1\right) - \omega_i^4 \Lambda_i p(p+1)}\right) \tag{3.2.48}$$

and with $R(\omega_i) \simeq 0$, Eq. (3.2.44) becomes, that is

$$n_s - 1 = -2\frac{(p+1)}{p+2}\frac{1}{N} \tag{3.2.49}$$

Eq. (3.2.48) gives the spectral index for the case of multifields and Eq. (3.2.49) represents the spectral index for the case when a single scalar field is taken into account. In this case the masses of all the fields considered at once are of same value at the time of horizon-crossing. This poses the case when the spectral index of the multifields is same and corresponds to the spectral index of a single scalar field (Alabidi & Lyth, 2006). It is also clear that the term $R(\omega_i)$ appears due to the consideration of multifields. It is also interesting to observe with regard to the fact that the value of $R(\omega_i)$ will be positive for $\omega_i < \omega_{i+1}$ and $m_i^2 < m_{i+1}^2$. It will turn, however into negative for $\omega_i < \omega_{i+1}$ and $m_i^2 > m_{i+1}^2$. The positive value of $R(\omega_i)$ is interpreted as having a spectrum being redder for multifields in comparison with its corresponding spectrum emerging from a single field. Therefore, the negativity here implies being its value less redder as is demonstrated in the corresponding case. Nonetheless, a stringent condition begs further work to develop in this perspective.

3.2.1.3 Analytical Analysis For the Case Related to $p = -2, +2$

Now, we will discuss some specific cases for the values of p. We will investigate for $p = 2, -2$ and will observe that what effect is bore upon the respective expressions of number of e-folds and the spectral indices.

Let us take first the case when $p = 2$. From Eqs. (3.2.1, 3.2.5, 3.2.31), we have

$$\sum_i V_i(\phi_i) = \sum_i \Lambda_i \left[1 - \left(\frac{\phi_i}{\mu_i}\right)^{-2}\right] \tag{3.2.50}$$

$$\sum_i V'_i(\phi_i) = 2\sum_i \frac{\Lambda_i}{\mu_i}\left(\frac{\phi_i}{\mu_i}\right)^{-3} \tag{3.2.51}$$

and

$$\sum_i V_i''(\phi_i) = -6\sum_i \frac{\Lambda_i}{\mu_i^2}\left(\frac{\phi_i}{\mu_i}\right)^{-4} \tag{3.2.52}$$

From Eq. (3.2.12) for the number of e-folds with $p = 2$, we get

$$N = \frac{1}{8M_p^2}\sum_i \mu_i^2 \left(\frac{\mu_i}{\phi_i^s}\right)^{-4} \tag{3.2.53}$$

Eq. (3.2.53) leads to the absurd result which is

$$N = \frac{1}{8\mu_i^2 M_p^2}\sum_i \left[\left(\frac{\phi_i^e}{M_{pl}}\right)^2 + \left(\frac{\phi_i^s}{M_p}\right)^2\right] \to 0 \tag{3.2.54}$$

similarly, the spectral index $n_s - 1$ from Eq. (3.2.48) for $p = 2$

$$n_s - 1 = -\frac{3}{2}\frac{1}{N}\left(1 + \sum_i \frac{2\left(\mu_i^2 m_i^2 + 6\omega_i^4\Lambda_i\right)}{\mu_i^2 m_i^2\left(\omega_i^2 - 1\right) - 6\omega_i^4\Lambda_i}\right) \tag{3.2.55}$$

for $N \simeq 0$, as we have an absurd result from above equation, Eq. (3.2.55) leads to the value of spectral index $n_s - 1$ approaching to ∞ which is again meaningless seemingly.

For $p = -2$, Eq. (3.2.1) takes the form

$$\sum_i V_i(\phi_i) = \sum_i \Lambda_i \left[1 - \left(\frac{\phi_i}{\mu_i}\right)^{2}\right] \tag{3.2.56}$$

Now, the Eqs. (3.2.5) and (3.2.31) reduce to the following expressions

$$\sum_i V'_i(\phi_i) = V'_i(\phi_i) = -2\sum_i \frac{\Lambda_i}{\mu_i^2}\phi_i \tag{3.2.57}$$

$$\sum_i V_i''(\phi_i) = V_i''(\phi_i) = -2\sum_i \frac{\Lambda_i}{\mu_i^2} \tag{3.2.58}$$

and the expression for the number of e-folds N is given by

$$N = -\frac{1}{2M_p^2}\sum_i \ln\left(\frac{\phi_i^s}{\phi_i^e}\right)\mu_i^2 \tag{3.2.59}$$

Finding the values of the following from Eq. (3.2.56) which comes out to be

$$\sum_i \left(V_i'\right)^2 = 4\sum_i \frac{\Lambda_i^2}{\omega_i^2\mu_i^2} \tag{3.2.60}$$

$$\sum_i \left(\frac{V_i}{V_i'}\right)^2 = \frac{1}{4}\sum_i \omega_i^2\mu_i^2 \tag{3.2.61}$$

similarly for

$$\sum_j \left(\frac{V_j}{V_j'}\right)^2 = \frac{1}{4}\sum_j \omega_j^2\mu_j^2 \tag{3.2.62}$$

and finally

$$\sum_i \left(\frac{V_i}{V_i'}\right)^2 V_i'' = -\frac{1}{2}\sum_i \Lambda_i\omega_i^2 \tag{3.2.63}$$

Substituting Eqs. (3.2.60)-(3.2.63) in Eq. (3.2.13) we find the spectral

$$n_s - 1 = -M_p^2\left(\frac{\sum\limits_i \Lambda_i\omega_i^2}{\sum\limits_i \Lambda_i \sum\limits_i \mu_j^2\omega_j^2}\right) \tag{3.2.64}$$

where we used the condition that $\omega_i^{-2} \simeq 0$ Now, from Eq. (3.2.3), we have

$$\frac{\dot{\phi}_i}{V'_i\left(\phi_i\right)} = \frac{\dot{\phi}_j}{V'_j\left(\phi_j\right)} \tag{3.2.65}$$

working out for finding $V'_i\left(\phi_i\right)$ and $V'_j\left(\phi_j\right)$ from Eq. (3.2.56) and using in Eq. (3.2.64), we obtain

$$\mu_i^2\frac{\dot{\phi}_i}{\Lambda_i\phi_i} = \mu_j^2\frac{\dot{\phi}_j}{\Lambda_j\phi_j} \tag{3.2.66}$$

Integrating the above equation between the limits ϕ_i^s, and ϕ_i^e for ith field whereas between ϕ_j^s and ϕ_i^e for the corresponding jth field

$$\frac{\mu_i^2}{\Lambda_i}\int_{\phi_i^s}^{\phi_i^e}\frac{\dot{\phi}_i}{\phi_i} = \frac{\mu_j^2}{\Lambda_j}\int_{\phi_j^s}^{\phi_j^e}\frac{\dot{\phi}_j}{\phi_j} \tag{3.2.67}$$

after simplification we get

$$\sum_i \mu_i^2 \ln\left(\frac{\phi_i^s}{\phi_i^e}\right) = \sum_k \mu_k^2 \ln\left(\frac{\phi_k^s}{\phi_k^e}\right)\sum_i \frac{\Lambda_i}{\Lambda_k} \tag{3.2.68}$$

for some fixed value of k we can drop $\sum\limits_k$

$$\sum_i \mu_i^2 \ln\left(\frac{\phi_i^s}{\phi_i^e}\right) = \mu_k^2 \ln\left(\frac{\phi_k^s}{\phi_k^e}\right)\sum_i \frac{\Lambda_i}{\Lambda_k} \tag{3.2.69}$$

or having a more simplified expression for it

$$\mu_i^2 \ln\left(\frac{\phi_i^s}{\phi_i^e}\right) = \mu_k^2 \ln\left(\frac{\phi_k^s}{\phi_k^e}\right)\frac{\Lambda_i}{\Lambda_k} \tag{3.2.70}$$

The number of e-folds in Eq. (3.2.59) becomes

$$N = -\frac{\mu_k^2}{2M_p^2} \ln\left(\frac{\phi_k^s}{\phi_k^e}\right) \sum_i \frac{\Lambda_i}{\Lambda_k} \tag{3.2.71}$$

from Eq. (3.2.71), we can find expression for Planck mass in terms of number of e-folds

$$M_p^2 = -\frac{1}{2N}\mu_k^2 \ln\left(\frac{\phi_k^s}{\phi_k^e}\right) \sum_i \frac{\Lambda_i}{\Lambda_k} \tag{3.2.72}$$

The expression for spectral index in Eq. (3.2.64) becomes with the use of Planck mass from above equation

$$n_s - 1 = \frac{2}{N} \ln\left(\frac{\phi_k^s}{\phi_k^e}\right) \frac{\sum\limits_i \left(\frac{\Lambda_i}{\Lambda_k}\right) \omega_i^2}{\sum\limits_j \left(\frac{\mu_j}{\mu_k}\right)^2 \omega_j^2} \tag{3.2.73}$$

for $\Lambda_i = \Lambda_k$, all the fields ϕ_i or ϕ_k will possess the same value of Λ_i. In this case the expression for the spectral index in above equation reduces to the following form

$$n_s - 1 = \frac{2}{N} \ln\left(\frac{\phi_k^s}{\phi_k^e}\right) \frac{\sum\limits_i \omega_i^2}{\sum\limits_j \left(\frac{\mu_j}{\mu_k}\right)^2 \omega_j^2} \tag{3.2.74}$$

The results presented in the Eqs. (3.2.73) and (3.2.74) are independent of the choice of the value of k that is being considered to the uncompromising level. In Eq. (3.2.74), if the multifields avail the chance of having the same μ_i and $\mu_j = \mu_k$, then we have

$$n_s - 1 = \frac{2}{N} \ln\left(\frac{\phi_k^s}{\phi_k^e}\right) \tag{3.2.75}$$

3.3 An Nflationary Phase Diagram with Multifield Polynomial Potential

In this section we bring into discussion two cases in order to calculate the field values and critical point.

3.3.1 Calculation of the Field Values and The Critical Point

The potential of a single scalar field ϕ is usually written as $V(\phi) = \Lambda^4 f\left(\frac{\phi}{\mu}\right)$. It is characterized by two independent mass scales Λ^4 and μ, where Λ^4 known as height corresponds to the density of the vacuum energy during inflationary phase and the second one μ called as width corresponds to the change in the field $\Delta\phi$ during inflation. The function $f\left(\frac{\phi}{\mu}\right)$ has distinct forms for the choice of different models. Here we consider a multifield polynomial potential of the form $V(\phi_j) = \Lambda_j^4 \left(\frac{\phi_j}{\mu_j}\right)^p$ and develop

further calculations to reach at the required results. We first find the total change $\Delta\phi$ in the field ϕ, which is important and plays significantly very basic role

$$\Delta\phi = \Delta\phi_1 + \Delta\phi_2 + \Delta\phi_2 + \cdots + \Delta\phi_j = \sum_j \Delta\phi_j = \sqrt{\sum_j \left(\Delta\phi_j\right)^2} \tag{3.3.1}$$

Now, the equation

$$\begin{cases} \frac{d\phi_j}{dt} = \left(H^{-1}\right)^{-1}\Delta\phi_j \\ \Delta\phi_j = \frac{\dot{\phi}_j}{H} \end{cases} \tag{3.3.2}$$

From equation of motion of scalar field

$$\frac{d^2\phi_j}{dt^2} - 3H\frac{d\phi_j}{dt} + \frac{dV\left(\phi_j\right)}{d\phi_j} = 0 \tag{3.3.3}$$

From Eq. (3.3.3) with

$$\frac{d^2\phi_j}{dt^2} = 0$$

during slow roll phase, therefore we obtain

$$\frac{d\phi_j}{dt} = \dot{\phi}_j = \frac{1}{3H}\frac{dV\left(\phi_j\right)}{d\phi_j} \tag{3.3.4}$$

Using Eqs. (3.3.2) and Eq. (3.3.4) in Eq. (3.3.1), we have

$$\Delta\phi = \sqrt{\frac{\sum\limits_j \left(\frac{dV(\phi_j)}{d\phi_j}\right)^2}{\left(3H^2\right)^2}} = \frac{\sqrt{\sum\limits_j \left(\frac{dV(\phi_j)}{d\phi_j}\right)^2}}{3H^2} \tag{3.3.5}$$

From first Friedmann's equation which describes the cosmological evolution of the universe

$$\left(\partial_t \ln a\right)^2 - ka^{-2} = \frac{8\pi G}{3}\rho \tag{3.3.6}$$

where $a = a\left(t\right)$ is the scale factor characterizing expansion rate of the universe, k gives the curvature of spacetime and ρ is the energy density of the universe. For flat universe $k = 0$, the energy density in Planck era $\rho = \rho\left(\phi\right)$, so that $\rho \sim \rho_{\phi_j} \sim V\left(\phi_j\right)$, $\partial_t \ln a = H$ and $M_p^2 = \frac{1}{8\pi G}$, then, Eq. (3.3.6) takes the form

$$H^2 = \frac{1}{3M_p^2}V\left(\phi_j\right) \tag{3.3.7}$$

now the potential

$$V\left(\phi_j\right) = \frac{\Lambda_j^4}{\mu_j^p}(\phi_j)^p = \sum_j m_j^p(\phi_j)^p = \left(mass - scales\right)\left(\phi_j\right)^p \tag{3.3.8}$$

so Eq. (3.3.7) takes the form with the use of Eq. (3.3.8) in it

$$H^2 = \frac{\sum\limits_j m_j^p(\phi_j)^p}{3M_p^2} \tag{3.3.9}$$

Further from Eq. (3.3.8), we have

$$\frac{dV\left(\phi_j\right)}{d\phi_j} = pm_j^p\phi_j^{p-1} \tag{3.3.10}$$

using the Eqs. (3.3.9) and (3.3.10) in Eq. (3.3.5), the term $\Delta\phi$ takes the form

$$\Delta\phi = \frac{\sqrt{\sum_j \left(pm_j^p\phi_j^{p-1}\right)^2}}{3\left(\frac{\sum_j m_j^p(\phi_j)^p}{3M_p^2}\right)} = \frac{pM_p^2\sqrt{\sum_j m_j^{2p}\phi_j^{2p-2}}}{\sum_j m_j^p\phi_j^p} \tag{3.3.11}$$

We calculate, now, the change in ϕ i.e., $\delta\phi$

$$\begin{cases} \delta\phi = \delta\phi_1 + \delta\phi_2 + \delta\phi_3 + \cdots + \delta\phi_j = \sum_j \delta\phi_j = \sqrt{\left(\sum_j \delta\phi_j\right)^2} \\ \delta\phi \propto \sqrt{\left(\sum_j \delta\phi_j\right)^2} \Rightarrow \delta\phi = \sqrt{N}\sqrt{\left(\sum_j \delta\phi_j\right)^2} \end{cases} \tag{3.3.12}$$

Now, using the value of $\delta\phi_j = \frac{H}{2\pi}$ and in addition to Eq. (3.3.9) in Eq. (3.3.12), we find

$$\delta\phi = \frac{\sqrt{N}}{2\sqrt{3}\pi}\frac{1}{M_p}\sqrt{\sum_j m_j^p\phi_j^p} \tag{3.3.13}$$

Equating Eq. (3.3.11) and Eq. (3.3.13) for both types of change in the values of ϕ, where we can determine the relation

$$12\pi^2p^2\frac{M_p^6}{N}\left(\sum_j m_j^{2p}\phi_j^{2p-2}\right) = \left(\sum_j m_j^p\phi_j^p\right)^3 \tag{3.3.14}$$

and from slow roll condition we have $\varepsilon = -\frac{\dot{H}}{H^2} = \frac{1}{16\pi G}\left(\frac{\partial_\phi V}{V}\right)^2, |\varepsilon| \simeq 1$

$$p^2\frac{M_p^2}{2}\left(\sum_j m_j^p\phi_j^{p-1}\right)^2 = \left(\sum_j m_j^p\phi_j^p\right)^2 \tag{3.3.15}$$

Now, either the mass-scales of fields are equivalent or different, so we discuss two cases accordingly

3.3.2 The Case of Equivalent Mass Scales

Now, from Eq. (3.3.14) and Eq. (3.3.15), we can find the case for the equivalent mass scales and the equivalent potentials for keeping the case simple and straightforward respectively i.e., $m_j = m$ and $\phi_j = \phi$

$$\frac{M_p^6}{N}12\pi^2p^2\left(m^{2p}\phi^{2p-2}\right) = \left(m^p\phi^p\right)^3 \Rightarrow \phi = \left(\frac{48\pi^2}{N^3}\right)^{\frac{1}{4}}\sqrt{\frac{M_p^3}{m}} \tag{3.3.16}$$

$$\frac{p^2}{2}M_p^2\left(m^p\phi^{p-1}\right)^2 = (m^p\phi^p)^2 \Rightarrow \phi = \sqrt{2}\frac{M_p}{\sqrt{N}} \tag{3.3.17}$$

The results calculated in Eqs. (3.3.16) and (3.3.17) are obtained by substituting the masses of all fields to be equivalent and that of the fields as well to keep the things simple and easy to handle. These equations represent the values of fields at the final stage of slow roll phase and at the boundary of eternal inflation respectively with respect to the number of fields N in order to derive the Nflationary phase. From Eq. (3.3.16), we can observe that $\phi = \sqrt{\frac{M_p^3}{m}4\pi(3)^{\frac{1}{2}}}\left(\frac{1}{N^3}\right)^{\frac{1}{4}}$ i.e., $\phi \propto \left(\frac{1}{N^3}\right)^{\frac{1}{4}} \propto \sqrt{\left(\frac{1}{N^{\frac{3}{2}}}\right)}$ that is the value of ϕ at the boundary of eternal inflation and varies as $N^{-\frac{3}{4}}$. We can plot the values of ϕ at the end of slow roll phase and at the boundary of eternal inflation crossing each other at a point of the fields, let it be N, which is obtained by comparing the values of field ϕ as given in Eqs. (3.3.16) and (3.3.17), that is

$$\left(\frac{48\pi^2}{N^3}\right)^{\frac{1}{4}}\sqrt{\frac{M_p^3}{m}} = \sqrt{2}\frac{M_p}{\sqrt{N}} \Rightarrow N \simeq 12\pi^2\frac{M_p^2}{m^2} \tag{3.3.18}$$

or by dropping the constant we can write in simple form

$$N \simeq \frac{M_p^2}{m^2} \tag{3.3.19}$$

The value $\left(\frac{M_p}{m}\right)^2$ represents a common point between the phase of slow roll and eternal inflation where the lines of two regions join each other as given in the diagram. This can be labelled as meeting point or crossing point. The slow roll phase beyond this point does not appear more. Once this point is achieved, the line of eternal inflation at the boundary does not move further extending downward which means that the crossing point can be considered as a critical point. The field values at the critical point can be calculated by substituting it in Eqs. (3.3.16) and (3.3.17). Eq. (3.3.16) at the critical point $N \simeq \frac{M_p^2}{m^2}$ gives the value of the field

$$\phi = \left(\frac{48\pi^2}{N^3}\right)^{\frac{1}{4}}\sqrt{\frac{M_p^3}{m}} = \left(\frac{48\pi^2}{\left(\frac{M_p^2}{m^2}\right)^3}\right)^{\frac{1}{4}}\sqrt{\frac{M_p^3}{m}} \simeq \frac{2\sqrt{\pi}(3)^{\frac{1}{4}}}{m^2} \tag{3.3.20}$$

and at the critical point $N \simeq \frac{M_p^2}{m^2}$, Eq. (3.3.17) produces the field value

$$\phi \simeq \sqrt{2}\frac{M_p}{\sqrt{N}} \simeq \sqrt{2}\frac{M_p}{\sqrt{\left(\frac{M_p^2}{m^2}\right)}} \simeq \sqrt{2}m \tag{3.3.21}$$

Below in Figure-3.2, we plot the phase transition diagram for Nflationary phase. In Eq. (3.3.20), behavior of the field with mass scale goes the way like $\phi \propto m^{-2}$ which means that the field value does not depend on number of fields N and is inversely proportional

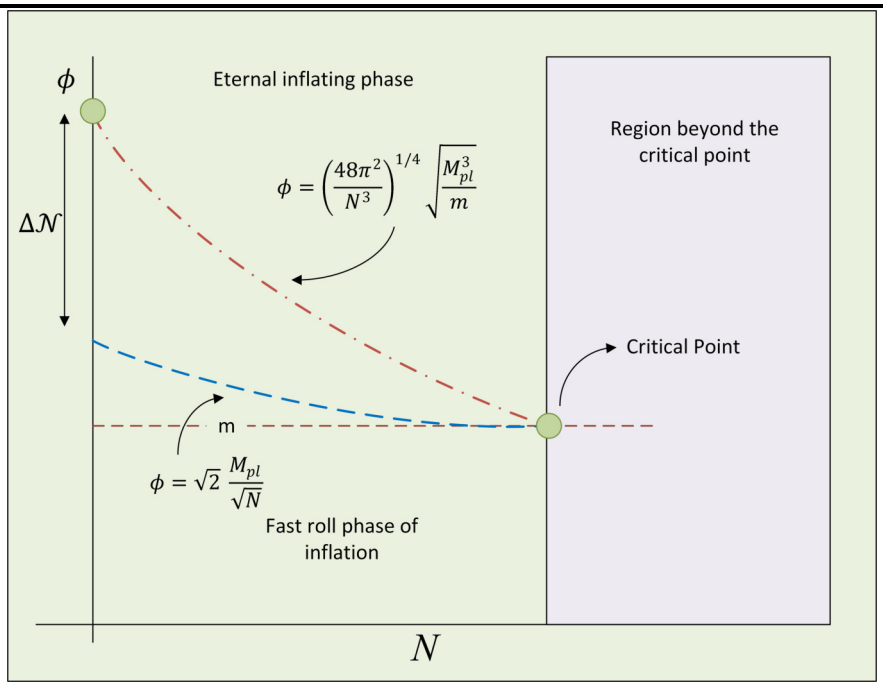

Figure– 3.2: The diagram of Nflationary phase between ϕ and N for a specific multifield potential $V(\phi_j) = \Lambda_j^4 \left(\frac{\phi_j}{\mu_j}\right)^p$. The two dotted lines divide the region of inflation into three phases as is shown in the diagram. The phase of slow roll appears to terminate on and beyond the critical point. It is complicated to predict about it due to disappearance of classical limit on and to the other side of the critical point. Two lower dotted lines and one upper represent the lasting values of slow roll phase and eternal inflation respectively

to the square of the mass scale of the fields which takes the responsibility for occurrence of the boundary in eternal inflation. Eq. (3.3.21) describes the behavior of the field $\phi \propto m$ and is independent of the number of fields N and for those values of ϕ which fall short than m, there are likely chances that the slow rolling phase would not occur during inflation. But we know that slow roll phase might necessarily occur in inflationary paradigm in order to resolve the cosmological problems occurring in the standard model of cosmology like horizon, flatness, monopole and entropy problems. The slow roll phase is also necessary to occur to generate the primordial quantum fluctuations to seed the present structure formation in the universe cosmologically. Beyond the critical point, it is expected that only the line representing the end value of slow roll phase would exist and the line representing the boundary of eternal inflation would terminate at the critical point as shown in the diagram. This is drawn as dotted line shifting away from the critical point. Since the value of eternal inflation at the boundary is dependent on extrapolating the value of slow roll phase, we argue that beyond and below the end value, the fast roll regime takes over and replaces it. In the scenario, the possibility of quantum fluctuations being suppressed is likely to happen and therefore it can hardly be probable for the quantum fluctuations to suppress the evolution of these fluctuations classically, however the case cannot be simple enough as expected. Next we will investigate that a restriction on entropy can be found as a bound on the number of fields N that at the critical point $\left(\frac{M_p}{m}\right)^2$ saturates. It means that our semiclassical investigations do not remain valid and become inapplicable beyond the critical point. Beyond the critical point quantum era is dominant and the investigation of phase diagram beyond it would constitute an interesting subject of exploration for further future work. In Nflation scenario, it is important to note that when the number of fields N is larger than the ratio of squares of Planck mass (M_p) to the average value of the masses of the fields (mass scales) ($\bar{m}$), then the region of slow roll inflation exits no more.

$$N \leq M_p^2 : m^2 \Rightarrow N \leq \frac{M_p^2}{m^2} \tag{3.3.22}$$

The case when field-masses are equivalent is simple to handle, for this reason we considered equivalent mass-scale case upto here. However, the scenario is not affected too much with different masses of the fields if we use some suitable technique. The Marčenko-Pastur law comes here to remedy for the case of different masses. It has already been investigated that the phase diagram does not change for the unequal masses, we just have to replace the mass m with average masses of the fields $\bar{m}$. It is, however significant to note here that all the fields implied by N are massive with no massless

scalar field contained in it. If we take the massless fields present under N, they will have no effect because the dynamics of massive scalar fields remains unaffected due to their negligible impact. Therefore, their presence and non-presence is equivalent and it can be supposed as if they are not present at all. From Eqs. (3.3.16) and (3.3.17) it can be seen that only massive fields are taken into account for which Eq. (3.3.21) is satisfied. This is the case when massive scalar fields are considered as dominant for cosmological evolution. However, the way fields behave as jumping random movement quantum mechanically along the trajectory of the field spaces during calculating of perturbations since isocurvature perturbations are only furnished by the fields which are massless and Eq. (3.3.16) and (3.3.17) do not bother about this mentioned case as such. The plots beneath are drawn in Figure-3.3 which give the behavior of logarithmic change in field ϕ values against the number of fields.

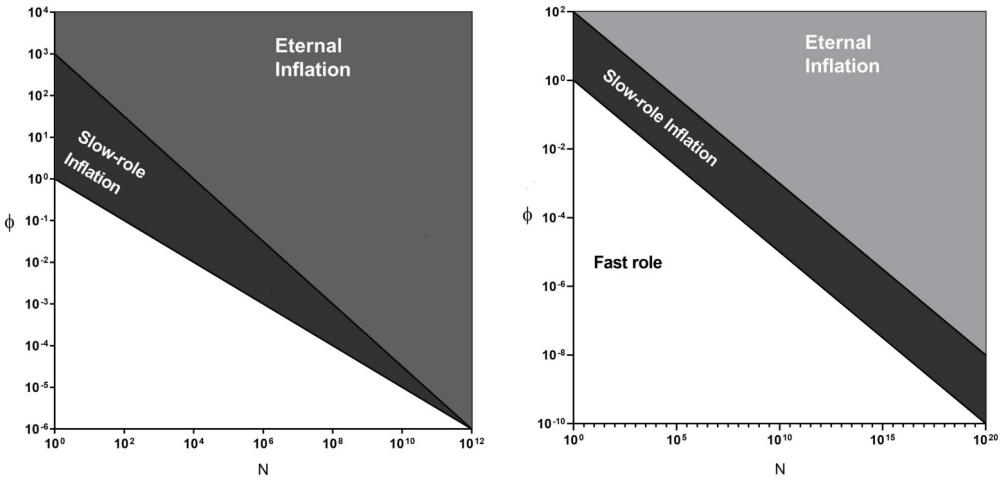

(a) **(b)**

Figure– 3.3: (a) The figure shows plot between the logarithmic change of ϕ and the number of fields N. It represents relationship of slow roll, eternal inflation and fast roll phases. It can clearly be seen that N has bound for which slow rolling phase disappears converging towards the critical point.

(b) The figure shows plot between the logarithmic change of ϕ and the number of fields N. It represents relationship of slow roll, eternal inflation and fast roll phases. It can clearly be seen that N does not have any bound for which slow rolling phase disappears converging towards some point. Therefore two lines separating the Nflationary phases move parallel to each other and never converge to some point

3.3.3 The Case of Different Mass Scales-An Application of Marčenko-Pastur law Concerned with Distribution of Masses in Nflation

The use of random matrix theory in Nflation model plays a significant role to show that spectrum for the distribution of different masses is in accordance with Marčenko-Pastur law. R. Easter and L. McAllister have suggested the mechanism to solve the problem of different scale of masses (Easther & McAllister, 2006). They have proposed a law regarding the general case of the distribution of mass scales which is known as Marčenko-Pastur law. The technique was first used in connection with the mass distribution of axion fields in string theory. we employ Marčenko-Pastur law for the distribution of mass scale factors μ. Marčenko-Pastur law uses $\bar{\mu}$ and β, where β is the ratio of rows and columns of mass scale factor μ. We can express it as $\beta = \frac{n}{n+r}$ for any mass scale matrix of order $(n+r) \times n$. Now the values related with μ for the smallest and the largest are given by

$$\mu_1^2 = x = \bar{\mu}^2\Big(1 - \sqrt{\beta}\Big)^2 \tag{3.3.23}$$

$$\mu_2^2 = y = \bar{\mu}^2\Big(1 + \sqrt{\beta}\Big)^2 \tag{3.3.24}$$

respectively and the field value during slow roll approximation comes out to be

$$\phi_j\left(t\right) \simeq \phi_j\left(t_0\right)\left[T\left(t\right)\right]^{\frac{\mu_1^2}{y}} \tag{3.3.25}$$

where $T\left(t\right) = \frac{\phi_n(t)}{\phi_n(t_0)}$ represents the ratio between the larger field at some time t and initial value at some time t_0. Defining now in Eq. (3.3.14) and Eq. (3.3.15), the following $z = 2\frac{\ln[T(t)]}{y}$, where ϕ_j^2 is replaced by $\phi_j^2\left(t_0\right)e^{z\mu_i^2}$. We can compute in a straightforward way the respective range of average values of mass distributions regardless of the initial field distributions when we neglect correlations between them. Now we employ the power series expansion and calculate the average value of the exponential term.

$$\begin{aligned}\langle e^{z\mu_i^2}\rangle &= \sum_i \langle\mu_i^2\rangle\frac{c^j}{j} = \bar{\mu}^{2i}\sum_{j=1}^{i} T\left(i,j\right)\beta^{j-1}\frac{c^j}{j} \\ &= \sum_{i=0}^{\infty}\bar{\mu}^{2i}F_1\left(1-i,-i,2,\beta\right)\frac{c^j}{j}\end{aligned} \tag{3.3.26}$$

Now, Eq. (3.3.14) can be expressed in the form

$$\mu_j^2\phi_j^2 = n\alpha\bar{\mu}^2\sum_{i=0}^{\infty}\bar{\mu}^{2i}F_1\left(-i,-i-1,2,\beta\right)\frac{c^i}{i} \tag{3.3.27}$$

where $\alpha = \langle\zeta_j^2\left(t_0\right)\rangle$, further we have

$$\mu_j^4\phi_j^2 = n\alpha\bar{\mu}^4\sum_{i=0}^{\infty}\bar{\mu}^{2i}F_1\left(-i-1,-i-2,2,\beta\right)\frac{c^i}{i} \tag{3.3.28}$$

We substitute Eq. (3.3.27) and Eq. (3.3.28) in Eq. (3.3.14) first and afterwards in Eq. (3.3.15), and obtain for α respectively

$$\begin{cases} \alpha = \left(\frac{48\pi^2}{N^3}\frac{M_p^3}{\tilde{m}}\right)^{\frac{1}{2}} f_1(t,\beta) \\ \alpha = 2\frac{M_p^2}{N} f_2(t,\beta) \end{cases} \tag{3.3.29}$$

where

$$\begin{cases} f_1(t,\beta) = \dfrac{\left(\sum\limits_{i=0}^{\infty} \bar{\mu}^{2i} F_1(-i-1,-i-2,2,\beta)\frac{c^i}{i}\right)^{\frac{1}{2}}}{\left(\sum\limits_{i=0}^{\infty} \bar{\mu}^{2i} F_1(-i,-i-1,2,\beta)\frac{c^i}{i}\right)^{\frac{3}{2}}} \\ f_2(t,\beta) = \dfrac{\left(\sum\limits_{i=0}^{\infty} \bar{\mu}^{2i} F_1(-i-1,-i-2,2,\beta)\frac{c^i}{i}\right)}{\left(\sum\limits_{i=0}^{\infty} \bar{\mu}^{2i} F_1(-i,-i-1,2,\beta)\frac{c^i}{i}\right)^{2}} \end{cases} \tag{3.3.30}$$

The Figure-3.4 below gives the distribution of masses according to Marčenko-Pastur law. For distinct values of z we can have $f_1(t,\beta)$ and $f_2(t,\beta)$. It can be observed from

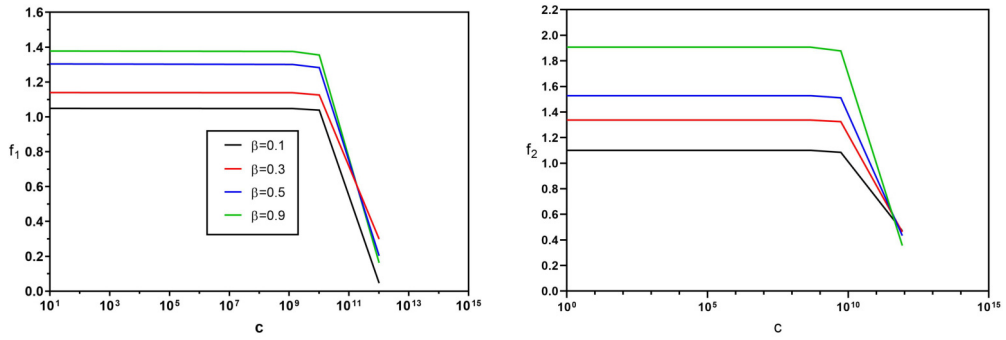

(a) **(b)**

Figure– 3.4: (a) Marčenko-Pastur law: This figure illustrates the mass distribution of axions versus dimensionless mass variables in the case β adopts different values. c is along parallel axis when the function $f_1(t,\beta)$. Note that the law of large numbers ensures that the mass distribution of N axions obeys the distribution probability of a single field.

(b) Marčenko-Pastur law: This figure illustrates the mass distribution of axions versus the dimensionless mass variables in the case β adopts different values. c is along parallel axis when the function $f_2(t,\beta)$. Note that the law of large numbers ensures that the mass distribution of N axions obeys the distribution probability of a single field

the diagrams of the two functions that when the values of z are taken in larger range the function's behavior is similar to that like of a constant. For equal values of mass scales

and fields the functions $f_1(t,\beta) = f_2(t,\beta) \simeq 1$ and from Eq. (3.3.29) the value of $\alpha \simeq \phi^2$ and $\bar{m} = m$, in this case we regain the values of ϕ as expressed in Eqs. (3.3.16, 3.3.17) i.e., $\phi = \left(\frac{48\pi^2}{N^3}\right)^{\frac{1}{4}} \sqrt{\frac{M_p^3}{m}}$ and $\phi = \sqrt{2}\frac{M_p}{\sqrt{N}}$.

3.4 Time Independent Schrödinger Equation Conforming to Wheeler-DeWitt Equation for the Evolution of Early Universe

In this section we discuss formulation of the problem.

3.4.1 Mathematical Formulation of the Problem

Wheeler-DeWitt equation leads to the time-independent Schrödinger equation with the condition of zero point energy. The time-independent Schrödinger equation gives evolution of the universe as state system and predicts even inflationary phase under special assumptions. From the Friedmann 1st equation of evolution, we have,

$$\left(\frac{\dot{a}}{a}\right)^2 + \frac{k}{a^2} = \frac{8\pi G}{3}\rho \tag{3.4.1}$$

assuming the energy density is sourced by the cosmological constant i.e., $\rho = \frac{\Lambda}{8\pi G}$ only and considering a positively curved spacetime geometry i.e., $k = +1$, that represents a close universe, we have from Eq. (3.4.1)

$$\frac{\dot{a}^2}{a^2} + \frac{1}{a^2} = \frac{1}{3}\Lambda \tag{3.4.2}$$

$$\frac{d^2a}{dt^2} - \frac{1}{3}\Lambda a^2 + 1 = 0 \tag{3.4.3}$$

Eq. (3.4.3) is satisfied by the following solution

$$a\left(t\right) = a_0 \cosh\left(\frac{t}{a_0}\right) \tag{3.4.4}$$

where $a_0 = \sqrt{\frac{\Lambda}{3}}$ and at $t = 0$ the universe shrinks to a radius of the maximally smallest size and the expansion at $t = 0$ is $a\left(0\right) = a_0 = \sqrt{\frac{\Lambda}{3}}$, however at some later time $t = t_0$, it keeps on expanding forever. From Eq. (3.4.1) we also have a generalized form for Eq. (3.4.3) as

$$\frac{d^2a}{dt^2} - \frac{8\pi G\rho}{3}a^2 = -k \tag{3.4.5}$$

Now, From Eq. (3.4.2), multiplying it by a^3 on both sides and after having simplified, we have

$$a\dot{a}^2 + a - \frac{1}{3}a^3\Lambda = 0 \tag{3.4.6}$$

Furthermore, making use of Einstein-Hilbert action we obtain

$$S_{EH} = -\frac{3\pi}{4G}\int\left(a\dot{a}^2 - a + \frac{1}{3}a^3\Lambda\right)dx^0 \tag{3.4.7}$$

Determining now the classical Lagrangian $\mathcal{L}$ and Hamiltonian H from it. We can write the Lagrange $\mathcal{L}$ classically from the above equation

$$\mathcal{L} = \mathcal{L}(a, \dot{a}) = -\frac{3\pi}{4G}\left(a\dot{a}^2 - a + \frac{1}{3}a^3\Lambda\right) \tag{3.4.8}$$

The conjugate momentum to the variable $a(t)$ is

$$\frac{\partial \mathcal{L}(a, \dot{a})}{\partial \dot{a}} = P = -\frac{3\pi}{2G}\dot{a}a \tag{3.4.9}$$

and Hamiltonian function taken classically could be written as

$$H = \frac{\partial \mathcal{L}(a, \dot{a})}{\partial \dot{a}}(\dot{a}) - \mathcal{L}(a, \dot{a}) = -\frac{3\pi}{2G}\dot{a}a(\dot{a}) + \frac{3\pi}{4G}\left(a\dot{a}^2 - a + \frac{1}{3}a^3\Lambda\right) \tag{3.4.10}$$

$$H = -\frac{3\pi}{4G}\left(a - \frac{1}{3}a^3\Lambda\right) - \frac{GP^2}{3\pi a} \tag{3.4.11}$$

When we use quantization where the conjugate momentum operator is $p \to i\frac{\partial}{\partial t} \Rightarrow p^2 = -\frac{\partial^2}{\partial t^2}$ and Eq. (3.4.11) takes the form with its use in it

$$H = -\frac{3\pi}{4G}\left(a - \frac{1}{3}a^3\Lambda\right) + \frac{G}{3\pi a}\frac{\partial^2}{\partial t^2} \tag{3.4.12}$$

The classical constraint $H = 0$ as an operator identity is not satisfied and proved here. Instead, it is taken as the constraint on the states of the theory that is

$$H\Psi(t) = 0 \tag{3.4.13}$$

Now, from Eq. (3.4.12), for $H = 0$

$$-\frac{3\pi}{4G}\left(a - \frac{1}{3}a^3\Lambda\right) + \frac{G}{3\pi a}\frac{\partial^2}{\partial t^2} = 0 \tag{3.4.14}$$

or

$$H = \frac{\partial^2}{\partial t^2} - \frac{9\pi^2}{4G^2}\left(a^2 - \frac{1}{3}a^4\Lambda\right) = 0 \tag{3.4.15}$$

and Eq. (3.4.13) takes the following form

$$\left(\frac{\partial^2}{\partial t^2} - \frac{9\pi^2}{4G^2}\left(a^2 - \frac{1}{3}a^4\Lambda\right)\right)\Psi(a) = 0 \tag{3.4.16}$$

Eq. (3.4.16) represents Wheeler-DeWitt (WDW) equation in minisuperspace where $\Psi(a)$ is the wave function of the observable universe expressed solely in terms of scale factor $a(t)$ and does not explicitly depend on time and can be said that it is independent of time. This equation can be viewed as the time-independent Schrödinger wave equation, that is

$$\left(-\frac{h^2}{2m}\frac{\partial^2}{\partial x^2} + V\right)\Psi = E\Psi \tag{3.4.17}$$

Having a comparative look on Eqs. (3.4.16) and (3.4.17)), it implies that Wheeler-DeWitt equation can be considered as Schrödinger wave equation with the zero-point energy wave function i.e. $(0)\,E$ at the right hand side (Vakili, 2012). Now, we consider an FLRW metric in minisuperspace that goes all the way

$$ds^2 = -N^2(t)\,dt^2 + a^2(t)\left[\frac{dr^2}{1-kr^2} + r^2 d\theta^2 + r^2 \sin^2\theta d\phi^2\right] \tag{3.4.18}$$

where the parameter $N(t)$ stands for the lapse function and describes the measure considerations for the rate of flow of proper time τ with respect to the coordinate time t as one shifts away along the unit normal vector to the hypersurface. The lapse function is defined in terms of the metric tensor $g_{\mu\nu}$ and slicing of it into timelike hypersurfaces. The parameter $a(t)$ is the scale factor that characterizes expansion of the universe whreas the term k is curvature of space (spacetime) representing three geometries namely spherical, elliptical and flat corresponding to $+1$, -1 and 0 respectively. The minisuperspace used here is the analogue of quantum version for FLRW universe which takes into account such model of the universe. It is here intended to work out a variable which could play suitably the role of time variable. Now, employing Einstein-Hilbert action, we proceed

$$S_{EH} = \frac{1}{16\pi G}\int \left(\sqrt{-g}R + \sqrt{-g}\mathcal{L}_\phi\right) d^4x \tag{3.4.19}$$

and substituting the value of Ricci scalar R from Eq. (3.4.18) and in addition taking $\mathcal{L}_\phi = \frac{1}{2}g^{\mu\nu}\partial_\mu\phi\partial_\nu\phi + V(\phi)$ and $N(t) = 16\pi G = 1$ in Eq. (3.4.19), we determine the Lagrangian $\mathcal{L}$ in the minisuperspace parameterized as $\{a, \phi\}$ in the following form

$$\mathcal{L} = -3\left(\frac{da}{dt}\right)^2 a + 3ka + \frac{1}{2}a^3\left(\frac{d\phi}{dt}\right)^2 - a^3 V(\phi) \tag{3.4.20}$$

We figure out the momenta conjugate to the variables a and ϕ respectively

$$\frac{\partial L}{\partial \dot{\phi}} = P_\phi = a^3\frac{d\phi}{dt} \tag{3.4.21}$$

and

$$\frac{\partial \mathcal{L}}{\partial \dot{a}} = P_a = -6a\frac{da}{dt} \tag{3.4.22}$$

Now, on the other hand, the canonical Hamiltonian H is given by

$$H = \dot{a}(t)\frac{\partial L}{\partial \dot{a}(t)} + \dot{\phi}(t)\frac{\partial \mathcal{L}}{\partial \dot{\phi}(t)} - \mathcal{L} \tag{3.4.23}$$

Eq. (3.4.23) becomes on substituting the values of momenta conjugate from Eq. (3.4.21) and Eq. (3.4.22) and of $\mathcal{L}$ from Eq. (3.4.20)

$$H = \frac{1}{2}\frac{P_\phi^2}{a^3} - \frac{1}{12}\frac{P_a^2}{a} + a^3 V(\phi) - 3ka \tag{3.4.24}$$

The canonical Hamiltonian as worked out in Eq. (3.4.24), now takes the form for the canonical transformations as given below

$$(\phi, P_\phi) \to (T, P_T) \tag{3.4.25}$$

we have

$$T = \frac{\phi}{P_\phi} \tag{3.4.26}$$

and

$$P_T = \frac{P_\phi^2}{2} \tag{3.4.27}$$

$$H_{CL} = \frac{P_T}{a^3} - \frac{1}{12}\frac{P_a^2}{a} + a^3 V(T) - 3ka \tag{3.4.28}$$

The subscript CL here indexed in H denotes classical Hamiltonian. It is arguable here that the momentum P_T which appears linearly in the expression can be regarded as parameter of time during the quantization of the model. To quantize the model and have the Wheeler-DeWitt equation there out

$$H\Psi(a, T) = 0 \tag{3.4.29}$$

here $\Psi(a, T)$ is the wave function of the universe in the minisuperspace. Using the transformations

$$P_T \to -i\frac{\partial}{\partial t} \tag{3.4.30}$$

and

$$P_{a(t)} \to -i\frac{\partial}{\partial a(t)} \tag{3.4.31}$$

The quantized version of Eq. (3.4.28) takes the form as is expressed below where the results from Eq. (3.4.30) and Eq. (3.4.31) are used for the operators

$$H_{QZ} = a^2(t)\frac{\partial^2}{\partial a^2} + sa(t)\frac{\partial}{\partial a} - i\left(12\frac{\partial}{\partial T}\right) - 36ka^4 \tag{3.4.32}$$

The subscript QZ here in H denotes the quantized Hamiltonian whereas s represents the mutual interaction in the term $-\frac{1}{12}\frac{P_a^2}{a}$ as the ambiguous order for the factors a and P_a. Using the quantized Hamiltonian in Eq. (3.4.32), we obtain the Wheeler-DeWitt equation in Eq. (3.4.29) in the form

$$\left(a^2(t)\frac{\partial^2}{\partial a^2} + sa(t)\frac{\partial}{\partial a} - i\left(12\frac{\partial}{\partial T}\right) - 36ka^4\right)\Psi(a, T) = 0 \tag{3.4.33}$$

Considering the case for a flat geometry ($k = 0$), we have from the above equation

$$\left(a^2(t)\frac{\partial^2}{\partial a^2} + sa(t)\frac{\partial}{\partial a} - 12i\frac{\partial}{\partial T}\right)\Psi(a, T) = 0 \tag{3.4.34}$$

From Eq. (3.4.34) we can have the Schrödinger equation by separating suitably its variables as $\Psi(a,T) = e^{iBT}\Psi(a)$. This leads to the equation in the following form

$$a^2\frac{d^2\Psi(a)}{da^2} + sa\frac{d\Psi(a)}{da} + 12B\Psi(a) = 0 \tag{3.4.35}$$

or

$$\left(a^2\frac{d^2}{da^2} + sa\frac{d}{da} + 12B\right)\Psi(a) = 0 \tag{3.4.36}$$

where s and B are the parameters which for different values falling in the feasible range of the solution suitable for the phenomena under consideration help in solving this equation numerically. We will solve this equation numerically by assigning different values to these parameters. The dependent variable $\Psi(a)$ is the wave function and is the function of scale factor $a(t)$ describing expansion evolutionary dynamics of the universe. In interpreting the wave function $\Psi(a)$ physically, it bears similarity to that of the wave function discussed in quantum mechanics. The scale factor parameter seems here somehow to play the role of a coordinate-like variable. For the scale factor $a(t)$, two initial conditions are possibly taken into account that is $a(0) = 0$ and $a(0) > 0$. When the solution is considered in the half plane $t \geq 0$, we observe $a(t) \to 0$ as $t \to \infty$. The observations evidence that $a(t)$ is always increasing function which means that the big crunch could not be attained and our simple approach may still be advantageous to describe the desired dynamics. In the case of a bound state as a quantum state possessing solution means that it does not present a good demonstration altogether. However, the Schrödinger equation possesses an infinite number of wave function solutions for any as large as possible number of continuous set of energies that diverge to $\pm\infty$ as $t \to \infty$ (Mielnik & Reyes, 1996). Determining such a solution and interpreting it probabilistically could reveal the weird features of the cosmic dynamics with providing dualistic nature of the cosmic scale factor. Below in the Figure-3.5, the graphical abstract is illustrated which presents the step by step procedural process of the working for solving the problem and describes how the early universe could evolve.

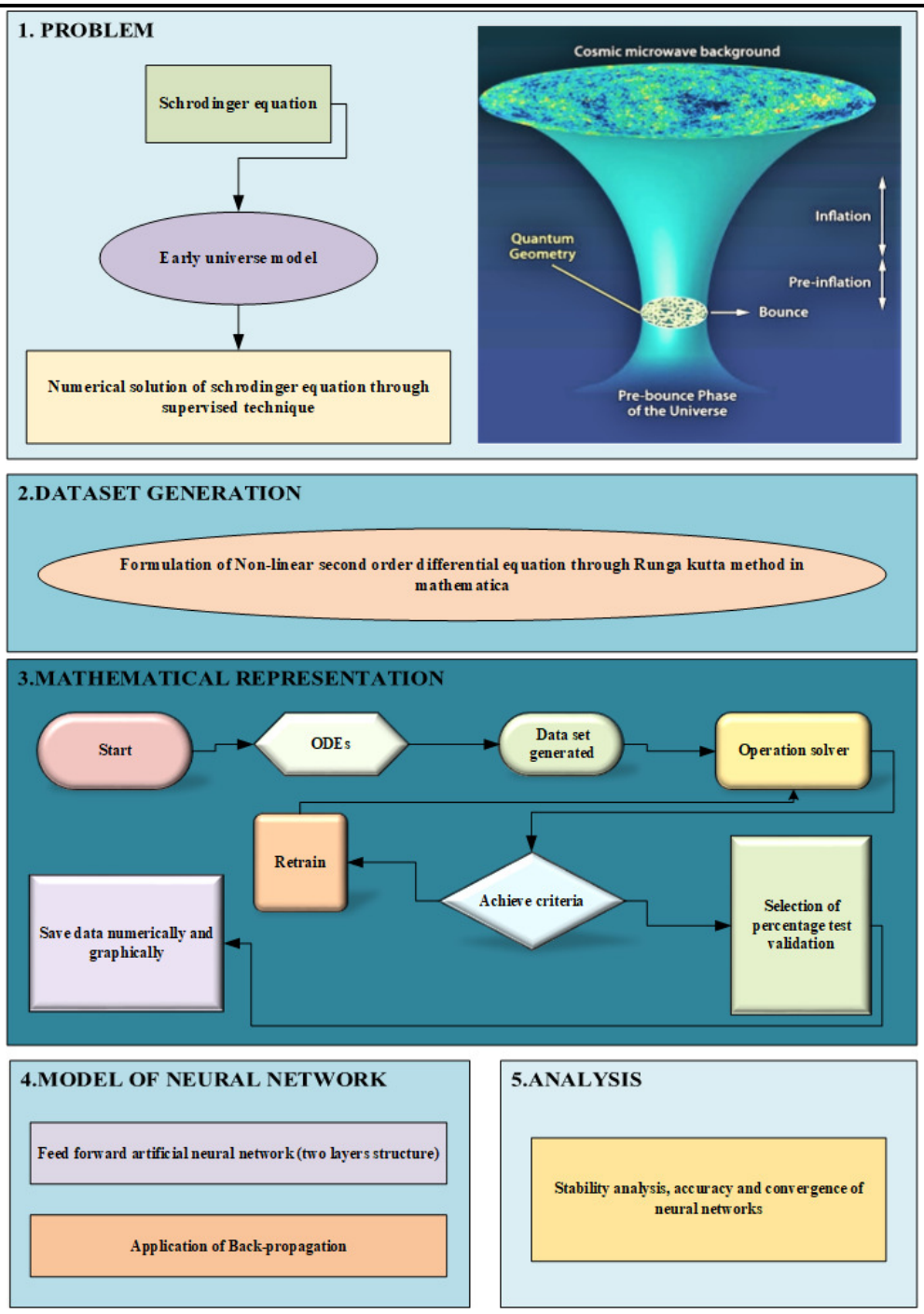

Figure– 3.5: The graphical abstract of the proposed problem

3.5 Accelerating Universe Driven by Multifield Tachyon-Quintom Dark Energy

In the first place, we begin with the development of the mathematical machinery required to discuss dark energy models under consideration using dynamical system approach.

3.5.1 Development Of the Mathematics For the Model

We take two homogeneous scalar fields namely multifield-tachyon $\sum_{i=1}^{n} \xi_i$ and multifield-phantom tachyon $\sum_{i=1}^{n} \eta_i$ which is known as tachyon-quintom (Shi et al., 2009). Their corresponding potentials are $\sum_{i=1}^{n} V(\xi_i)$ and $\sum_{i=1}^{n} V(\eta_i)$ respectively. In the background we consider the FLRW universe with four-dimensional flat spacetime. Since we shall use equation of state parameter w expressed in terms of pressure and density as ratio of the two, therefore we are going to take the fluid whose density is the function of pressure only i.e., $\rho = \rho(p)$. The barotropic fluid is disseminated through and replenished in the universe with equation $p_\gamma = (\gamma - 1)\ \rho_\gamma$ with the condition $0 < \gamma \leq 2$, where γ has different values for dust and radiation etc. The system of this type will have action of the form

$$S = \int \left(\frac{M_p^2 R}{2} + \sum_{i=1}^{n} \mathcal{L}_{\xi_i} + \sum_{i=1}^{n} \mathcal{L}_{\eta_i} + \mathcal{L}_m \right) \sqrt{-g} d^4x \tag{3.5.1}$$

where

$$\sum_{i=1}^{n} \mathcal{L}_{\xi_i} = -\sum_{i=1}^{n} V(\xi_i) \sqrt{1 + g^{\mu\nu} \sum_{i=1}^{n} \partial_\mu \xi_i \partial_\nu \xi_i} \tag{3.5.2}$$

and

$$\sum_{i=1}^{n} \mathcal{L}_{\eta_i} = -\sum_{i=1}^{n} V(\eta_i) \sqrt{1 - g^{\mu\nu} \sum_{i=1}^{n} \partial_\mu \eta_i \partial_\nu \eta_i} \tag{3.5.3}$$

are the scalar field Lagrangian densities where as $\mathcal{L}_m$ represents the Lagrangian density of the matter fields as Lagrangian. The spatial homogeneity will imply $\sum_{i=1}^{n} \partial_i \xi_i = \sum_{i=1}^{n} \partial_i \eta_i = 0$, that is only spatially homogeneous solutions that evolve in time i.e., time dependent solutions will be considered. The generalized energy densities of the fields result in the form

$$\rho_{\sum_{i=1}^{n} \xi_i} = \frac{\sum_{i=1}^{n} V(\xi_i)}{\sqrt{1 - \sum_{i=1}^{n} \dot{\xi}_i^2}} \tag{3.5.4}$$

$$\rho_{\sum_{i=1}^{n}\eta_i} = \frac{\sum_{i=1}^{n} V(\eta_i)}{\sqrt{1+\sum_{i=1}^{n}\dot{\eta}_i^2}} \tag{3.5.5}$$

and the generalized pressures for both fields

$$p_{\sum_{i=1}^{n}\xi_i} = -\sum_{i=1}^{n} V(\xi_i)\sqrt{1-\sum_{i=1}^{n}\dot{\xi}_i^2} \tag{3.5.6}$$

$$p_{\sum_{i=1}^{n}\eta_i} = -\sum_{i=1}^{n} V(\eta_i)\sqrt{1+\sum_{i=1}^{n}\dot{\eta}_i^2} \tag{3.5.7}$$

Now, the equations of the scalar fields for generalized tachyon and generalized phantom tachyon read in the following forms

$$\frac{\sum_{i=1}^{n}\ddot{\xi}_i}{1-\sum_{i=1}^{n}\dot{\xi}_i^2} + 3H\sum_{i=1}^{n}\dot{\xi}_i + \frac{\sum_{i=1}^{n} V_{,\xi_i}(\xi_i)}{\sum_{i=1}^{n} V(\xi_i)} = 0 \tag{3.5.8}$$

and

$$\frac{\sum_{i=1}^{n}\ddot{\eta}_i}{1-\sum_{i=1}^{n}\dot{\eta}_i^2} + 3H\sum_{i=1}^{n}\dot{\eta}_i - \frac{\sum_{i=1}^{n} V_{,\eta_i}(\eta_i)}{\sum_{i=1}^{n} V(\eta_i)} = 0 \tag{3.5.9}$$

and from equation of continuity, substituting for $p_\gamma = (\gamma-1)\rho_\gamma$, we obtain evolution equation for barotropic perfect fluid

$$\frac{d\rho}{dt} + 3H(\rho+p) = 0, \tag{3.5.10}$$

$$\Rightarrow \qquad \frac{d\rho_\gamma}{dt} + 3H(\rho_\gamma + p_\gamma) \tag{3.5.11}$$

$$\Rightarrow \qquad \frac{d\rho_\gamma}{dt} - 3H\gamma\rho_\gamma = 0 \tag{3.5.12}$$

In order to find the equation for acceleration, we have now to compute first the following two parameters $\dot{H}$ and H^2. We know from Friedmann's Equations that

$$H^2 = \left(\frac{\dot{a}}{a}\right)^2 = \frac{8\pi G}{3}\rho + \frac{k}{a^2} \tag{3.5.13}$$

$$\dot{H} + H^2 = \frac{\ddot{a}}{a} = -\frac{4\pi G}{3}(\rho+3p) \tag{3.5.14}$$

from above Eq. (3.5.13) and Eq. (3.5.14), we have

$$\dot{H} = -\frac{4\pi G}{3}(\rho+p) \tag{3.5.15}$$

Now, Eq. (3.5.15) can be written for the densities and pressures of the generalized fields considered in the model and for the barotropic pressure and density, that is

$$\dot{H} = -\frac{1}{2M_p^2}\left(\rho_{\sum_{i=1}^{n}\xi_i} + \rho_{\sum_{i=1}^{n}\eta_i} + p_{\sum_{i=1}^{n}\xi_i} + p_{\sum_{i=1}^{n}\eta_i} + \rho_\gamma + p_\gamma \right) \tag{3.5.16}$$

Now, substituting the values for the generalized energy densities and pressures, we have

$$\begin{aligned} \dot{H} = -\tfrac{1}{2M_p^2}\Bigg[& \left(\frac{\sum_{i=1}^{n} V(\xi_i)}{\sqrt{1-\sum_{i=1}^{n}\dot{\xi}_i^2}} + \frac{\sum_{i=1}^{n} V(\eta_i)}{\sqrt{1+\sum_{i=1}^{n}\dot{\eta}_i^2}} \right) \\ & + \left(\begin{array}{l} -\sum_{i=1}^{n} V(\xi_i)\sqrt{1-\sum_{i=1}^{n}\dot{\xi}_i^2} - \sum_{i=1}^{n} V(\eta_i)\sqrt{1+\sum_{i=1}^{n}\dot{\eta}^2} \\ +\rho_\gamma + (\gamma-1)\,\rho_\gamma \end{array} \right) \Bigg] \end{aligned} \tag{3.5.17}$$

after having simplified the above expression, we obtain

$$\dot{H} = -\frac{1}{2M_p^2}\left(\frac{\sum_{i=1}^{n} V(\xi_i)\dot{\xi}_i^2}{\sqrt{1-\sum_{i=1}^{n}\dot{\xi}_i^2}} - \frac{\sum_{i=1}^{n} V(\eta_i)\dot{\eta}_i^2}{\sqrt{1+\sum_{i=1}^{n}\dot{\eta}_i^2}} + \gamma\rho_\gamma \right) \tag{3.5.18}$$

Now, from Eq. (3.5.13)

$$H^2 = \left(\frac{\dot{a}}{a}\right)^2 = \frac{8\pi G}{3}\rho + \frac{k}{a^2}$$

With $k = 0$ for flat universe

$$H^2 = \frac{8\pi G}{3}\rho \tag{3.5.19}$$

Since the energy density ρ is contributed by $\sum_{i=1}^{n}\xi_i$ and $\sum_{i=1}^{n}\eta_i$ and ρ_γ, and for $M_p^2 = \frac{1}{8\pi G}$, we have

$$H^2 = \frac{1}{3M_p^2}\rho = \frac{1}{3M_p^2}\left(\rho_{\sum_{i=1}^{n}\xi_i} + \rho_{\sum_{i=1}^{n}\eta_i} + \rho_\gamma \right) \tag{3.5.20}$$

Using Eq. (3.5.4) and Eq. (3.5.5), we have

$$H^2 = \frac{1}{3M_p^2}\left(\frac{\sum_{i=1}^{n} V(\xi_i)}{\sqrt{1-\sum_{i=1}^{n}\dot{\xi}_i^2}} + \frac{\sum_{i=1}^{n} V(\eta_i)}{\sqrt{1+\sum_{i=1}^{n}\dot{\eta}_i^2}} + \rho_\gamma \right) \tag{3.5.21}$$

Now, dividing both sides of above equation by H^2

$$1 = \frac{1}{3H^2M_p^2}\left(\frac{\sum_{i=1}^{n} V(\xi_i)}{\sqrt{1-\sum_{i=1}^{n}\dot{\xi}_i^2}} + \frac{\sum_{i=1}^{n} V(\eta_i)}{\sqrt{1+\sum_{i=1}^{n}\dot{\eta}_i^2}} + \rho_\gamma \right) \tag{3.5.22}$$

or

$$1=\left(\frac{\sum\limits_{i=1}^{n}V\left(\xi_i\right)\backslash 3H^2M_p^2}{\sqrt{1-\sum\limits_{i=1}^{n}\dot{\xi}_i^2}}+\frac{\sum\limits_{i=1}^{n}V\left(\eta_i\right)\backslash 3H^2M_p^2}{\sqrt{1+\sum\limits_{i=1}^{n}\dot{\eta}_i^2}}+\frac{\rho_\gamma}{3H^2M_p^2}\right) \tag{3.5.23}$$

From Eq. (3.5.23), we are going now to define some parameters which are dimensionless and can facilitate our calculations. Further we will construct dynamical system with the help of these parameters

$$x_{\sum\limits_{i=1}^{n}\xi_i}=\sum_{i=1}^{n}\dot{\xi}_i \tag{3.5.24}$$

$$x_{\sum\limits_{i=1}^{n}\eta_i}=\sum_{i=1}^{n}\dot{\eta}_i \tag{3.5.25}$$

and

$$y_{\sum\limits_{i=1}^{n}\xi_i}=\frac{\sum\limits_{i=1}^{n}V\left(\xi_i\right)}{3H^2M_p^2} \tag{3.5.26}$$

$$y_{\sum\limits_{i=1}^{n}\eta_i}=\frac{\sum\limits_{i=1}^{n}V\left(\eta_i\right)}{3H^2M_p^2} \tag{3.5.27}$$

and

$$z=\frac{\rho_\gamma}{3H^2M_p^2} \tag{3.5.28}$$

Now, using the defined parameters from Eqs. (3.5.24)-(3.5.28), Eq. (3.5.23) becomes

$$1=\left(\frac{y_{\sum\limits_{i=1}^{n}\xi_i}}{\sqrt{1-x^2_{\sum\limits_{i=1}^{n}\xi_i}}}+\frac{y_{\sum\limits_{i=1}^{n}\eta_i}}{\sqrt{1+x^2_{\sum\limits_{i=1}^{n}\eta_i}}}+z\right) \tag{3.5.29}$$

For obtaining the equation of acceleration, we divide both sides of Eq. (3.5.18) by H^2 and making use of the defined parameters from Eqs. (3.5.24)-(3.5.28), we get the following simplified form

$$\frac{\dot{H}}{H^2}=-\frac{3}{2}\left(\frac{y_{\sum\limits_{i=1}^{n}\xi_i}x^2_{\sum\limits_{i=1}^{n}\xi_i}}{\sqrt{1-x^2_{\sum\limits_{i=1}^{n}\xi_i}}}+\frac{y_{\sum\limits_{i=1}^{n}\eta_i}x^2_{\sum\limits_{i=1}^{n}\eta_i}}{\sqrt{1+x^2_{\sum\limits_{i=1}^{n}\eta_i}}}+\gamma z\right) \tag{3.5.30}$$

Using the value of z from Eq. (3.5.29) in Eq. (3.5.30) and performing simplification, we have

$$\frac{H'}{H}=-\frac{3}{2}\left(-\frac{y_{\sum\limits_{i=1}^{n}\xi_i}\left(\gamma-x^2_{\sum\limits_{i=1}^{n}\xi_i}\right)}{\sqrt{1-x^2_{\sum\limits_{i=1}^{n}\xi_i}}}-\frac{y_{\sum\limits_{i=1}^{n}\eta_i}\left(\gamma+x^2_{\sum\limits_{i=1}^{n}\eta_i}\right)}{\sqrt{1+x^2_{\sum\limits_{i=1}^{n}\eta_i}}}+\gamma\right) \tag{3.5.31}$$

here H' denotes the derivative of H with respect to the logarithm of the scale factor i.e., $lna = N$ and $H = \partial_t \ln a = \frac{dN}{dt}$ and $\dot{H} = \frac{dH}{dN} \times \frac{dN}{dt} = H'H$ Now, from Eq. (3.5.29)

$$\Omega_{DE} = 1 - \frac{1}{3}\left(\rho_\gamma H^{-2} M_p^{-2}\right) \tag{3.5.32}$$

where we used Eq. (3.5.28) and for $\frac{y\sum_{i=1}^{n}\xi_i}{\sqrt{1-x^2\sum_{i=1}^{n}\xi_i}} + \frac{y\sum_{i=1}^{n}\eta_i}{\sqrt{1+x^2\sum_{i=1}^{n}\eta_i}} = \Omega_{DE}$ The parameter Ω_{DE} weighs out the energy density of dark energy as a fraction of the critical density ρ_{cd}. The EoS $w = \frac{p}{\rho}$ of dark energy for the system of multifield scalars is given by

$$w = \frac{p_{\sum_{i=}^{n}\xi_i} + p_{\sum_{i=}^{n}\eta_i}}{\rho_{\sum_{i=}^{n}\xi_i} + \rho_{\sum_{i=}^{n}\eta_i}} \tag{3.5.33}$$

using Eqs. (3.5.4)-(3.5.7), we obtain

$$w = \frac{-\sum_{i=1}^{n} V(\xi_i)\sqrt{1-\sum_{i=1}^{n}\xi_i^2} - \sum_{i=1}^{n} V(\eta_i)\sqrt{1+\sum_{i=1}^{n}\eta_i^2}}{\frac{\sum_{i=1}^{n} V(\xi_i)}{\sqrt{1-\sum_{i=1}^{n}\xi_i^2}} + \frac{\sum_{i=1}^{n} V(\eta_i)}{\sqrt{1+\sum_{i=1}^{n}\eta_i^2}}} \tag{3.5.34}$$

dividing and multiplying by $\frac{8\pi G}{3H^2}$

$$w = \frac{\frac{8\pi G}{3H^2}\left(-\sum_{i=1}^{n} V(\xi_i)\sqrt{1-\sum_{i=1}^{n}\xi_i^2} - \sum_{i=1}^{n} V(\eta_i)\sqrt{1+\sum_{i=1}^{n}\eta_i^2}\right)}{\frac{8\pi G}{3H^2}\left(\frac{\sum_{i=1}^{n} V(\xi_i)}{\sqrt{1-\sum_{i=1}^{n}\xi_i^2}} + \frac{\sum_{i=1}^{n} V(\eta_i)}{\sqrt{1+\sum_{i=1}^{n}\eta_i^2}}\right)} \tag{3.5.35}$$

after simplification we get

$$w = \frac{-y_{\sum_{i=1}^{n}\xi_i}\sqrt{1-x^2_{\sum_{i=1}^{n}\xi_i}} - y_{\sum_{i=1}^{n}\eta_i}\sqrt{1+x^2_{\sum_{i=1}^{n}\eta_i}}}{\frac{y\sum_{i=1}^{n}\xi_i}{\sqrt{1-x^2\sum_{i=1}^{n}\xi_i}} + \frac{y\sum_{i=1}^{n}\eta_i}{\sqrt{1+x^2\sum_{i=1}^{n}\eta_i}}} \tag{3.5.36}$$

Carrying out some numerical analysis shows that there is correspondence between e-folding number N and the redshift z. The redshift is related to the scale factor $a(t)$ by the relation $z = \frac{a_0(t)}{a(t)-1}$ and $a_0(t) = 1$, we have $z = \frac{1}{a(t)-1}$. For $z \approx 10^{10}$, the number of e-folds maps the nucleosynthesis at the time of big bang to $N_{nbb} \simeq -21$. On the other hand, for $z \approx 3300$, the number of e-folds maps the equality of matter-radiation at the time slightly after big bang to $N_{emr} \simeq -10$. We take $N = -10$ as the initial number of e-folds which could be a convenient choice and conforming to it consider $\gamma = 1$ in

Eqs. (3.5.38) and (3.5.41) which may prove a suitable approximation. In the below in Figure-3.6, it is shown how the equation of state and dark energy evolves conforming to the number of e-folds. Now, we develop an autonomous dynamical system. we use

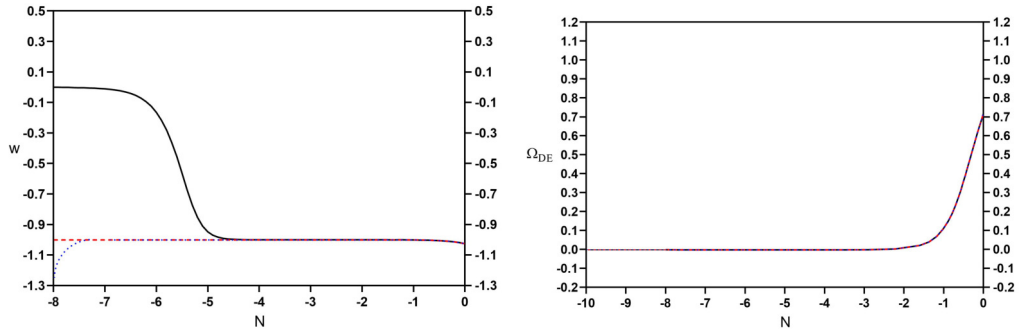

(a) **(b)**

Figure– 3.6: The figure shows how does the growth of equation of state parameter w and the parameter of dark energy density Ω_{DE} occur with evolution of the number of e-folds N and for $\gamma = 1$ and $\lambda_{\sum_{i=1}^{n}\xi_i}$ and $\lambda_{\sum_{i=1}^{n}\eta_i}$ as 0.33

inverse square potentials to study the dynamics of our model constructed for tachyon and phantom tachyon. Inverse square potential renders the similar role to tachyon field as does the exponential potential to the standard scalar field. These potentials have been used extensively in the study of tachyon models and allow to develop the dynamical system (Padmanabhan, 2002; Bagla et al., 2003; Calcagni & Liddle, 2006; Copeland et al., 2005; Aguirregabiria & Lazkoz, 2004). From Eqs. (3.5.8) and (3.5.24) and with inverse square potential defined for multifield scalars $\sum_{i=1}^{n}\xi_i$ as $\sum_{i=1}^{n} V(\xi_i) = M^2_{\sum_{i=1}^{n}\xi_i} \sum_{i=1}^{n}\xi_i^{-2}$ for evolution of the system. Here $M^2_{\sum_{i=1}^{n}\xi_i}$ is the mass scale of multifield scalars $\sum_{i=1}^{n}\xi_i$.

$$
\begin{aligned}
x'_{\sum_{i=1}^{n}\xi_i} &= \frac{d\left(x_{\sum_{i=1}^{n}\xi_i}\right)}{dN} \\
&= -3\left(1 - x^2_{\sum_{i=1}^{n}\xi_i}\right)\left(x_{\sum_{i=1}^{n}\xi_i} - \sqrt{\lambda_{\sum_{i=1}^{n}\xi_i} y_{\sum_{i=1}^{n}\xi_i}}\right)
\end{aligned}
\tag{3.5.37}
$$

From Eq. (3.5.26) and Eq. (3.5.31) with using inverse square potential $\sum_{i=1}^{n} V(\xi_i) = M^2_{\sum_{i=1}^{n}\xi_i} \sum_{i=1}^{n} \xi_i^{-2}$, we find

$$\begin{aligned} y'_{\sum_{i=1}^{n}\xi_i} &= \frac{d\left(y_{\sum_{i=1}^{n}\xi_i}\right)}{dN} \\ &= 3y_{\sum_{i=1}^{n}\xi_i} \left(\begin{array}{l} -\frac{y_{\sum_{i=1}^{n}\xi_i}\left(\gamma - x^2_{\sum_{i=1}^{n}\xi_i}\right)}{\sqrt{1-x^2_{\sum_{i=1}^{n}\xi_i}}} - \frac{y_{\sum_{i=1}^{n}\eta_i}\left(\gamma + x^2_{\sum_{i=1}^{n}\eta_i}\right)}{\sqrt{1+x^2_{\sum_{i=1}^{n}\eta_i}}} \\ -\sqrt{\lambda_{\sum_{i=1}^{n}\xi_i} y_{\sum_{i=1}^{n}\xi_i}} x_{\sum_{i=1}^{n}\xi_i} + \gamma \end{array} \right) \end{aligned} \tag{3.5.38}$$

where

$$\lambda_{\sum_{i=1}^{n}\xi_i} = \frac{4M_p^2}{3M^2_{\sum_{i=1}^{n}\xi_i}} \tag{3.5.39}$$

Now, from Eq. (3.5.9) and Eq. (3.5.25) with inverse square potential defined for multifield scalars $\sum_{i=1}^{n} \eta_i$ as

$$V\left(\sum_{i=1}^{n}\eta_i\right) = M^2_{\sum_{i=1}^{n}\eta_i} \sum_{i=1}^{n} \eta_i^{-2}$$

for evolution of the system. Here $M^2_{\sum_{i=1}^{n}\eta_i}$ is the mass scale for multifield scalars $\sum_{i=1}^{n} \eta_i$.

$$x'_{\sum_{i=1}^{n}\eta_i} = \frac{d\left(x_{\sum_{i=1}^{n}\eta_i}\right)}{dN} = -3\left(1 + x^2_{\sum_{i=1}^{n}\eta_i}\right)\left(x_{\sum_{i=1}^{n}\eta_i} + \sqrt{\lambda_{\sum_{i=1}^{n}\eta_i} y_{\sum_{i=1}^{n}\eta_i}}\right) \tag{3.5.40}$$

From Eq. (3.5.27) and Eq. (3.5.31) with using inverse square potential $V\left(\sum_{i=1}^{n}\eta_i\right) = M^2_{\sum_{i=1}^{n}\eta_i} \sum_{i=1}^{n} \eta_i^{-2}$, we find $y'_{\sum_{i=1}^{n}\eta_i} = \frac{d\left(y_{\sum_{i=1}^{n}\eta_i}\right)}{dN}$

$$\begin{aligned} &= 3y_{\sum_{i=1}^{n}\eta_i} \left[\begin{array}{l} -\frac{y_{\sum_{i=1}^{n}\xi_i}\left(\gamma - x^2_{\sum_{i=1}^{n}\xi_i}\right)}{\sqrt{1-x^2_{\sum_{i=1}^{n}\xi_i}}} - \frac{y_{\sum_{i=1}^{n}\eta_i}\left(\gamma + x^2_{\sum_{i=1}^{n}\eta_i}\right)}{\sqrt{1+x^2_{\sum_{i=1}^{n}\eta_i}}} \\ -\sqrt{\lambda_{\sum_{i=1}^{n}\eta_i} y_{\sum_{i=1}^{n}\eta_i}} x_{\sum_{i=1}^{n}\eta_i} + \gamma \end{array} \right] \end{aligned} \tag{3.5.41}$$

where

$$\lambda_{\sum_{i=1}^{n}\eta_i} = \frac{4M_p^2}{3M^2_{\sum_{i=1}^{n}\eta_i}} \tag{3.5.42}$$

The Figure-3.7 describes and illustrates the growth of general points of the scalar fields as the number of e-folds grows.

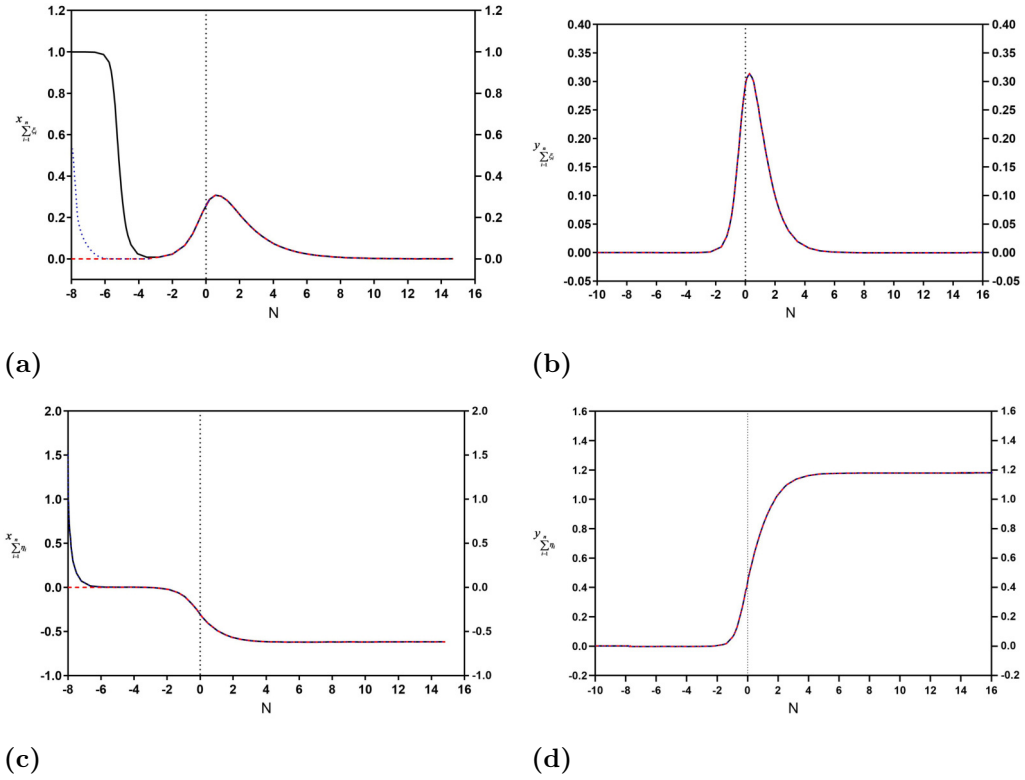

Figure– 3.7: The above figures indicate the behavior of general points of scalar multifields as the number of e-folds N evolve. The points $x_{\sum_{i=1}^{n}\xi_i}$, $y_{\sum_{i=1}^{n}\xi_i}$, $x_{\sum_{i=1}^{n}\eta_i}$ and $y_{\sum_{i=1}^{n}\eta_i}$ develop gradually as the function of e-folding number N for $\gamma = 1$ and $\lambda_{\sum_{i=1}^{n}\xi_i}$ and $\lambda_{\sum_{i=1}^{n}\eta_i}$ both with assigned a value equivalent to 0.33

3.6 Accelerating Universe in the Framework of $f(R)$ Modified Gravity

Here we revise the theoretical framework of $f(R)$ modified gravity which provides the methodology for finding out the results in study of these models.

3.6.1 Theoretical Framework of $f(R)$ Modified Gravity

In Section 2 here, we briefly review the theoretical background in which the cosmological dynamics of $f(R)$ modified gravity is developed. Taking start from Einstein Field Equation (EFE) of general relativity, that is

$$G_{\mu\nu} = R_{\mu\nu} - \frac{1}{2}g_{\mu\nu}R = 8\pi T_{\mu\nu} \tag{3.6.1}$$

we move forward to develop $f(R)$ dynamics. Eq. (3.6.1) corresponds to Einstein-Hilbert action with Lagrangian density $\mathcal{L} = \sqrt{-g}R$

$$S_{EH} = \frac{1}{16\pi G}\int d^4x\sqrt{-g}R + \int d^4x\sqrt{-g}\mathcal{L}_m \tag{3.6.2}$$

In scalar field models we usually modify RHS of EFE i.e., matter sector represented by energy-momentum tensor $T_{\mu\nu}$ and accordingly add some terms in it for a scalar field usually. On the other hand, the gravitational sector is modified which means that RHS is kept unaltered and LHS is modified that stands for the geometry of spacetime mimicking the role of gravity in $f(R)$, and this is why it is called model of modified gravity. The LHS of EFE is derived solely from the curvature invariant term i.e., Ricci scalar R, therefore, in the modified gravity we replace it by a general function of it in the action. Replacing Ricci scalar R in Einstein-Hilbert action given in Eq. (3.6.1) by a general function of R, that is $f(R)$ i.e., $R \to f(R)$, we have

$$S_{EH(f(R))} = \frac{1}{16\pi G}\int d^4x\sqrt{-g}f(R) + \int d^4x\sqrt{-g}\mathcal{L}_m \tag{3.6.3}$$

The variation of Eq. (3.6.2) for the curved geometry would be written as

$$\delta S_{EH(f(R))} = \int d^4x\delta\left(\sqrt{-g}f(R)\right) \tag{3.6.4}$$

where the variation of Eq. (3.6.2) with inverse metric $g^{\mu\nu} \to g^{\mu\nu} + \delta g^{\mu\nu}$ yields the following modified gravity equation through performing tedious calculations

$$F(R)R_{\mu\nu} - \frac{1}{2}f(R)g_{\mu\nu} - (\nabla_\mu\nabla_\nu - g_{\mu\nu}\Box)F(R) = k^2T_{\mu\nu} \tag{3.6.5}$$

where $\Box = g^{\mu\nu}\nabla_\mu\nabla_\nu = \nabla_\nu\nabla^\nu$ and ∇_μ are the covariant d'Alembert operator or d'Alembertian and covariant derivative operator respectively whereas $F(R) = f_{,R}(R)$.

The modified $f(R)$ gravity equation expressed in Eq. (3.6.5) reduces to general relativity equation for $f(R) = R$ and $\frac{\partial f(R)}{\partial R} = F(R) = 1$. In Eq. (3.6.4), the LHS is the modified form of Einstein tensor $G_{\mu\nu} = R_{\mu\nu} - \frac{1}{2}g_{\mu\nu}R$ and represents the modified geometry in the framework of $f(R)$. We can contract Eq. (3.6.4) with $g^{\mu\nu}$ to determine the trace of modified EFE

$$F(R)R + 3\Box F(R) - 2f(R) = k^2 T \tag{3.6.6}$$

For a vacuum solution $T = 0$, the de Sitter space with curvature term R to be constant

$$F(R)R + 3\Box F(R) - 2f(R) = 0 \tag{3.6.7}$$

Eq. (3.6.7) represents an inflationary solution with the term $3\Box F(R) = 0$ at the de Sitter point.

$$F(R)R - 2f(R) = 0 \tag{3.6.8}$$

If the condition in Eq. (3.6.8) is fulfilled, the late time de Sitter solution can be obtained in $f(R)$-based models that play the role of dark energy through modification of the geometry of spacetime.

3.6.1.1 Modified Version of Friedmann's Equations In the Framework of $f(R)$ Gravity For a Spatially Flat and Homogeneous Universe

For a homogeneous, isotropic and spatially flat and expanding FLRW universe with a time-dependent scale factor $a(t)$

$$ds^2 = g_{\mu\nu}dx^\mu dx^\nu = -dt^2 + a^2(t)\left(dx^2 + dy^2 + dz^2\right) \tag{3.6.9}$$

Now, Friedmann's equations for the modified Einstein field equation as given by Eq. (3.6.5) can be determined going through the lengthy calculations. Where we find

$$R_{00} = -3\left(\dot{H} + H^2\right) \tag{3.6.10}$$

$$R_{ii} = 2\dot{a}^2 + a\ddot{a} \tag{3.6.11}$$

and

$$R = 6\left(\dot{H} + 2H^2\right) \tag{3.6.12}$$

Eq. (3.6.10) can be further re-expressed using Eq. (3.6.12)

$$R_{00} = -\frac{1}{2}R + 3H^2 \tag{3.6.13}$$

for

$$T_{\mu\nu} = diag\left(-\rho_m, p_m, p_m, p_m\right) \tag{3.6.14}$$

where trace of $T_{\mu\nu}$ is $(-\rho_m + 3p_m)$. Now, on using $\mu = \nu = 0$ in Eq. (3.6.5) gives

$$F(R) R_{00} - \frac{1}{2} f(R) g_{00} - \nabla_0 \nabla_0 F(R) + g_{00} \Box F(R) = k^2 T_{00} \tag{3.6.15}$$

Solving through tedious calculations by using Eq. (3.6.10) and Eq. (3.6.14), we reach at

$$3H^2 F = \frac{1}{2}(FR - f) - 3H\dot{F} + k^2(\rho_m + \rho_r) \tag{3.6.16}$$

again for $\mu = \nu = i$ in Eq. (3.6.5), we have

$$F(R) R_{ii} - \frac{1}{2} f(R) g_{ii} - \nabla_i \nabla_i F(R) + g_{ii} \Box F(R) = k^2 T_{ii} \tag{3.6.17}$$

We find

$$g_{ii} \Box F(R) = -2a^2 H\dot{F} - a^2 \ddot{F} + \nabla_i \nabla_i F \tag{3.6.18}$$

Using Eq. (3.6.11), Eq. (3.6.14) and Eq. (3.6.8) in Eq. (3.6.17), we obtain

$$2\dot{H}F = -\ddot{F} + H\dot{F} - k(\rho_m + p_m) \tag{3.6.19}$$

Eq. (3.6.16) and Eq. (3.6.19) taken together determine the background dynamics of a flat FLRW universe governed by $f(R)$ gravity. From Eq. (3.6.16), on dividing by $3H^2F$ and for $\rho = \rho_r + \rho_m$, we can construct a dynamical autonomous system in the framework of $f(R)$, that is

$$-\frac{\dot{F}}{HF} + \left(-\frac{f}{6H^2F}\right) + \frac{R}{6H^2} + \frac{k^2\rho_r}{3H^2F} + \frac{k^2\rho_m}{3H^2F} = 1 \tag{3.6.20}$$

Now, the following parameters (Amendola et al., 2007) are defined

$$x_1 = -\frac{\dot{F}}{HF} \tag{3.6.21}$$

$$x_2 = -\frac{f}{6H^2F} \tag{3.6.22}$$

$$x_3 = \frac{R}{6H^2} \tag{3.6.23}$$

$$x_4 = \frac{k^2\rho_r}{3H^2F} \tag{3.6.24}$$

$$x_5 = \frac{k^2\rho_m}{3H^2F} \tag{3.6.25}$$

Eq. (3.6.23) can be recast by using Eq. (3.6.12)

$$x_3 = \frac{\dot{H}}{H^2} + 2 = \frac{R}{6H^2} \tag{3.6.26}$$

We have a constraint from Eq. (3.6.20) on using the defined dimensionless parameters in it

$$x_1 + x_2 + x_3 + x_4 + x_5 = 1 \tag{3.6.27}$$

Now, for $p_m = \frac{4}{3}\rho_r$, $N = \ln a$ and $\dot{H} = H'H$, where dot "." and prime "′" denote differentiation with respect to the cosmic time "t" and "N" that is natural logarithm of the scale factor a, respectively, so that we can determine the following dynamical system, after going through a process of tedious calculations

$$\frac{dx_1}{dN} = x_1^2 - x_1x_3 - 3x_2 - x_3 + x_4 - 1 \tag{3.6.28}$$

$$\frac{dx_2}{dN} = x_1x_2 - 2x_2\left(x_3 - 2\right) + \frac{x_1x_3}{m} \tag{3.6.29}$$

$$\frac{dx_3}{dN} = -2x_3\left(x_3 - 2\right) - \frac{x_1x_3}{m} \tag{3.6.30}$$

$$\frac{dx_4}{dN} = x_4\left(x_1 - 2x_3\right) \tag{3.6.31}$$

$$\frac{dx_5}{dN} = x_5\left(x_1 - 2x_3\right) \tag{3.6.32}$$

where,

$$m = \frac{Rf_{,RR}}{f_{,R}} = \frac{d\log f_{,R}}{d\log R} \tag{3.6.33}$$

It is important to note that m is the most significant definition in the construct of $f(R)$ whereas the derivative terms $f_{,R} = \frac{\partial f}{\partial R}$ and $f_{,RR} = \frac{\partial^2 f}{\partial R^2}$. The variable m measures the deviation of $f(R)$ cosmology from the flat ΛCDM cosmological model that corresponds to the vanishing of m (Amendola & Tsujikawa, 2008). The notation "," written in the place of subscript or as subscript denotes the partial differentiation with respect to the variable written adjacent to it such as here is R. Another variable (parameter) r, in addition to m is defined as

$$r = -\frac{Rf_{,R}}{f} = -\frac{d\log f}{d\log R} = \frac{x_3}{x_2} \tag{3.6.34}$$

It can be observed from the coordinates x_2 and x_3 in the points P_5 and P_6 respectively in terms of which r is described that they are joined with the line $m(r) = -r - 1$ in the light of Eq. (3.6.34) above. The effective equation of state parameter w_{eff}, can also be written with the help of Eq. (3.6.16) and Eq. (3.6.19) through division

$$w_{eff} = -1 - \frac{2\dot{H}}{3H^2} \tag{3.6.35}$$

or using Eq. (3.6.26), it gives

$$w_{eff} = -\frac{1}{3}\left(-1 + 2x_3\right) \tag{3.6.36}$$

Further, another form can also be written as

$$w_{DE} = -1 + \frac{\ddot{F} - H\dot{F} + k\left(\rho + p\right)}{\frac{1}{2}\left(FR - f\right) - 3H\dot{F} + k\rho_M} \tag{3.6.37}$$

It can be written in terms of critical points as well

$$w_{DE} = -\frac{1}{3}\frac{-1 + 2x_3 + \frac{F}{F_0}x_4}{1 - \frac{F}{F_0}(1 - x_1 - x_2 - x_3)} \tag{3.6.38}$$

The model dependent values can be determined for the points x_1, x_2, x_3, x_4 and x_5. The fixed points corresponding to any $f(R)$ model can be determined from the system defined above. The certain properties of these points similar to the effective equation of state parameter that describe the evolution of the universe are described below. For the matter-dominated epoch these are determined for the dynamical system developed above generally. For this epoch $x_4 = w = \frac{k^2\rho_r}{3FH^2} = 0$. These fixed points in the context of $f(R)$ are responsible for the description of universe through their different properties. The properties of these fixed points $(P_1 - P_6)$ are very interesting and are given underneath.

P_1: $(x_1, x_2, x_3, x_4) = (-4, 5, 0, 0), P_{1(EV)} : \left(-5, -4, -3, \frac{4(1+m)}{m}\right), w_{eff} = \frac{1}{3}, \Omega_m = 0, \Omega_r = 0, \Omega_{GC} = 1$

The point P_1 is unable to produce matter dominated epoch since $\Omega_m = 0$ and it generates irrelevant effective equation of state $w_{eff} = \frac{1}{3}$ which could not be used to derive the epoch of accelerated expansion of the late time universe as it requires negative value of unity or closer to it. Figure-3.8 below gives evolution of P_1.

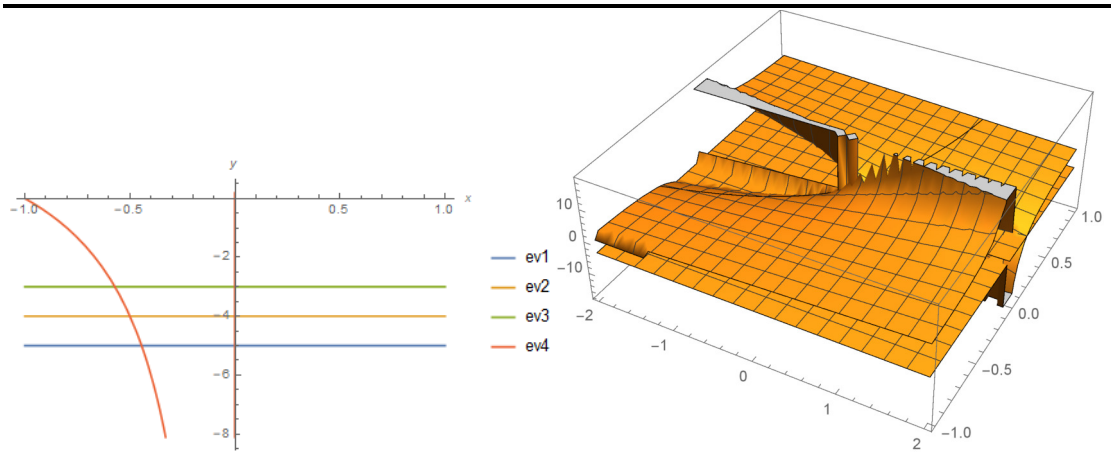

(a) **(b)**

Figure– 3.8: The evolution of point P_1 for general $f(R)$ for $-1 < m = \frac{Rf_{,RR}}{f_{,R}} < 1$. In Fig1(a) shows a plot in two dimensions whereas in Fig1(b) a three dimensional plot is given

P_2: $(x_1, x_2, x_3, x_4) = (-1, 0, 0, 0)\,, P_{2(EV)} : \left(-2, -1, 3, \frac{1+4m}{m}\right), w_{eff} = \frac{1}{3}, \Omega_m = 2, \Omega_r = 0, \Omega_{GC} = -1$

The point P_2 could not give perfect matter dominated epoch before the expansion begins accelerating. Similarly, its effective equation of state $w_{eff} = \frac{1}{3}$ which could not shed light on the late time accelerated expansion is irrelevant. The point is, however dominated by geometric curvature. Figure-3.9 below gives evolution of P_2.

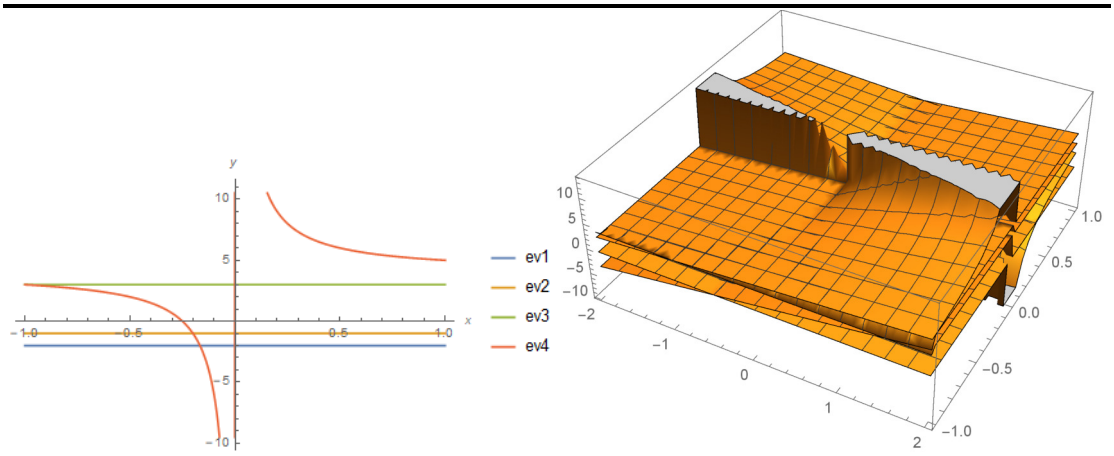

(a) **(b)**

Figure– 3.9: The evolution of point P_2 for general $f(R)$ for $-1 < m = \frac{Rf_{,RR}}{f_{,R}} < 1$. In Fig1(a) shows a plot in two dimensions whereas in Fig1(b) a three dimensional plot is given

P_3: $(x_1, x_2, x_3, x_4) = (0, 0, 0, 1)\,, P_{3(EV)} : (4, 4, -1, 1)\,, w_{eff} = \frac{1}{3}, \Omega_m = 0, \Omega_r = 1, \Omega_{GC} = 0$

The point P_3 could not give matter dominated epoch before the expansion begins to accelerate as it considers matter density to be vanishing. Similarly, its effective equation of state is $w_{eff} = \frac{1}{3}$ which could not shed light on the late time accelerated expansion rather is irrelevant. The geometric curvature also vanishes at this point. Figure-3.10 below gives evolution of P_3.

P_4: $(x_1, x_2, x_3, x_4) = (0, -1, 2, 0)\,, P_{4(EV)} : \left(-4, -3, \frac{-3m-\sqrt{m}\sqrt{-16+25m}}{2m}, \frac{-3m+\sqrt{m}\sqrt{-16+25m}}{2m}\right)$ $w_{eff} = -1, \Omega_m = 0, \Omega_r = 0, \Omega_{GC} = 1$. It is very important point as it gives $w_{eff} = -1$ which leads to the late time de Sitter point with $R = -2$ satisfying

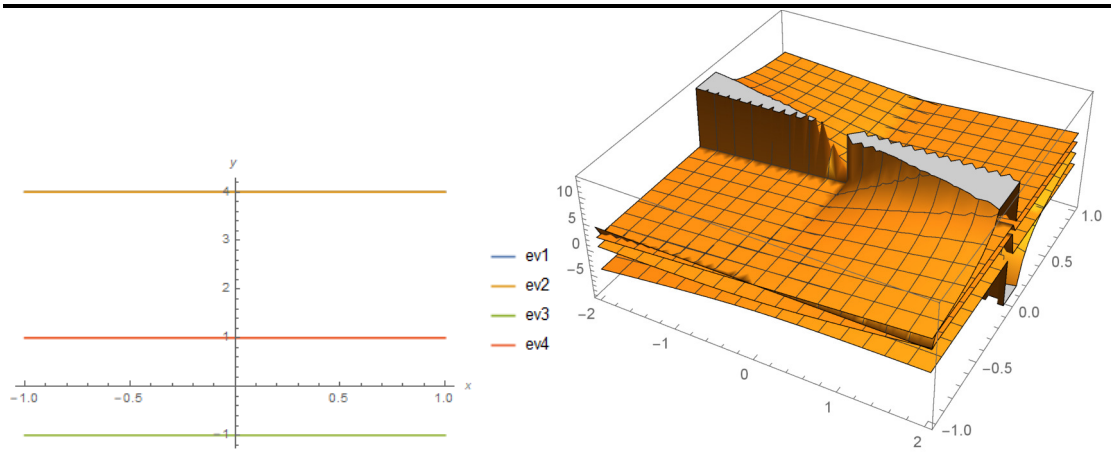

(a) **(b)**

Figure– 3.10: The evolution of point P_3 for general $f(R)$ for $-1 < m = \frac{Rf_{,RR}}{f_{,R}} < 1$. In Fig1(a) shows a plot in two dimensions whereas in Fig1(b) a three dimensional plot is given

the condition $F(R)R - 2f(R) = 0$. The point is related with the accelerated expansion of the universe and is dominated by curvature geometrically. Figure-3.11 below gives evolution of P_4.

P_5: $(x_1, x_2, x_3, x_4) = (1, 0, 0, 0), P_{3(EV)} : \left(1, 2, 5, \frac{-1+4m}{m}\right), w_{eff} = \frac{1}{3}, \Omega_m = 0, \Omega_r = 0, \Omega_{GC} = 1$

The point P_5 could not give matter dominated epoch as $\Omega_m = 0$ and is concerned as well with the irrelevant effective equation of state since $w_{eff} = \frac{1}{3}$ which could not throw light on the accelerated expansion of the late time. It is, however dominated by geometric curvature. Figure-3.12 below gives evolution of P_5.

P_6: $(x_1, x_2, x_3, x_4) = \left(\frac{3m}{1+m}, \frac{1}{6}\left(-6 + \frac{9m}{(1+m)^2} + \frac{18m^2}{(1+m)^2} + \frac{3}{1+m} - \frac{12m}{1+m}\right), \frac{1+4m}{2(1+m)}, 0\right), P_{6(EV)} :$
$\left(\begin{array}{c} -1, \frac{3\left(m+2m^2+m^3\right)}{m(1+m)^2}, \frac{-3m-3m^2-\sqrt{m}(1+m)\sqrt{-16-31m+160m^2+256m^3}}{4m(1+m)^2}, \\ \frac{-3m-3m^2+\sqrt{m}(1+m)\sqrt{-16-31m+160m^2+256m^3}}{4m(1+m)^2} \end{array}\right), w_{eff} = -\frac{m}{1+m}, \Omega_m = \frac{2-3m-8m^2}{2(1+m)^2}, \Omega_r = 0, \Omega_{GC} = \frac{m(7+10m)}{2(1+m)^2}$

The point P_6 gives matter dominated epoch as for a range of values between -1 and +1 and is concerned as well with effective equation of state. It could not produce radiation epoch, however is related with curvature domination for values of m. Figure-3.13 below gives evolution of P_6.

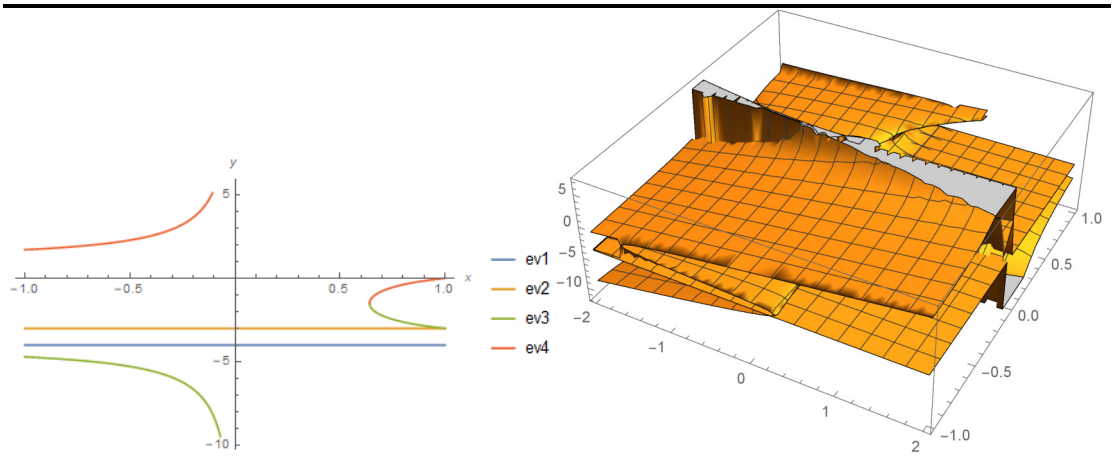

(a) **(b)**

Figure– 3.11: The evolution of point P_4 for general $f(R)$ for $-1 < m = \frac{Rf_{,RR}}{f_{,R}} < 1$. In Fig1(a) shows a plot in two dimensions whereas in Fig1(b) a three dimensional plot is given

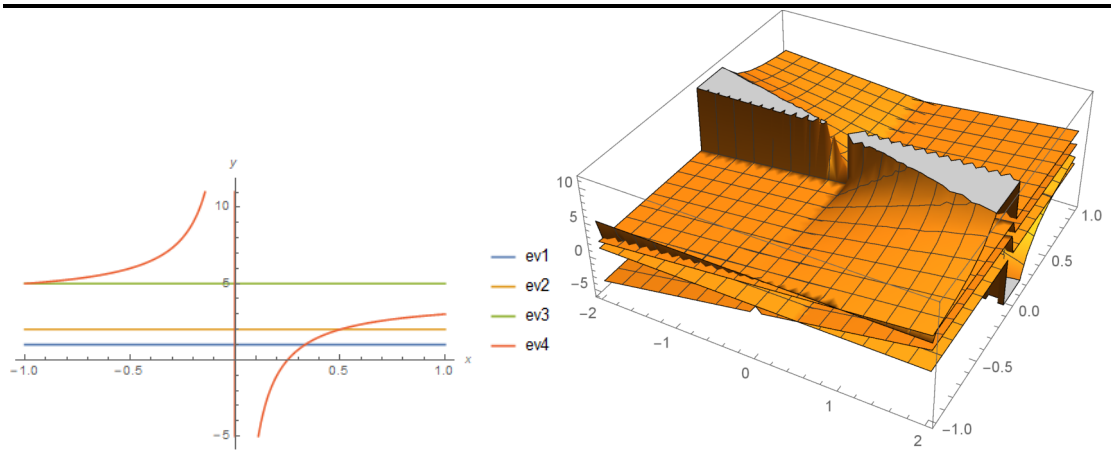

(a) **(b)**

Figure– 3.12: The evolution of point P_5 for general $f(R)$ for $-1 < m = \frac{Rf_{,RR}}{f_{,R}} < 1$. In Fig1(a) shows a plot in two dimensions whereas in Fig1(b) a three dimensional plot is given

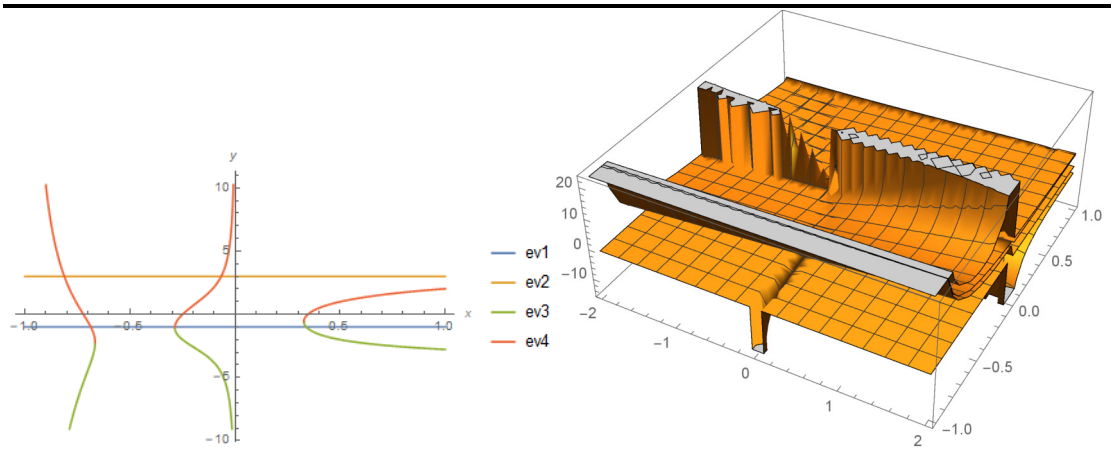

(a) **(b)**

Figure– 3.13: The evolution of point P_6 for general $f(R)$ for $-1 < m = \frac{Rf_{,RR}}{f_{,R}} < 1$. In Fig1(a) shows a plot in two dimensions whereas in Fig1(b) a three dimensional plot is given

P_7: $(x_1, x_2, x_3, x_4) = \left(\frac{4m}{1+m}, -\frac{2m}{(1+m)^2}, \frac{2m}{1+m}, \frac{1-2m-5m^2}{(1+m)^2}\right)$,

$P_{7(EV)}$: $\begin{pmatrix} 1, \frac{4\left(1+2m+m^2\right)}{(1+m)^2}, \frac{-1+m^2-\sqrt{3}\sqrt{-5+42m^2+64m^3+27m^4}}{2(1+m)^2}, \\ \frac{-1+m^2+\sqrt{3}\sqrt{-5+42m^2+64m^3+27m^4}}{2(1+m)^2} \end{pmatrix}$, $w_{eff} = \frac{1-3m}{3+3m}, \Omega_m = 0, \Omega_r = \frac{1-2m-5m^2}{(1+m)^2}, \Omega_{GC} = \frac{2m(2+3m)}{(1+m)^2}$

The point P_7 is very significant as it allows the formation of matter-domination era. The matter-dominated era corresponding to $\Omega_m = 1 - \frac{(10m+7)m}{2(m+1)^2}$ with effective equation of state $w_{eff} < 0$ can be achieved for the value of m being close to 0 i.e $m \to 0$. This point can launch the universe enter into the acceleratedly expanding phase for small value of m. Figure-3.14 below gives evolution of P_7.

P_8: $(x_1, x_2, x_3, x_4) = \left(-\frac{2(-1+m)}{1+2m}, -\frac{1-4m}{m+2m^2}, \frac{-1+3m+4m^2}{m(1+2m)}, 0\right)$,

$P_{8(EV)}$: $\left(-\frac{2\left(-1+2m+5m^2\right)}{m(1+2m)}, \frac{2m-3m^2-8m^3}{m^2(1+2m)}, \frac{m-2m^2-8m^3}{m^2(1+2m)}, -\frac{2\left(-m+m^3\right)}{m^2(1+2m)}\right)$

$w_{eff} = \frac{2-5m-6m^2}{3m+6m^2}, \Omega_m = 0, \Omega_r = 0, \Omega_{GC} = 1$. The point P_8 is very important with regard to the accelerated expansion with effective equation of state $w_{eff} < -\frac{1}{3}$ provided that $-\frac{1}{2} < m < 0$ or $\frac{\sqrt{3}-1}{2} < m < -\frac{\sqrt{3}+1}{2}$. Figure-3.15 below gives evolution of P_8.

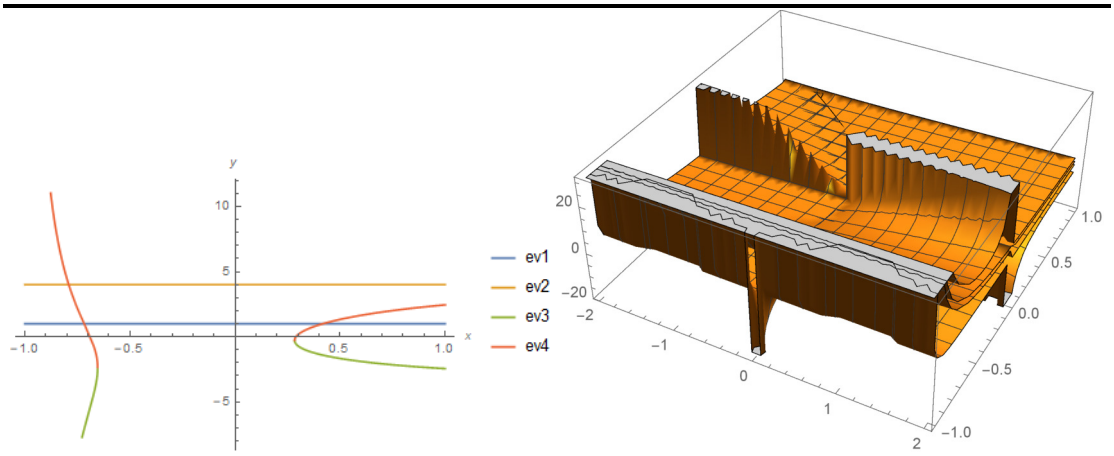

(a) **(b)**

Figure– 3.14: The evolution of point P_7 for general $f(R)$ for $-1 < m = \frac{Rf_{,RR}}{f_{,R}} < 1$. In Fig1(a) shows a plot in two dimensions whereas in Fig1(b) a three dimensional plot is given

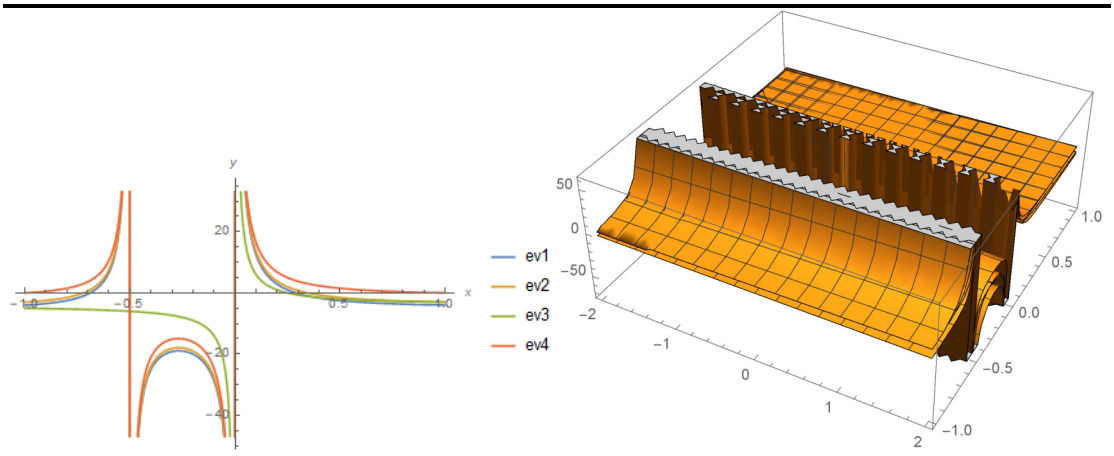

(a) **(b)**

Figure– 3.15: The evolution of point P_8 for general $f(R)$ for $-1 < m = \frac{Rf_{,RR}}{f_{,R}} < 1$. In Fig1(a) shows a plot in two dimensions whereas in Fig1(b) a three dimensional plot is given

3.6.1.2 Constraints For Viable $f(R)$ Models at Local and Cosmological Scales

In $f(R)$ gravity perspective, inflation as the accelerated expansion in the early universe was first described by Starobinsky model $f(R) = R + \alpha R^2$ (Starobinsky, 1980). Since that time, it is known that the model has viability only for inflation and is not any more concerned with the late time accelerated expansion. The reason behind it is that as long as the quadratic term R^2 maintains itself, inflationary phase continues, however the moment it begins growing smaller in comparison with linear term R, the early accelerated expansion comes to the end. Likewise, the models with the negative powers of scalar invariant undergo the similar situation and limitations. There are, however some models that do not show viability for local gravity constraints (Hu & Sawicki, 2007; Capozziello & Tsujikawa, 2008) and some are not viable for global constraints. Therefore, it is important to know which models are viable and which are the otherwise. In this regard, there some viability constraints that a $f(R)$ model must fulfill. The set of viability conditions or constraints which must be satisfied for an $f(R)$ model to be viable and to be working realistically, are expressed below (Amendola & Tsujikawa, 2010; Shah & Samanta, 2019; Bamba, 2013):

1. $F = \frac{df(R)}{dR} > 0$.
2. $F_{,R} = \frac{d^2 f(R)}{dR} > 0$.
3. $f \to R - 2\Lambda$.
4. $0 < m < 1$ at $r = -2$, where $m = \frac{R\frac{d^2 f}{dR}}{\frac{df}{dR}} = \frac{RF_{,R}}{F}$.
5. Constraints due to violation of the equivalence principle.

CHAPTER-04

RESULTS AND DISCUSSION

4.1 On the Cosmological Dynamics of Spacetime and Basics of Cosmology

This section is retained for the sake of keeping the corresponding sections in order as it is related with introduction section1.1. Therefore, it has no significant analytical or numerical results.

4.2 Multifield Inflationary Universe and Spectrum of Curvature Perturbation

It can be noted from Eq. (3.2.75) in chapter 3 of methodology that all the terms included in the $\ln\left(\frac{\phi_k^s}{\phi_k^e}\right)$ might be equivalent on account of what is expressed in Eq. (3.2.71). Now, the Eq. (3.2.75) is representing the same equation for the corresponding single field case. The value of $\ln\left(\frac{\phi_k^s}{\phi_k^e}\right)$ in Eq. (3.2.71) will be smaller for the bigger value of μ_i when Λ_i are taken equivalent to the μ_i. If we consider $\mu_k = Max\,(\mu_n)$ where n denotes natural numbers. This gives rise to $\frac{\mu_i}{\mu_k} < 1$ which implies that the spectrum is more redder than its corresponding spectrum resulting from Eq. (3.2.75) for a single scalar field ϕ_k. In this case the value of $\ln\left(\frac{\phi_k^s}{\phi_k^e}\right)$ would represent almost the smallest from all the values of $\ln\left(\frac{\phi_i^s}{\phi_i^e}\right)$ which indicates that in Eq. (3.2.75) the case of single scalar field ϕ_k the value of k approaches nearer to unity. On the other hand If we take into account $\mu_k = Min\,(\mu_n)$ where n denotes natural numbers. This gives rise to $\frac{\mu_i}{\mu_k} > 1$ which leads to the factual result that the spectrum is less redder than its corresponding spectrum resulting from Eq. (3.2.75) for a single scalar field ϕ_k. In this case the value of $\ln\left(\frac{\phi_k^s}{\phi_k^e}\right)$ would represent almost the biggest one out of all the values of $\ln\left(\frac{\phi_i^s}{\phi_i^e}\right)$ which shows that in Eq. (3.2.75) the case of single scalar field ϕ_k the value of k shifts away from unity. It means that the value of the scalar spectral index falls between that of single field in general for the biggest μ_k and the smallest accordingly. Below in Table-4.1 and Table-4.2 are listed the corresponding range of spectral indices resulting from variant values of N and against the values of p, the corresponding range of N respectively. Below in Figure-4.1 and Figure-4.2, spectral index (n_s) is plotted against e-folding number N for a range of values.

Table– 4.1: Spectral index (n_s) in terms of e-fold number N for a range of values of p

Sr.No	**values of** p	**spectral index in terms of e-folding number** (N)
2	$p = -300$	$0-\frac{4}{N}$
3	$p = -200$	$0-\frac{3}{N}$
4	$p = -100$	0 undefined
5	$p = 000$	$0-\frac{1}{N}$
6	$p = 100$	$0-\frac{4}{3N}$
7	$p = 200$	$0-\frac{3}{2N}$
8	$p = 300$	$0-\frac{8}{5N}$
9	$p = 400$	$0-\frac{5}{3N}$

Table– 4.2: Spectral index (n_s) against the number of e-folds N

Sr.No	**e-folding Number** (N)	**spectral index** (n_s)
1	30	0.90
2	35	0.914
3	40	0.925
4	45	0.93
5	50	0.94
6	55	0.945
7	60	0.95
8	65	0.953
9	70	0.96

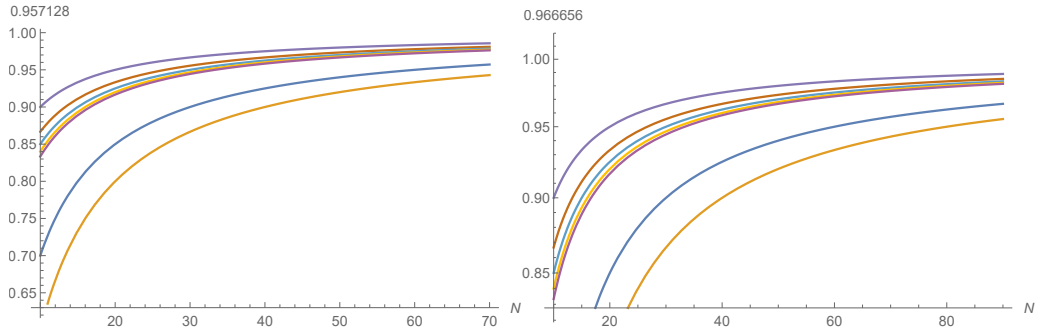

(a) **(b)**

Figure– 4.1: Plot of spectral index (n_s) against the e-folding Number (N) for the values of p. At the right there is logarithm of the plot

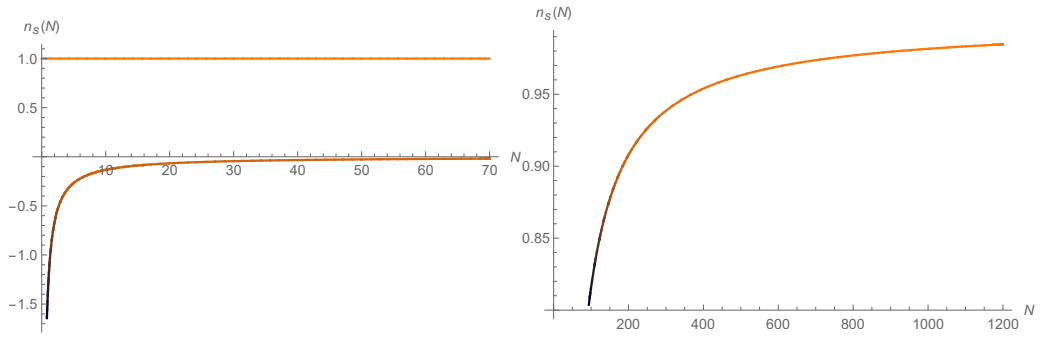

(a) **(b)**

Figure– 4.2: Plot of spectral index (n_s) against the e-folding Number (N)

Now, considering that the fields are uncoupled so that the dynamics during slow roll proceeds as

$$\Delta\phi \simeq \sqrt{\sum_i \left(\frac{\partial_t \phi_i}{H}\right)^2} \tag{4.2.1}$$

and Friedmann equation

$$H^2 = \frac{8\pi G}{3}\rho + \frac{k^2}{a^2} \tag{4.2.2}$$

using Eq. (3.2.3), Eq. (3.2.5) and Eq. (4.2.2) in Eq. (4.2.1) above, we have

$$\Delta\phi \simeq pM_p^2 \frac{\sqrt{\sum_i \left(\frac{\Lambda_i}{\mu_i}\left(\frac{\phi_i}{\mu_i}\right)^{-(p+1)}\right)^2}}{\sum_i \Lambda_i \left(1 - \left(\frac{\phi_i}{\mu_i}\right)^{-p}\right)} \tag{4.2.3}$$

The quantum fluctuations during this phase

$$\delta\phi \simeq \sqrt{\sum_i (\delta\phi_i)} \tag{4.2.4}$$

where $\delta\phi_i \sim \frac{H}{2\pi}$ and making use of Eqs. (3.2.1, 4.2.2), it gives

$$\delta\phi \simeq \frac{1}{\pi M_p}\sqrt{\frac{N}{12}}\sqrt{\sum_i \Lambda_i \left(1 - \left(\frac{\phi_i}{\mu_i}\right)^{-p}\right)} \tag{4.2.5}$$

The critical field values can be reached at $\Delta\phi \simeq \delta\phi$, for $p = 2$, we have

$$p^2 M_p^6 \sum_i \left(\frac{\Lambda_i}{\mu_i}\left(\frac{\phi_i}{\mu_i}\right)^{-(p+1)}\right)^2 \simeq \frac{N}{12\pi^2}\sum_i \left(\Lambda_i \left(1 - \left(\frac{\phi_i}{\mu_i}\right)^{-p}\right)\right)^3 \tag{4.2.6}$$

using now the slow roll condition $\varepsilon << 1$, from Eq. (3.2.1) and Eq. (3.2.5) we get the following relation

$$\frac{1}{2}pM_p^2 \sum_i \left(\frac{\Lambda_i}{\mu_i}\left(\frac{\phi_i}{\mu_i}\right)^{-(p+1)}\right)^2 << \sum_i \left(\Lambda_i \left(1 - \left(\frac{\phi_i}{\mu_i}\right)^{-p}\right)\right)^2 \tag{4.2.7}$$

or towards the end of slow roll phase

$$\frac{1}{2}pM_p^2 \sum_i \left(\frac{\Lambda_i}{\mu_i}\left(\frac{\phi_i}{\mu_i}\right)^{-(p+1)}\right)^2 \simeq \sum_i \left(\Lambda_i \left(1 - \left(\frac{\phi_i}{\mu_i}\right)^{-p}\right)\right)^2 \tag{4.2.8}$$

R. Easter and L. McAllister have developed a very powerful technique in order to work out the problem of different scale of masses (Easther & McAllister, 2006). The method is frequently employed in Nflation or multiple field scenarios. They have proposed a law regarding the general case of the distribution of mass scales which is known as Marčenko-Pastur law or distribution. In multifield models of inflation it is customary to make use of random matrix theory which might play a very basic and important role

in the distribution of different masses related to the spectrum. This is accomplished by using some suitable law, the one best example is Marčenko-Pastur distribution. The law was first used in string theory where the problem of mass distribution axion field was being faced. In multifield models there occur different trajectorie of inflation and therefore become susceptible to the initial conditions as the values of the fields laying in the background dynamics. As is the case in most cases inflationary scenarios are based on the hypothesis taken ad hoc which pose the problem of finding the initial conditions to not much reliable. Based on it, inflationary parameters, in some specific scenarios are predicted not to depend largely on priors of initial conditions (Easther, Frazer, Peiris, & Price, 2014). We utilize Marčenko-Pastur law here for the distribution of mass scale factors μ or Λ_i. Marčenko-Pastur law makes the use of the parameters $\bar{\mu}$ and β, where β is the ratio of rows and columns of mass scale factor μ. We can express it as $\beta = \frac{n}{n+r}$ for any mass scale matrix of order $(n+r) \times n$. Now the values related with μ for the smallest and for the largest are given by

$$\mu_1^2 = x = \bar{\mu}^2\Big(1 - \sqrt{\beta}\Big)^2 \tag{4.2.9}$$

$$\mu_2^2 = y = \bar{\mu}^2\Big(1 + \sqrt{\beta}\Big)^2 \tag{4.2.10}$$

respectively and the field value during slow roll approximation comes out to be

$$\phi_j\left(t\right) \simeq \phi_j\left(t_0\right)\left[T\left(t\right)\right]^{\frac{\mu_1^2}{y}} \tag{4.2.11}$$

where $T\left(t\right) = \frac{\phi_n(t)}{\phi_n(t_0)}$ represents the ratio between the larger field at some time t and initial value at some time t_0. Defining now in Eq. (4.2.6) and Eq. (4.2.8) $z = 2\frac{\ln[T(t)]}{y}$ where ϕ_j^2 is replaced by $\phi_j^2\left(t_0\right)e^{z\mu_i^2}$. We can compute in a straightforward way the respective range of average values of mass distributions regardless of the initial field distributions when we neglect correlations between them. Now we employ the power series expansion and calculate the average value of the exponential term.

$$\begin{aligned}\langle e^{z\mu_i^2}\rangle &= \sum_i \langle\mu_i^2\rangle\tfrac{c^j}{j} = \bar{\mu}^{2i}\sum_{j=1}^{i} T\left(i,j\right)\beta^{j-1}\tfrac{c^j}{j} \\ &= \sum_{i=0}^{\infty}\bar{\mu}^{2i}F_1\left(1-i,-i,2,\beta\right)\tfrac{c^j}{j}\end{aligned} \tag{4.2.12}$$

Now, Eq. (4.2.6) can be expressed in the form

$$\mu_j^2\phi_j^2 = n\alpha\bar{\mu}^2\sum_{i=0}^{\infty}\bar{\mu}^{2i}F_1\left(-i,-i-1,2,\beta\right)\frac{z^i}{i} \tag{4.2.13}$$

where $\alpha = \langle\zeta_j^2\left(t_0\right)\rangle$, moreover, we have

$$\mu_j^4\phi_j^2 = n\alpha\bar{\mu}^4\sum_{i=0}^{\infty}\bar{\mu}^{2i}F_1\left(-i-1,-i-2,2,\beta\right)\frac{z^i}{i} \tag{4.2.14}$$

We substitute Eq. (4.2.13) and Eq. (4.2.14) in Eq. (4.2.6) first and afterwards in Eq. (4.2.8), and obtain for α respectively

$$\begin{cases} \alpha = p^2 M_p^6 \sum\limits_i \left(\frac{\Lambda_i}{\mu_i} \left(\frac{\phi_i}{\mu_i} \right)^{-(p+1)} \right)^2 f_1(t,\beta) \\ \alpha = \frac{1}{2} p M_p^2 \sum\limits_i \left(\frac{\Lambda_i}{\mu_i} \left(\frac{\phi_i}{\mu_i} \right)^{-(p+1)} \right)^2 f_2(t,\beta) \end{cases} \tag{4.2.15}$$

where

$$\begin{cases} f_1(t,\beta) = \frac{\left(\sum\limits_{i=0}^{\infty} \bar{\mu}^{2i} F_1(-i-1,-i-2,2,\beta) \frac{z^i}{i} \right)^{\frac{3}{2}}}{\left(\sum\limits_{i=0}^{\infty} \bar{\mu}^{2i} F_1(-i,-i-1,2,\beta) \frac{z^i}{i} \right)^{\frac{5}{2}}} \\ f_2(t,\beta) = \frac{\left(\sum\limits_{i=0}^{\infty} \bar{\mu}^{2i} F_1(-i-1,-i-2,2,\beta) \frac{z^i}{i} \right)^{\frac{1}{2}}}{\left(\sum\limits_{i=0}^{\infty} \bar{\mu}^{2i} F_1(-i,-i-1,2,\beta) \frac{z^i}{i} \right)^{2}} \end{cases} \tag{4.2.16}$$

In Figure-4.3, distribution of mass scales is plotted in accordance with Marčenko-Pastur law. we can have values of the functions $f_1(t,\beta)$ and $f_2(t,\beta)$ corresponding to the

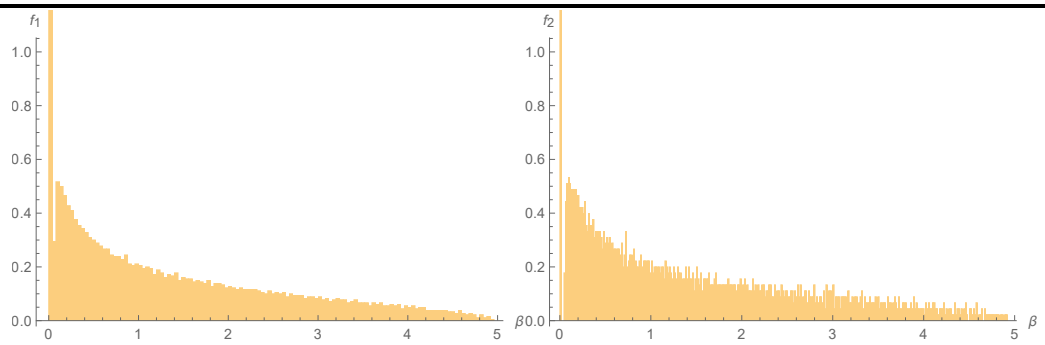

(a) **(b)**

Figure– 4.3: This figure demonstrates the mass distribution according to Marčenko-Pastur law, where it takes place against the dimensionless mass variables in the case β takes on different values. c is along parallel axis when the functions are along vertical axes. It can be noted that the law of large numbers of mass scales ensures that the mass distribution of N fields obeys the distribution probability like that of a single field

distinct values as adapted by or assigned to the parameter z. However, for comparatively bigger values of it, the functions behave like a constant as the figures show it. In the case, when values of the fields and mass scales are equivalent, the functions $f_1(t,\beta) = f_2(t,\beta) \simeq 1$ and from Eq. (4.2.15) the value of $\alpha \simeq \phi^2$ and $\bar{m} = m$, in this case we regain the values of the fields.

4.2.1 Discussion and Concluding Remarks

In this problem related to multifield inflation, we discussed the inflationary phase by considering a small multifield potential written in the generalized form $\sum_i V_i(\phi_i) = \sum_i \Lambda_i \left[1 - \left(\frac{\phi_i}{\mu_i}\right)^p\right]$ with p being negative. This potential represents the small field inflationary model and can be regarded as Taylor series expansion about the origin of its minima and maxima in its lowest order. In small field models of inflation the field is usually considered beginning with about an unstable equilibrium around the origin and then rolling down along its potential about the origin. As the field expression denotes a generalized potential to stand for the multifield inflationary potential. i denotes any ith field taken into account multiple fields. The parameters Λ_i and μ_i denote the height and tilt of the ith potential in the multiple fields. The spectrum of curvature perturbations which give rise to the growth of cosmic structure are important relic from inflation. We investigated this spectrum for the potential under consideration. At first, we considered the case for the value of p larger than 2. In the case, in general, when inflaton fields have the equivalent masses the equations of motion give rise to those of single field inflation producing the phase of non-perturbations. This occurs due to relative mass differences in the inflaton fields. It is observed that the spectrum comes out to be more or less redder in comparison with the corresponding single field model accordingly. Included fields and their effective masses play a very significant role because the results depend upon these at the time of horizon-crossing. It is noted that the result corresponds to that of single scalar field when the effective masses of all the fields are taken to be equivalent. The spectrum in this case results to be similar and therefore coincides with the spectrum of single field. It is concluded that the results for the values of $p > 2$, $p = 2$ and $p = -2$ are different and the behaviour of the field potentials and the corresponding spectrums are distinct as well as different.

It can be noted that all the terms included in the factor $\ln\left(\frac{\phi_k^s}{\phi_k^e}\right)$ might be equivalent on account of the result reached. With some extra term the two expressions represent the same equation for the corresponding single field case. The value of $\ln\left(\frac{\phi_k^s}{\phi_k^e}\right)$ for the result reached at, will be smaller for the larger value of μ_i when Λ_i are taken equivalent to the μ_i. If we consider $\mu_k = Max\,(\mu_n)$ where n denotes natural numbers. This gives rise to $\frac{\mu_i}{\mu_k} < 1$ which implies that the spectrum is more redder than its corresponding spectrum resulting from the result for a single scalar field ϕ_k. In this case the value of $\ln\left(\frac{\phi_k^s}{\phi_k^e}\right)$ would represent almost the smallest from all the values of $\ln\left(\frac{\phi_i^s}{\phi_i^e}\right)$ which indicates that

in Eq. (3.2.75) the case of single scalar field ϕ_k the value of k tends to get nearer to unity. On the other hand if we are taking the $\mu_k = Min\,(\mu_n)$ where n denotes natural numbers. This gives rise to $\frac{\mu_i}{\mu_k} > 1$ which resultantly leads to the result that the spectrum is less redder than its corresponding spectrum resulting from the result for a single scalar field ϕ_k. In this case the value of $\ln\left(\frac{\phi_k^s}{\phi_k^e}\right)$ would represent almost larger one out of all the values of $\ln\left(\frac{\phi_i^s}{\phi_i^e}\right)$ which shows that the case of single scalar field ϕ_k, where the value of k shifts away from unity. It means that the value of the scalar spectral index falls between that of single field in general for the biggest μ_k and the smallest accordingly.

The results we came across depend upon the effective masses and the values of the fields, however they emerge irrespective of the consideration for the initial conditions. Due to the spectrum being calculated on the time of horizon-crossing these occur on this time. To have these results we only require to satisfy the slow-rolling approximation of the fields in the initial and not any further action for it. The imposition of the condition $\frac{\delta\phi_j}{\dot{\phi}_j} = \frac{\delta\phi_i}{\dot{\phi}_i}$ is ensured in order to neglect the isocurvature perturbations. With this condition it appears that the fields are confined to some specific trajectories. Although the incorporation of the isocurvature perturbation modes look plausible however, is not taken into account for keeping simplicity and for remaining stuck with the our main theme.

It is investigated how the observables such as slow roll parameters, e-folding number and spectral index affect the inflationary models of multi-fields. Multi-field models might predict a range of values for the spectral index, although initial values of the inflaton scalar field depend upon the coefficient μ. The models of the inflationary universe which come out of the potential representing the models of scalar fields are namely the natural inflation model, double-well inflationary model, and brane inflationary model. First, we performed calculations of inflationary parameters taking single field models from these scalar field potentials. These models of scalar fields are very well-known inflationary models. Slow roll parameters are calculated for all three models taken into consideration. Then we computed the spectral indices for all three models expressed in terms of slow-roll parameters. The number of e-folds is calculated by the formula expressed in terms of the potential and its derivatives. In the natural inflation model, we used the limiting value of the potential for $\phi \longrightarrow 0$. In our calculations for the natural inflation model, we set the limiting case for both $\sin\phi$ and $\cos\phi$, so that the result we obtained is the good approximated solution. In Table-4.1 and Table-4.2 are listed the corresponding range of spectral index resulting from the variant values of N

and against the values of p, the corresponding range of N respectively. Where the range of values for spectral index with an increasing number of e-fold N is observed. Whereas, in Figure-4.1 and Figure-4.2, spectral index (n_s) is plotted against e-folding number N for a range of values. The behavior and the trend of spectral index against the number of e-folds N is diagramed graphically for the range $N = 30, 35, 40, 45, 50, 55, 60, 65, 70$. The range of values for spectral index with an increasing number of e-fold is listed in Table-4.1 and Table-4.2 for the corresponding cases. In Figure-4.3, distribution of mass scales is plotted in accordance with Marčenko-Pastur law or distribution for the case when a large number of scalar fields is taken into account.

4.3 An Nflationary Phase Diagram with Multifield Polynomial Potential

We discuss the following results in this section for an Nflationary phase diagram with the multifield polynomial potential.

4.3.1 Relation Between Number of Fields N, Number of e-Folds $\mathcal{N}$ and Entropy S

The entropy S during Nflation is given by de Sitter (dS) i.e., $S \sim \left(H^{-1}\right)^2 M_p^2$ where $S = S_{dS}$. We are considering entropy on the boundary of eternal inflation such that it can be expressed in the form

$$S \sim \frac{M_p^2}{H^2} \sim \frac{M_p^2}{\left({}^{Nm^2\phi^2}/_{M_p^2}\right)} = \frac{M_p^4}{Nm^2\phi^2} \tag{4.3.1}$$

From Eq. (3.3.16), making use of the expression $\phi = \left(\frac{48\pi^2}{N^3}\right)^{\frac{1}{4}} \sqrt{\frac{M_p^3}{m}}$ in Eq. (4.3.1), we find

$$S \sim \sqrt{\frac{N}{48\pi^2}} \frac{M_p}{m} \simeq \sqrt{N} \sqrt{\left(\frac{1}{(48)^{\frac{1}{2}}\pi}\right)^2 \left(\frac{M_p}{m}\right)^2} \Rightarrow S \propto N^{\frac{1}{2}} \tag{4.3.2}$$

From Eq. (4.3.2), we note that the entropy S is in direct proportion to the square root of the number of fields N, it simply means that the entropy decreases with decrease in the number of fields and increases with increase in the number of fields. The case of such entropy is similar to the entanglement entropy related with event horizon of a black hole where it depends on the N number of species (fields). This entropy represents a general case for N species (Dvali & Solodukhin, 2008). Although this does not appear to agree with black hole entanglement entropy due to equal contributions of all the fields in its entropy. The problem is resolved by proposing a suitable gravity cutoff (Λ) which is

given as $\Lambda \sim \frac{M_{pl}}{\sqrt{N}}$ (Dvali, 2010; Dvali & Solodukhin, 2008; Arkani-Hamed, Dubovsky, Nicolis, Trincherini, & Villadoro, 2007). We use Eq. (4.3.2) and put to test it for the gravity cutoff as described below

$$S \sim \sqrt{\frac{N}{48\pi^2}}\frac{M_p}{m} = \frac{\sqrt{N}\sqrt{N}}{\sqrt{48}\pi m}\frac{M_p}{\sqrt{N}} = \frac{N}{\sqrt{48}\pi}\frac{\Lambda}{m} \tag{4.3.3}$$

From above the value of gravity cutoff $\Lambda \sim \frac{M_p}{\sqrt{N}} \Rightarrow \Lambda\sqrt{N} \sim \Lambda \cdot N \sim M_p$, substituting in Eq. (4.3.3), we find

$$S \sim \frac{N}{\sqrt{48}\pi}\frac{\Lambda}{m} \sim \frac{1}{\sqrt{48}\pi}\frac{M_p}{m} \sim \frac{M_p}{m} \tag{4.3.4}$$

The result in Eq. (4.3.4) represents the entropy for the case of a single field at the boundary of the eternal inflation. Now, we develop a relation between e-folding number $\mathcal{N}$, number of fields N and entropy S, we will use the following expression for the number of e-folds $\mathcal{N}$

$$\mathcal{N} \sim \frac{N\phi^2}{M_p^2} \tag{4.3.5}$$

Using $\phi = \left(\frac{48\pi^2}{N^3}\right)^{\frac{1}{4}}\sqrt{\frac{M_p^3}{m}}$ from Eq. (4.3.6) in Eq. (4.3.5), we find the expression for the number of e-folds

$$\mathcal{N} \sim \frac{\sqrt{48}\pi M_p}{m\sqrt{N}} \tag{4.3.6}$$

Using for $\frac{M_p}{m} = \sqrt{\frac{48}{N}}\pi S$ from Eq. (4.3.2) in Eq. (4.3.6), we find a relation between number of e-folds $\mathcal{N}$, number of fields N and entropy S in the form

$$\mathcal{N} \cdot N \sim 48\pi^2 S \tag{4.3.7}$$

For simplicity, we can drop the constant terms to have

$$\mathcal{N} \cdot N \sim S \tag{4.3.8}$$

In Figure-3.2, at the boundary of eternal inflation the initial value of the field ϕ is given by Eq. (3.3.16) and for a specific number of fields N along the axis of ϕ, the total number of e-folds $\mathcal{N}$ shall correspond to the line of slow roll phase accordingly. However, Eq. (4.3.7) represents a general condition on entropy with number of fields N and number of e-folds $\mathcal{N}$. We observe now that

$$\mathcal{N} \cdot N \leq S \tag{4.3.9}$$

will be the case below the boundary line of eternal inflation. Eq. (4.3.9) indicates the fact that for a certain number of fields N, total number of e-folds in case of slow roll phase along the axis representing ϕ and along the line in parallel with N axis both are

bounded by the entropy bound S while at the boundary of eternal inflation the entropy bound is saturated. Further from Eq. (4.3.7) or Eq. (4.3.8) for N tending to unity we can recover the result for single field such that total number of e-folds turns out to be of the order of entropy (Arkani-Hamed et al., 2007; Kaloper, Kleban, Lawrence, & Sloth, 2016; Huang, 2008).

$$\mathcal{N} \cdot N \simeq 48\pi^2 S \Rightarrow \mathcal{N} \cdot 1 \simeq 48\pi^2 S \Rightarrow \mathcal{N} \simeq 48\pi^2 S \Rightarrow \mathcal{N} \simeq S \tag{4.3.10}$$

On the other hand when N is near the critical point and the number of e-folds tends approximately to unity i.e.,

$$\mathcal{N} \simeq 1 \Rightarrow 1 \cdot N \simeq S \Rightarrow N \simeq S \tag{4.3.11}$$

Eq. (4.3.11) describes the fact that the entropy is equivalent to the number of fields N. From Eq. (3.3.18) the number of fields N is given as $N \simeq 12\pi^2 \frac{M_p^2}{m^2} \Rightarrow \frac{M_p}{m} = \sqrt{\frac{N}{12}} \frac{1}{\pi}$, substituting this value of $\frac{M_p}{m}$ in Eq. (4.3.2) we can have the same value as found in Eq. (4.3.11), that is

$$S \sim \sqrt{\frac{N}{48\pi^2}} \frac{M_p}{m} = S \sim \sqrt{\frac{N}{48\pi^2}} \sqrt{\frac{N}{12\pi^2}} \sim \frac{N}{12\sqrt{2}\pi^2} \tag{4.3.12}$$

$$12\sqrt{2}\pi^2 S \sim N \Rightarrow S \sim N \tag{4.3.13}$$

However, below the critical point $N \leq S$ and from Eq. (4.3.2), $S \sim \sqrt{\frac{N}{48\pi^2}} \frac{M_p}{m} \geq N$ can be found which becomes as $N \leq 12\pi^2 \frac{M_p^2}{m^2}$. G. dvali et al. has suggested (Dvali & Solodukhin, 2008, 2008; Dvali, 2010; Arkani-Hamed et al., 2007) about the renormalizability of the planck mass M_p in the presence of the number of fields N at the scale of the order m such that $M_p^2 \geq Nm^2$. It means in other words that $N \geq \left(\frac{M_p}{m}\right)^2$ do not show consistency. If we consider the case $N \geq \left(\frac{M_p}{m}\right)^2$ keeping in mind the case of Eq. (4.3.2), $S \sim \sqrt{\frac{N}{48\pi^2}} \frac{M_p}{m}$, we find that number of fields N is larger than the entropy dS of the critical point i.e., $N \geq S$. It intuitionally looks impossible because it suggests that at least each field has one degree of freedom. We argue that in a system consisting of N number of fields, total degrees of freedom, in addition to the entropy limit must also be equivalent to N. In this case the entropy dS represents the entropy of the system maximally. It is interesting to note that for comparatively larger N, we can determine the relation given in Eq. (4.3.10) and from Eq. (4.3.1) as well, $\phi^2 \simeq \frac{M_p^4}{m^2 SN}$ substituting this value in Eq. (4.3.5), we have $\mathcal{N} \simeq \left(\frac{M_p}{m}\right)^2 S^{-1}$, differentiating it with respect to S, it results in the following expression

$$\frac{d\mathcal{N}}{dS} \simeq -\frac{1}{S^2} \left(\frac{M_p}{m}\right)^2 \tag{4.3.14}$$

By integrating Eq. (4.3.14) alongside the axis in which ϕ is evolving as illustrated in the Figure-**??**, and using the value of $\frac{M_p^2}{m^2}$ from Eq. (4.3.1), we find $\mathcal{N} \cdot N \simeq S$ which corresponds again with Eq. (4.3.10).

4.3.2 Eternal Inflationary Phase and Primordial Density Perturbations That Appear At Its Boundary

A smooth universe can be described by the ratio approaching to unity i.e., $\frac{\delta\rho}{\rho} \approx 1$, clearly the value unity for this ratio requires both of the denominator and numerator to be of value 1 i.e., $\delta\rho = 1$ and $\rho = 1$. This poses the case of a universe without any structure cosmologically existing in it. Because the inhomogeneities such as stars, galaxies, cluster of galaxies and whatever is observed in the condensed form or like that are smoothed out. If there be any homogeneity will be negligibly small to grow in the present form. But we know the case is not like this. When the ratio $\frac{\delta\rho}{\rho}$ has to deviate from unity, The quantity $\delta\rho$ has to take values either less than 1 or larger than it with respect to a fixed complete single value assigned to ρ. This is the value 1 representing the energy density budget of the universe. In this case either $\frac{\delta\rho}{\rho}$ is larger or smaller than 1, accordingly we can predict the presence of inhomogeneities in the universe in the form of structure formation like planets, stars, galaxies and cluster of galaxies etc. In this way we utilize the ratio $\frac{\delta\rho}{\rho}$ and it serves our purpose of detecting inhomogeneities of structure in the geometric structure of spacetime. We know how inflation is obtained from a single scalar field and its mechanism as well. When the scalar field inflaton is at the boundary of eternal inflation the primordial density perturbations are of the order of unity that is

$$\frac{\delta\rho}{\rho} \sim 1 \tag{4.3.15}$$

But in case of Nflation, we can use a formula for the primordial density perturbations developed by Sasaki et al. for the primordial density perturbations (Sasaki & Stewart, 1996; Sasaki & Tanaka, 1998). These perturbations during the phase of slow roll are approximated (Kim & Liddle, 2006; Lyth & Riotto, 1999) by S.A. Kim et al. and the expression for these is given by

$$\left(\frac{\delta\rho}{\rho}\right)^2 \sim m^2 N^2 \phi^4 M_p^{-6} \tag{4.3.16}$$

The dynamics of the boundary of eternal inflation satisfies the Eq. (3.3.16), using $\phi = \left(\frac{48\pi^2}{N^3}\right)^{\frac{1}{4}}\sqrt{\frac{M_p^3}{m}}$ from Eq. (3.3.16) in Eq. (4.3.16), we can reach at the following result

$$\left(\frac{\delta\rho}{\rho}\right)^2 \sim m^2N^2\left(\left(\frac{48\pi^2}{N^3}\right)^{\frac{1}{4}}\sqrt{\frac{M_p^3}{m}}\right)^4 M_p^{-6} \tag{4.3.17}$$

$$\Rightarrow \frac{\delta\rho}{\rho} \sim \sqrt{48}\pi\frac{1}{\sqrt{N}} \Rightarrow \frac{\delta\rho}{\rho} \propto \frac{1}{\sqrt{N}} \tag{4.3.18}$$

If we observe the two results determined in Eq. (4.3.15) and Eq. (4.3.18) respectively, we see that $\frac{\delta\rho}{\rho}$ tends to unity always in Eq. (4.3.15) but in Eq. (4.3.18), $\frac{\delta\rho}{\rho}$ is inversely proportional to the square root of number of fields N i.e., $\frac{\delta\rho}{\rho}$ decreases with increasing N and it increases with decreasing N and it will always remain less than unity for each value of N. This is clearly distinctive from that of single scalar field results. We can investigate such behavior as the case is in single field inflation at the boundary of the eternal inflation and the point of primordial density perturbations approaching unity are same but change of the fields in the two cases is different as can be seen from Eq. (3.3.11) and Eq. (3.3.13) in the corresponding section of previous chapter of methodology.

4.3.3 Discussion and Concluding Remarks

We investigated pertaining to the problem of the multifield model of inflation and studied its Nflationary phase transition properties. The study is carried out for the properties of inflationary phase with the help of phase diagram which gradually decreases and finally vanishes in the slow roll phase of this Nflation model. It is observed that as the number of fields is increased the critical point and the end point of slow rolling phase shift to smaller average values of the fields. The motion of these two points, however takes place at different rates. It is the critical point that splits between the regions of eternal inflation and slow roll. Generally the critical point shifts towards end phase faster than the end point of the slow roll which indicates that the region of eternal inflation wiil dominate over the slow roll inflation. The slow roll region completely disappears when there is a large number of fields. Therefore Nflation might have some bound on the number of fields that assist each other to drive inflationary phase for evolution of the universe. From black hole entropy in its event horizon a bound is found between number of fields N, with masses m and planck mass. The properties of Nflation models correspond to the properties of single field models which help to check their real existence. Inflation was here demonstrated for a large number of fields when large N phase transitions occur in Nflation. By drawing the phase transition diagram for Nflationary model considering the

multifield potential $V(\phi_j) = \Lambda_j^4 \left(\frac{\phi_j}{\mu_j}\right)^p$, we explained how the slow roll phase diminishes. Further conditions on entropy as a bound that conforms to the number of fields N and the outcomes occurring in it have also been addressed. It is investigated that all the de Sitter (dS) entropy around or at the critical point remains concentrated about it and is condensed in the number of fields N for the considered potential. We observe the behavior of two regions, the slow roll phase and the eternal inflationary phase separated by the critical point at the boundary and at the initial points respectively which move gradually at slightly distinct rates towards field values smaller on the average. The boundary of the slow roll is likely to be engulfed slowly by the eternal inflation as the pace of critical point might be faster than the ending point, in principle. It can also be seen that the bounding limit from the theory of black holes for the number of fields N and Planck mass M_p does not almost show viability for the massless scalar fields which generate density perturbations as entropy. Marčenko-Pastur distribution or law gives the likely distribution of field masses that assigns average mass to all the large and small masses. We found approximately similar order for a specific value of β which incorporates all the masses naturally.

4.4 Time Independent Schrödinger Equation Conforming to Wheeler-DeWitt Equation For the Evolution of Early Universe

Below we discuss the results and simulations which are the outcomes of numerical solutions of the problem.

4.4.1 Results and Simulations

In Figure-4.4 below the numerical values and absolute errors of $\Psi(a)$ for all scenarios are plotted using the developed code in Matlab for the problem emerging from Wheeler-DeWitt equation. It is concerned with the early stage evolution of cosmic expansion. The figure incorporates all the scenarios for all cases inclusive. The subfigures (a), (b) and (c) correspond to numerical values whereas (d), (e) and (f) are related to absolute errors. Moreover, the datasets as tabulated in Table-4.3 in the follwing are generated for the time independent Schrodinger equation conforming to the Wheeler-DeWitt equation for three scenarios. Each scenario consists of three cases that are generated through Runge-Kutta method (RK4). Afterwards, these datasets are trained through LMBN algorithm in order to perform testing, validation and training of these for the enhanced accuracy

of results. Now, the following plots presented in Figure-4.5 are showing the Error

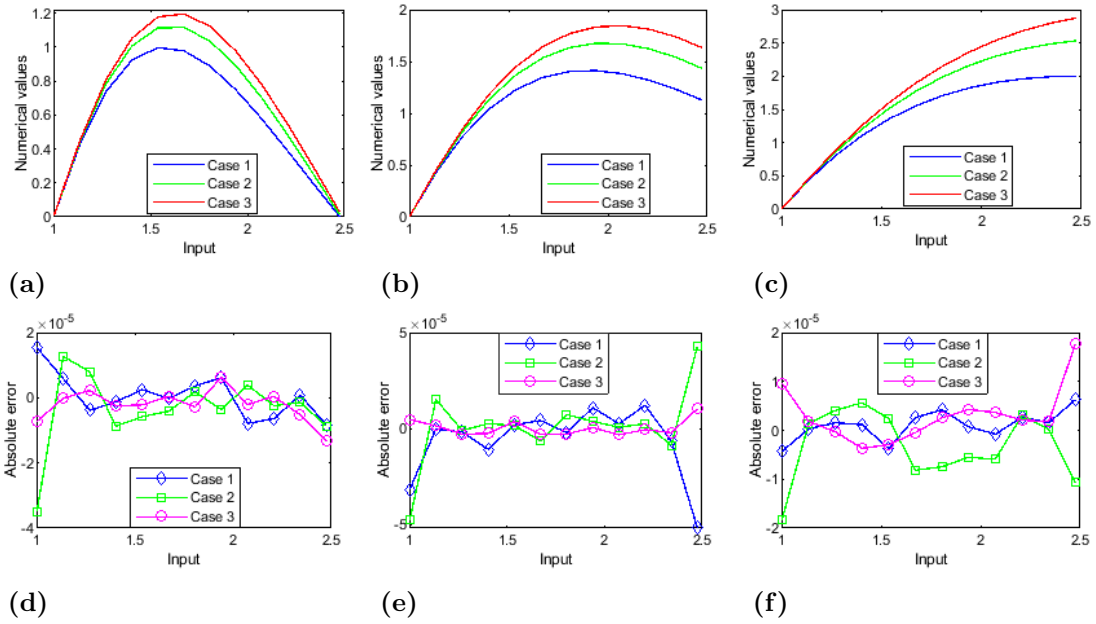

Figure– 4.4: These figures demonstrate the plots of numerical values and absolute errors of $\Psi(a)$ for all scenarios. The figures (a), (b) and (c) are the numerical values of $\Psi(a)$ for scenarios 1, 2 and 3 respectively, whereas the figures (d), (e) and (f) are the absolute errors of $\Psi(a)$ for scenarios 1, 2 and 3 respectively

Autocorrelation Analysis for all scenarios. Again, the following plots presented in Figure-4.6 describe Error Histogram Analysis for all three scenarios with their corresponding cases.

4.4.2 Discussion With Results And Simulations

The datasets are generated for the Schrödinger equation for three scenarios. Each scenario consists of three cases that are generated through Runge-Kutta method (RK4). Afterwards these datasets are trained through LMBN algorithm in order to perform testing, validation and training of these for the enhanced accuracy of results. The graphical abstract displays the stepwise procedure of the proposed scheme for the problem to solve in a comparatively better understanding of the reader as shown in Figure-3.5 in the corresponding section of previous chapter 3 of methodology. The results of performance analysis are presented in Table-4.3 by varying the parameters s and B for all scenarios

Table– 4.3: Tabulation of the complete numerical analysis of each case for all scenarios taken into consideration

	Cases	Time (sec)	Performance	Grad	Mu	MSE			Epoch
						Training	Testing	Validation	
Sceario 1	1	21.00	2.730E-11	9.860E-11	1.00E-09	2.73E-11	1.83E-11	2.70255E-11	243
	2	25.00	1.88E-11	9.820E-08	1.000E-09	1.88E-11	2.13E-11	1.66184E-11	314
	3	16.00	9.770E-12	9.830E-08	1.000E-09	9.77E-12	1.06E-11	1.15203E-11	170
Sceario 2	1	39.00	8.200E-11	1.000E-07	1.000E-08	8.20E-11	8.49E-11	7.98158E-11	456
	2	32.00	6.340E-11	9.940E-08	1.000E-08	6.34E-11	5.41E-11	8.783903E-11	421
	3	29.00	5.200E-12	9.910E-08	1.000E-09	5.20E-12	6.35E-12	5.83225E-12	389
Sceario 3	1	34.00	6.620E-12	9.970E-08	1.000E-09	6.62E-12	1.01E-11	7.43161E-12	466
	2	20.00	3.570E-11	9.970E-08	1.000E-08	3.57E-11	4.55E-11	3.92013E-11	277
	3	56.00	6.740E-12	9.960E-08	1.000E-09	6.74E-12	1.06E-11	7.60358E-12	766

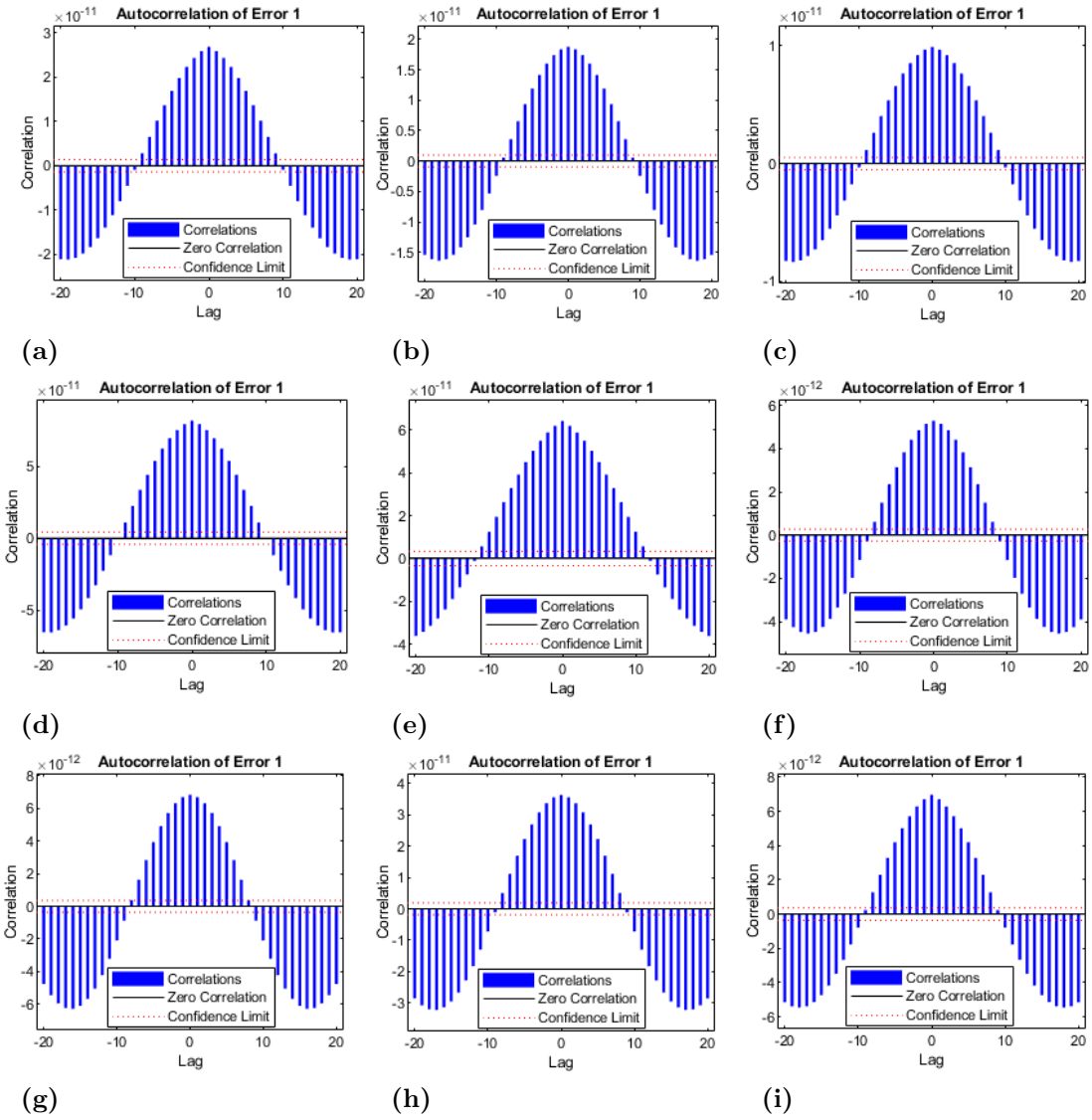

Figure– 4.5: These figures are showing the error autocorrelation analysis and are presenting the results through graphical display of all scenarios inclusive with all nine cases. The figures (a), (b) and (c) illustrate three cases of error autocorrelation analysis corresponding to scenario 1 respectively, whereas the figures (d), (e) and (f) depict three cases of error autocorrelation analysis corresponding to scenario 2 respectively, whereas the figures (g), (h) and (i) demonstrate three cases of error autocorrelation analysis corresponding to scenario 3 respectively

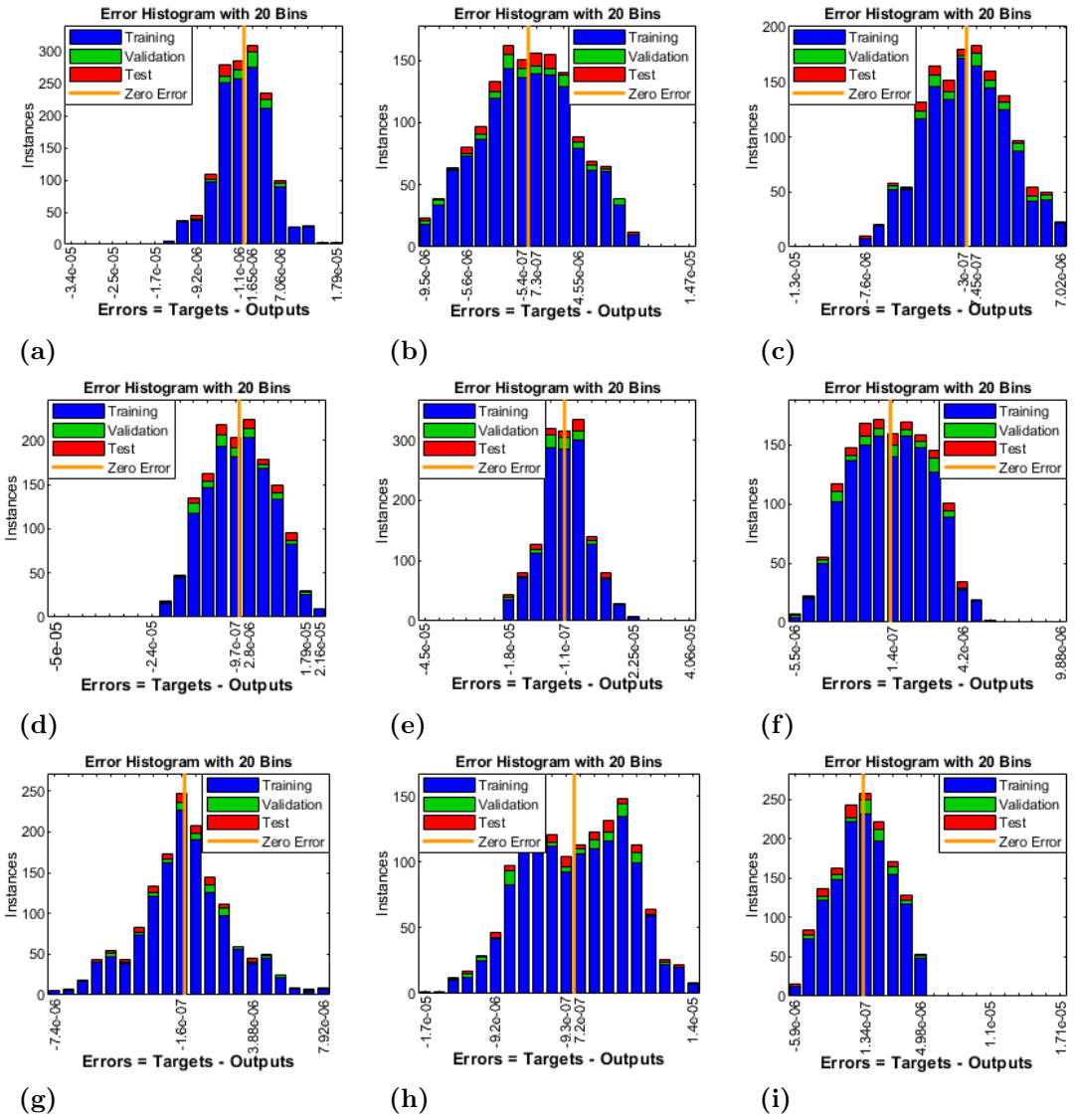

Figure– 4.6: The figure shows error histogram analysis and presents graphical display of all three scenarios inclusive with all nine cases. The figures (a), (b) and (c) represent three cases of error histogram analysis corresponding to scenario 1 respectively, whereas the figures (d), (e) and (f) illustrate three cases of error histogram analysis corresponding to scenario 2 respectively, whereas the figures (g), (h) and (i) demonstrate three cases of error histogram analysis corresponding to scenario 3 respectively

and their corresponding cases.

The obtained datasets through LMBN scheme is optimized for different weights in ntstool by setting 5% of the whole dataset as testing and validation, 90% for training with 100 hidden layers and 2 delays in order to train the dataset with the LMBN algorithm. The complete numerical data that is obtained in detail for the plots of performance and error analysis using LMBN scheme is evaluated for the parameter s and for the profiles B as the 2nd parameter. The process is repeated for scenarios inclusively and for the adjacent cases as well and the results of both cases are tabulated in Table-4.3. The numerical results with absolute errors for error histogram analysis and error autocorrelation analysis for $\Psi(a)$ with regard to each case are presented in Figure-4.5 and Figure-4.6 with their subfigures (a-f) illustrating the behaviour.

It is significant to mention that the hidden layers and the neurons in these hidden layers play very important role in the quality of the solvers. The choice in preferring the number of hidden layers and the number of neurons assimilated in the hidden layer requires a great deal of precautionary measures because these have great impact on the performance of the network. Usually error and trial method is used to fix the number of these parameters and it would be almost impossible to determine the number of hidden layers for a specific learning procedure. In most of ANN applications, it is however observed that one layer would suffice (Smith et al., 1997; Trzaska & Dobrzański, 2006; Tan, Mat, Abd Rahim, Lile, & Yaacob, 2011). The incremental updating of weights helps carry out the network training which is meant for the entry of responses which provide a successive learning vector and is taken to be determined each time and are changed as well (Zajkowski, 2014). Now, the following plots as presented in Figure-4.7 illustrate Performance Analysis for all scenarios and the corresponding cases. The following plots are drawn for Regression Analysis as given in Figure-4.8 and Figure-4.9 and demonstrate the analysis for all scenarios related to it in addition to their corresponding cases. Further, the following plots are drawn for Training State Analysis as given in Figure-

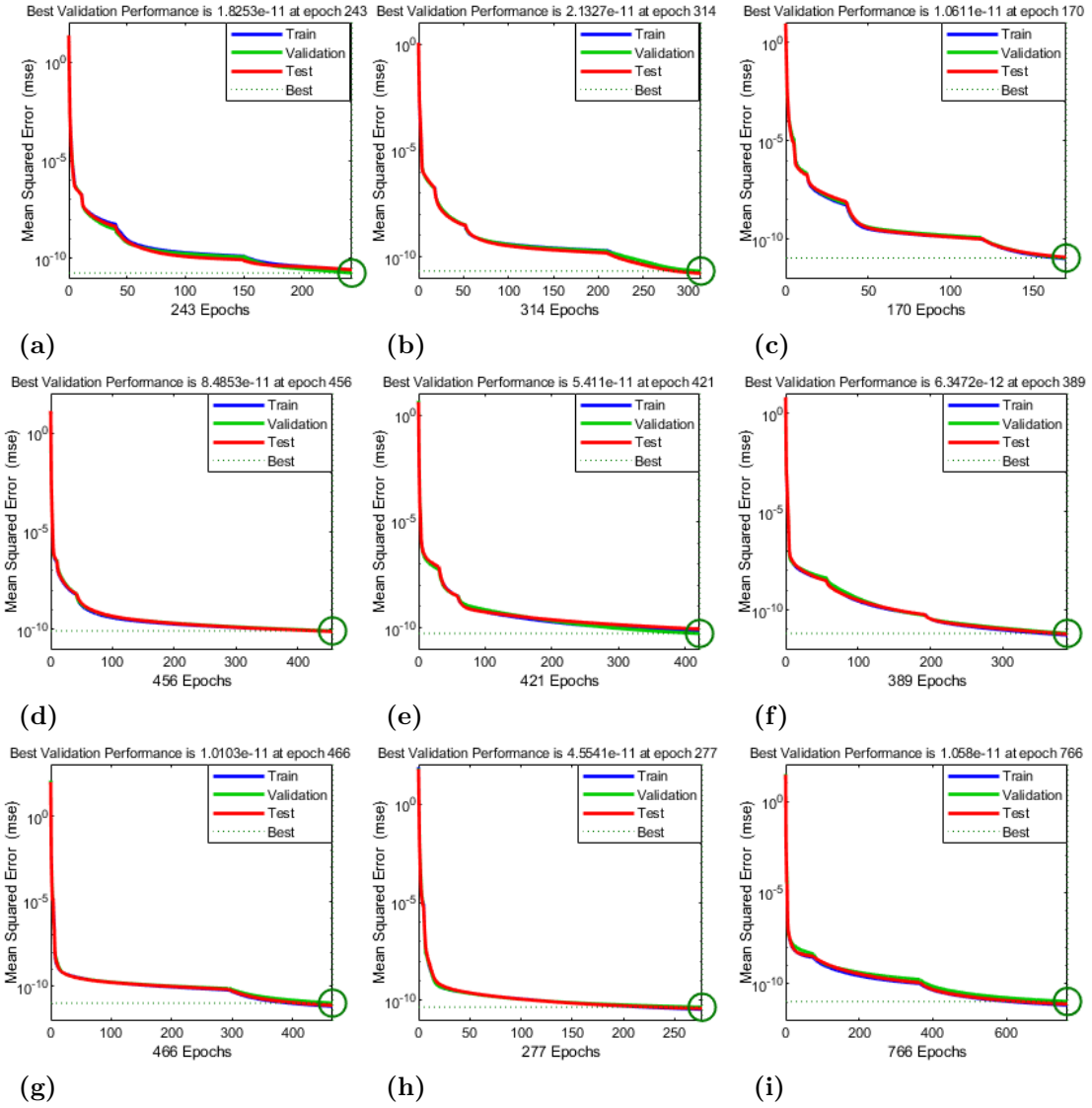

Figure– 4.7: The figure presents the performance analysis and presents graphical display of all three scenarios inclusive with all nine cases. The figures (a), (b) and (c) describe three cases of performance analysis corresponding to scenario 1 respectively, whereas the figures (d), (e) and (f) represent three cases of performance analysis corresponding to scenario 2 respectively, whereas the figures (g), (h) and (i) illustrate three cases of performance analysis corresponding to scenario 3 respectively

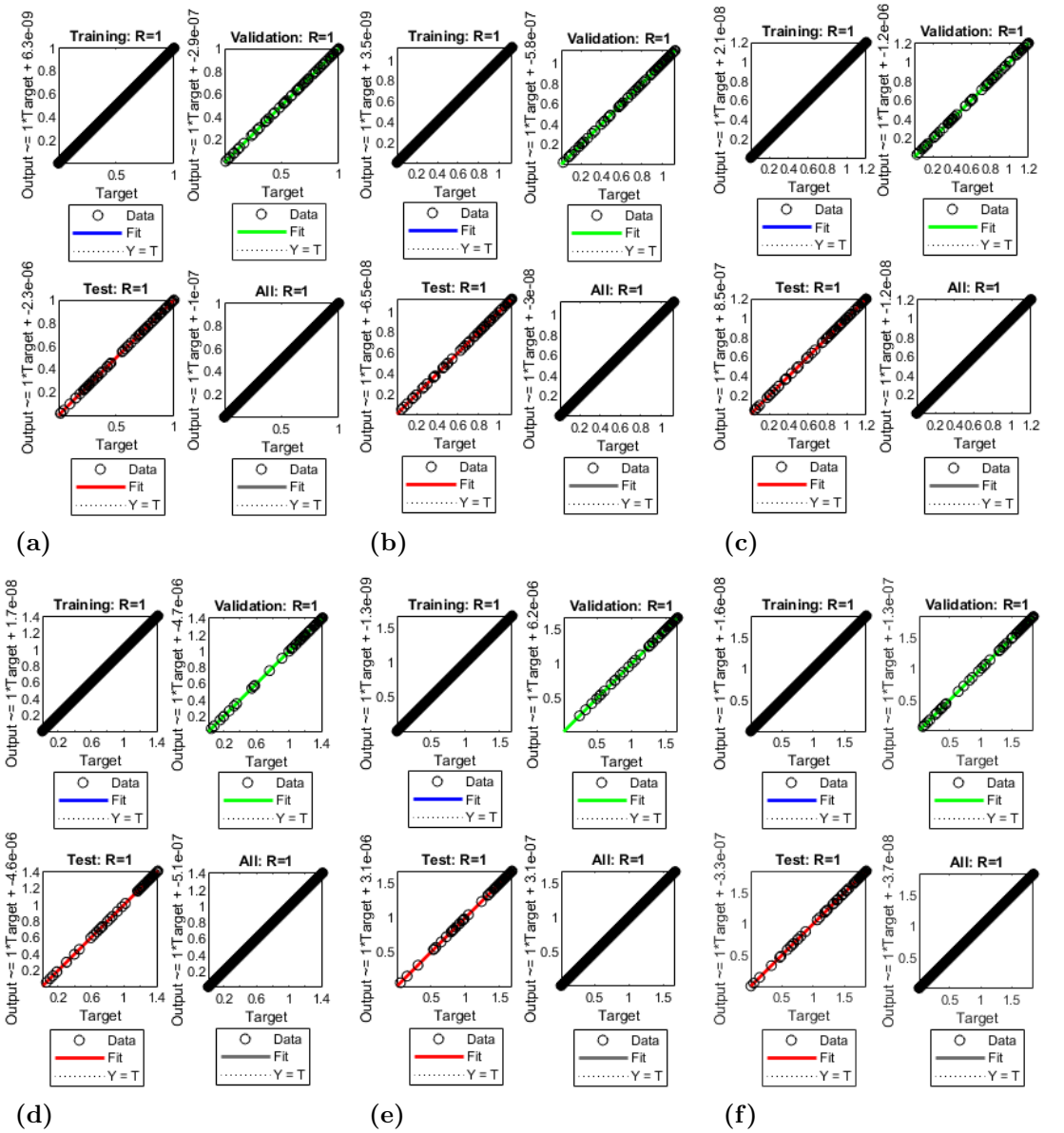

Figure– 4.8: These figures illustrate the analysis for regression and present graphical display of two scenarios incorporating six cases. The figures (a), (b) and (c) demonstrate three cases of regression analysis corresponding to scenario 1 respectively, whereas the figures (d), (e) and (f) show three cases of regression analysis corresponding to scenario 2 respectively. The figures on the next page are integral part of the analysis for regression and give graphical display of third scenario incorporating three cases

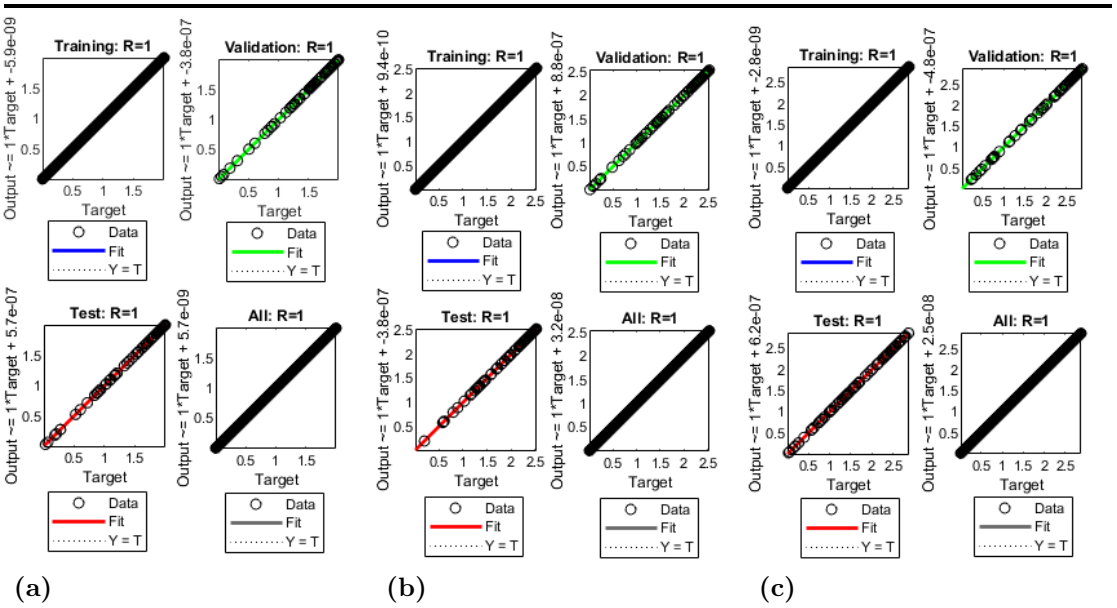

Figure– 4.9: This figure with subfigures (a), (b) and (c) are the integral part of Figure-4.11 however is labeled as a separate figure due to shifting of it to the next page. It shows three cases of regression analysis corresponding to scenario 3 respectively

4.10 and illustrate the analysis for all the related scenarios and their corresponding cases. Now, the following diagrams are plotted for Time-Series Response Analysis as shown in Figure-4.11 and explain the analysis for all three scenarios in relation to it and their corresponding cases. The following results presented in the Table-4.4) as given below describe the comparative study through absolute errors for all the cases inclusive. The scenarios are also shown as well. and the following results presented below in the Table-4.5 are outcomes of the study of comparative statistics analysis for the scenario 1-3 for all cases inclusively based on absolute errors. In Figure-4.4, the figures plotted as its subfigures are formed with the help of developed code in Matlab for the problem emerging from Wheeler-DeWitt equation conforming to time independent Schrodinger equation. It is concerned with the early phase growth of cosmic evolution and is therefore related with cosmological quantum states in its very early evolutionary stages. The figure incorporates all the scenarios with all the cases inclusive. Figure-4.5 represents overall the autocorrelation of error for all three scenarios including nine cases are presented in subfigures [4.5(a) - 4.5(i)] three for each scenario. In Figure-4.5 autocorrelation measures the degree to which a lagging value of a variable have a connection with its non-lagging

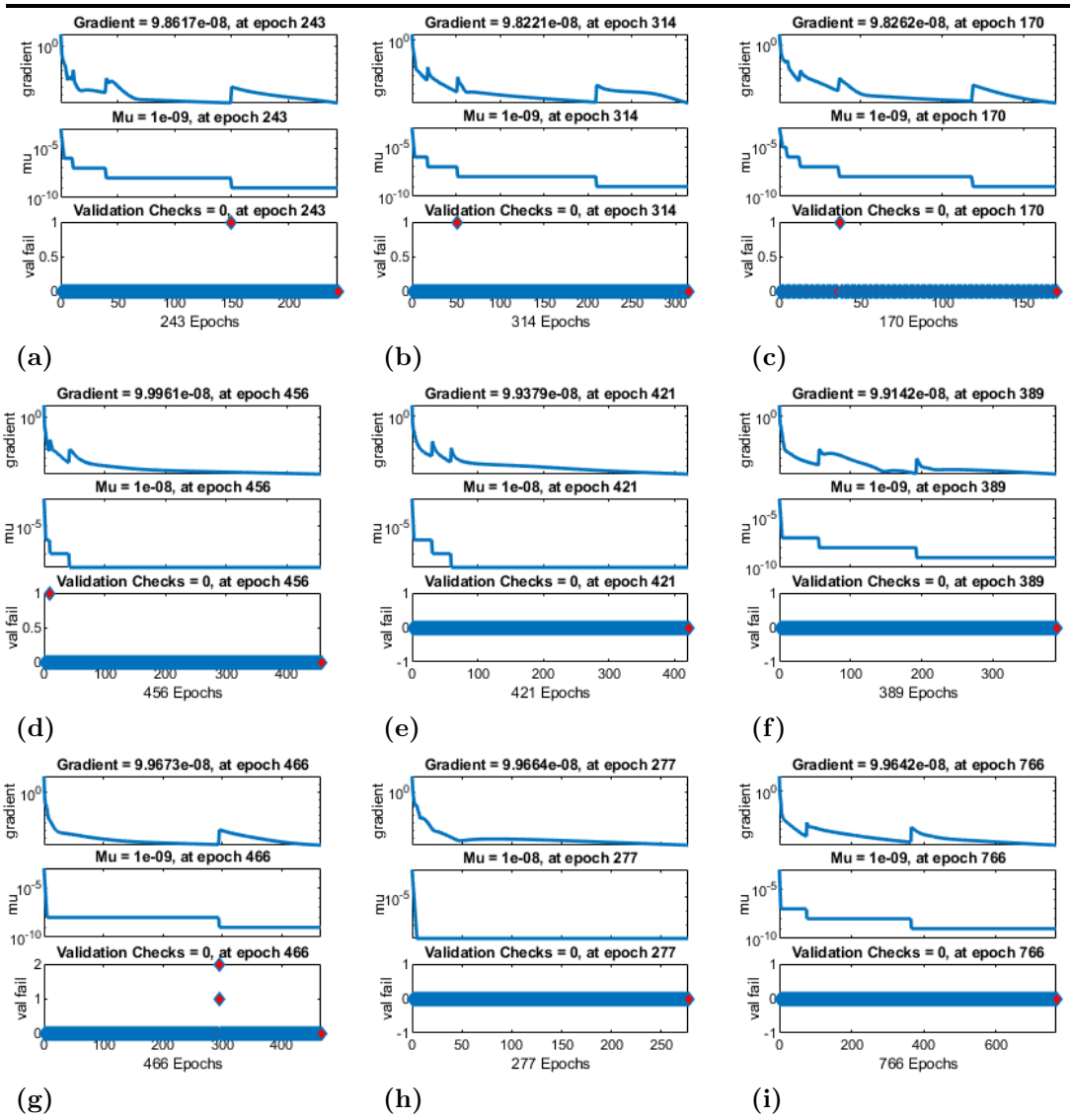

Figure– 4.10: These figures describe the training state analysis and presents graphical display of all three scenarios inclusive with all nine cases. The figures (a), (b) and (c) indicate three cases of training state analysis corresponding to scenario 1 respectively, whereas the figures (d), (e) and (f) demonstrate three cases of training state analysis corresponding to scenario 2 respectively, whereas the figures (g), (h) and (i) represent three cases of training state analysis corresponding to scenario 3 respectively

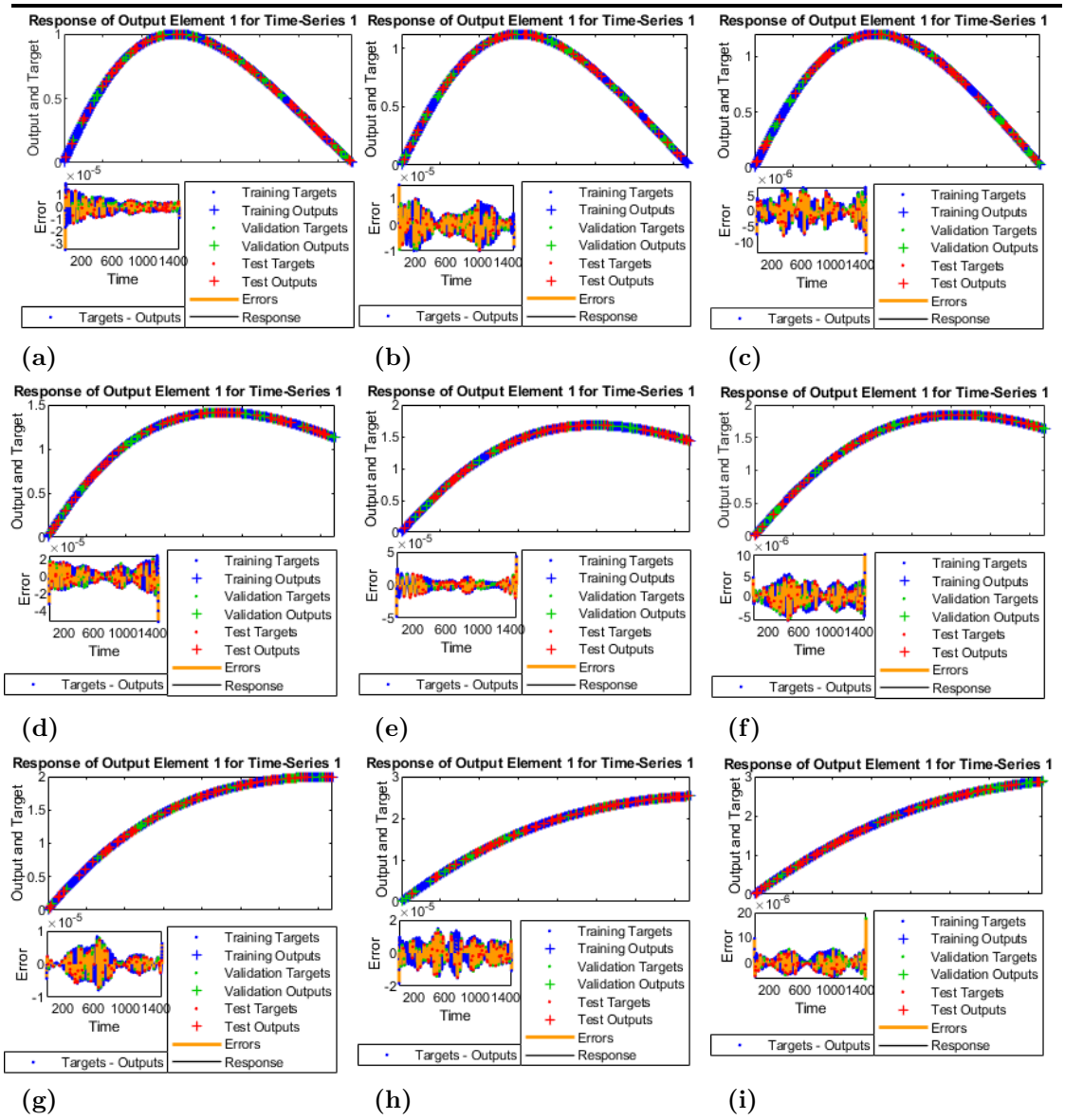

Figure– 4.11: These figures represents the time series response analysis and gives graphical display of all three scenarios inclusive with all nine cases. The figures (a), (b) and (c) demonstrate three cases of time series response analysis corresponding to scenario 1 respectively, whereas the figures (d), (e) and (f) show three cases of time series response analysis corresponding to scenario 2 respectively, whereas the figures (g), (h) and (i) illustrate three cases of time series response analysis corresponding to scenario 3 respectively

Table– 4.4: The comparative numerical study of the scenarios 1-3 for all cases through absolute errors

Input	Scenario 1			Scenario 2			Scenario 3		
	Case 1	**Case 2**	**Case 3**	**Case 1**	**Case 2**	**Case 3**	**Case 1**	**Case 2**	**Case 3**
1.00	1.5370E-05	3.4930E-05	7.2707E-06	3.1640E-05	4.7608E-05	4.6241E-06	4.3234E-06	3.4930E-05	9.6568E-06
1.10	7.5262E-06	9.5904E-06	3.3755E-06	1.5272E-05	1.3752E-05	1.1905E-07	4.3876E-07	9.5904E-06	2.2173E-06
1.20	4.2786E-06	9.3247E-06	2.3644E-06	8.5347E-06	1.6748E-05	2.1420E-06	1.1072E-06	9.3247E-06	5.1390E-07
1.30	4.2830E-06	1.1446E-06	1.6137E-06	7.8205E-06	1.4157E-05	6.0576E-07	9.9590E-07	1.1446E-06	1.6423E-06
1.40	3.0140E-06	7.8716E-06	4.4655E-06	9.7018E-06	4.9630E-07	3.6533E-06	9.6343E-07	7.8716E-06	2.3614E-06
1.50	3.5081E-07	6.0878E-06	2.0277E-06	7.0767E-07	3.2679E-06	1.4681E-06	2.5264E-06	6.0878E-06	1.1695E-06
1.60	3.3863E-06	5.6776E-06	2.0495E-06	6.7244E-06	1.4091E-06	1.4509E-06	5.1452E-06	5.6776E-06	4.4705E-07
1.70	3.1379E-06	2.2377E-06	4.5295E-06	5.8736E-07	6.3255E-06	3.6845E-06	1.3006E-06	2.2377E-06	2.3045E-07
1.80	2.8440E-06	1.6570E-06	3.8836E-06	6.3733E-07	5.5402E-06	2.7692E-06	2.8303E-06	1.6570E-06	3.0398E-06
1.90	4.8161E-06	2.8366E-06	2.7387E-06	1.0721E-05	6.8000E-07	6.8359E-07	4.8001E-07	2.8366E-06	3.9156E-06
2.00	4.3807E-06	2.1888E-06	2.1957E-06	1.1490E-05	4.4650E-06	2.1271E-06	2.9687E-07	2.1888E-06	1.0137E-06
2.10	2.4266E-06	2.9498E-06	8.7247E-07	6.0185E-06	4.5773E-06	2.3140E-06	1.7301E-06	2.9498E-06	5.0672E-06
2.20	7.2275E-07	8.8166E-07	7.6888E-07	6.0430E-06	1.1226E-06	2.7286E-06	1.7154E-06	8.8166E-07	6.5793E-07
2.30	9.2762E-07	2.0030E-06	1.7772E-07	7.1900E-06	1.0879E-07	1.5916E-06	1.5141E-06	2.0030E-06	1.6721E-06
2.40	1.9767E-06	2.5962E-06	4.8004E-06	1.8487E-05	1.3470E-05	2.8194E-06	3.0584E-07	2.5962E-06	1.1407E-07

Table– 4.5: The comparative statistics analysis of the scenario 1-3 for all cases on the basis of absolute errors

Operator	Scenario 1			Scenario 2			Scenario 3		
	Case 1	**Case 2**	**Case 3**	**Case 1**	**Case 2**	**Case 3**	**Case 1**	**Case 2**	**Case 3**
Max	5.00E-09	1.25E-08	4.07E-10	1.09E-08	4.18E-09	3.44E-10	1.82E-09	1.36E-09	1.07E-09
Min	1.54E-05	3.49E-05	1.34E-05	5.19E-05	4.76E-05	1.03E-05	8.33E-06	1.83E-05	1.77E-05
Mean	3.55E-06	4.02E-06	2.56E-06	7.43E-06	6.24E-06	1.93E-06	1.98E-06	5.15E-06	2.13E-06
Std	2.48E-06	3.27E-06	1.82E-06	5.19E-06	5.02E-06	1.25E-06	1.71E-06	3.14E-06	1.56E-06

value (normal) for the same variable in given time series i.e., it quantifies the relationship observation and the points. It measures the location of the different points in time and searches out their relationship to the observations by developing a trend template over the time series. The same variable between two successive intervals of time becomes of great interest in this regard. It figures out the degree of correlation for the same variable between two successive time intervals. The analysis of autocorrelation focusses short-term trends on the parametric values. The range set of Autocorrelation is $\{-1, 1\}$ and between -1 and 0 it represents negative autocorrelation and a positive correlation has a value between 0 and 1. Thus it can be observed how the correlation go alongside the lag in Figure-4.5 and sub-figures[4.5(a) - 4.5(i)].

Now, Figure-4.6 as well as its subfigures [4.6(a) - 4.6(i)] represents the histogram of error for all three scenarios including nine cases. Figure-4.6 represents the error histogram for the errors. After we have performed training to a feed forward neural network it shows the histogram of error between predicted and target values. The error values as manifested in the error histogram can be negative this is due to the reason that this negativity of values explains the predicted values are varying from the target values. The number of vertical bars on the graph display we observe are known as bins. In the present case the error range in totality is split from 0 to 300 into tinier bins along the vertical axis. Horizontal axis displays the target outputs i.e., the number of samples of our dataset that falls in a particular bin in the histogram. The error histogram illustrates the conditions of behaviour of the neural network with training of the datasets.

For example, on considering subfigure [4.6(a)] from Figure-4.6, the bins on the horizontal axis spans between 0 to 300, and the positive correlations falling between this limit range

between 0 and 300 correlations on the vertical axis. We have a bin corresponding to the error ranging $-3.40-05$ to $1.790-05$. For the training dataset, the altitude of the that bar falls below 10 but very near to this value in the case of validation and training. The datasets of the test occur between 10 and 300 values. This explains that a large number of sample datasets from the given multifaceted datasets possess an error which situates in that specific range. Further, the line which corresponds to zero error is situated there which also conforms to the zero error value the axis of the error which usually taken as X-axis. The existence of low or small values oferror is also manifest from the diagram of error histogram almost occurring for every dataset of values. It is also obvious that most of the error lie between the range given as $-3.40-05$ to $1.790-05$.

Figure-4.7 with subfigures [4.7(a) - 4.7(i)] represents the performance plot of the training for all three scenarios including nine cases. We may observe that the performance of the training attains the minimum value at epoch 170 and reaches its maximum value at 766. It is further obvious that the training remains continuing to the iteration 766 and stops after it as a temporary halt. This figure does not indicate any significant problem occurring during the training and the outstanding validating performance at epoch 389 is $6.3472e-12$. The performance value for different number of hidden nodes with gradient values and the total number of epochs are listed and displayed in Table-4.3. The above values as listed in the Table-4.4 are represented graphically and the plots in graphical illustration in order to make a understandable sense as displayed in the Figure-4.7 with subfigures [4.7(a) - 4.7(i)]. The artificial neural network with 100 points, it was noted, in hidden layers possesses the least performance value at epoch 389 to be $6.3472e-12$ with total number of 766 epochs. It was observed that the minimum gradient decent was meaningfully effective for this network. In order to decide the choice for number of hidden variable the analysis was further performed with the convergence of network performance plots. We observe a colossal distinction and contrast if we plot the network training performance with 100 nodes in the convergence of network. On the other hand with 100 hidden variables the network had considerably rapid convergence of network as presented in Figure-4.7.

Figure-4.8 and Figure-4.9 with subfigures [4.8(a) - 4.8(f)] and its integral subfigures on the next page [4.9(a) - 4.9(c)] represent the regression analysis for scenarios $1-2$ and for scenario 3 respectively including nine cases. In ANN after training, testing and validation is accomplished, then regression analysis is performed. It is the process based on the statistics in order to estimate the relation between targets and outputs of the system.

The plot of the regression picks two parametric values namely outputs and targets and plots the linear regression of the targets in relation to the outputs. The miniscule circle placed on the plots indicates the representation of specific values of data. After the regression plot it is significant to check the goodfit of the data in the model. Regression as a statistical technique employed almost in all disciplines that determine the strength and the character of the relationship between one dependent variable and a series of other independent variables. Linear, multiple linear and non-linear regression techniques are usually used for different problems. Simple linear regression put to use one independent variable to explicate or predict the result outcome of the dependent variable. On the other hand multiple linear regression makes use of two or more independent variables to explain and predict the result outcome of the dependent variable.The regression analysis helps us sorting out which of the variables involved does indeed have an impact and which factors we can ignore. The regression values are plotted for 0 to 3 and 100 hidden nodes as can be seen in Table-4.5) to further investigate the conduct of these distinct several hidden nodes or variables.

In LMBN model, the regression analysis is carried out after the network finalizes the processes of training, testing and validation. The plot of regression function grabs two parameteric values (targets, outputs) and draw plots of the linear regression of the targets in relation to the outputs. It is a mechanism of statistical procedure for assessing the relationships between the outcomes of output and the target of the network. Moreover, the Figure-4.8 and Figure-4.9 with subfigures [4.8(a) - 4.8(i)] and [4.9(a) - 4.9(c)] on the next page represents the plots of regression for the training, testing, validation and over all regression. The tiny circle indicates the representation of data in the model. It is very important to authenticate the goodfit of the datasets as the diagnosis after the plots of regression have been generated.

Figure-4.10 with subfigures [4.10(a) - 4.10(i)] represents training for all three scenarios including nine cases. The main aim and purpose of training the network is to reduce as much as the mean square error (MSE). The choice to fix and decide the number of hidden layers and the number of neurons in these hidden layers requires that we must be carefully select these because it has significant impact on the network performance. It is not easy target to decide the number of hidden layers for a specific learning procedure. These parameters are determined usually by error and trial method. In most ANN applications it is, however in general observed that one hidden layer is sufficient. The training procedure might employ the largest datasets and might govern the network

to follow and understand the samples existing in the in the datasets. The process of training carries on up to the network slowly and gradually rectifies and improves on the checks of validating.

Figure-4.11 with subfigures [4.11(a) - 4.11(i)] illustrates the Time Series Response for all three scenarios including nine cases. Time Series Response analysis investigates the previous behavior of the historical series by making use of several distinct techniques where the randomness, trend and the quality of being periodical in the given datasets are verified in two different methods. When the observations swing about a pivotal axis that is horizontal, it is known as stationary and it becomes non-stationary when it begins oscillating about the varying values. The most suitable and proper model for a particular dataset is the coefficient of determination which is labelled by R, the mean absolute error written in abridged form as MAE, and the third is the mean squared error in short form expressed abridgedly as MSE (Abraham et al., 2020; Escolano & Espín, 2016).

4.5 Accelerating Universe Driven by Multifield Tachyon-Quintom Dark Energy

We study the stability of the system here as a result of our developed mathematics for the model in methodology section.

4.5.1 Stability Of the Model

The fixed points which we have determined in the previous chapter 3 of methodology from the dynamical system, which are $x'_{\sum_{i=1}^{n}\xi_i}$, $y'_{\sum_{i=1}^{n}\xi_i}$, $x'_{\sum_{i=1}^{n}\eta_i}$ and $y'_{\sum_{i=1}^{n}\eta_i}$, it is observed that where these points diminish to zero, the existence of these critical points $x_{\left(\sum_{i=1}^{n}\xi_i\right)crt}$, $y_{\left(\sum_{i=1}^{n}\xi_i\right)crt}$, $x_{\left(\sum_{i=1}^{n}\eta_i\right)crt}$ and $y_{\left(\sum_{i=1}^{n}\eta_i\right)crt}$ corresponds to that. These critical points have been calculated for the system and are enlisted in the Table-4.6 given below. Now, from Eq. (3.5.31) calculated in previous chapter 3 of methodology, we determine the solutions of the self-similar nature, that is

$$\frac{H'}{H}=\frac{\dot{H}}{H^2}=-\frac{3}{2}\left(-\frac{y_{\sum_{i=1}^{n}\xi_i}\left(\gamma-x^2_{\sum_{i=1}^{n}\xi_i}\right)}{\sqrt{1-\sum_{i=1}^{n}\dot{\xi}_i^2}}-\frac{y_{\sum_{i=1}^{n}\eta_i}(\gamma-x^2_{\sum_{i=1}^{n}\eta_i}}{\sqrt{1-\sum_{i=1}^{n}\dot{\eta}_i^2}}+\gamma\right) \tag{4.5.1}$$

Table– 4.6: The table enlisting the critical points

Sr.No	$x_{\left(\sum_{i=1}^{n}\xi_i\right)crt}$	$y_{\left(\sum_{i=1}^{n}\xi_i\right)crt}$	$x_{\left(\sum_{i=1}^{n}\eta_i\right)crt}$	$y_{\left(\sum_{i=1}^{n}\eta_i\right)crt}$	**Existence Status**
I	0	0	0	0	$\sum_{j>0}^{2}\gamma_j$
II	0	0	$-\sqrt{\lambda_{\left(\sum_{i=1}^{n}\eta_i\right)}y_{\left(\sum_{i=1}^{n}\eta_i\right)crt}}$	$\frac{1}{2}\left(\sqrt{\lambda^2_{\left(\sum_{i=1}^{n}\eta_i\right)}+4}-\lambda_{\left(\sum_{i=1}^{n}\eta_i\right)}\right)$	$\sum_{j>0}^{2}\gamma_j$
III	±1	0	0	0	$\sum_{j>0}^{2}\gamma_j$
IV	±1	0	$-\sqrt{\lambda_{\left(\sum_{i=1}^{n}\eta_i\right)}y_{\left(\sum_{i=1}^{n}\eta_i\right)crt}}$	$\frac{1}{2}\left(\sqrt{\lambda^2_{\left(\sum_{i=1}^{n}\eta_i\right)}+4}+\lambda_{\left(\sum_{i=1}^{n}\eta_i\right)}\right)$	$\sum_{j>0}^{2}\gamma_j$
V	1	$\frac{1}{\lambda_{\left(\sum_{i=1}^{n}\xi_i\right)}}$	0	0	$\sum_{j=1}\gamma_j$
VI	-1	$\frac{1}{\lambda_{\left(\sum_{i=1}^{n}\xi_i\right)}}\left(\lambda^2_{\left(\sum_{i=1}^{n}\eta_i\right)}y^2_{\left(\sum_{i=1}^{n}\eta_i\right)crt}\right)$	$-\sqrt{\lambda_{\left(\sum_{i=1}^{n}\eta_i\right)}y_{\left(\sum_{i=1}^{n}\eta_i\right)crt}}$	$\frac{1}{2}\left(\sqrt{\lambda^2_{\left(\sum_{i=1}^{n}\eta_i\right)}+4}+\lambda_{\left(\sum_{i=1}^{n}\eta_i\right)}\right)$	$\sum_{j=1}\gamma_j$
VII	$\sqrt{\gamma}$	$\frac{\gamma}{\lambda_{\left(\sum_{i=1}^{n}\xi_i\right)}}$	0	0	$\frac{\lambda_{\left(\sum_{i=1}^{n}\xi_i\right)}\sqrt{\lambda^2_{\left(\sum_{i=1}^{n}\xi_i\right)}+4}-\lambda^2_{\left(\sum_{i=1}^{n}\xi_i\right)}}{2}>\gamma$
VIII	$\sqrt{\lambda_{\left(\sum_{i=1}^{n}\xi_i\right)}y_{\left(\sum_{i=1}^{n}\xi_i\right)crt}}$	$\frac{1}{2}\left(\sqrt{\lambda^2_{\left(\sum_{i=1}^{n}\xi_i\right)}+4}-\lambda_{\left(\sum_{i=1}^{n}\xi_i\right)}\right)$	0	0	$\sum_{j>0}^{2}\gamma_j$

This corresponds to an expanding universe such that the scale factor $a(t)$ is directly proportional to the power p of time t, i.e., scales like $a(t) \propto t^p$, where

$$p = \frac{2}{3\left(-\frac{y_{\sum_{i=1}^{n}\xi_i}\left(\gamma - x^2_{\sum_{i=1}^{n}\xi_i}\right)}{\sqrt{1-\sum_{i=1}^{n}\dot{\xi}_i^2}} - \frac{y_{\sum_{i=1}^{n}\eta_i}\left(\gamma - x^2_{\sum_{i=1}^{n}\eta_i}\right)}{\sqrt{1-\sum_{i=1}^{n}\dot{\eta}_i^2}} + \gamma\right)} \tag{4.5.2}$$

We now study the stability around the critical points given in Table-4.6 for which we consider small perturbations $\delta x_{\sum_{i=1}^{n}\xi_i}$, $\delta y_{\sum_{i=1}^{n}\xi_i}$, $\delta x_{\sum_{i=1}^{n}\eta_i}$, $\delta y_{\sum_{i=1}^{n}\eta_i}$ about the critical points $x_{\left(\sum_{i=1}^{n}\xi_i\right)crt}$, $y_{\left(\sum_{i=1}^{n}\xi_i\right)crt}$, $x_{\left(\sum_{i=1}^{n}\eta_i\right)crt}$ and $y_{\left(\sum_{i=1}^{n}\eta_i\right)crt}$ respectively such that

$$\begin{aligned}
x_{\left(\sum_{i=1}^{n}\xi_i\right)crt} &\to x_{\left(\sum_{i=1}^{n}\xi_i\right)crt} + \delta x_{\sum_{i=1}^{n}\xi_i} \\
y_{\left(\sum_{i=1}^{n}\xi_i\right)crt} &\to y_{\left(\sum_{i=1}^{n}\xi_i\right)crt} + \delta y_{\sum_{i=1}^{n}\xi_i} \\
x_{\left(\sum_{i=1}^{n}\eta_i\right)crt} &\to x_{\left(\sum_{i=1}^{n}\eta_i\right)crt} + \delta x_{\sum_{i=1}^{n}\eta_i} \\
y_{\left(\sum_{i=1}^{n}\eta_i\right)crt} &\to y_{\left(\sum_{i=1}^{n}\eta_i\right)crt} + \delta y_{\sum_{i=1}^{n}\eta_i}
\end{aligned}$$

when we substitute the above small perturbations around the critical points in Eqs. (3.5.37 - 3.5.38) and Eqs. (3.5.40 - 3.5.41) as described in previous chapter 3 of methodology, these lead to the following equations in matrix form which represents differential equations of the first order.

$$\begin{pmatrix} \delta x'_{\sum_{i=1}^{n}\xi_i} \\ \delta y'_{\sum_{i=1}^{n}\xi_i} \\ \delta x'_{\sum_{i=1}^{n}\eta_i} \\ \delta y'_{\sum_{i=1}^{n}\eta_i} \end{pmatrix} = X \begin{pmatrix} \delta x_{\sum_{i=1}^{n}\xi_i} \\ \delta y_{\sum_{i=1}^{n}\xi_i} \\ \delta x_{\sum_{i=1}^{n}\eta_i} \\ \delta y_{\sum_{i=1}^{n}\eta_i} \end{pmatrix} \tag{4.5.3}$$

where the X represents matrix depending upon the critical points $x_{\left(\sum_{i=1}^{n}\xi_i\right)crt}$, $y_{\left(\sum_{i=1}^{n}\xi_i\right)crt}$, $x_{\left(\sum_{i=1}^{n}\eta_i\right)crt}$ and $y_{\left(\sum_{i=1}^{n}\eta_i\right)crt}$.

The dependence of the matrix X on $x_{\left(\sum_{i=1}^{n}\xi_i\right)crt}$ $y_{\left(\sum_{i=1}^{n}\xi_i\right)crt}$ $x_{\left(\sum_{i=1}^{n}\eta_i\right)crt}$ and $y_{\left(\sum_{i=1}^{n}\eta_i\right)crt}$ is clear. Now the general solution for the evolution of linear perturbations can be expressed in the following way using the eigenvalues a, b, c, and d of the matrix X. Thus it is the nature of the eigenvalues upon which stability around the fixed points depends.

$$\delta x_{\sum_{i=1}^{n}\xi_i} = v_{11}e^{aN} + v_{12}e^{bN} + v_{13}e^{cN} + v_{14}e^{dN} \tag{4.5.4}$$

$$\delta y_{\sum_{i=1}^{n}\xi_i} = v_{21}e^{aN} + v_{22}e^{bN} + v_{23}e^{cN} + v_{24}e^{dN} \tag{4.5.5}$$

$$\delta x_{\sum_{i=1}^{n}\eta_i} = v_{31}e^{aN} + v_{32}e^{bN} + v_{33}e^{cN} + v_{34}e^{dN} \tag{4.5.6}$$

$$\delta y_{\sum_{i=1}^{n}\eta_i} = v_{41}e^{aN} + v_{42}e^{bN} + v_{43}e^{cN} + v_{44}e^{dN} \tag{4.5.7}$$

The following Table-4.7 enlists the eigenvalues and the status of stability for the critical or fixed points determined from the equations. The points h and k are given below

Table– 4.7: The table enlisting the eigenvalues and the status of stability

Labels	**a**	**b**	**c**	**d**	**Status of Stability**
I	-3	3γ	-3	3γ	unstable
II	-3	$-3x^2\left(\sum_{i=1}^{n}\eta_i\right)_{crt}$	$-3-\frac{3}{2}x^2\left(\sum_{i=1}^{n}\eta_i\right)_{crt}$	$-3\gamma-3x^2\left(\sum_{i=1}^{n}\eta_i\right)_{crt}$	stable
III	6	3γ	-3	3γ	unstable
IV	6	$-3x^2\left(\sum_{i=1}^{n}\eta_i\right)_{crt}$	$-3-\frac{3}{2}x^2\left(\sum_{i=1}^{n}\eta_i\right)_{crt}$	$-3\gamma-3x^2\left(\sum_{i=1}^{n}\eta_i\right)_{crt}$	unstable
V	0	$-\frac{3}{2}$	-3	3	unstable
VI	$6\left(1+x^2\left(\sum_{i=1}^{n}\eta_i\right)_{crt}\right)$	$\frac{3}{2}x^2\left(\sum_{i=1}^{n}\eta_i\right)_{crt}$	$-3-\frac{3}{2}x^2\left(\sum_{i=1}^{n}\eta_i\right)_{crt}$	$-3\gamma-3x^2\left(\sum_{i=1}^{n}\eta_i\right)_{crt}$	unstable
VII	h	k	-3	3γ	unstable
VIII	$3\left(-\gamma+x^2\left(\sum_{i=1}^{n}\xi_i\right)_{crt}\right)$	$\frac{3}{2}\left(-2+x^2\left(\sum_{i=1}^{n}\xi_i\right)_{crt}\right)$	-3	$3x^2\left(\sum_{i=1}^{n}\xi_i\right)_{crt}$	unstable

$$h = \frac{3\left[(\gamma-2)\lambda\sum_{i=1}^{n}\xi_i \mp \sqrt{16\lambda\sum_{i=1}^{n}\xi_i\gamma^2\sqrt{(-\gamma+1)}+\lambda^2\sum_{i=1}^{n}\xi_i(17\gamma^2-20\gamma+4)}\right]}{4\lambda\sum_{i=1}^{n}\xi_i} \tag{4.5.8}$$

and

$$k = \frac{3\left[(\gamma-2)\lambda\sum_{i=1}^{n}\xi_i \mp \sqrt{16\lambda\sum_{i=1}^{n}\xi_i\gamma^2\sqrt{(-\gamma+1)}+\lambda^2\sum_{i=1}^{n}\xi_i(17\gamma^2-20\gamma+4)}\right]}{4\lambda\sum_{i=1}^{n}\xi_i} \tag{4.5.9}$$

It has been described by E.J. Copeland et al. (Copeland et al., 2005) and Z.K. Guo et al. (Guo & Zhang, 2004) have shown that the real parts of all eigenvalues might be negative for the remaining stable points. Table-4.7 lists all the eigenvalues and the status of their stability. A fixed critical point I gives a solution with fluid domination, the

points II and III represent a phantom tachyon and tachyon domination in the solutions respectively. A two- field dominated solution is manifested by the fixed critical point IV. For the γ to remain unity, the fixed critical points V and VI owe their existence to it. The energy densities $\rho_{\sum_{i=1}^{n}\xi_i}$ and ρ_γ show a decrease at the same rate in the point VII when the point VIII indicates a solution where tachyon field energy dominates. The Figure-4.12 below demonstrates the evolution of the equation of state (EoS) parameter w and the development of the parameter of dark energy Ω_{DE} in the very early universe and their development during its behavior in the late time accelerated expansion where $\gamma = 1$ and $\lambda_{\left(\sum_{i=1}^{n}\xi_i\right)}$ and $\lambda_{\left(\sum_{i=1}^{n}\eta_i\right)}$ both take on the value 0.33. The above diagrams in

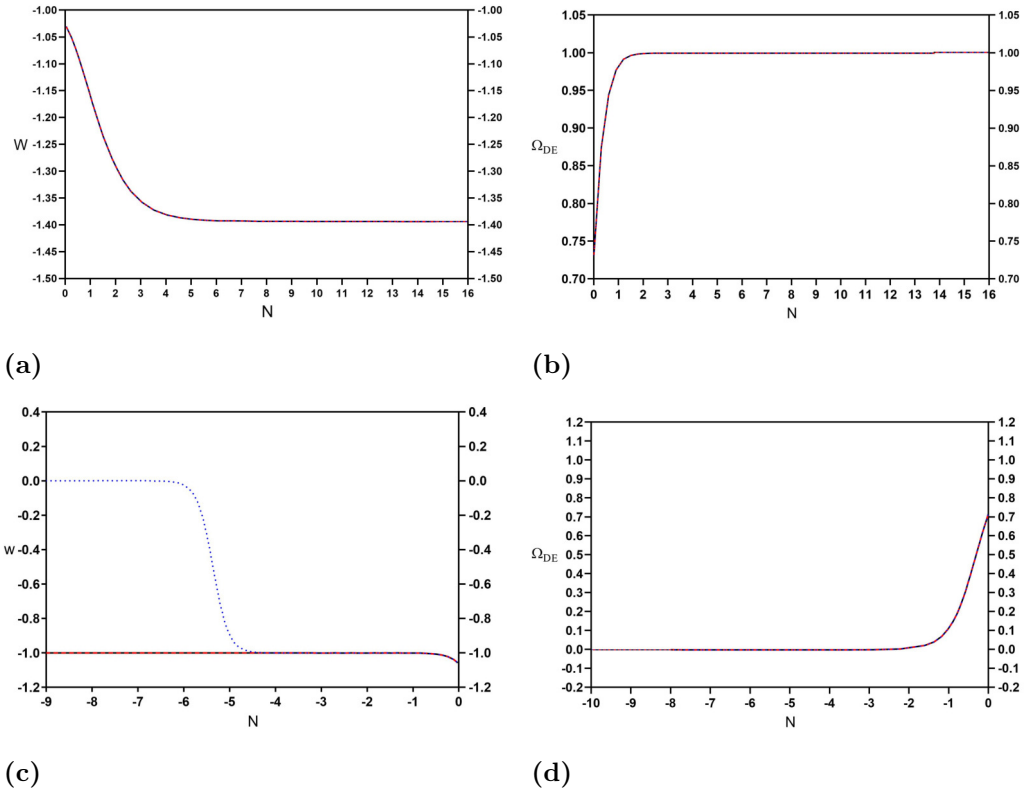

Figure– 4.12: The diagrams demonstrating the evolution of equation of state parameter w and the development of the parameter of dark energy Ω_{DE} in the very early universe. The figure also demonstrates their developmental growth during the cosmic behavior in late time accelerated expansion where $\gamma = 1$ and $\lambda_{\left(\sum_{i=1}^{n}\xi_i\right)}$ and $\lambda_{\left(\sum_{i=1}^{n}\eta_i\right)}$ both take on the value 0.33

Figure-4.12 illustrate the plots for the evolution of the equation of state parameter w

and dark energy parameter Ω_{DE} cosmologically against the growth of e-folding number N, It can be seen that the evolutionary path cosmologically bends towards the point II which is a fixed stability point in the Table-4.6 in the model. A comparison between the plots of the Figure-3.6 in the previous chapter 3 of Methodology and the values of the critical points listed in Table-4.6, can in addition clarify the situation more clearly . When we substitute $\frac{1}{3}$ the value of $\lambda_{\left(\sum_{i=1}^{n}\eta_i\right)}$ in point II the stable critical point i.e., $x_{\left(\sum_{i=1}^{n}\xi_i\right)crt} = 0$, $y_{\left(\sum_{i=1}^{n}\xi_i\right)crt} = 0$, $x_{\left(\sum_{i=1}^{n}\eta_i\right)crt} = -\sqrt{\lambda_{\left(\sum_{i=1}^{n}\eta_i\right)} y_{\left(\sum_{i=1}^{n}\eta_i\right)crt}}$ and

$$y_{\left(\sum_{i=1}^{n}\eta_i\right)crt} = \frac{\sqrt{\lambda^2_{\left(\sum_{i=1}^{n}\eta_i\right)} + 4} + \lambda_{\left(\sum_{i=1}^{n}\eta_i\right)}}{2} \tag{4.5.10}$$

we obtain the values of these points $x_{\left(\sum_{i=1}^{n}\xi_i\right)crt} = 0$, $y_{\left(\sum_{i=1}^{n}\xi_i\right)crt} = 0$, $x_{\left(\sum_{i=1}^{n}\eta_i\right)crt} = -\sqrt{\lambda_{\left(\sum_{i=1}^{n}\eta_i\right)} y_{\left(\sum_{i=1}^{n}\eta_i\right)crt}} = -0.627285$ and

$$y_{\left(\sum_{i=1}^{n}\eta_i\right)crt} = \frac{\sqrt{\lambda^2_{\left(\sum_{i=1}^{n}\eta_i\right)} + 4} + \lambda_{\left(\sum_{i=1}^{n}\eta_i\right)}}{2} = 1.180460 \tag{4.5.11}$$

which shows consistency with plots as described in Figure-4.12. Further with the help of Eq. (3.5.34), at the fixed point II, we possess $w = \frac{p}{\rho} = -1 - x^2_{\left(\sum_{i=1}^{n}\eta_i\right)crt} = -1.03367$ which also shows consistency with the plots drawn in Figure-3.6 in previous chapter 3 of methodology. In Table-4.7, We have described the initial values of the fixed points $x_{\left(\sum_{i=1}^{n}\xi_i\right)}, y_{\left(\sum_{i=1}^{n}\xi_i\right)}, x_{\left(\sum_{i=1}^{n}\eta_i\right)}$ and $y_{\left(\sum_{i=1}^{n}\eta_i\right)}$ would evolve towards stability If these are not the values of unstable points in the model granted the condition $1 - x^2_{\left(\sum_{i=1}^{n}\xi_i\right)} > 0$ does not get violated as physical constraint. When the values of the points $x_{\left(\sum_{i=1}^{n}\xi_i\right)}, y_{\left(\sum_{i=1}^{n}\xi_i\right)}, x_{\left(\sum_{i=1}^{n}\eta_i\right)}$ and $y_{\left(\sum_{i=1}^{n}\eta_i\right)}$ deviate slightly by a quantity amounting $\vec{\delta}$ from the values of $x_{\left(\sum_{i=1}^{n}\xi_i\right)crt}$, $y_{\left(\sum_{i=1}^{n}\xi_i\right)crt}$, $x_{\left(\sum_{i=1}^{n}\eta_i\right)crt}$, $y_{\left(\sum_{i=1}^{n}\eta_i\right)crt}$ from the Eqs. (4.5.4) - (4.5.7), it can be envisaged that $\vec{\delta}$ can be larger enough despite being diminishing.

4.5.2 Discussion and Final remarks

The analysis shows that the model does not indicate sensitivity to the kinetic energy density of under consideration multi-field scalars initially. It has been shown that there exists a stable unique critical point during the analysis of the background spatially flat

universe in the phase space. We make its comparison with the tachyon model altogether. The scale for sum-masses $M_{\left(\sum_{i=1}^{n}\xi_i\right)}$ of the multifield scalars $\sum_{i=1}^{n}\xi_i$ should be enough larger (Copeland et al., 2005) than Planck mass M_p in case of dark energy of multi-field tachyon with inverse square potential of the type $\sum_{i=1}^{n}V(\xi_i) = M^2_{\left(\sum_{i=1}^{n}\xi_i\right)}\sum_{i=1}^{n}\xi_i^{-2}$ in order to meet the late time accelerated expansion of the universe i.e., $a(t) \propto [time]^{\frac{1}{2}a}$, where $a = \left(\frac{M_{\left(\sum_{i=1}^{n}\xi_i\right)}}{M_p}\right)^2 >> 1$. This huge mass pushes the solutions towards dense energy regions where even general theory of relativity fails, therefore the potential $\sum_{i=1}^{n}V(\xi_i) = M^{4-p}_{\left(\sum_{i=1}^{n}\xi_i\right)}\sum_{i=1}^{n}\xi_i^{-2}$ where p lies between 0 and 2. The phantom tachyon fields $\sum_{i=1}^{n}\eta_i$ in our model take the responsibility of this late time acceleration with equation of state parameter $w_{\left(\sum_{i=1}^{n}\xi_i\right)} < -1$. From Eqs. (3.5.37) and (3.5.38), it becomes clear that the value of $M_{\left(\sum_{i=1}^{n}\xi_i\right)}$ is not still smaller as required by the recent observational constraints. This is due to the reason for $\lambda_{\left(\sum_{i=1}^{n}\xi_i\right)} = \frac{4}{3}\frac{M_p^2}{\left(\sum_{i=1}^{n}\xi_i\right)^2}$ being larger, therefore $1 - \left(\sum_{i=1}^{n}\dot{\xi}_i\right)^2$ falls in risk of non-positive behavioral increment.

In our multi-fields model of tachyon and phantom tachyon there is only one stable critical point namely II whose value does not rest on the value of γ, on the other hand in reference to (Aguirregabiria & Lazkoz, 2004), it is shown that in tachyon model of dark energy the sole source of dark energy is tachyon scalar field and it has three critical stable points, existence of whose hinges upon the factor γ. Further we have seen the values of scalar fields $\sum_{i=1}^{n}\dot{\xi}_i$ and $\sum_{i=1}^{n}\dot{\eta}_i$ are zero at critical points in our model of tachyon and phantom tachyon but in tachyon model of dark energy singly, the values of both fields at critical points can be non-zero also as expressed in the Table-4.7. The values of $x_{\left(\sum_{i=1}^{n}\xi_i\right)crt}$, $y_{\left(\sum_{i=1}^{n}\xi_i\right)crt}$, $x_{\left(\sum_{i=1}^{n}\eta_i\right)crt}$ and $y_{\left(\sum_{i=1}^{n}\eta_i\right)crt}$ at the critical points are fixed with the value of $x_{\left(\sum_{i=1}^{n}\eta_i\right)crt}$ becoming non-zero and if its value is zero then $y_{\left(\sum_{i=1}^{n}\eta_i\right)crt}$ turns out to be zero, this is obvious from the Eq. (3.5.40), it further ensues the impossibility

that $x_{\left(\sum_{i=1}^{n}\eta_i\right)crt}$ and $\rho_{\left(\sum_{i=1}^{n}\eta_i\right)crt}$ are zero i.e.,

$$\begin{cases} \rho_{\left(\sum_{i=1}^{n}\xi_i\right)_{crt}} = \frac{\sum_{i=1}^{n}V(\xi_i)_{crt}}{\sqrt{1-\left(\sum_{i=1}^{n}\dot{\xi}_i^2\right)_{crt}}} = \frac{3y_{\left(\sum_{i=1}^{n}\xi_i\right)_{crt}}}{\sqrt{1-x^2_{\left(\sum_{i=1}^{n}\xi_i\right)_{crt}}}}M_p^2H^2 \\ p_{\left(\sum_{i=1}^{n}\xi_i\right)_{crt}} = \left(w_{\left(\sum_{i=1}^{n}\xi_i\right)_{crt}}\right)\left(\rho_{\left(\sum_{i=1}^{n}\xi_i\right)_{crt}}\right) \\ \Rightarrow w_{\left(\sum_{i=1}^{n}\xi_i\right)_{crt}} = -1+\left(\sum_{i=1}^{n}\dot{\xi}_i^2\right)_{crt} = -1+x^2_{\left(\sum_{i=1}^{n}\xi_i\right)_{crt}} \geq -1 \end{cases} \tag{4.5.12}$$

and

$$\begin{cases} \rho_{\left(\sum_{i=1}^{n}\eta_i\right)_{crt}} = \frac{\sum_{i=1}^{n}V(\eta_i)_{crt}}{\sqrt{1-\left(\sum_{i=1}^{n}\dot{\eta}_i^2\right)_{crt}}} = \frac{3y_{\left(\sum_{i=1}^{n}\eta_i\right)_{crt}}}{\sqrt{1-x^2_{\left(\sum_{i=1}^{n}\eta_i\right)_{crt}}}}M_p^2H^2 \\ p_{\left(\sum_{i=1}^{n}\eta_i\right)_{crt}} = \left(w_{\left(\sum_{i=1}^{n}\eta_i\right)_{crt}}\right)\left(\rho_{\left(\sum_{i=1}^{n}\eta_i\right)_{crt}}\right) \\ \Rightarrow w_{\left(\sum_{i=1}^{n}\eta_i\right)_{crt}} = -1-\left(\sum_{i=1}^{n}\dot{\eta}_i^2\right)_{crt} = 1-x^2_{\left(\sum_{i=1}^{n}\eta_i\right)_{crt}} < -1 \end{cases} \tag{4.5.13}$$

It is clear from Eq. (4.5.12) that H^2 becomes non-increasing for non-zero $y_{\left(\sum_{i=1}^{n}\xi_i\right)crt}$ at the points which are fixed, with $\rho_{\left(\sum_{i=1}^{n}\xi_i\right)crt}$ also non-increasing. The same is not inapplicable from Eq. (4.5.13) for $y_{\left(\sum_{i=1}^{n}\eta_i\right)crt}$ and $\rho_{\left(\sum_{i=1}^{n}\eta_i\right)crt}$ making one of the two critical points $y_{\left(\sum_{i=n}^{n}\xi_i\right)crt}$, $y_{\left(\sum_{i=1}^{n}\eta_i\right)crt}$ equal to zero. Therefore $y_{\left(\sum_{i=n}^{n}\xi_i\right)crt}$ is set to zero for $\rho_{\left(\sum_{i=1}^{n}\xi_i\right)crt}$ as non-increasing and $\rho_{\left(\sum_{i=1}^{n}\eta_i\right)crt}$ as increasing. Moreover if $1-x^2_{\left(\sum_{i=1}^{n}\xi_i\right)crt} > 0$ does not get violated and for $y_{\left(\sum_{i=1}^{n}\xi_i\right)crt}$ being zero, the critical point $x_{\left(\sum_{i=1}^{n}\xi_i\right)crt}$ also becomes zero. In tachyon model of dark energy, the speed of sound c_s^2 is described by the following expression

$$c_s^2 = \frac{p_{\left(\sum_{i=1}^{n}\xi_i\right)}\frac{1}{2}\left(\sum_{i=1}^{n}\partial_\mu\xi_i\right)^2}{\rho_{\left(\sum_{i=1}^{n}\xi_i\right)}\frac{1}{2}\left(\sum_{i=1}^{n}\partial_\mu\xi_i\right)^2} = 1-\sum_{i=1}^{n}\dot{\xi}_i^2 \leq 0 \tag{4.5.14}$$

In order to investigate whether a ghost dark energy model is stable or the otherwise, we use the theory of perturbation. In case the model is unstable we can find ghost modes for ghost instability therein. In the energy density of the background we consider a perturbation of very small size and investigate to observe whether it will collapse or will grow cosmologically. We can write from the linear theory of perturbation $\rho(x,t) = \rho(t) + \delta\rho(x,t)$, here the term $\rho(t)$ represents the energy density in the background that

remains unperturbed. Now from Eq. (3.5.10) or from covariant divergence of energy-momentum tensor $\nabla_i T^{ij} = 0$, we obtain the following equation

$$\delta\left(\partial_{tt}\rho\right) = c_s^2 \nabla^2 \delta\rho\left(x,t\right) \tag{4.5.15}$$

here c_s^2 is described as the term with speed of sound squared and is expressed as $\frac{dp}{d\rho}$. Two solutions $\delta\rho = \delta\rho_0 \exp\left(i\vec{k}\cdot\vec{x} \pm i\omega t\right)$ come out, where for the case when $c_s^2 > 0$, the first solution comes out to be oscillatory wave solution $\delta\rho = \delta\rho_0 \exp\left(i\vec{k}\cdot\vec{x} - i\omega t\right)$ which demonstrates propagation mode for the perturbations of energy density. When the second solution is $\delta\rho = \delta\rho_0 \exp\left(i\vec{k}\cdot\vec{x} + i\omega t\right)$ for $c_s^2 < 0$. This describes that the density perturbation would grow out because in this case the oscillation frequency comes out to be purely imaginary. This propagation mode as growing perturbation marks the possibility for ghost instabilities to emerge. The unwanted consequence of $c_s^2 < 0$ is principally interpreted as the growth of amplitude exponentially for the modes with short wavelengths. The robust coupling scale being light during $c_s^2 < 0$, excludes the validity range of an effective field theory for the dangerous short wavelength modes to incorporate. The occurrence of ghost instability is related to the field having negative kinetic energy term. In the field theories these are usually followed by the violation of Null Energy Condition (NEC) in the development of singularity-free cosmological models in effective field theories. The problem of ghosts is resolved by considering the theory of Galileon, its generalized forms and the theories beyond it, see References (Y. Cai et al., 2017) and the references therein. Gradient instability arises when the field has a negative momentum squared and is related to negative speed of sound squared. This may lead to perturbations grow exponentially. Some spatial operators cure this instability. However it was shown that tachyon dark energy models have speed of sound squared c_s^2 to be positive. Therefore, these models are supposed to be stable against small perturbations (Gorini, Kamenshchik, Moschella, Pasquier, & Starobinsky, 2005; Sandvik, Tegmark, Zaldarriaga, & Waga, 2004). The speed of sound squared is to be found

$$c_s^2 = \frac{\dot{c}_3 - a c_2}{a c_1} \tag{4.5.16}$$

from the quadratic action of scalar perturbations where $c_2 = M_p^2 f\left(t\right)$ and the action is

$$S_\xi^2 = \int \left[c_1 \dot{\xi}^2 - \left(\frac{\dot{c}_3}{a} - c_2\right) \frac{\left(\partial\xi\right)^2}{a^2} + \frac{c_4}{a_a}\left(\partial^2\xi\right)^2 - \frac{16\lambda\left(t\right)}{M_p^2 a^6}\left(\partial^2\xi\right)^2 \right] a^3 d^4x \tag{4.5.17}$$

The condition to avoid the ghost instability is $c_1 > 0$ and the gradient instability is avoided by the condition $\dot{c}_3 - a c_2 > 0$. Similarly, from quadratic action of tensor

perturbations

$$S_{\gamma}^{2} = \frac{M_p^2}{8}\int\left(\gamma_{\mu\nu}^{2} - c_T^2\frac{\left(\gamma_{\mu\nu,\rho}\right)^2}{a^2}\right)a^3 Q_T d^4x \tag{4.5.18}$$

we have $Q_T = f + 2\left(\frac{m_4}{M_p}\right)^2$ and $c_T^2 = \frac{f}{Q_T}$. The conditions for avoiding the gradient and ghost instabilities for tensor modes are $c_T^2 > 0$ and $Q_T > 0$ respectively.

In relation to the Eq. (4.5.14), we explain that due to the presence of under-root in the Lagrangian density $\mathcal{L}$, the difference term $1 - \sum_{i=1}^{n}\dot{\xi}_i^2$ will be non-positive accordingly and it keeps as a consequence, the pressure and energy to remain in the realm of real, therefore a positive sound speed is attributed to the homogeneous perturbations which owes stability. We can put to use independent sound speed of each component of the multi-fields tachyon and phantom tachyon in our case here to give a description to the model. It is, however, notable that J.Q. Xia et al. (Xia, Cai, Qiu, Zhao, & Zhang, 2008; Myung, 2007; Bean & Dore, 2004) and H. Kodama et al. (Kodama & Sasaki, 1984) have shown the use of effective sound speed because using of two or more independent components of sound does not coincide with the present juncture of the constraints of dark energy. The effective sound speed for larger N in the case when the energy density is considered as a fraction of dark energy density of phantom tachyon, when $\Omega_{\sum_{i=1}^{n}\eta_i}$ approaches to unity, is

$$c_s^2 = \frac{p_{\sum_{i=1}^{n}\eta_i}\frac{1}{2}\left(\sum_{i=1}^{n}\partial_\mu\eta_i\right)^2}{\rho_{\sum_{i=1}^{n}\eta_i}\frac{1}{2}\left(\sum_{i=1}^{n}\partial_\mu\eta_i\right)^2} = 1 + \sum_{i=1}^{n}\dot{\eta}_i^2 > 1 \tag{4.5.19}$$

for the effective density in the Lagrangian $\mathcal{L}$ of Eq. (3.5.2) in previous chapter 3. It can be interpreted as the perturbations of the scalar field in the background that can move with a speed larger than the speed of light in the preferred and privileged frame of reference where the field is existing homogeneously in the background. In concluding remarks, we investigated a dark energy model consisting of multi-field tachyon and multi-field phantom tachyon known as the multi-field tachyon-quintom model. During evolution of the universe, the equation of state parameter w in $p = w\rho$ changes its direction from $w < -1$ to $w > -1$ in the model we considered. The inverse square potentials are used in the development of the autonomous system as dynamical system for performing the analysis in phase space where we found stable points that have power-law solutions. The analysis of spatially flat background universe of FLRW metric manifests the existence of a unique critical point which is compared with the tachyon dark energy model. We observed that neither multi-field tachyon nor the multi-field phantom tachyon showed

sensitivity to the kinetic energy of initial conditions. It happens approximately when the e-folding number is near to ten and the variation of multi-field tachyons by the order of magnitude four is still observed coinciding with the observations conducted in the recent past.

The results for multiple tachyon and phantom tachyon fields are presented graphically, in which slightly changed behaviour of the parameters involved as compared to single field. At the fixed point II in Table-4.7, we obtained $w = \frac{p}{\rho} = -1 - x^2_{\left(\sum_{i=1}^{n} \eta_i\right)crt} = -1.03367$ which also shows consistency with the plots drawn in Figure-3.6 presented in previous chapter of Methodology and has minute difference with single scalar fields. The evolution of equation of state parameter w and dark energy parameter Ω_{DE} as function of number of e-folds N is plotted beginning with the initial condition -10. In accordance with it the initial values of the fields have slight variations which impacts the overall results very lightly. The different initial values of the scalar fields have convergence towards a track that evolves in common with all for $N \geq 2$. From this point onwards the values of the fields become slightly larger, however the convergence of these fields with distinct and different initial values stay constant and do no change.

4.6 Accelerating Universe in the Framework of $f(R)$ Modified Gravity

The following results are obtained for the model under consideration in the framework of $f(R)$ modified gravity. We discuss four cases by modifying the autonomous dynamical system as each case demands correspondingly imposing conditions on the cosmic stuff i.e. matter, radiation and dark energy. By determining fixed points in each, their eigenvalues are calculated. Stability of all the systems considered is discussed in the light of eigenvalues. For other related eras, parameters of density of all kinds and equation of state parameters are computed and interpreted.

4.6.1 Calculations For the Model Under Consideration and Construction Of Autonomous System

After reviewing the necessary mathematical machinery for the sake of retrospection employed for investigating more possibilities in the framework of $f(R)$ gravity, we are now to apply that for a particular viable $f(R)$ model in order to carry out its analysis and study of its stability properties in phase space through dynamical system approach. The use of puissant and powerful approach of dynamical systems is very frequent nowadays to

study the cosmological evolution of our universe. The dynamical system approach proves very advantageous in understanding the cosmic dynamics globally in the context of any proposed model with regard to early universe and specifically the late time dynamics of the accelerated expansion. In perspective of a dynamical system, we construct an autonomous system of differential equations for the given cosmological model by introducing suitable dynamical variables in the model. By doing this, we can suitably carry out the analysis of many of the features of the model in the phase space through studying the critical points and their stability analysis. This may provide realization and insight into the large scale behaviour of the model under consideration for the geometry of global dynamics of the model. We assume first that the universe is composed of radiation and matter only that do not interact with each other i.e., $\int \left(\frac{1}{2k^2} f(R) + \mathcal{L}_m + \mathcal{L}_r\right) d^4x\sqrt{-g}$. The characteristics of being mutually interaction-free renders the equation of continuity $\dot{\rho} + 3\partial_t a(\rho + p) = 0$ to assume the forms i.e., $\dot{\rho}_m + 3\partial_t a\rho_m = 0$ and $\dot{\rho}_r + 4\partial_t a\rho_r = 0$ for the corresponding epoches with i.e., $p_m = 0$ and $p_m = \frac{4}{3}\rho_r$ respectively. The modified Friedmann equations as determined for a spatially flat, homogeneous and expanding universe in Eq. (3.6.16) and Eq. (3.6.19) of methodology chapter 3 are

$$3H^2F = \frac{1}{2}(FR - f) - 3H\dot{F} + k^2(\rho_m + \rho_r) \tag{4.6.1}$$

$$2\dot{H}F = -\ddot{F} + H\dot{F} - k^2(\rho_m + p_m) \tag{4.6.2}$$

where $p_m = \frac{4}{3}\rho_r$. In first Friedmann equation (4.6.1), the following dimensionless variables or parameters are defined

$$x_1 = -\frac{\dot{F}}{HF}, x_2 = -\frac{f}{6H^2F}, x_3 = \frac{R}{6H^2}, x_4 = \Omega_r = \frac{k^2\rho_r}{3H^2F} \tag{4.6.3}$$

Moreover, we have a constraint from Eq. (3.6.27) in previous chapter 3 of methodology

$$x_1 + x_2 + x_3 + x_4 = 1 \tag{4.6.4}$$

In Eq. (4.6.4), $x_4 = \Omega_r = w = \frac{k^2\rho_r}{3H^2F}$ and it gives

$$\Omega_m = 1 - \Omega_r - (x_1 + x_2 + x_3) \tag{4.6.5}$$

The parameter for energy density contributed by geometric curvature Ω_{GC} is the sum of variables x_1, x_2 and x_3 i.e.,

$$\Omega_{GC} = x_1 + x_2 + x_3 = H^{-2}\left(\dot{H} + 2H^2 - H\frac{\dot{F}}{F} - \frac{f}{6F}\right) \tag{4.6.6}$$

we consider the following particular model in order to study its stability analysis by constructing an autonomous system whose dynamics will describe the physical universe

as a system in phase space.

$$f(R) = R^p \exp(qR) \tag{4.6.7}$$

and

$$f_{,R}(R) = \exp(qR)\left[pR^{p-1} + qR^p\right] \tag{4.6.8}$$

$$f_{,RR}(R) = \exp(qR)\left[p(p-1)R^{p-2} + 2pqR^{p-1} + q^2R^p\right] \tag{4.6.9}$$

and

$$m = \frac{Rf_{,RR}(R)}{f_{,R}(R)} = \frac{p(p-1) + 2pqR + q^2R^2}{p + qR} \tag{4.6.10}$$

and

$$r = -\frac{Rf_{,R}(R)}{f(R)} = -(p + qR) \tag{4.6.11}$$

Now, with the help of Eq. (4.6.8) and Eq. (4.6.9), we determine the value of m in terms of r or as a function of it i.e., $m(r)$

$$m(r) = \frac{p}{r} - r \tag{4.6.12}$$

which comes out to be independent of parameter q. By writing now the parameter m in terms of the variable r i.e., $m = m(r)$, we can realize the possible existence of matter-dominated era followed by radiation era after which the late time accelerated expansion epoch would has started. The properties of the model can also be studied from the curves drawn for $m(r)$ in the plane (m, r) as given below in the Figure-4.13. The expression of $m(r)$ can be re-evaluated using for r from Eq. (3.6.34) in it as

$$m(r) = \frac{-x_3^2 + x_2^2 p}{x_2 x_3} \tag{4.6.13}$$

The derivative of m in Eq. (4.6.7) is

$$\frac{dm}{dr} = -\frac{p}{r^2} - 1 \tag{4.6.14}$$

We can check the conditions for m and $\frac{dm}{dr}$ to understand the viability of matter dominated era and the late time accelerated expansion epoch. For matter dominated epoch $m(r)|_{r=-1} = -p + 1$, for $p = 1$, it leads to $m(r) = 0$. Now $\left.\frac{dm(r)}{dr}\right|_{r=-1} = -p - 1$, at $p = 1$, $\left.\frac{dm(r)}{dr}\right|_{r=-1} = -2$, it leads to $\left.\frac{dm(r)}{dr}\right|_{r=-1} < -1$ as $-2 < -1$, however we require $\left.\frac{dm(r)}{dr}\right|_{r=-1} > -1$. Therefore for $p = 1$, the conditions of viable matter dominated epoch are partially achieved which means that the model $f(R) = R^p e^{qR}$ does not yield matter dominated epoch at $r = -1$ and $p = 1$. For $p < 0$, the condition $\left.\frac{dm(r)}{dr}\right|_{r=-1} < -1$ is satisfied i.e., for $p \neq 1$. For a viable epoch of late time accelerated expansion we have $m(r)|_{r=-2} = -\frac{p}{2} + 2$ and $\left.\frac{dm(r)}{dr}\right|_{r=-2} = -\frac{p}{4} - 1$, whereas either we have to satisfy

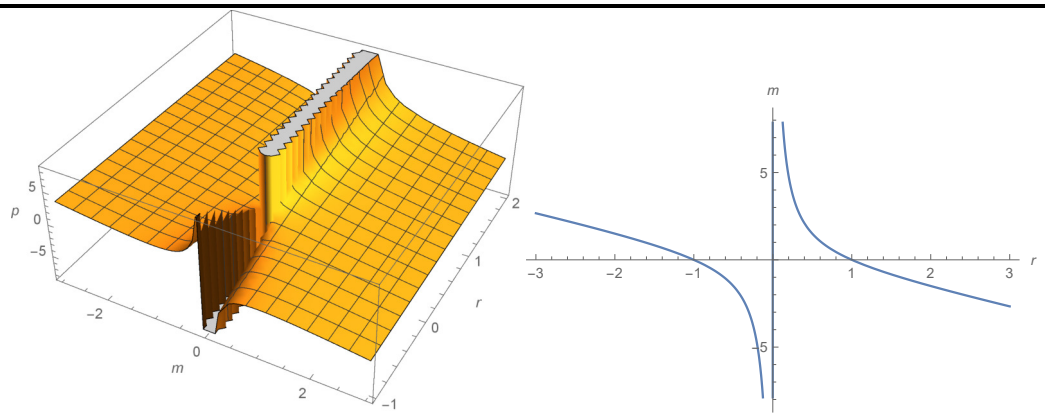

(a) **(b)**

Figure– 4.13: The evolution of the geometric curve for the model under consideration. The plots between the parameter m and r for the function $m(r) = \frac{p}{r} - r$ determined for the model $f(R) = R^p \exp(qR)$ in the plane (m, r). In Fig1(a), $p = 1$ whereas in Fig1(b) $p = 0$

$m(r) = -r - 1$, $\frac{dm(r)}{dr} < 1$ with $\frac{\sqrt{3}-1}{2} < m \leq 1$ at $r = -2$ or at $r = -2$ just $0 \leq m \leq 1$. Now at $p = 1$ it is not satisfied, however at $p = 2$ it is fulfilled and it remains valid for $p \geq 2$. Further, in Eq. (4.6.7) for $p = 1$, we have $m(r) = -r$ which purely presents the exponential case of the model evolution (Amendola et al., 2007). Now, we substitute the value of $m(r)$ from above equation in the dynamical system described in Eqs. (3.6.28)-(3.6.31), and after simplification, we obtain the following set of differential equations for the model under consideration. This is how we transform fourth order gravity equations of $f(R)$ in a system of linear equations.

$$x'_1 = -1 + x_1^2 - x_1 x_3 - 3x_2 - x_3 + x_4 \tag{4.6.15}$$

$$x'_2 = -x_2(-4 - x_1 + 2x_3) + \frac{x_1 x_2 x_3^2}{p x_2^2 - x_3^2} \tag{4.6.16}$$

$$x'_3 = -2x_3(x_3 - 2) - \frac{x_1 x_2 x_3^2}{p x_2^2 - x_3^2} \tag{4.6.17}$$

$$x'_4 = x_4(x_1 - 2x_3) \tag{4.6.18}$$

and the effective equation of state parameter w_{eff}, matter density parameter Ω_m and radiation density parameter Ω_r for this system will be determined by

$$w_{eff} = -1 - \frac{2\dot{H}}{3H^2} = -\frac{1}{3}(2x_3 - 1) \tag{4.6.19}$$

$$\Omega_r = x_4 = w = \frac{k^2\rho_r}{3H^2F} \tag{4.6.20}$$

and

$$\Omega_m = \frac{k^2\rho_m}{3H^2F} = 1 - (x_1 + x_2 + x_3 + x_4) \tag{4.6.21}$$

and from Eq. (3.6.27)

$$x_1 + x_2 + x_3 = 1 - x_4 \tag{4.6.22}$$

or

$$\Omega_{GC} = \Omega_{DE} = 1 - \Omega_r - \Omega_m \tag{4.6.23}$$

where $\Omega_{GC} = x_1 + x_2 + x_3$ and Ω_{GC} signifies the gravity due to curvature playing the role of dark energy. Now, we determine the critical points, their eigenvalues and the related density parameters Ω_{GC}, Ω_m and Ω_r using these points.

4.6.2 Stability Analysis For Cosmic Dynamics Without Including Cosmological Constant Λ as Dark Energy

The critical points are usually categorized into three cases discerned on the basis of the signs of eigenvalues. Firstly, a stable point or an attractor is the one for which the eigenvalues of the Jacobian matrix have all the real parts of them to be negative. In this case, all the nearby trajectories are attracted toward the critical point. Secondly, an unstable point or a repeller is the one for which the eigenvalues of the Jacobian matrix possess all the real parts of them to be positive. In this case, the trajectories are repelled from the critical point. Thirdly, a critical point is a saddle point if one half the eigenvalues of the Jacobian matrix has positive signs and the other half possesses negative signs. This case nonetheless becomes relevant if the two eigenvalues at the lowest possess the real parts with opposite signs. In this case, some of the nearby trajectories are attracted toward the critical point and some are repelled away from the critical point. Moreover, eigenvalues are used to determine whether a critical point (fixed or equilibrium point) is stable or unstable. On displacing a system in beginning around a critical point, if the system comes back ultimately to its original position and ensures its stay over that point, the critical point is stable. On the other hand, around an unstable critical point, the system does not return to its initial state. Now, the eigenvalues of the system linearized around the critical point can determine the stability modus operandi about that point. The particular behavior of stability is dependent upon the existence and nature of the eigenvalues. The real and imaginary components of eigenvalues, in addition to the signatures of real parts and in addition their being

distinct are very fundamental to the study of stability analysis. Some properties of eigenvalues are mentioned below

1. Eigenvalues with only real component

   The Eigenvalues possessing only real components are

a. All Positive

   The set of eigenvalues of a point are positive, distinct and real, the point is unstable and the system at this point is unstable as well.

b. All Negative

   When all the eigenvalues of a point are negative, distinct and real, the point is unstable and the system at this point is unstable as well.

c. Negative and positive

   When the set of eigenvalues of a point contains both positive and negative, then critical point represents a saddle point that is unstable.

d. Repeated and Real

   For two positive repeated eigenvalues, the critical point is unstable source whereas for two negative repeated it is stable sink. Moreover, or the real and repeated eigenvalues, the role of associated eigenvector decides whether the critical point is stable or unstable depending upon whether it is linearly independent or orthogonal. In this case the eigenvector degenerates and an eigenvalue possess more than one eigenvector associated with it.

e. Zero eigenvalues

   If the set of eigenvalues of a point consists of both real and imaginary parts as zero, the system is unstable with unstable point.

2. Complex eigenvalues

   For a set of imaginary eigenvalues i.e., $x + iy$, stability analysis depends upon the existence and nature of real part with a non-zero complex component. The following three cases belong to it

a. Zero Real Component

   For zero real component, the system mimics the role of an undamped oscillator

b. Positive Real component

   For a positive real part, the point is unstable making the system unstable behaving

like an unstable oscillator.

c. Negative Real component

For a negative real part, the point is stable and consequently the system is stable at this point behaving as a damped oscillator. It makes a necessary and sufficient condition for a stable system to have the real parts of all eigenvalues negative signs in this case.

We determine now the Jacobian matrix for the system given in Eqs. (4.6.15-4.6.18) which comes out

$$J = \begin{pmatrix} 2x_1 - x_3 & -3 & -1 - x_1 & 1 \\ x_2 + \frac{x_2 x_3^2}{p x_2^2 - x_3^2} & 4 + x_1 - 2x_3 - \frac{2p x_1 x_2^2 x_3^2}{\left(p x_2^2 - x_3^2\right)^2} + \frac{x_1 x_3^2}{p x_2^2 - x_3^2} & -2x_2 + \frac{2x_1 x_2 x_3^3}{\left(p x_2^2 - x_3^2\right)^2} + \frac{2x_1 x_2 x_3}{p x_2^2 - x_3^2} & 0 \\ -\frac{x_2 x_3^2}{p x_2^2 - x_3^2} & \frac{2p x_1 x_2^2 x_3^2}{\left(p x_2^2 - x_3^2\right)^2} - \frac{x_1 x_3^2}{p x_2^2 - x_3^2} & -2\left(-2 + x_3\right) - 2x_3 - \frac{2x_1 x_2 x_3^3}{\left(p x_2^2 - x_3^2\right)^2} - \frac{2x_1 x_2 x_3}{p x_2^2 - x_3^2} & 0 \\ x_4 & 0 & -2x_4 & x_1 - x_3 \end{pmatrix} \tag{4.6.24}$$

The dynamical system for the model in Eq. (4.6.15) to Eq. (4.6.18), has the following critical points as solutions of these equations $\frac{dx_1}{dN} = 0$, $\frac{dx_2}{dN} = 0$, $\frac{dx_3}{dN} = 0$, $\frac{dx_4}{dN} = 0$. We will calculate their corresponding eigenvalues with the help of Jacobian matrix, the effective equation of state parameter w_{eff}, and parameters for matter, radiation and curvature densities i.e. Ω_m, Ω_r, and Ω_{GC} respectively for analysing its stability.

P_1: $(x_1, x_2, x_3, x_4) = (-4, 5, 0, 0)$

The characteristic polynomial $\lambda^4+8\lambda^3-\lambda^2-128\lambda-240$ gives the following eigenvalues of point P_1: -5, -4, 4, 3. $w_{eff} = \frac{1}{3}$, $\Omega_m = \frac{k^2\rho_m}{3FH^2} = 1-(x_1 + x_2 + x_3 + x_4) = 0$, $\Omega_r = x_4 = 0$ and $\Omega_{GC} = 1$. For a point to be stable the signs of its all eigenvalues must be negative, however in case of I, one of the eigenvalues 4 is positive which makes the point insusceptible to stability. On the other hand, the value of the effective equation of state parameter is positive which means that the cosmic accelerated expansion could not be realized through this point. Similarly, through this point the matter dominated epoch could not be yielded. The point is, however predominated thoroughly by Ω_{GC} i.e., curvature density is prevalent.

P_2: $(x_1, x_2, x_3, x_4) = (0, -1, 2, 0)$

The eigenvalues of point P_2 are -4, -3, $\frac{12-3p-\sqrt{272-168p+25p^2}}{2(-4+p)}$, $\frac{12-3p+\sqrt{272-168p+25p^2}}{2(-4+p)}$. $w_{eff} = -1$, $\Omega_m = 0$, $\Omega_r = 0$ and $\Omega_{GC} = 1$. It can be observed on simplification that the real parts of all four eigenvalues are negative which makes the point P_2 stable, however spirally stable. On the other hand, from the negative value of the

effective equation of state parameter w_{eff}, it is clear that this point produces acceleration. It means that the cosmic accelerated expansion could be realized through this point. However, matter dominated epoch could not be achieved through this point. However the point is completely dominated by the curvature geometrically $\Omega_{GC} = 1$.

P_3: $(x_1, x_2, x_3, x_4) = (-1, 0, 2, 0)$

The eigenvalues of point III are -5, -4, -4, 0. $w_{eff} = -1$, $\Omega_m = 0$, $\Omega_r = 0$ and $\Omega_{GC} = 1$. The real parts of three eigenvalues are negative while 4rth is zero which makes the point P_3 unstable. On the other hand, from the signature of the effective equation of state parameter w_{eff}, it is clear that this point could produce acceleration which means that the cosmic accelerated expansion could be realized through this point. However, matter dominated epoch could not be achieved through this point. However the point is thoroughly dominated by the curvature geometrically $\Omega_{GC} = 1$.

P_4: $(x_1, x_2, x_3, x_4) = (3, 0, 2, 0)$

The eigenvalues of point IV are -4, 4, -1, 0. $w_{eff} = -1$, $\Omega_m = -4$, $\Omega_r = 0$ and $\Omega_{GC} = 5$. The real parts of two eigenvalues are negative, one zero and 4rth has positive signature which makes the point P_4 unstable. On the other hand, from the negative value of the effective equation of state parameter w_{eff}, it is concluded that this point is related with the accelerated expansion. Matter dominated epoch, nonetheless, could not be obtained through this point as Ω_m has negative value violating the definition for this era. The value of curvature density is also problematic and may pose unjustified difficulty in interpretation as $\Omega_{GC} = 5$.

P_5: $(x_1, x_2, x_3, x_4) = (4, 0, 2, -5)$

The eigenvalues of point P_5 are: 5, -4, 1, 0. $w_{eff} = -1$, $\Omega_m = 0$, $\Omega_r = -5$ and $\Omega_{GC} = 6$. One of the eigenvalues is negative, however, due to presence of zero, and positive signatures of other eigenvalues, the point P_5 unstable. On the other hand, from w_{eff}, the point shows viability to yield the epoch of accelerated expansion. It means that the cosmic accelerated expansion could be realized through this point. However, matter dominated epoch could not be achieved through this point as Ω_m has zero value. The value of curvature density is also problematic and may pose much difficulty in interpretation as $\Omega_{GC} = 6$.

P_6: $(x_1, x_2, x_3, x_4) = \left(\frac{4(-1+p)}{p}, \frac{2(-1+p)}{p^2}, \frac{2(-1+p)}{p}, \frac{-2+8p-5p^2}{p^2}\right)$

The eigenvalues of point P_6 are: $1, -\frac{4\left(-p+p^2\right)}{(-1+p)p^2}, \frac{2p-3p^2+p^3-\sqrt{3}\sqrt{12p^2-68p^3+127p^4-98p^5+27p^6}}{2(-1+p)p^2}$, $\frac{2p-3p^2+p^3+\sqrt{3}\sqrt{12p^2-68p^3+127p^4-98p^5+27p^6}}{2(-1+p)p^2}$. $w_{eff} = -1+\frac{4}{3p}$, $\Omega_m = 0$, $\Omega_r = -5-\frac{2}{p^2}+\frac{8}{p}$ and $\Omega_{GC} = 6+\frac{2}{p^2}-\frac{8}{p}$. Due to presence of 1 as positive eigenvalue, the point gets deprived of stability and remains unstable. Matter dominated epoch could not be achieved through this point as Ω_m is vanishing. Moreover, the value of p is decisive in having other properties related with point P_6. For $p < 0$ and $p \geq 2$, it produces different possibilities in yielding various eras of energy density, however the point is not viable for accelerated expansion. The eigenvalue plot for the point P_6 is presented in Figure-4.14 below.

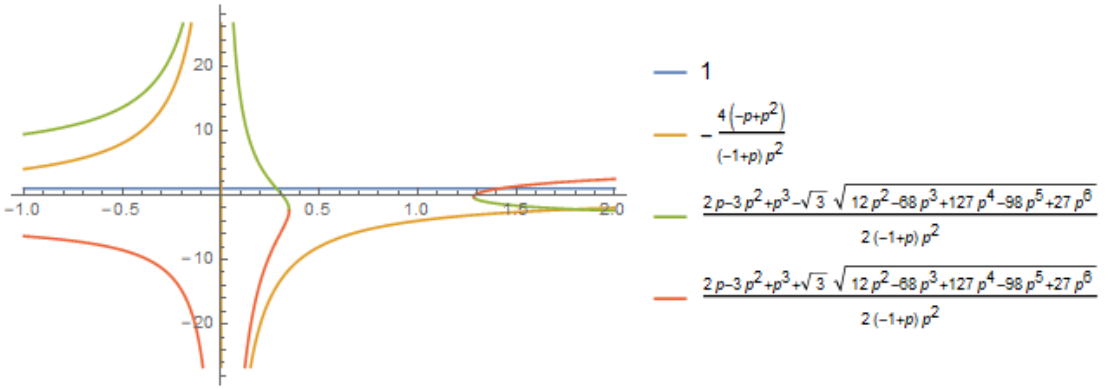

Figure– 4.14: Plot of the eigenvalues for point P_6 for $-1 < p < 2$

P_7: $(x_1, x_2, x_3, x_4) = \left(\frac{3(-1+p)}{p}, \frac{3-4p}{2p^2}, \frac{-3+4p}{2p}, 0\right)$

The eigenvalues of point P_7 are $-1, -\frac{3\left(-p+p^2\right)}{(-1+p)p^2}, \frac{3p-3p^2-p\sqrt{81-498p+1025p^2-864p^3+256p^4}}{4(-1+p)p^2}$, $\frac{3p-3p^2+p\sqrt{81-498p+1025p^2-864p^3+256p^4}}{4(-1+p)p^2}$. Other related parameters are $w_{eff} = -1+\frac{1}{p}$, $\Omega_m = -\frac{3-13p+8p^2}{2p^2}$, $\Omega_r = 0$ and $\Omega_{GC} = 5+\frac{3}{2p^2}-\frac{13}{2p}$. Further, the value of p will play an important role in having other properties related with point P_7. For $p < 0$ and $p \geq 2$, it presents different possibilities in yielding various eras of energy density of he universe. The point becomes spiral stable for the range of p. The graph displaying the plot of eigenvalues for the point P_7 is presented in Figure-4.15 in the below.

P_8: $(x_1, x_2, x_3, x_4) = \left(-\frac{2(-2+p)}{-1+2p}, \frac{5-4p}{1-3p+2p^2}, \frac{p(-5+4p)}{1-3p+2p^2}, 0\right)$

, where $\frac{-20+36p-16p^2-\frac{50p}{1-3p+2p^2}+\frac{130p^2}{1-3p+2p^2}-\frac{112p^3}{1-3p+2p^2}+\frac{32p^4}{1-3p+2p^2}}{5-4p} = -\frac{2(-2+p)}{-1+2p}$ is simplified.

The eigenvalues of point P_8 are:

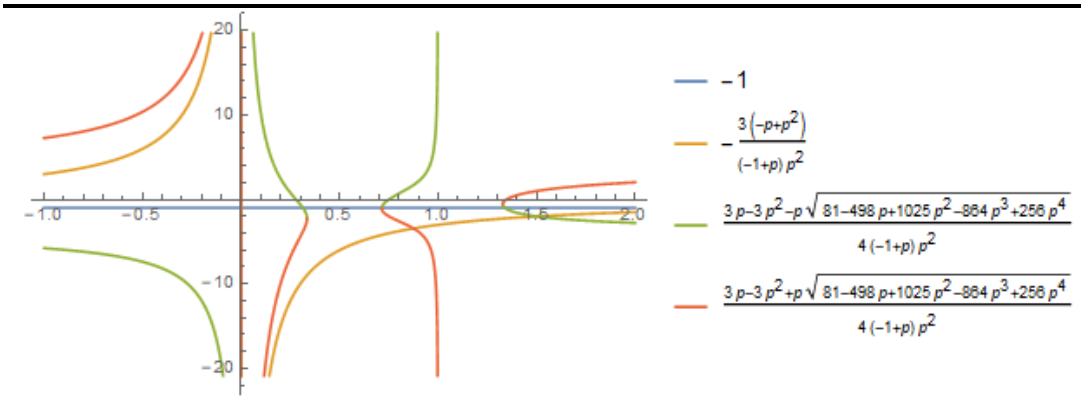

Figure– 4.15: Plot of the eigenvalues for point P_7 for $-1 < p < 2$

$\frac{2\left(2-3p+p^2\right)}{(-1+p)^2(-1+2p)}$, $-\frac{2\left(2-8p+5p^2\right)}{(-1+p)(-1+2p)}$, $\frac{3-16p+21p^2-8p^3}{(-1+p)^2(-1+2p)}$, $\frac{5-19p+22p^2-8p^3}{(-1+p)^2(-1+2p)}$. $w_{eff} = -\frac{1}{3}\left(\frac{-1-7p+6p^2}{1-3p+2p^2}\right)$, $\Omega_m = 0$, $\Omega_r = 0$ and $\Omega_{GC} = 1$. For the given range of p, when eigenvalues of the point are plotted we observe that it shows stability. Additionally, we remark that the point is susceptible to various other possibilities for different values of p in the range. The cases emerging for $p = 0$ and $p = \pm\infty$ are very interesting. The point can produce accelerated expansion in the range of values for p. The eigenvalues are plotted for the point P_8 in the mentioned range in Figure-4.16 given below.

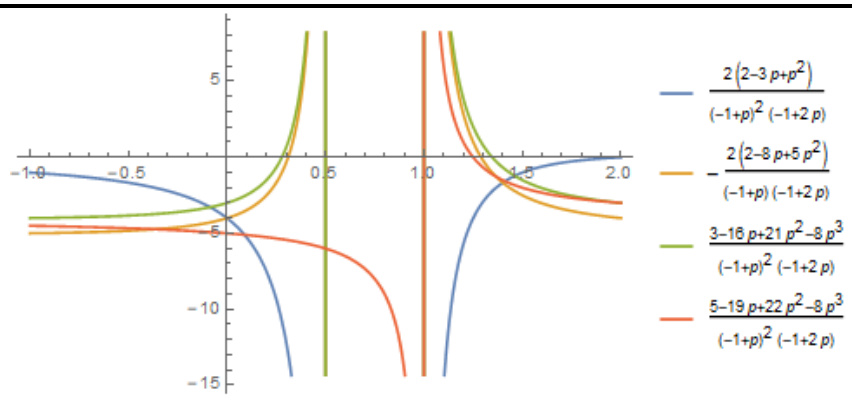

Figure– 4.16: Plot of the eigenvalues for point P_8 for $-1 < p < 2$

Now, we tabulate the results of all points collectively for this case in Table-4.8 given below

Table– 4.8: Description of results for all points for the first case of dynamical system

Sr.No	Fixed Points	Status of stability	Existence of acceleration
1	P_1	Unstable	No
2	P_2	Spiral stable	Yes
3	P_3	Unstable	Yes
4	P_4	Unstable	Yes
5	P_5	Unstable	Yes
6	P_6	Unstable	No
7	P_7	Spiral stable	Yes
8	P_8	Stable	Yes

4.6.3 Development Of Dynamical System With the Cosmological Constant Λ Representing Dark Energy

Now we propose to incorporate the cosmological constant Λ in addition to matter and radiation densities which represents dark energy as an additional cosmic component. This impels us to consider the problem in five dimensional world with taking into account dark energy as extra component. The calculations are similar to that of performed in the previous case for evaluating the accelerated expansion phase. We use Jacobian matrix, signs of eigenvalues for carrying out the analysis of stability alongwith equation of state parameter. It is assumed here that there does not exist interaction of any kind between the components of cosmic fluids as a whole. The modified Friedmann equations given in Eq. (3.6.16) and Eq. (3.6.19) can be written now

$$3H^2F = \frac{1}{2}\left(FR - f\right) - 3H\dot{F} + k^2\left(\rho_m + \rho_r + \rho_\Lambda\right) \tag{4.6.25}$$

$$2\dot{H}F = -\ddot{F} + H\dot{F} - k^2\left(\rho_m + p_m\right) \tag{4.6.26}$$

where $p_m = \frac{4}{3}\rho_r$. In above Eq. (4.6.25), the first modified Friedmann which is slightly different now than Eq. (3.6.16) due to inclusion of cosmological constant term, the following dimensionless variables are defined

$$x_1 = -\frac{\dot{F}}{HF}, x_2 = -\frac{f}{6H^2F}, x_3 = \frac{R}{6H^2}, x_4 = \frac{k^2\rho_r}{3H^2F}, x_5 = \frac{k^2\rho_m}{3H^2F} \tag{4.6.27}$$

Further, we have from Eq. (3.6.27) for the above mentioned corresponding variables

$$x_1 + x_2 + x_3 + x_4 + x_5 = 1 \tag{4.6.28}$$

In Eq. (4.6.27), the variables $x_4 = \Omega_r$ and $x_5 = \Omega_m$ and from Eq. (4.6.6), $\Omega_{GC} = x_1 + x_2 + x_3$. Using these in Eq. (4.6.28), we obtain

$$x_1 + x_2 + x_3 = 1 - \Omega_r - \Omega_m \tag{4.6.29}$$

The parameter for energy density contributed by Λ i.e., Ω_Λ can be determined from above as we have proposed in this fashion,

$$\Omega_\Lambda = 1 - x_1 - x_2 - x_3 - x_4 - x_5 \tag{4.6.30}$$

or

$$\Omega_\Lambda = 1 - \Omega_{GC} - \Omega_r - \Omega_m \tag{4.6.31}$$

Now, forthrightly we can write the autonomous system with the help of Eq. (4.6.25), Eq. (4.6.27) and Eq. (4.6.14), in the form given below

$$x_1' = -4 + 3x_1 + 2x_3 + 4x_4 + 3x_5 - x_1x_3 + x_1^2 \tag{4.6.32}$$

$$x_2' = -x_2\left(-4 - x_1 + 2x_3\right) + \frac{x_1x_2x_3^2}{px_2^2 - x_3^2} \tag{4.6.33}$$

$$x'_3 = -2x_3\left(x_3 - 2\right) - \frac{x_1x_2x_3^2}{px_2^2 - x_3^2} \tag{4.6.34}$$

$$x'_4 = x_4\left(x_1 - 2x_3\right) \tag{4.6.35}$$

$$x'_5 = x_5\left(x_1 - 2x_3\right) + x_5 \tag{4.6.36}$$

For the system described above, the effective equation of state parameter w_{eff}, matter density parameter Ω_m and radiation density parameter Ω_r are

$$w_{eff} = -1 - \frac{2\dot{H}}{3H^2} = -\frac{1}{3}\left(-1 + 2x_3\right) \tag{4.6.37}$$

$$\Omega_r = x_4 = w = \frac{k^2\rho_r}{3H^2F} \tag{4.6.38}$$

and

$$\Omega_m = x_5 = u = \frac{k^2\rho_m}{3H^2F} \tag{4.6.39}$$

and from Eq. (4.6.6)

$$x_1 + x_2 + x_3 = 1 - x_4 - x_5 \tag{4.6.40}$$

$$\Omega_{GC} = 1 - \Omega_m - \Omega_r \tag{4.6.41}$$

where Ω_{GC} signifies the gravity due to curvature mimicking the role of dark energy in $f(R)$ gravity. Now, we determine the critical points, their eigenvalues and the density parameters Ω_Λ, Ω_m and Ω_r using these points. The Jacobian matrix for the system of equations is

$$J = \begin{pmatrix} 3+2x_1-x_3 & 0 & 2-x_1 & 4 & 3 \\ x_2+\frac{x_2x_3^2}{px_2^2-x_3^2} & 4+x_1-2x_3-\frac{2px_1x_2^2x_3^2}{\left(px_2^2-x_3^2\right)^2}+\frac{x_1x_3^2}{px_2^2-x_3^2} & -2x_2+\frac{2x_1x_2x_3^3}{\left(px_2^2-x_3^2\right)^2}+\frac{2x_1x_2x_3}{px_2^2-x_3^2} & 0 & 0 \\ -\frac{x_2x_3^2}{px_2^2-x_3^2} & \frac{2px_1x_2^2x_3^2}{\left(px_2^2-x_3^2\right)^2}-\frac{x_1x_3^2}{px_2^2-x_3^2} & -2(-2+x_3)-2x_3-\frac{2x_1x_2x_3^3}{\left(px_2^2-x_3^2\right)^2}-\frac{2x_1x_2x_3}{px_2^2-x_3^2} & 0 & 0 \\ x_4 & 0 & -2x_4 & x_1-2x_3 & 0 \\ x_5 & 0 & -2x_5 & 0 & 1+x_1-2x_3 \end{pmatrix} \tag{4.6.42}$$

4.6.4 Stability Analysis Of the System Describing For Cosmic Dynamics With Cosmological Constant Λ

The dynamical system for the model in Eq. (4.6.32) to Eq. (4.6.36), has the following critical points and their corresponding eigenvalues. In addition, the effective equation of state parameter w_{eff}, matter density parameter Ω_m are also worked out.

P_1: $(x_1, x_2, x_3, x_4, x_5) = (-1, 0, 2, 0, 0)$

Eigenvalues of this point are: -5, -4, -4, -1, 0. $w_{eff} = -1$, $\Omega_r = 0$, $\Omega_m = 0$ and $\Omega_{GC} = 0$. One of the eigenvalues is 0, the point is not stable. Matter and radiation eras could not be obtained through this point, however, accelerated expansion is possible to achieve. The plot of eigenvalues for the point is laid out in Figure-4.17 underneath.

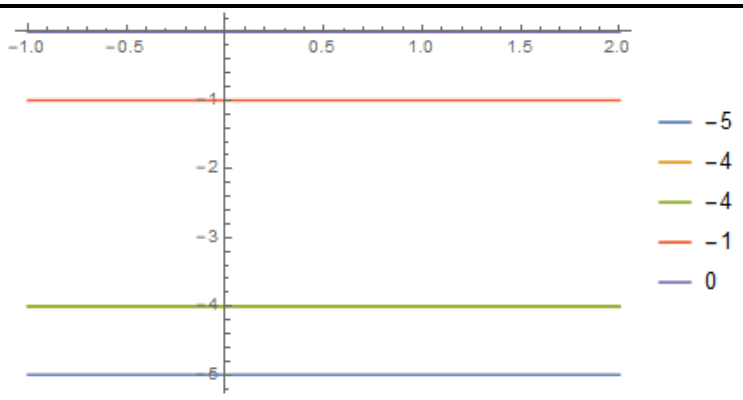

Figure– 4.17: Plot of the eigenvalues for point P_1 for $-1 < p < 2$

P_2: $(x_1, x_2, x_3, x_4, x_5) = (0, 0, 2, 0, 0)$

eigenvalues of this point are: -4, -4, -3, 1, 0. $w_{eff} = -1$, $\Omega_r = 0$, $\Omega_m = 0$ and the $\Omega_\Lambda = -1$. One of the eigenvalues is 0, while another is positive, which bars the point to be stable, therefore the point is unstable. However the point is predominated by Ω_Λ phase. The can produce accelerated expansion as the effective parameter of equation of state is negative.

P_3: $(x_1, x_2, x_3, x_4, x_5) = (3, 0, 2, 0, -4)$

eigenvalues of this point are: -4, 4, 3, -1, 0. $w_{eff} = -1$, $\Omega_r = 0$, $\Omega_m = -4$ and the $\Omega_{GC} = 0$. It is unstable point and other eras can be easily explained.

P_4: $(x_1, x_2, x_3, x_4, x_5) = (4, 0, 2, -5, 0)$

the eigenvalues of this point are: 5, -4, 4, 1, 0. $w_{eff} = -1$, $\Omega_r = -5$, $\Omega_m = 0$ and $\Omega_{GC} = 0$. It is not a stable point and values of other parameters can be interpreted easily.

P_5: $(x_1, x_2, x_3, x_4, x_5) = \left(\frac{4(-1+p)}{p}, -\frac{2(-1+p)}{p^2}, \frac{2(-1+p)}{p}, \frac{-2+8p-5p^2}{p^2}, 0\right)$

The eigenvalues of this point read as:

1, $-\frac{4\left(-p+p^2\right)}{(-1+p)p^2}$, $\frac{4\left(-p^2+p^3\right)}{(-1+p)p^2}$,

$\frac{2p-3p^2+p^3-\sqrt{3}\sqrt{12p^2-68p^3+127p^4-98p^5+27p^6}}{2(-1+p)p^2}$, $\frac{2p-3p^2+p^3+\sqrt{3}\sqrt{12p^2-68p^3+127p^4-98p^5+27p^6}}{2(-1+p)p^2}$.

Whereas, other related parameters are: $w_{eff} = -1 + \frac{4}{3p}$, $\Omega_r = -5 - \frac{2}{p^2} + \frac{8}{p}$, $\Omega_m = 0$ and $\Omega_\Lambda = \frac{4-4p}{p^2}$. In the range of p, acceleration could be achieved, however stability is not possible to obtain. The eigenvalue plot is given below for this point in Figure-4.18 below.

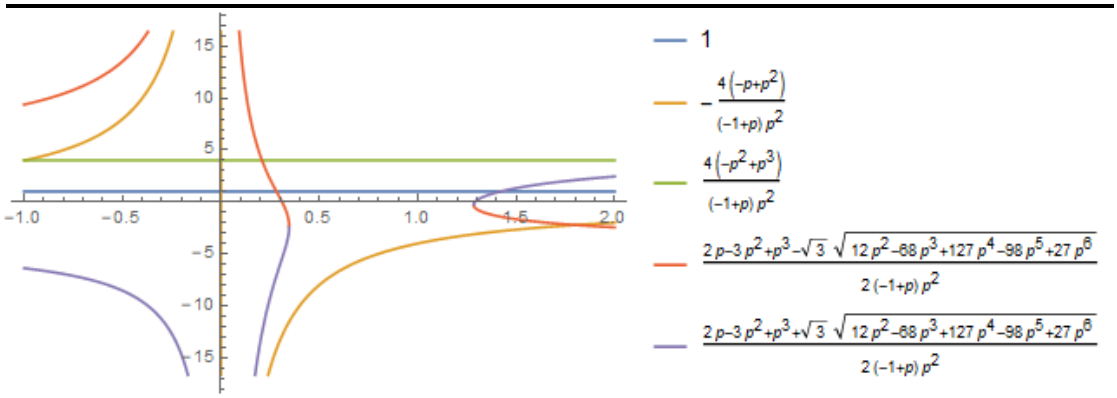

Figure– 4.18: Plot of the eigenvalues for point P_5 for $-1 < p < 2$

P_6: $(x_1, x_2, x_3, x_4, x_5) = \left(\frac{3(-1+p)}{p}, \frac{3-4p}{2p^2}, \frac{-3+4p}{2p}, 0, \frac{-3+13p-8p^2}{2p^2}\right)$

The eigenvalues of this point are:
$-\frac{3\left(-p+p^2\right)}{(-1+p)p^2}$, $-\frac{-p^2+p^3}{(-1+p)p^2}$, $\frac{3\left(-p^2+p^3\right)}{(-1+p)p^2}$, -5, $\frac{3p-3p^2\pm p\sqrt{81-498p+1025p^2-864p^3+256p^4}}{4(-1+p)p^2}$.
Other parameters related to the point are $w_{eff} = -1 + \frac{1}{p}$, $\Omega_r = 0$, $\Omega_m = -\frac{3-13p+8p^2}{2p^2}$ and $\Omega_\Lambda = 0$. It has similar properties to the point P_5. The eigenvalues of this point are plotted in Figure-4.19 in the below.

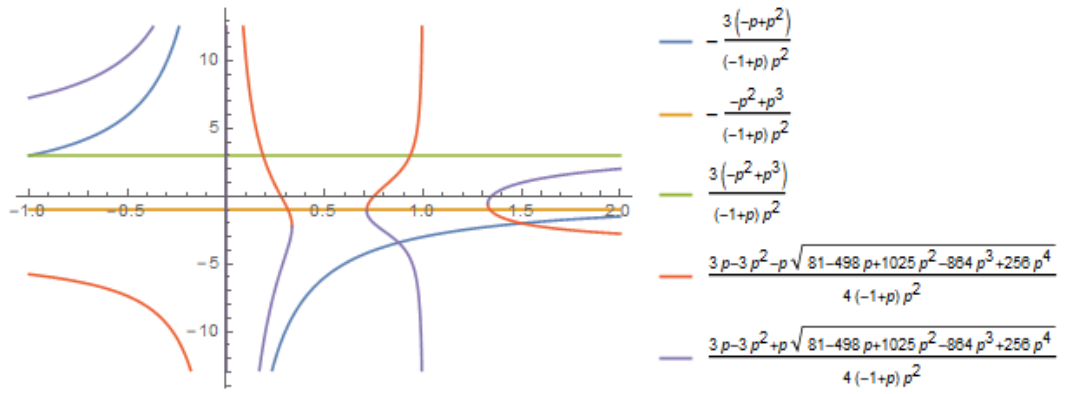

Figure– 4.19: Plot of the eigenvalues for point P_6 for $-1 < p < 2$

P_7: $(x_1, x_2, x_3, x_4, x_5) = \left(-\frac{2(-2+p)}{-1+2p}, \frac{5-4p}{1-3p+2p^2}, \frac{p(-5+4p)}{1-3p+2p^2}, 0, 0\right)$

The eigenvalues of this point are: $\frac{2\left(2-3p+p^2\right)}{(-1+p)^2(-1+2p)}$, $-\frac{2\left(2-8p+5p^2\right)}{(-1+p)(-1+2p)}$, $-\frac{3-13p+8p^2}{(-1+p)(-1+2p)}$, $\frac{5-19p+22p^2-8p^3}{(-1+p)^2(-1+2p)}$, $-\frac{2\left(2p-3p^2+p^3\right)}{(-1+p)^2(-1+2p)}$. $w_{eff} = \frac{1+7p-6p^2}{3-9p+6p^2}$, $\Omega_r = 0$, $\Omega_m = 0$ and $\Omega_\Lambda = 0$. Stability of this point could be achieved for this point in the range given for p. The accelerated expansion is also possible to have for the range of values in p. The plot of eigenvalues of the point is drawn below in Figure-4.20, where each colour live corresponds to a certain eigenvalue.

Now, we tabulate the results of all points collectively for this case in Table-4.9 given below

4.6.5 Dynamical Systems With Interaction Terms Between Cosmic Fluids

It will constitute an interesting issue to explore the effect of interaction between the cosmic fluids namely radiation, matter and dark energy. In order to understand the nature of mutual interaction between the cosmological fluids we will discuss both kinds of interactions i.e., linear and non-linear and develop the autonomous systems accordingly.

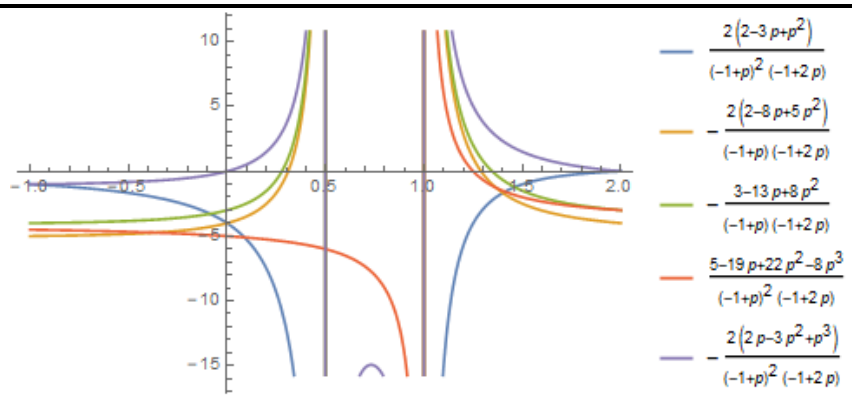

Figure– 4.20: Plot of the eigenvalues for point P_7 for $-1 < p < 2$

Table– 4.9: Description of results for all points for the second case of dynamical system

Sr.No	Fixed Points	Status of stability	Existence of acceleration
1	P_1	Unstable	Yes
2	P_2	Unstable	Yes
3	P_3	Unstable	Yes
4	P_4	Unstable	Yes
5	P_5	Unstable	Yes
6	P_6	Unstable	Yes
7	P_7	Stable	Yes

The dimensionless variables will be defined on the same lines as earlier in previous two cases. The conservation equation for cosmic fluids is however described in the following way for the corresponding epoches. Equation of continuity $\dot{\rho}+3\partial_t a\,(\rho+p)=0$ assumes the forms i.e., $\dot{\rho}_m+3\partial_t a\rho_m=0$ and $\dot{\rho}_r+4\partial_t a\rho_r=0$ for the corresponding epoches with i.e., $p_m=0$ and $p_m=\frac{4}{3}\rho_r$ respectively.

4.6.6 When Linear Interaction is Considered

The linear interaction is defined as $Q=H\rho_t$ in accordance with the references (Shah & Samanta, 2019; Arevalo, Bacalhau, & Zimdahl, 2012; Garcia-Salcedo, Gonzalez, & Quiros, 2012; Golchin, Jamali, & Ebrahimi, 2017; Pan, de Haro, Yang, & Amorós, 2020; Bolotin, Kostenko, Lemets, & Yerokhin, 2015). The modified Friedmann equations given in Eqs (4.6.25, 4.6.26) are put to use for this case. The dimensionless parameters are also defined similarly as given in Eq. (4.6.27). The dynamical system in case of linear interaction remains unaltered except for the equation $\frac{dx_5}{dN}$ in Eq. (4.6.47) underneath which is modified slightly. The autonomous system reads as

$$x_1'=-4+3x_1+2x_3+4x_4+3x_5-x_1x_3+x_1^2 \tag{4.6.43}$$

$$x_2'=-x_2\,(-4-x_1+2x_3)+\frac{x_1x_2x_3^2}{px_2^2-x_3^2} \tag{4.6.44}$$

$$x'_3=-2x_3\,(x_3-2)-\frac{x_1x_2x_3^2}{px_2^2-x_3^2} \tag{4.6.45}$$

$$x'_4=x_4\,(x_1-2x_3) \tag{4.6.46}$$

$$x'_5=x_5\,(x_1-2x_3)+x_5+1-(x_1+x_2+x_3) \tag{4.6.47}$$

For the system described above, the effective equation of state parameter w_{eff}, matter density parameter Ω_m and radiation density parameter Ω_r are

$$w_{eff}=-1-\frac{2\dot{H}}{3H^2}=-\frac{1}{3}\,(-1+2x_3) \tag{4.6.48}$$

$$\Omega_r=x_4=w=\frac{k^2\rho_r}{3H^2F} \tag{4.6.49}$$

and

$$\Omega_m=x_5=u=\frac{k^2\rho_m}{3H^2F} \tag{4.6.50}$$

and from Eq. (4.6.6)

$$x_1+x_2+x_3=1-x_4-x_5 \tag{4.6.51}$$

$$\Omega_{GC}=1-\Omega_m-\Omega_r \tag{4.6.52}$$

The parameter for energy density contributed by Λ i.e., Ω_Λ can be determined from above as we have assumed the case,

$$\Omega_\Lambda = 1 - x_1 - x_2 - x_3 - x_4 - x_5 \tag{4.6.53}$$

or

$$\Omega_\Lambda = 1 - \Omega_{GC} - \Omega_r - \Omega_m \tag{4.6.54}$$

where Ω_{GC} signifies the gravity due to curvature term playing the role of dark energy. Now, we determine the critical points, their eigenvalues and the density parameters Ω_{GC}, Ω_m and Ω_r using these points. The Jacobian matrix of the system in Eq. (4.6.43) to Eq. (4.6.47) is calculated to be

$$J = \begin{pmatrix} 3+2x_1-x_3 & 0 & 2-x_1 & 4 & 3 \\ x_2+\frac{x_2x_3^2}{px_2^2-x_3^2} & 4+x_1-2x_3-\frac{2px_1x_2^2x_3^2}{\left(px_2^2-x_3^2\right)^2}+\frac{x_1x_3^2}{px_2^2-x_3^2} & -2x_2+\frac{2x_1x_2x_3^3}{\left(px_2^2-x_3^2\right)^2}+\frac{2x_1x_2x_3}{px_2^2-x_3^2} & 0 & 0 \\ -\frac{x_2x_3^2}{px_2^2-x_3^2} & \frac{2px_1x_2^2x_3^2}{\left(px_2^2-x_3^2\right)^2}-\frac{x_1x_3^2}{px_2^2-x_3^2} & -2\left(-2+x_3\right)-2x_3-\frac{2x_1x_2x_3^3}{\left(px_2^2-x_3^2\right)^2}-\frac{2x_1x_2x_3}{px_2^2-x_3^2} & 0 & 0 \\ x_4 & 0 & -2x_4 & x_1-2x_3 & 0 \\ -1+x_5 & -1 & 1-2x_5 & 0 & 1+x_1-2x_3 \end{pmatrix} \tag{4.6.55}$$

4.6.7 Stability Analysis Of the System With Linear Interaction

The dynamical system for the model in Eq. (4.6.43) to Eq. (4.6.47), has the following critical points and their corresponding eigenvalues.

P_1: $(x_1, x_2, x_3, x_4, x_5) = \left(4, 0, 2, -\frac{35}{4}, 5\right)$

The eigenvalues of this point are: $5,\ -4,\ \frac{1}{2}\left(5+i\sqrt{3}\right),\ \frac{1}{2}\left(5-i\sqrt{3}\right),\ 0$. Other parameters are found to be $w_{eff} = -1$, $\Omega_r = -\frac{35}{4}$, $\Omega_m = 5$ and $\Omega_\Lambda = -\frac{5}{4}$. It is an unstable point as the signatures of eigenvalues manifest. It can yield accelerated expansion phase, however, radiation and matter dominations are not satisfied by this point.

P_2: $(x_1, x_2, x_3, x_4, x_5) = \left(\frac{1}{2}\left(3-i\sqrt{3}\right), 0, 2, 0, \frac{1}{3}\left(3-2\left(3-i\sqrt{3}\right)\right)\right)$

The eigenvalues of this point are: $-4,\ -\frac{1}{2}i\left(-5i+\sqrt{3}\right),\ \frac{1}{2}\left(5-i\sqrt{3}\right),\ -i\sqrt{3},\ 0$. Moreover, equation of state and other parameters are $w_{eff} = -1$, $\Omega_r = 0$, $\Omega_m = -1+\frac{2i}{\sqrt{3}}$ and $\Omega_\Lambda = -\frac{1}{6}i\left(-9i+\sqrt{3}\right)$. The point is not stable on account of positive real parts of the eigenvalues.

P_3: $(x_1, x_2, x_3, x_4, x_5) = \left(\frac{1}{2}\left(3+i\sqrt{3}\right), 0, 2, 0, \frac{1}{3}\left(3-2\left(3+i\sqrt{3}\right)\right)\right)$

The eigenvalues of this point are: $-4,\ \frac{1}{2}i\left(5i+\sqrt{3}\right),\ \frac{1}{2}\left(5+i\sqrt{3}\right), i\sqrt{3},\ 0$. Other

parameters for the density and the equation of state are $w_{eff} = -1$, $\Omega_r = 0$, $\Omega_m = -1 - \frac{2i}{\sqrt{3}}$ and $\Omega_\Lambda = \frac{1}{6}i\left(9i + \sqrt{3}\right)$. This is also an unstable point. The point produces accelerated expansion as effective equation of state parameter has negative 1 value.

P_4: $(x_1, x_2, x_3, x_4, x_5) = \left(\frac{4(-1+p)}{p}, -\frac{2(-1+p)}{p^2}, \frac{2(-1+p)}{p}, -\frac{7\left(2-8p+5p^2\right)}{4p^2}, \frac{2-8p+5p^2}{p^2}\right)$

The eigenvalues of this point are:

$-\frac{4\left(-p+p^2\right)}{(-1+p)p^2}$, $\frac{-5p^2+5p^3-\sqrt{3}\sqrt{-p^4+2p^5-p^6}}{2(-1+p)p^2}$, $\frac{-5p^2+5p^3+\sqrt{3}\sqrt{-p^4+2p^5-p^6}}{2(-1+p)p^2}$,

$\frac{2p-3p^2+p^3-\sqrt{3}\sqrt{12p^2-68p^3+127p^4-98p^5+27p^6}}{2(-1+p)p^2}$, $\frac{2p-3p^2+p^3+\sqrt{3}\sqrt{12p^2-68p^3+127p^4-98p^5+27p^6}}{2(-1+p)p^2}$.

The related parameters to the points are:

$w_{eff} = -1 + \frac{4}{3p}$, $\Omega_r = -\frac{7\left(2-8p+5p^2\right)}{4p^2}$, $\Omega_m = 5 + \frac{2}{p^2} - \frac{8}{p}$ and $\Omega_\Lambda = -\frac{2-8p+5p^2}{4p^2}$. It is an unstable point, however, it gives accelerated expansion phase for the range of p and is viable for other eras as well. The eigenvalue plot for the point is diagramed in Figure-4.21 as presented below.

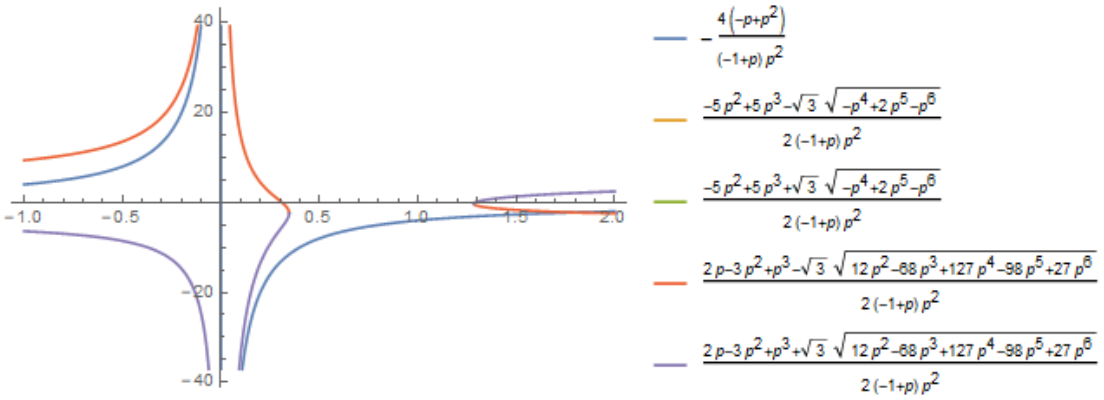

Figure– 4.21: Plot of the eigenvalues for point P_4 for $-1 < p < 2$

P_5: $(x_1, x_2, x_3, x_4, x_5) = \left(\frac{(3+i\sqrt{3})(-1+p)}{2p}, \frac{3+i\sqrt{3}-8p}{4p^2}, \frac{-3-i\sqrt{3}+8p}{4p}, 0, \frac{-3-3i\sqrt{3}+21p+13i\sqrt{3}p-12p^2-8i\sqrt{3}p^2}{12p^2} \right)$.

The eigenvalues of this point are:

$\frac{3p+i\sqrt{3}p-3p^2-i\sqrt{3}p^2}{2(-1+p)p^2}$, $\frac{5p^2-i\sqrt{3}p^2-5p^3+i\sqrt{3}p^3}{2(-1+p)p^2}$, $\frac{i\left(-\sqrt{3}p^2+\sqrt{3}p^3\right)}{(-1+p)p^2}$,

$$\frac{3p+i\sqrt{3}p+3p^2-3i\sqrt{3}p^2-6p^3+2i\sqrt{3}p^3}{8(-1+p)p^2} \pm i \frac{\sqrt{\left(\begin{array}{l} -54p^2 - 54i\sqrt{3}p^2 + 540p^3 + 332i\sqrt{3}p^3 - 1742p^4 \\ -574i\sqrt{3}p^4 + 1920p^5 + 400i\sqrt{3}p^5 - 664p^6 - 104i\sqrt{3}p^6 \end{array} \right)}}{8(-1+p)p^2},$$

Other related parameters are:

$w_{eff} = \frac{3+i\sqrt{3}-6p}{6p}$, $\Omega_r = 0$, $\Omega_m = \frac{-3-3i\sqrt{3}+\left(21+13i\sqrt{3}\right)p+\left(-12-8i\sqrt{3}\right)p^2}{12p^2}$ and $\Omega_\Lambda = \frac{-3+\left(15-2i\sqrt{3}\right)p+i\left(9i+\sqrt{3}\right)p^2}{6p^2}$. The point is unstable, however for the accelerated expansion and other eras it shows feasibility.

$$P_6\text{: } (x_1, x_2, x_3, x_4, x_5) = \left(\begin{array}{l} -\frac{2(-2+p)}{-1+2p}, \frac{5-4p}{1-3p+2p^2}, \frac{p(-5+4p)}{1-3p+2p^2}, 0, \\ \frac{1}{3}\left(\begin{array}{l} 12 - 8p - \frac{4(-2+p)^2}{(-1+2p)^2} + \frac{2(-2+p)}{-1+2p} + \frac{2p^2(-5+4p)^2}{(1-3p+2p^2)^2} - \frac{2p^3(-5+4p)^2}{(1-3p+2p^2)^2} \\ -\frac{10p(-5+4p)}{1-3p+2p^2} + \frac{8p^2(-5+4p)}{1-3p+2p^2} \end{array} \right) \end{array} \right)$$

The eigenvalues of this point come out to be:

$\frac{2\left(2-3p+p^2\right)}{(-1+p)^2(-1+2p)}$, $\frac{5-19p+22p^2-8p^3}{(-1+p)^2(-1+2p)}$, $-\frac{2\left(-2+10p-13p^2+5p^3\right)}{(-1+p)^2(-1+2p)}$,

$\frac{3-20p+27p^2-10p^3\pm\sqrt{3}\sqrt{-1+8p-26p^2+44p^3-41p^4+20p^5-4p^6}}{2(-1+p)^2(-1+2p)}$.

The related other parameters are: $w_{eff} = \frac{1+7p-6p^2}{3-9p+6p^2}$, $\Omega_r = 0$,

$$\Omega_m = \frac{1}{3}\left(\begin{array}{l} 12 - 8p - \frac{4(-2+p)^2}{(-1+2p)^2} + \frac{2(-2+p)}{-1+2p} + \frac{2p^2(-5+4p)^2}{(1-3p+2p^2)^2} - \frac{2p^3(-5+4p)^2}{(1-3p+2p^2)^2} - \frac{10p(-5+4p)}{1-3p+2p^2} \\ +\frac{8p^2(-5+4p)}{1-3p+2p^2} \end{array} \right)$$

and $\Omega_\Lambda = 0$. The eigenvalue plot for this point is drawn in Figure-4.22 given below. It produces accelerated expansion for $p < 0$. From the plot it can be seen that the point is unstable.

Now, we tabulate the results of all points collectively for this case in Table-4.10 given below

4.6.8 When Non-Linear Interaction is Considered

The Non-linear interaction has been described as $Q = H\rho_t$ in accordance with the references (Shah & Samanta, 2019; Arevalo et al., 2012; Garcia-Salcedo et al., 2012; Golchin et al., 2017; Pan et al., 2020; Bolotin et al., 2015). The modified Friedmann equations given in Eqs. (4.6.25, 4.6.26) are put to use for this case. The dynamical autonomous system in this non-linear interaction perspective keeps itself unmodified

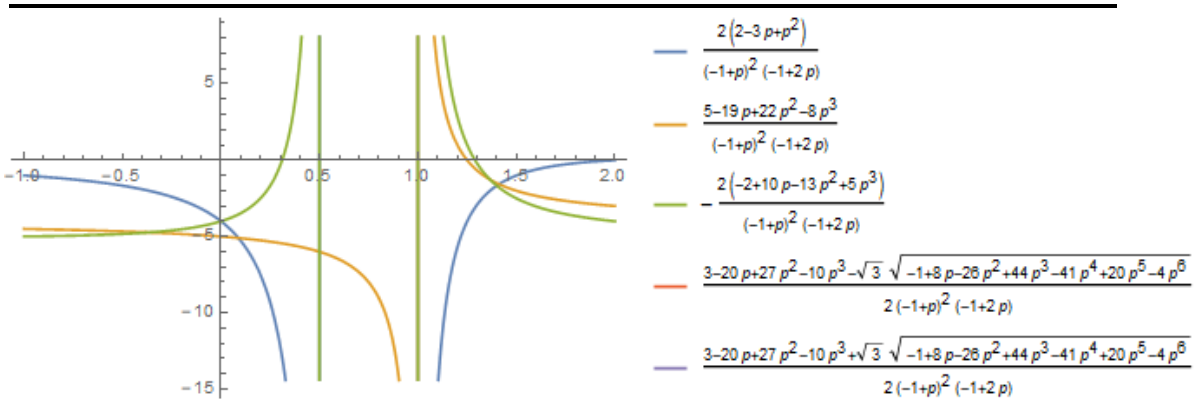

Figure– 4.22: Plot of the eigenvalues for point P_6 for $-1 < p < 2$

Table– 4.10: Description of results for all points for third case of dynamical system

Sr.No	Fixed Points	Status of stability	Existence of acceleration
1	P_1	Unstable	Yes
2	P_2	Unstable	Yes
3	P_3	Unstable	Yes
4	P_4	Spiral stable	Yes
5	P_5	Unstable	Yes
6	P_6	Unstable	Yes

except for $\frac{dx_5}{dN}$ which is modified slightly. The dimensionless parameters are also defined similarly as given in Eq. (4.6.27). The autonomous system is

$$x_1' = -4 + 3x_1 + 2x_3 + 4x_4 + 3x_5 - x_1x_3 + x_1^2 \tag{4.6.56}$$

$$x_2' = -x_2\left(-4 - x_1 + 2x_3\right) + \frac{x_1x_2x_3^2}{px_2^2 - x_3^2} \tag{4.6.57}$$

$$x'_3 = -2x_3\left(x_3 - 2\right) - \frac{x_1x_2x_3^2}{px_2^2 - x_3^2} \tag{4.6.58}$$

$$x'_4 = x_4\left(x_1 - 2x_3\right) \tag{4.6.59}$$

$$x_5' = \frac{x_5\left(1 - x_2 - 3x_3 - x_4 - x_1^2 + 2x_3^2 + x_1x_3 + 2x_2x_3 - x_1x_2 - x_1x_5 - x_2x_5 - x_3x_5\right)}{1 - (x_1 + x_2 + x_3)} \tag{4.6.60}$$

For the system described above, the effective equation of state parameter w_{eff}, matter density parameter Ω_m and radiation density parameter Ω_r are

$$w_{eff} = -1 - \frac{2\dot{H}}{3H^2} = -\frac{1}{3}\left(-1 + 2x_3\right) \tag{4.6.61}$$

$$\Omega_r = x_4 = w = \frac{k^2\rho_r}{3H^2F} \tag{4.6.62}$$

and

$$\Omega_m = x_5 = u = \frac{k^2\rho_m}{3H^2F} \tag{4.6.63}$$

and from Eq. (4.6.6)

$$x_1 + x_2 + x_3 = 1 - x_4 - x_5 \tag{4.6.64}$$

$$\Omega_{GC} = 1 - \Omega_m - \Omega_r \tag{4.6.65}$$

The parameter for energy density contributed by Λ i.e., Ω_Λ can be determined from above as we have assumed the case,

$$\Omega_\Lambda = 1 - x_1 - x_2 - x_3 - x_4 - x_5 \tag{4.6.66}$$

or

$$\Omega_\Lambda = 1 - \Omega_{GC} - \Omega_r - \Omega_m \tag{4.6.67}$$

where Ω_{GC} signifies the gravity due to curvature playing the role of dark energy. Now, we determine the critical points, their eigenvalues and the density parameters Ω_{GC}, Ω_m and Ω_r using these points. The Jacobian matrix of the system of equations is

$$J = \begin{pmatrix} 3 + 2x_1 - x_3 & 0 & 2 - x_1 & 4 & 3 \\ x_2 + \frac{x_2x_3^2}{px_2^2 - x_3^2} & 4 + x_1 - 2x_3 - \frac{2px_1x_2^2x_3^2}{\left(px_2^2 - x_3^2\right)^2} + \frac{x_1x_3^2}{px_2^2 - x_3^2} & -2x_2 + \frac{2x_1x_2x_3^3}{\left(px_2^2 - x_3^2\right)^2} + \frac{2x_1x_2x_3}{px_2^2 - x_3^2} & 0 & 0 \\ -\frac{x_2x_3^2}{px_2^2 - x_3^2} & \frac{2px_1x_2^2x_3^2}{\left(px_2^2 - x_3^2\right)^2} - \frac{x_1x_3^2}{px_2^2 - x_3^2} & -2\left(-2 + x_3\right) - 2x_3 - \frac{2x_1x_2x_3^3}{\left(px_2^2 - x_3^2\right)^2} - \frac{2x_1x_2x_3}{px_2^2 - x_3^2} & 0 & 0 \\ x_4 & 0 & -2x_4 & x_1 - 2x_3 & 0 \\ a_{51} & a_{52} & a_{53} & -\frac{x_5}{1 - x_1 - x_2 - x_3} & a_{55} \end{pmatrix} \tag{4.6.68}$$

where

$$a_{51} = \frac{x_5\left(-x_5 - 2x_1 - x_2 + x_3\right)}{1 - x_1 - x_2 - x_3} + \frac{x_5\left(\begin{array}{l} 1 - x_4 - x_1x_5 - x_1^2 - x_2 - x_2x_5 - x_1x_2 - 3x_3 - x_3x_5 \\ \\ +x_1x_3 + 2x_2x_3 \end{array}\right)}{\left(1 - x_1 - x_2 - x_3\right)^2}$$

$$a_{52} = \frac{x_5\left(-1 - x_5 - x_1 + 2x_3\right)}{1 - x_1 - x_2 - x_3} + \frac{x_5\left(\begin{array}{l} 1 - x_4 - x_1x_5 - x_1^2 - x_2 - x_2x_5 - x_1x_2 - 3x_3 - x_3x_5 \\ \\ +x_1x_3 + 2x_2x_3 \end{array}\right)}{\left(1 - x_1 - x_2 - x_3\right)^2}$$

$$a_{53} = \frac{x_5\left(-3 - x_5 + x_1 + 2x_2\right)}{1 - x_1 - x_2 - x_3} + \frac{x_5\left(\begin{array}{l} 1 - x_4 - x_1x_5 - x_1^2 - x_2 - x_2x_5 - x_1x_2 - 3x_3 - x_3x_5 \\ \\ +x_1x_3 + 2x_2x_3 \end{array}\right)}{\left(1 - x_1 - x_2 - x_3\right)^2}$$

$$a_{55} = \frac{1 - x_4 - 2x_1x_5 - x_1^2 - x_2 - 2x_2x_5 - x_1x_2 - 3x_3 - 2x_3x_5 + x_1x_3 + 2x_2x_3}{1 - x_1 - x_2 - x_3}$$

4.6.9 Stability Analysis Of the System With Non-Linear Interaction

The dynamical system for the model in Eq. (4.6.56) to Eq. (4.6.60), has the following critical points. These critical points as solutions of the autonomous system of differential equations can determine stability of the system. The corresponding eigenvalues of these points and other related density parameters play their fundamental role in stability analysis. We will analyze stability of the dynamical system through properties of eigenvalues and viability for the accelerated expansion as well with the help of these points. In this system some points have very larger eigenvalues that can not be put here, therefore are skipped. The eigenvalues of almost all points are shown figuratively through plots for the range $(-1 \leq p \leq 2)$ where it applies.

P_1: $(x_1, x_2, x_3, x_4, x_5) = (0, 0, 2, 0, 0)$

The eigenvalues of this point are: -4, -4, 0, 1, 5 and the related other parameters are: $w_{eff} = -1$, $\Omega_r = 0$, $\Omega_m = 0$, $\Omega_\Lambda = -1$. As the two repeated eigenvalues are negative, in addition to the one other to be positive, therefore the system is not stable at this point. However the point can yield accelerated expansion.

P_2: $(x_1, x_2, x_3, x_4, x_5) = \left(4, 0, 2, -\frac{27}{2}, -\frac{32}{21}\right)$

The eigenvalues of this point are:

$$Root\left[18144+2252\#1-5271\#1^2+735\#1^3\&,3\right],-4,$$

$$Root\left[18144+2252\#1-5271\#1^2+735\#1^3\&,2\right],$$

$$Root\left[18144+2252\#1-5271\#1^2+735\#1^3\&,1\right],0$$

The remaining parameters related to the point are: $w_{eff} = -1$, $\Omega_r = -\frac{27}{7}$, $\Omega_m = -\frac{32}{21}$, $\Omega_\Lambda = \frac{8}{21}$. Stability of the system, however at this point is not possible. Matter dominated era has incorrect definition as the similar case is with the radiation epoch. The accelerated expansion is also not possible to yield through this point for the system.

P_3: $(x_1, x_2, x_3, x_4, x_5) = (4, 0, 2, -5, 0)$

The eigenvalues of this point are:

5, -4, 4, $\frac{8}{5}$, 0, and other parameters are determined to be:

$w_{eff} = -1$, $\Omega_r = -5$, $\Omega_m = 0$ and $\Omega_\Lambda = 0$. It is an unstable point as can be seen from the signs of eigenvalues and other parameters are obvious where to lead straightforwardly.

P_4: $(x_1, x_2, x_3, x_4, x_5) = \left(0, \frac{5}{3}, 2, 0, 0\right)$

The eigenvalues of this point are:

0, 0, -4, $\frac{108-75p-\sqrt{5}\sqrt{9936-11400p+3125p^2}}{2(-36+25p)}$, $\frac{108-75p+\sqrt{5}\sqrt{9936-11400p+3125p^2}}{2(-36+25p)}$.

The related parameters to the point are found to be: $w_{eff} = -1$, $\Omega_r = 0$, $\Omega_m = 0$, $\Omega_\Lambda = -\frac{8}{3}$. For the given range of the values of p, at this point acceleration could be generated. The eigenvalue plot for the point is presented in Figure-4.23 as given underneath.

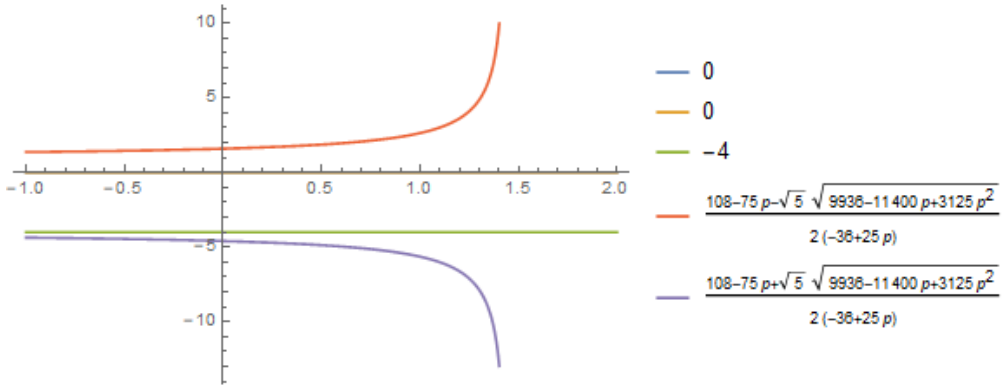

Figure– 4.23: Plot of the eigenvalues for point P_4 for $-1 < p < 2$

P_5: $(x_1, x_2, x_3, x_4, x_5) = \left(\frac{4(-1+p)}{p}, -\frac{2(-1+p)}{p^2}, \frac{2(-1+p)}{p}, \frac{-2+8p-5p^2}{p^2}, 0\right)$

The eigenvalues of this point are:

$\frac{8(-1+p)^2}{2-8p+5p^2}$, $-\frac{4\left(-2p+10p^2-13p^3+5p^4\right)}{(-1+p)p^2(2-8p+5p^2)}$, $\frac{4\left(-2p^2+10p^3-13p^4+5p^5\right)}{(-1+p)p^2(2-8p+5p^2)}$,

$\frac{4p-22p^2+36p^3-23p^4+5p^5}{2(-1+p)p^2(2-8p+5p^2)} + \frac{\sqrt{3}\sqrt{a}}{2(-1+p)p^2(2-8p+5p^2)}$, $\frac{4p-22p^2+36p^3-23p^4+5p^5}{2(-1+p)p^2(2-8p+5p^2)} - \frac{\sqrt{3}\sqrt{a}}{2(-1+p)p^2(2-8p+5p^2)}$

where $a = 48p^2-656p^3+3692p^4-11128p^5+19652p^6-20956p^7+13283p^8-4610p^9+675p^{10}$

Now, the related density parameters to the point are: $w_{eff} = -1 + \frac{4}{3p}$, $\Omega_r = -5 - \frac{2}{p^2} + \frac{8}{p}$, $\Omega_m = 0$, $\Omega_\Lambda = 0$. The point is unstable, however, accelerated expansion is possible through this point. Radiation and matter epoches could not be yielded through this point. The eigenvalue plot is drawn below in Figure-4.24 which shows its properties.

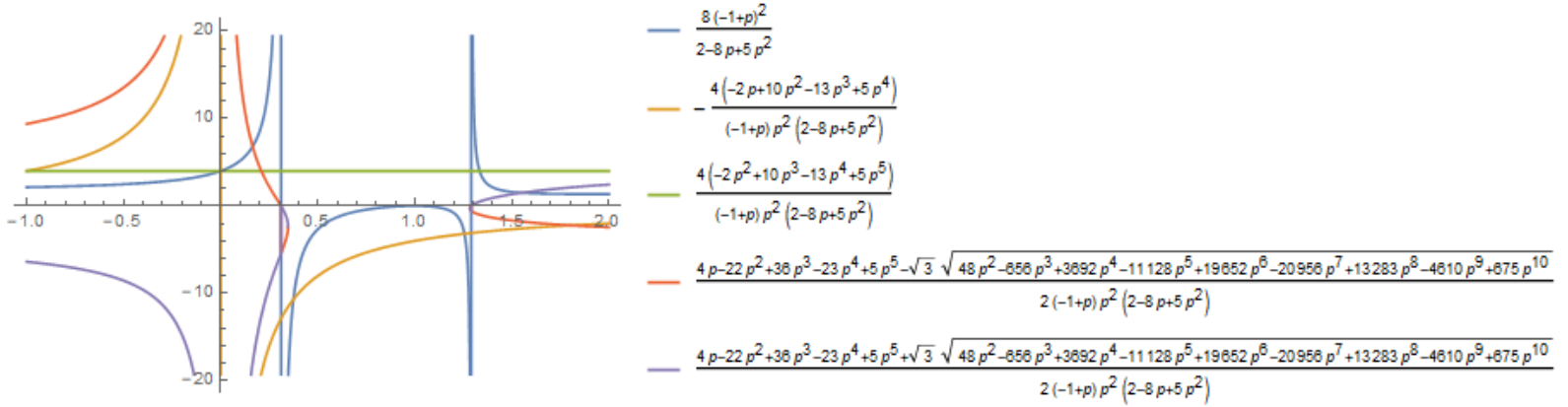

Figure– 4.24: Plot of the eigenvalues for point P_5 for $-1 < p < 2$

$$P_6\text{: } (x_1, x_2, x_3, x_4, x_5) = \left(\begin{array}{c} \frac{4(-1+p)}{p}, -\frac{2(-1+p)}{p^2}, \frac{2(-1+p)}{p}, \frac{-16+128p-314p^2+280p^3-81p^4}{p^2(8-32p+21p^2)}, \\ -\frac{32\left(1-2p+p^2\right)}{8-32p+21p^2} \end{array} \right)$$

The eigenvalues of this point are enormously larger and cannot be manually written here. It is, however clear that for $p < 0$ and $p > 2$, the resulting values do not make a stable point. $w_{eff} = -1 + \frac{4}{3p}$, $\Omega_r = \frac{-16+128p-314p^2+280p^3-81p^4}{p^2(8-32p+21p^2)}$, $\Omega_m = -\frac{32(-1+p)^2}{8-32p+21p^2}$, $\Omega_\Lambda = \frac{8(-1+p)^2}{8-32p+21p^2}$. The point gives accelerated expansion for the range of values of p, however, matter and radiation dominated eras could not be properly achieved. The plot for the eigenvalues is presented in Figure-4.25 underneath and can be interpreted suitably. Eigenvalue expressions could not be placed due to their colossal sizes, however plot for each expression is labelled.

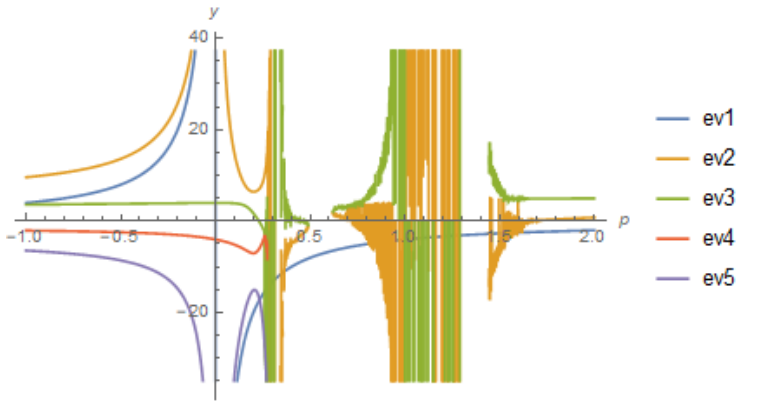

Figure– 4.25: Plot of the eigenvalues for point P_6 for $-1 < p < 2$

Now, we tabulate the results of all points collectively for this case in Table-4.11 given below

Table– 4.11: Description of results for all points for fourth case of dynamical system

Sr.No	Fixed Points	Status of stability	Existence of acceleration
1	P_1	Unstable	Yes
2	P_2	Unstable	Yes
3	P_3	Unstable	Yes
4	P_4	Unstable	Yes
5	P_5	Unstable	Yes
6	P_6	Unstable	Yes

4.6.10 Discussion and Concluding Remarks

The study of dark universe in the context of $f(R)$ dynamics has engrossing characteristics. To explain the late time accelerated expansion in its perspective is very attractive due to being it comprehensive and simple. In this paper we studied a particular model of $f(R)$ modified gravity by investigating its stability analysis through dynamical system analysis approach. A very challenging issue faced by $f(R)$ models is their viability for yielding the matter-dominated era. However these models were categorized (Amendola et al., 2007) based on the viability conditions that can produce the matter epoch followed by the late time accelerated expansion. With regard to it a straightforward method to investigate the cosmological viability is to study $f(R)$ models established on the geometric curves $m(r)$ and the critical line $m(r) = -r - 1$ plotted in the (m, r) two dimensional plane. The model we studied belongs to so called ϕMDE matter era where the scale factor $a(t)$ is proportional to $t^{\frac{1}{2}}$. The existence of such matter-dominated era, however is debatable and is related with a specific class of $f(R)$ models. In addition to these, there are cosmological viability conditions directly based on $f(R)$ derivatives $f_{,R}$ and $f_{,RR}$. Moreover, it is obvious from the definition of $m = \frac{Rf_{,RR}}{f_{,R}}$ that it contributes significantly in establishing the viability of these cosmological models.

In the result of this problem, we reviewed first briefly the $f(R)$ mathematical framework and derived the modified gravity equation that governs the cosmic dynamics. The modified Freidmann equations are presented then considering the FLRW metric for a spatially flat and homogeneous universe. Defining the dimensionless parameters or variables, the

autonomous dynamical system of differential equations is derived. Critical points, different density parameters and the eigenvalues of the critical points for the general $f(R)$ are listed solving the autonomous system simultaneously. We also discussed the viability conditions in general for these models and for the model under consideration. By calculating the first two derivatives, the parameters m and r are determined, from where m is expressed as a function of r i.e., $m = m(r)$. The mass of scalaron is somhow affected by the presence of standard matter in the background and is closely related with m. The value of $m = m(r)$ for the selected model obviously would be similar for all the discussed cases. We study four cases for studying the stability of the system developed for the model describing our universe. In the first case a universe consisting of radiation and matter only is proposed and accordingly defining the dimensionless parameters, the dynamical system is constructed. We did not consider any interaction term between these cosmic stuff. Determining the critical points, relevant density parameters and eigenvalues of these points in the perspective of the autonomous system plots are drawn. The signature of eigenvalues shed light on stability of the system in addition to the values of density parameters. The points which could cause accelerated expansion are discussed in detail.

In the second case we considered cosmological constant Λ representing dark energy density ρ_Λ in the cosmic fluidic stuff and incorporated into the modified Friedmann equations. In accordance with first modified Friedmann equation, defining dimensionless parameters in it, we constructed the autonomous system of differential equations whose stability is investigated. Going through the same procedure of determining the critical points, their eigenvalues in the context of newly developed autonomous system with the help of Jacobian matrix and other density parameters, the stability analysis is performed. The signs of eigenvalues of the points lend help in understanding the stability and the plots of it give their graphical behaviour. In first two cases, the interaction between matter and dark energy was not taken into account. Now, however the interaction of two kinds linear and non-linear would present an interesting case to study. In third case, linear interaction terms are taken into consideration and using conservation equation for cosmic fluidic stuff we drew up a program of modifying autonomous system accordingly following the references (Amendola et al., 2007; Shah & Samanta, 2019). The dimensionless parameters, however are not disrupted in this whole process. It is observed that only first and fifth equations in the autonomous system are slightly changed.

For stability analysis, the method of critical points, eigenvalues with finding density parameters is adapted. The graphical display similar to the earlier discussed cases is laid out. It can be observed that at some points accelerated expansion is achieved, however stability and violation of other closely related parameters is lost altogether. Finally, we considered the non-linear case and following the similar procedure of case third stability is analyzed. It is observed that it is the range of values for p which makes the points in most cases to help undergo the system through the phase of accelerated expansion.

It is important to notice that in many cases the roots of the eigenvalues are not so simple and straightforward in general and entails implications and complications, however we considered the range of values for $-2 \leq p \leq 0$ that sets the trend of stability analysis efficiently and very close to precision and accuracy. Another thing which is important to note is that the addition of cosmological constant in the framework of $f(R)$ modified gravity makes no difference and is therefore redundant. This is because in the construct of $f(R)$, it is the curvature of spacetime itself that is responsible for driving the cosmic expansion acceleratingly. The fact is also clear from our discussion and calculational aspects in addition to the behaviour of points P_2 and P_3 in case of 3rd autonomous system which makes it more plausible. Therefore in $f(R)$ gravity models, the stability of the system describing the universe phenomenologically and the late time behaviour of expanding acceleratingly can be described self sufficiently within its perspective.

In general, the work can be enlarged for any $f(R)$ model for modified gravity and for other extended theories of modified gravity as well if it fulfils the necessary required conditions of viability as are understood and discussed.

CHAPTER-05

CONCLUSIONS

Relativistic cosmology was founded on general relativity with the introduction of cosmological principle where Weyl's principle was implicitly implied, in addition. In the beginning, two cosmological models were presented by Einstein and de Sitter, although, now of historical interest, yet they both are very significant as the first initiates modern cosmology relativistically and scientifically and the latter, later on, was used to provide the initial conditions of the big bang model with a slight change in time translation symmetry. The first theoretical models for the possibility of a dynamic universe evolved beginning with Friedmann, Lemaitre and were observationally determined by Edwin Hubble. In 1929, E. Hubble found exactly the same expanding universe that Friedmann did theoretically in 1922. Therefore, it was Friedmann who championed the cause of dynamic universes; however, his work was recognized later when he was no more in the world. The theory of the big bang that was based on the standard cosmological model faced Horizon, Flatness, Entropy problems, etc. To resolve these problems a phase of exponentially expanding universe was introduced in its very early history which proposed to have occurred in a very small fraction of time (about $\frac{1}{10^{43}}$s of the very 1st second after time creation) known as inflation. Inflation is identified as the initial conditions under which the big bang might have taken place. The introduction of inflation caused the name inflationary cosmology to surface and it is about forty years since its birth to date. The inflationary paradigm stands now on the firm observational footing and is accepted irrevocably in cosmology as the viable description for the early universe. Starobinsky, Guth, and Linde are credited with setting the foundations of inflationary cosmology. The inflationary cosmology is being hailed as successful in explaining the origin of structure formation through cosmological quantum fluctuations as relicts of cosmic inflation. The observations conducted on cosmic microwave background (CMB) radian and the recent discoveries of gravitational waves and black holes lend confirmatory support to the underlying principles of inflationary cosmology. Dark energy is one of the most challenging issues of standard cosmology both on theoretical and observational grounds. In the framework of ΛCDM it has equation of state (EoS) $w = -1$, however Λ is confronted with fine-tuning problem. An alternative remedy to tackle the problems related to Λ is the construction of models based on canonical and non-canonical scalar

fields. These models modify the matter sector on the right-hand side of the Einstein field equation, nonetheless, in non-scalar field models, the gravitational sector which is the curved geometry of spacetime is modified such as in $f(R)$ gravity. ΛCDM model, a parametrization of the big bang is accepted for being in good agreement with the recent observations. There exists now, however, a well-elaborated scenario to unify inflation with dark energy in modified gravity which was first proposed by S. Nojiri and S.D. Odintsov, See Ref. (Nojiri & Odintsov, 2003).

We discussed the multifield inflation by considering a small multifield potential written in the generalized form $\sum_i V_i(\phi_i) = \sum_i \Lambda_i \left[1 - \left(\frac{\phi_i}{\mu_i}\right)^p\right]$ with p being negative. This potential represents the small field inflationary model and can be regarded as Taylor series expansion about the origin of its minima and maxima in its lowest order. In small field models of inflation the field is usually considered beginning with about an unstable equilibrium around the origin and then rolling down along its potential about the origin. As the field expression denotes a generalized potential to stand for the multifield inflationary potential. i denotes any ith field taken into account multiple fields. The parameters Λ_i and μ_i denote the height and tilt of the ith potential in the multiple fields. The spectrum of curvature perturbations which give rise to the growth of cosmic structure are important relic from inflation. We investigated this spectrum for the potential under consideration. At first, we considered the case for the value of p larger than 2. In the case, in general, when inflaton fields have the equivalent masses the equations of motion give rise to those of single field inflation producing the phase of non-perturbations. This occurs due to relative mass differences in the inflaton fields. It is observed that the spectrum comes out to be more or less redder in the respective cases in comparison with the corresponding single field model accordingly. Included fields and their effective masses play a very significant role because the results depend upon these at the time of horizon-crossing. It is noted that the result corresponds to that of single scalar field when the effective masses of all the fields are taken to be equivalent. The spectrum in this case results to be similar and therefore coincides with the spectrum of single field. It is concluded that the results for the values of $p > 2$, $p = 2$ and $p = -2$ are different and the behaviour of the field potentials and the corresponding spectrums are distinct as well as different.

It can be noted that all the terms included in the factor $\ln\left(\frac{\phi_k^s}{\phi_k^e}\right)$ might be equivalent on account of the result reached. With some extra terms, the two expressions represent the same equation for the corresponding single field case. The value of $\ln\left(\frac{\phi_k^s}{\phi_k^e}\right)$ for the

result reached at, will be smaller for the larger value of μ_i when Λ_i are taken equivalent to the μ_i. If we consider $\mu_k = Max\,(\mu_n)$ where n denotes natural numbers. This gives rise to $\frac{\mu_i}{\mu_k} < 1$ which on the other hand implies that the spectrum is more redder than its corresponding spectrum resulting from the result for a single scalar field ϕ_k. In this case the value of $\ln\left(\frac{\phi_k^s}{\phi_k^e}\right)$ would represent almost the smallest from all the values of $\ln\left(\frac{\phi_i^s}{\phi_i^e}\right)$ which indicates that in Eq. (3.2.75), the case of single scalar field ϕ_k, the value of k tends to get nearer or approach to unity. On the other hand if we are taking the $\mu_k = Min\,(\mu_n)$ where n denotes natural numbers, then this gives rise to $\frac{\mu_i}{\mu_k} > 1$ which resultantly leads to the result that the spectrum is less redder than its corresponding spectrum resulting from a single scalar field ϕ_k. In this case the value of $\ln\left(\frac{\phi_k^s}{\phi_k^e}\right)$ would represent almost larger one out of all the values of $\ln\left(\frac{\phi_i^s}{\phi_i^e}\right)$ which shows that the case of single scalar field ϕ_k, where the value of k shifts away from unity. It means that the value of the scalar spectral index falls between that of single field in general for the biggest μ_k and the smallest accordingly.

Further, we considered a multifield model of inflation and studied its Nflationary phase transition properties. The study is carried out for the properties of inflationary phase with the help of phase diagram which gradually decreases and finally vanishes during slow roll phase of this Nflation model. It is observed that as the number of fields is increased, the critical point and the end point of slow rolling phase shift towards the smaller average values of the fields. The motion of these two points, however, takes place at different rates. It is the critical point that splits between the regions of eternally inflating phase and slow roll phase. In general, the critical point shifts towards the end phase faster than the end point of the slow roll phase indicating that the region of eternal inflation will dominate over the slow roll inflation. The slow roll region completely disappears when there is a large number of fields. Therefore Nflation might have some bound on the number of fields that might assist each other to drive the inflationary phase for evolution of the universe. From black hole entropy in its event horizon a bound is determined between number of fields N, with masses m and planck mass M_p. The properties of Nflation models correspond to that of the properties of single field models which help to investigate their real existence. Inflation is demonstrated for a large number of fields when large N phase transitions occur in Nflation. By plotting the phase transition diagram for Nflationary model by considering the multifield potential $V\,(\phi_j) = \Lambda_j^4\left(\frac{\phi_j}{\mu_j}\right)^p$, we explained how the slow roll phase diminishes. Further conditions on entropy in the form of a bound which conforms to the number of fields

N and the outcomes occurring in it have also been addressed. It is further investigated that all de Sitter (dS) entropy around or at the critical point remains concentrated about it and is completely condensed in the number of fields N for the considered potential. We observe the behavior of two regions, the slow roll phase and the eternal inflationary phase separated by the critical point at the boundary and at the initial points respectively which move gradually at slightly distinct rates towards field values smaller on the average. The boundary of the slow roll is likely to be engulfed slowly by the eternal inflation as the pace of critical point might be faster than the ending point, in principle. It can also be seen that the bounding limit from the theory of black holes for the number of fields N and Planck mass M_p does not almost show viability for the massless scalar fields which generate density perturbations as entropy. Marčenko-Pastur law gives the likely distribution of field masses that assigns average mass to all the large and small masses. We determined approximately similar order for specific value of β which incorporates all the masses naturally.

For understanding the earliest phase of cosmic evolution, Wheeler-DeWitt equation motivated the study of quantum cosmology around 1960 for investigating the early quantum phases of the universe. When the universe was evolving beyond the classical reign the quantum cosmology although hitherto perfectly unknown turns out to be important with Wheeler-DeWitt equation. The time-independent Schrödinger equation conforming to the Wheeler DeWitt equation is briefly reviewed for modelling the quantized behavior in the early universe. Therefore by solving Schrödinger equation we can get insight into the early universe evolution phases where the inflationary paradigm since the last forty years has become a dominant paradigm to the extent of irrefutable status. We solve it numerically for a single scalar field in flat spacetime with FLRW metric using artificial neural networks (ANN) and observe how it governs the early universe as it evolves through the inflationary phase following the big bang. To construct a continuous neural network mapping the explicit Runge-Kutta method is used as the target parameter to generate the datasets. To determine the solution datasets for different scenarios the processes of training, testing and validation are employed to take advantage of these in the learning of neural network models established upon the backpropagation technique of Levenberg-Marquardt. The work can be extended in future prospective using the technique of proposed ANN-LMB for the evolution of different system dynamics by solving numerically. This presents a viable technique to be applied to solve the problems of this nature.

To study the accelerating universe in the context of general relativity, we explore both sectors i.e. gravitational and matter sectors of the field equation. By modifying first the matter sector a multi-field model of dark energy is investigated to drive accelerated expansion. In order to understand accelerating universe in the framework of general relativity, we investigated both matter and gravitational sectors of Einstein field equation. For this purpose, at first we used modification of the matter sector for constructing a multi-field model of dark energy which drives the accelerated expansion. By considering two multiple scalar fields, namely tachyon, and phantom tachyon, we analyze the autonomous system in phase space making use of inverse square potentials suitable for such models. The critical points and their eigenvalues for the autonomous system stability analysis is performed. It is observed that stable critical points are satisfied by power-law solutions. Significant feature of the model is that the equation of state changes from $w \geq -1$ to $w \leq -1$ that is related to so called phantom divide and is decisive in evolutionary phases of the universe in these models. In principle, such models can be extended for understanding the cosmic viability for its late time accelerated phase.

On the other hand, accelerating universe is also explored using the gravitational sector of Einstein field equation. The gravitational sector is effectively modified through $f(R)$ gravity, which offers a viable candidacy for accelerating universe, where Ricci scalar invariant R is basically replaced to some general non-linear function of it which consists of higher-order curvature terms. Following the dynamical system approach for a particular $f(R)$ model, its stability analysis is carried out for cosmological inferences.

A particular model $f(R) = R^p \exp(qR)$ with $m = \frac{Rf_{,RR}}{f_{,R}} = \frac{p(p-1)+2pqR+q^2R^2}{p+qR}$ and $r = -\frac{Rf_{,R}}{f} = -(p+qR)$ and with the geometric curve $m(r) = -\frac{r^2-p}{r}$, is considered for investigation. Following the geometric approach for the curve $m(r)$ in the plane (r, m) which provides some properties of the model, study is carried out. In the case of matter-dominated era the viability conditions at $r = -1$, $m(r) = 0$ and $\frac{dm}{dr} > -1$ are examined. On the other hand, for the late time acceleration however, at $r = -2$, either of the two conditions $m(r) = -r - 1$ with $\frac{dm}{dr} < -1$, $1 \geq m > \frac{1}{2}\left(\sqrt{3}-1\right)$ and $1 \geq m \geq 0$ are sought to satisfied.

In the first place, cosmic content is assumed to be comprised of matter and radiation only in absence of cosmological constant term Λ. In this case interaction of any kind is disregarded. Afterward, as second consideration, the interaction term in the presence of cosmological constant term representing dark energy is taken into account. The effects of linear and non-linear interaction terms between matter and dark energy are also taken

into consideration for the case orderly. The results are presented for each case alongside the discussion carried out for the critical points, their eigenvalues, and the equation of state parameter. We present the stability analysis of the autonomous system of the model which is extended afterward by considering the cosmological constant as dark energy, which proves, however, to be redundant. The cases of linear and non-linear interactions between cosmic fluids are also discussed. The analysis shows that at some points accelerated expansion is yielded with a viable epoch of matter domination. In general, the work can be enlarged for any arbitrary $f(R)$ and for other extended theories of modified gravity if these fulfil the required conditions of viability.

REFERENCES

Abraham, E. R., Mendes dos Reis, J. G., Vendrametto, O., Oliveira Costa Neto, P. L. d., Carlo Toloi, R., Souza, A. E. d., & Oliveira Morais, M. d. (2020). Time series prediction with artificial neural networks: An analysis using brazilian soybean production. *Agriculture*, *10*(10), 475.

Abramo, L. R., & Finelli, F. (2003). Cosmological dynamics of the tachyon with an inverse power-law potential. *Physics Letters B*, *575*(3-4), 165–171.

Adler, I., Resende, M. G., Veiga, G., & Karmarkar, N. (1989). An implementation of karmarkar's algorithm for linear programming. *Mathematical programming*, *44*(1), 297–335.

Adshead, P., Easther, R., & Lim, E. A. (2009). Cosmology with many light scalar fields: stochastic inflation and loop corrections. *Physical Review D*, *79*(6), 063504.

Aghanim, N., Akrami, Y., Ashdown, M., Aumont, J., Baccigalupi, C., Ballardini, M., ... others (2020). Planck 2018 results-vi. cosmological parameters. *Astronomy & Astrophysics*, *641*, A6.

Aghanim, N., Akrami, Y., Ashdown, M., Aumont, J., Baccigalupi, C., Ballardini, M., ... others (2021). Corrigendum: Planck 2018 results. *Astronomy and Astrophysics-A&A*, *652*, C4.

Aguirregabiria, J. M., & Lazkoz, R. (2004). Tracking solutions in tachyon cosmology. *Physical Review D*, *69*(12), 123502.

Ahmad, I. (2012). Observational constraints on nfields phantom power-law. *arXiv preprint arXiv:1208.0021*.

Ahmad, I., Piao, Y.-S., & Qiao, C.-F. (2008). On the number of nflation fields. *Journal of Cosmology and Astroparticle Physics*, *2008*(06), 023.

Ahmad, I., Piao, Y.-S., & Qiao, C.-F. (2009). Phase diagram for nflation. *Physics Letters B*, *673*(1), 1–4.

Alabidi, L., & Lyth, D. H. (2006). Inflation models and observation. *Journal of Cosmology and Astroparticle Physics*, *2006*(05), 016.

Albrecht, A., & Steinhardt, P. J. (1982). Cosmology for grand unified theories with radiatively induced symmetry breaking. *Physical Review Letters*, *48*(17), 1220.

Albrecht, A., Steinhardt, P. J., Turner, M. S., & Wilczek, F. (1982). Reheating an inflationary universe. *Physical Review Letters*, *48*(20), 1437.

Allahverdi, R., Brandenberger, R., Cyr-Racine, F.-Y., & Mazumdar, A. (2010). Reheating in inflationary cosmology: theory and applications. *Annual Review of Nuclear and Particle Science*, *60*, 27–51.

ALPHER, R., & Herman, R. (1988). Reflections on early work on'big bang' cosmology. *Physics Today*, *41*(8), 24–34.

Amato, F., López, A., Peña-Méndez, E. M., Vaňhara, P., Hampl, A., & Havel, J. (2013). *Artificial neural networks in medical diagnosis.* Elsevier.

Amendola, L., Gannouji, R., Polarski, D., & Tsujikawa, S. (2007). Conditions for the cosmological viability of f (r) dark energy models. *Physical Review D*, *75*(8), 083504.

Amendola, L., Gordon, C., Wands, D., & Sasaki, M. (2002). Correlated perturbations from inflation and the cosmic microwave background. *Physical review letters*, *88*(21), 211302.

Amendola, L., Mayer, A. B., Capozziello, S., Gottlober, S., Muller, V., Occhionero, F., & Schmidt, H.-J. (1993). Generalized sixth-order gravity and inflation. *Classical and Quantum Gravity*, *10*(5), L43.

Amendola, L., & Tsujikawa, S. (2008). Phantom crossing, equation-of-state singularities, and local gravity constraints in f (r) models. *Physics Letters B*, *660*(3), 125–132.

Amendola, L., & Tsujikawa, S. (2010). *Dark energy: theory and observations*. Cambridge University Press.

Arevalo, F., Bacalhau, A. P., & Zimdahl, W. (2012). Cosmological dynamics with nonlinear interactions. *Classical and Quantum Gravity*, *29*(23), 235001.

Arkani-Hamed, N., Dubovsky, S., Nicolis, A., Trincherini, E., & Villadoro, G. (2007). A measure of de sitter entropy and eternal inflation. *Journal of High Energy Physics*, *2007*(05), 055.

Armendariz-Picon, C., Damour, T., & Mukhanov, V.-i. (1999). k-inflation. *Physics Letters B*, *458*(2-3), 209–218.

Armendariz-Picon, C., Mukhanov, V., & Steinhardt, P. J. (2000). Dynamical solution to the problem of a small cosmological constant and late-time cosmic acceleration. *Physical Review Letters*, *85*(21), 4438.

Armendariz-Picon, C., Mukhanov, V., & Steinhardt, P. J. (2001). Essentials of k-essence. *Physical Review D*, *63*(10), 103510.

Asadi, K., & Nozari, K. (2019). Reheating constraints on a two-field inflationary model. *Nuclear Physics B*, *949*, 114827.

Ashoorioon, A., Krause, A., & Turzynski, K. (2009). Energy transfer in multi field inflation and cosmological perturbations. *Journal of Cosmology and Astroparticle Physics*, *2009*(02), 014.

Astier, P., & Pain, R. (2012). Observational evidence of the accelerated expansion of the universe. *Comptes Rendus Physique*, *13*(6-7), 521–538.

Atkatz, D., & Pagels, H. (1982). Origin of the universe as a quantum tunneling event. *Physical Review D*, *25*(8), 2065.

Avgoustidis, A., Cremonini, S., Davis, A.-C., Ribeiro, R. H., Turzyński, K., & Watson, S. (2012). The importance of slow-roll corrections during multi-field inflation. *Journal of Cosmology and Astroparticle Physics*, *2012*(02), 038.

Bagla, J., Jassal, H. K., & Padmanabhan, T. (2003). Cosmology with tachyon field as dark energy. *Physical Review D*, *67*(6), 063504.

Bahamonde, S., Böhmer, C. G., Carloni, S., Copeland, E. J., Fang, W., & Tamanini,

N. (2018). Dynamical systems applied to cosmology: dark energy and modified gravity. *Physics Reports*, *775*, 1–122.

Bamba, K. (2013). Equation of state for dark energy in modified gravity theories. In *Quest for the origin of particles and the universe* (pp. 73–79). World Scientific.

Bamba, K., Capozziello, S., Nojiri, S., & Odintsov, S. D. (2012). Dark energy cosmology: the equivalent description via different theoretical models and cosmography tests. *Astrophysics and Space Science*, *342*(1), 155–228.

Bamba, K., & Odintsov, S. D. (2015). Inflationary cosmology in modified gravity theories. *Symmetry*, *7*(1), 220–240.

Banks, T., & Fischler, W. (2003). An upper bound on the number of e-foldings. *arXiv preprint astro-ph/0307459*.

Barbosa-Cendejas, N., & Reyes, M. (2009). The schrodinger picture of standard cosmology. *arXiv preprint arXiv:1001.0084*.

Barreiro, T., Copeland, E. J., & Nunes, N. a. (2000). Quintessence arising from exponential potentials. *Physical Review D*, *61*(12), 127301.

Bartolo, N., Matarrese, S., & Riotto, A. (2002). Non-gaussianity from inflation. *Physical Review D*, *65*(10), 103505.

Barvinsky, A. O. (2011). Standard model higgs inflation: Cmb, higgs mass and quantum cosmology. *Progress of Theoretical Physics Supplement*, *190*, 1–19.

Bassett, B. A., Tsujikawa, S., & Wands, D. (2006). Inflation dynamics and reheating. *Reviews of Modern Physics*, *78*(2), 537.

Battefeld, D., & Battefeld, T. (2007). Non-gaussianities in n-flation. *Journal of Cosmology and Astroparticle Physics*, *2007*(05), 012.

Battefeld, D., & Battefeld, T. (2009). Multi-field inflation on the landscape. *Journal of Cosmology and Astroparticle Physics*, *2009*(03), 027.

Bauer, F., & Demir, D. A. (2011). Higgs–palatini inflation and unitarity. *Physics Letters B*, *698*(5), 425–429.

Baumann, D. (2009). Tasi lectures on inflation. *arXiv preprint arXiv:0907.5424*.

Baumann, D. (2012). Cosmology. *Part III Mathematical Tripos*.

Baumann, D. (2018a). Primordial cosmology. In *Theoretical advanced study institute summer school 2017" physics at the fundamental frontier"* (Vol. 305, p. 009).

Baumann, D. (2018b). Tasi lectures on primordial cosmology. *arXiv preprint arXiv:1807.03098*.

Bean, R., & Dore, O. (2004). Probing dark energy perturbations: the dark energy equation of state and speed of sound as measured by wmap. *Physical Review D*, *69*(8), 083503.

Bekov, S., Myrzakulov, K., Myrzakulov, R., & Sáez-Chillón Gómez, D. (2020). General

slow-roll inflation in f (r) gravity under the palatini approach. *Symmetry*, *12*(12), 1958.

Benisty, D., & Staicova, D. (2021). Testing late-time cosmic acceleration with uncorrelated baryon acoustic oscillation dataset. *Astronomy & Astrophysics*, *647*, A38.

Bergmann, P. G. (1968). Comments on the scalar-tensor theory. *International Journal of Theoretical Physics*, *1*(1), 25–36.

Bernardeau, F., Kofman, L., & Uzan, J.-P. (2004). Modulated fluctuations from hybrid inflation. *Physical Review D*, *70*(8), 083004.

Bernardeau, F., & Uzan, J.-P. (2002). Non-gaussianity in multifield inflation. *Physical Review D*, *66*(10), 103506.

Berti, E., Barausse, E., Cardoso, V., Gualtieri, L., Pani, P., Sperhake, U., ... others (2015). Testing general relativity with present and future astrophysical observations. *Classical and Quantum Gravity*, *32*(24), 243001.

Bertotti, B., Balbinot, R., Bergia, S., & Messina, A. (1990). *Modern cosmology in retrospect*. Cambridge University Press.

Bijari, K., Zare, H., Veisi, H., & Bobarshad, H. (2018). Memory-enriched big bang–big crunch optimization algorithm for data clustering. *Neural Computing and Applications*, *29*(6), 111–121.

Bohr, N. (1928). *The quantum postulate and the recent development of atomic theory 1.* Nature Publishing Group.

Bohr, N. (1961). *Atomic theory and the description of nature* (Vol. 1). CUP Archive.

Bojowald, M. (2011). *Quantum cosmology: a fundamental description of the universe* (Vol. 835). Springer Science & Business Media.

Bolotin, Y. L., Kostenko, A., Lemets, O. A., & Yerokhin, D. A. (2015). Cosmological evolution with interaction between dark energy and dark matter. *International Journal of Modern Physics D*, *24*(03), 1530007.

Boubekeur, L., & Lyth, D. H. (2005). Hilltop inflation. *Journal of Cosmology and Astroparticle Physics*, *2005*(07), 010.

Bouhmadi-Lopez, M., & Moniz, P. V. (2005). Frw quantum cosmology with a generalized chaplygin gas. *Physical Review D*, *71*(6), 063521.

Bransden, B., & Joachain, C. (n.d.). Quantum mechanics,(2000). *Prentice Hall.*.

Brejzman, B., Gurovich, V. T., & Sokolov, V. (1970). On the possibility of setting up regular cosmological solutions. *Zhurnal Eksperimentalnoi i Teoreticheskoi Fiziki*, *59*, 288–294.

Brout, R., Englert, F., & Gunzig, E. (1978). The creation of the universe as a quantum phenomenon. *Annals of Physics*, *115*(1), 78–106.

Buchdahl, H. A. (1970). Non-linear lagrangians and cosmological theory. *Monthly Notices of the Royal Astronomical Society*, *150*(1), 1–8.

Byrnes, C. T., & Wands, D. (2006). Curvature and isocurvature perturbations from two-field inflation in a slow-roll expansion. *Physical Review D*, *74*(4), 043529.

Cai, R.-G., Guo, Z.-K., & Wang, S.-J. (2015). Reheating phase diagram for single-field slow-roll inflationary models. *Physical Review D*, *92*(6), 063506.

Cai, R.-G., Hu, B., & Piao, Y.-S. (2009). Entropy perturbations in n-flation. *Physical Review D*, *80*(12), 123505.

Cai, Y., Wan, Y., Li, H.-G., Qiu, T., & Piao, Y.-S. (2017). The effective field theory of nonsingular cosmology. *Journal of High Energy Physics*, *2017*(1), 1–18.

Cai, Y.-F., Li, H., Piao, Y.-S., & Zhang, X. (2007). Cosmic duality in quintom universe. *Physics Letters B*, *646*(4), 141–144.

Cai, Y.-F., Li, M., Lu, J.-X., Piao, Y.-S., Qiu, T., & Zhang, X. (2007). A string-inspired quintom model of dark energy. *Physics Letters B*, *651*(1), 1–7.

Cai, Y.-F., Qiu, T., Zhang, X., Piao, Y.-S., & Li, M. (2007). Bouncing universe with quintom matter. *Journal of High Energy Physics*, *2007*(10), 071.

Calcagni, G., & Liddle, A. R. (2006). Tachyon dark energy models: Dynamics and constraints. *Physical Review D*, *74*(4), 043528.

Caldwell, R. R., Kamionkowski, M., & Weinberg, N. N. (2003). Phantom energy: dark energy with w¡- 1 causes a cosmic doomsday. *Physical Review Letters*, *91*(7), 071301.

Capozziello, S., Carloni, S., & Troisi, A. (2003). Quintessence without scalar fields. *arXiv preprint astro-ph/0303041*.

Capozziello, S., & De Laurentis, M. (2011). Extended theories of gravity. *Physics Reports*, *509*(4-5), 167–321.

Capozziello, S., & De Laurentis, M. (2015). F (r) theories of gravitation. *Scholarpedia*, *10*(2), 31422.

Capozziello, S., De Laurentis, M., & Faraoni, V. (2009). A bird's eye view of f (r)-gravity. *arXiv preprint arXiv:0909.4672*.

Capozziello, S., Feoli, A., & Lambiase, G. (2000). Oscillating universe as eigensolutions of cosmological schrödinger equation. *International Journal of Modern Physics D*, *9*(02), 143–154.

Capozziello, S., Mantica, C. A., & Molinari, L. G. (2019). Cosmological perfect-fluids in f (r) gravity. *International Journal of Geometric Methods in Modern Physics*, *16*(01), 1950008.

Capozziello, S., Nojiri, S., & Odintsov, S. D. (2018). The role of energy conditions in f (r) cosmology. *Physics Letters B*, *781*, 99–106.

Capozziello, S., & Tsujikawa, S. (2008). Solar system and equivalence principle constraints on f (r) gravity by the chameleon approach. *Physical Review D*, *77*(10), 107501.

Carroll, S. M. (2004). Why is the universe accelerating? In *Aip conference proceedings* (Vol. 743, pp. 16–32).

Carroll, S. M., Hoffman, M., & Trodden, M. (2003). Can the dark energy equation-of-state parameter w be less than- 1? *Physical Review D*, *68*(2), 023509.

Cervantes-Cota, J. L., & Dehnen, H. (1995). Induced gravity inflation in the standard model of particle physics. *Nuclear Physics B*, *442*(1-2), 391–409.

Chiba, T., Okabe, T., & Yamaguchi, M. (2000). Kinetically driven quintessence. *Physical Review D*, *62*(2), 023511.

Cicoli, M., Dutta, K., & Maharana, A. (2014). N-flation with hierarchically light axions in string compactifications. *Journal of Cosmology and Astroparticle Physics*, *2014*(08), 012.

Clesse, S. (2011). Hybrid inflation: Multi-field dynamics and cosmological constraints. *arXiv preprint arXiv:1109.5575*.

Clifton, T., Ferreira, P. G., Padilla, A., & Skordis, C. (2012). Modified gravity and cosmology. *Physics reports*, *513*(1-3), 1–189.

Cline, J. M., Jeon, S., & Moore, G. D. (2004). The phantom menaced: constraints on low-energy effective ghosts. *Physical Review D*, *70*(4), 043543.

Copeland, E. J., Garousi, M. R., Sami, M., & Tsujikawa, S. (2005). What is needed of a tachyon if it is to be the dark energy? *Physical Review D*, *71*(4), 043003.

Copeland, E. J., Sami, M., & Tsujikawa, S. (2006). Dynamics of dark energy. *International Journal of Modern Physics D*, *15*(11), 1753–1935.

Covi, L. (2001). Models of inflation, supersymmetry breaking and observational constraints. In *Dark matter in astro-and particle physics* (pp. 163–175). Springer.

Das, K., & Dutta, K. (2014). N-flation in supergravity. *Physics Letters B*, *738*, 457–463.

de Barros, J. A., Silva, E. C., Monerat, G., Oliveira-Neto, G., Ferreira Filho, L., & Romildo Jr, P. (2007). Tunneling probability for the birth of an asymptotically de sitter universe. *Physical Review D*, *75*(10), 104004.

de Broglie, L. (1925). Research on the theory of quanta. In *Annales de physique* (Vol. 10, pp. 22–128).

De Felice, A., & Tsujikawa, S. (2010). f (r) theories. *Living Reviews in Relativity*, *13*(1), 1–161.

Demirtas, M., Kim, M., McAllister, L., Moritz, J., & Rios-Tascon, A. (2021). A cosmological constant that is too small. *arXiv preprint arXiv:2107.09065*.

De Sitter, W. (1916). On einstein's theory of gravitation and its astronomical consequences. second paper. *Monthly notices of the royal astronomical society*, *77*, 155–184.

DeWitt, B. S. (1967a). Quantum theory of gravity. iii. applications of the covariant theory. *Physical Review*, *162*(5), 1239.

DeWitt, B. S. (1967b). Quantum theory of gravity. ii. the manifestly covariant theory. *Physical Review*, *162*(5), 1195.

DeWitt, B. S. (1967c). Quantum theory of gravity. i. the canonical theory. *Physical Review*, *160*(5), 1113.

Dias, M., Frazer, J., Retolaza, A., Scalisi, M., & Westphal, A. (2019). Pole n-flation. *Journal of High Energy Physics*, *2019*(2), 1–29.

Dimopoulos, S., Kachru, S., McGreevy, J., & Wacker, J. G. (2008). N-flation. *Journal of Cosmology and Astroparticle Physics*, *2008*(08), 003.

D'Inverno, R. A., & Harvey, A. (1993). Introducing einstein's relativity. *Physics Today*, *46*(8), 59.

Di Valentino, E., Melchiorri, A., & Silk, J. (2020). Cosmological constraints in extended parameter space from the planck 2018 legacy release. *Journal of Cosmology and Astroparticle Physics*, *2020*(01), 013.

Dvali, G. (2010). Black holes and large n species solution to the hierarchy problem. *Fortschritte der Physik*, *58*(6), 528–536.

Dvali, G., Gruzinov, A., & Zaldarriaga, M. (2004). New mechanism for generating density perturbations from inflation. *Physical Review D*, *69*(2), 023505.

Dvali, G., & Solodukhin, S. N. (2008). Black hole entropy and gravity cutoff. *arXiv preprint arXiv:0806.3976*.

Earman, J., & Mosterin, J. (1999). A critical look at inflationary cosmology. *Philosophy of Science*, *66*(1), 1–49.

Easther, R., Frazer, J., Peiris, H. V., & Price, L. C. (2014). Simple predictions from multifield inflationary models. *Physical review letters*, *112*(16), 161302.

Easther, R., & McAllister, L. (2006). Random matrices and the spectrum of n-flation. *Journal of cosmology and astroparticle physics*, *2006*(05), 018.

Einstein, A. (1922). The general theory of relativity. In *The meaning of relativity* (pp. 54–75). Springer.

Einstein, A. (1925). Sitzung-ber preuss akad. *Wiss. Phys.-Math. Kl*, *23*(3).

Einstein, A. (1950). On the generalized theory of gravitation. *Scientific American*, *182*(4), 13–17.

Einstein, A. (1986). Cosmological considerations on the general theory of relativity. *Cosmological Constants*, 16.

Escolano, N. R., & Espín, J. J. L. (2016). *Econometría: series temporales y modelos de ecuaciones simultáneas*. Universidad Miguel Hernández.

Esposito, G. (2011). An introduction to quantum gravity. *arXiv preprint arXiv:1108.3269*.

Fairbairn, M., & Tytgat, M. H. (2002). Inflation from a tachyon fluid? *Physics Letters B*, *546*(1-2), 1–7.

Fang, W., Tu, H., Huang, J., & Shu, C. (2016). Dynamical system of scalar field from

2-dimension to 3-d and its cosmological implications. *The European Physical Journal C*, *76*(9), 1–12.

Faraoni, V., & Capozziello, S. (2011). *Beyond einstein gravity*.

Feinstein, A. (2002). Power-law inflation from the rolling tachyon. *Physical Review D*, *66*(6), 063511.

Feng, B., Li, M., Piao, Y.-S., & Zhang, X. (2006). Oscillating quintom and the recurrent universe. *Physics Letters B*, *634*(2-3), 101–105.

Feng, B., Wang, X., & Zhang, X. (2005). Dark energy constraints from the cosmic age and supernova. *Physics Letters B*, *607*(1-2), 35–41.

Feng, C.-J., Zhai, X.-H., & Li, X.-Z. (2020). Multi-pole dark energy. *Chinese Physics C*, *44*(10), 105103.

Ferraro, R. (2012). f (r) and f (t) theories of modified gravity. In *Aip conference proceedings* (Vol. 1471, pp. 103–110).

Frazer, J. (2014). Predictions in multifield models of inflation. *Journal of Cosmology and Astroparticle Physics*, *2014*(01), 028.

Freese, K., Frieman, J. A., & Olinto, A. V. (1990). Natural inflation with pseudo nambu-goldstone bosons. *Physical Review Letters*, *65*(26), 3233.

Friedmann, A. (1924). Über die möglichkeit einer welt mit konstanter negativer krümmung des raumes. *Zeitschrift für Physik*, *21*(1), 326–332.

Friedmann, A. (1999). On the possibility of a world with constant negative curvature of space. *General Relativity and Gravitation*, *31*(12), 2001–2008.

Friedmann, A. A. (2014). *The world as space and time*. Minkowski Institute Press.

Frieman, J. A., Turner, M. S., & Huterer, D. (2008). Dark energy and the accelerating universe. *Annu. Rev. Astron. Astrophys.*, *46*, 385–432.

Frolov, A., Kofman, L., & Starobinsky, A. (2002). Prospects and problems of tachyon matter cosmology. *Physics Letters B*, *545*(1-2), 8–16.

Fujiwara, Y., Higuchi, S., Hosoya, A., Mishima, T., & Siino, M. (1991). Nucleation of a universe in (2+ 1)-dimensional gravity with a negative cosmological constant. *Physical Review D*, *44*(6), 1756.

Fujiwara, Y., Ishihara, H., & Kodama, H. (1993). Comments on closed bianchi models. *Classical and Quantum Gravity*, *10*(5), 859.

Fukushima, M., & Tseng, P. (2002). An implementable active-set algorithm for computing a b-stationary point of a mathematical program with linear complementarity constraints. *SIAM Journal on Optimization*, *12*(3), 724–739.

Garcia-Salcedo, R., Gonzalez, T., & Quiros, I. (2012). Phase space dynamics of non-gravitational interactions between dark matter and dark energy: The case of ghost dark energy. *arXiv preprint arXiv:1211.2738*.

Gibbons, G. (2002). Cosmological evolution of the rolling tachyon. *Physics Letters B*, *537*(1-2), 1–4.

Gibbons, G. (2003). Thoughts on tachyon cosmology. *Classical and Quantum Gravity*, *20*(12), S321.

Gliner, E. B. (1966). Algebraic properties of the energy-momentum tensor and vacuum-like states o+ matter. *Soviet Journal of Experimental and Theoretical Physics*, *22*, 378.

Golchin, H., Jamali, S., & Ebrahimi, E. (2017). Interacting dark energy: Dynamical system analysis. *International Journal of Modern Physics D*, *26*(09), 1750098.

Gong, J.-O. (2006). Modular thermal inflation without slow-roll approximation. *Physics Letters B*, *637*(3), 149–155.

Gong, J.-O. (2007). End of multifield inflation and the perturbation spectrum. *Physical Review D*, *75*(4), 043502.

González-Díaz, P. F. (2003). You need not be afraid of phantom energy. *Physical Review D*, *68*(2), 021303.

González-Dıaz, P. F. (2004). K-essential phantom energy: Doomsday around the corner? *Physics Letters B*, *586*(1-2), 1–4.

Gordon, C., Wands, D., Bassett, B. A., & Maartens, R. (2000). Adiabatic and entropy perturbations from inflation. *Physical Review D*, *63*(2), 023506.

Gorini, V., Kamenshchik, A., Moschella, U., & Pasquier, V. (2004). Tachyons, scalar fields, and cosmology. *Physical Review D*, *69*(12), 123512.

Gorini, V., Kamenshchik, A., Moschella, U., Pasquier, V., & Starobinsky, A. (2005). Stability properties of some perfect fluid cosmological models. *Physical Review D*, *72*(10), 103518.

Gotay, M. J., & Demaret, J. (1983). Quantum cosmological singularities. *Physical Review D*, *28*(10), 2402.

Gott, J. R., & Slepian, Z. (2011). Dark energy as double n-flation–observational predictions. *Monthly Notices of the Royal Astronomical Society*, *416*(2), 907–916.

Gottlober, S., Schmidt, H.-J., & Starobinsky, A. A. (1990). Sixth-order gravity and conformal transformations. *Classical and Quantum Gravity*, *7*(5), 893.

Guo, Z.-K., Ohta, N., & Zhang, Y.-Z. (2005). Parametrization of quintessence and its potential. *Physical Review D*, *72*(2), 023504.

Guo, Z.-K., Ohta, N., & Zhang, Y.-Z. (2007). Parametrizations of the dark energy density and scalar potentials. *Modern Physics Letters A*, *22*(12), 883–890.

Guo, Z.-K., Piao, Y.-S., Cai, R.-G., & Zhang, Y.-Z. (2003). Inflationary attractor from tachyonic matter. *Physical Review D*, *68*(4), 043508.

Guo, Z.-K., Piao, Y.-S., Zhang, X., & Zhang, Y.-Z. (2005). Cosmological evolution of a quintom model of dark energy. *Physics Letters B*, *608*(3-4), 177–182.

Guo, Z.-K., Piao, Y.-S., Zhang, X., & Zhang, Y.-Z. (2006). Two-field quintom models in the $w - w'$ plane. *Physical Review D*, *74*(12), 127304.

Guo, Z.-K., & Zhang, Y.-Z. (2004). Cosmological scaling solutions of multiple tachyon fields with inverse square potentials. *Journal of Cosmology and Astroparticle Physics*, *2004*(08), 010.

Guo, Z.-K., & Zhang, Y.-Z. (2005). Interacting phantom energy. *Physical Review D*, *71*(2), 023501.

Guth, A. H. (1981). Inflationary universe: A possible solution to the horizon and flatness problems. *Physical Review D*, *23*(2), 347.

Guth, A. H., & Kaiser, D. I. (2005). Inflationary cosmology: Exploring the universe from the smallest to the largest scales. *Science*, *307*(5711), 884–890.

Guth, A. H., Kaiser, D. I., & Nomura, Y. (2014). Inflationary paradigm after planck 2013. *Physics Letters B*, *733*, 112–119.

Guth, A. H., & Pi, S.-Y. (1982). Fluctuations in the new inflationary universe. *Physical Review Letters*, *49*(15), 1110.

Guth, A. H., & Weinberg, E. J. (1983). Could the universe have recovered from a slow first-order phase transition? *Nuclear Physics B*, *212*(2), 321–364.

Halliwell, J. J., & Hawking, S. W. (1985). Origin of structure in the universe. *Physical Review D*, *31*(8), 1777.

Halliwell, J. J., & Louko, J. (1990). Steepest-descent contours in the path-integral approach to quantum cosmology. iii. a general method with applications to anisotropic minisuperspace models. *Physical Review D*, *42*(12), 3997.

Hao, J.-g., & Li, X.-z. (2002). Reconstructing the equation of state of the tachyon. *Physical Review D*, *66*(8), 087301.

Hao, J.-g., & Li, X.-z. (2003). Phantom with born-infeld-type lagrangian. *Physical Review D*, *68*(4), 043501.

Hartle, J. B., & Hawking, S. W. (1983). Wave function of the universe. *Physical Review D*, *28*(12), 2960.

Hawking, S. (2009). *A brief history of time: from big bang to black holes*. Random House.

Hawking, S. W. (1982). The development of irregularities in a single bubble inflationary universe. *Physics Letters B*, *115*(4), 295–297.

Hawking, S. W. (1984). The quantum state of the universe. *Nuclear Physics B*, *239*(1), 257–276.

Hawking, S. W., Moss, I., & Stewart, J. (1982). Bubble collisions in the very early universe. *Physical Review D*, *26*(10), 2681.

Heisenberg, L. (2019). A systematic approach to generalisations of general relativity and their cosmological implications. *Physics Reports*, *796*, 1–113.

Heisenberg, W. (n.d.). The physical content of quantum kinematics and mechanics (1927). *Quantum Theory and Measurement*, 62–84.

Hotinli, S. C., Frazer, J., Jaffe, A. H., Meyers, J., Price, L. C., & Tarrant, E. R. (2018). Effect of reheating on predictions following multiple-field inflation. *Physical Review D*, *97*(2), 023511.

Hu, W. (2005). Crossing the phantom divide: Dark energy internal degrees of freedom. *Physical Review D*, *71*(4), 047301.

Hu, W., & Sawicki, I. (2007). Models of f (r) cosmic acceleration that evade solar system tests. *Physical Review D*, *76*(6), 064004.

Huang, Q.-G. (2008). Weak gravity conjecture for effective field theories with n species. *Physical Review D*, *77*(10), 105029.

Hubble, E. P. (2013). *106. a relation between distance and radial velocity among extra-galactic nebulae*. Harvard University Press.

Hughes, J. (2019). The quintessential dark energy theory: Quintessence.

Huterer, D., & Turner, M. S. (1999). Prospects for probing the dark energy via supernova distance measurements. *Physical Review D*, *60*(8), 081301.

Ishak, M. (2019). Testing general relativity in cosmology. *Living Reviews in Relativity*, *22*(1), 1–204.

Ivanov, M. M., Simonović, M., & Zaldarriaga, M. (2020). Cosmological parameters from the boss galaxy power spectrum. *Journal of Cosmology and Astroparticle Physics*, *2020*(05), 042.

Jørgensen, L., Cardozo, D. L., & Thibierge, E. (2011). Numerical resolution of the schrödinger equation.

Kachru, S., Kallosh, R., Linde, A., Maldacena, J., McAllister, L., & Trivedi, S. P. (2003). Towards inflation in string theory. *Journal of Cosmology and Astroparticle Physics*, *2003*(10), 013.

Kallosh, R., & Linde, A. (2010). New models of chaotic inflation in supergravity. *journal of Cosmology and Astroparticle Physics*, *2010*(11), 011.

Kaloper, N., Kleban, M., Lawrence, A., & Sloth, M. S. (2016). Large field inflation and gravitational entropy. *Physical Review D*, *93*(4), 043510.

Kaloper, N., & Liddle, A. R. (2000). Dynamics and perturbations in assisted chaotic inflation. *Physical Review D*, *61*(12), 123513.

Kang, G.-Z., Zhang, D.-S., Jun, L., & Zong, H.-S. (2020). Fine tuning problem of the cosmological constant in a generalized randall-sundrum model. *Chinese Physics C*, *44*(12), 125102.

Kanti, P., & Olive, K. A. (1999). On the realization of assisted inflation. *Physical Review D*, *60*(4), 043502.

Kawasaki, M., & Yamaguchi, M. (2002). Supersymmetric topological inflation model.

Physical Review D, *65*(10), 103518.

Kazanas, D. (1980). Dynamics of the universe and spontaneous symmetry breaking. *The Astrophysical Journal*, *241*, L59–L63.

Kiefer, C. (2006). Quantum gravity: general introduction and recent developments. *Annalen der Physik*, *15*(1-2), 129–148.

Kim, S. A., & Liddle, A. R. (2006). N-flation: Multifield inflationary dynamics and perturbations. *Physical Review D*, *74*(2), 023513.

Kim, S. A., & Liddle, A. R. (2007). N-flation: Observable predictions from the random matrix mass spectrum. *Physical Review D*, *76*(6), 063515.

Kim, S. A., Liddle, A. R., & Seery, D. (2010). Non-gaussianity in axion n-flation models. *Physical review letters*, *105*(18), 181302.

Kinney, W. H., & Mahanthappa, K. (1996). Inflation at low scales: General analysis and a detailed model. *Physical Review D*, *53*(10), 5455.

Kinney, W. H., & Riotto, A. (1998). A signature of inflation from dynamical supersymmetry breaking. *Physics Letters B*, *435*(3-4), 272–276.

Kinney, W. H., & Riotto, A. (1999). Dynamical supersymmetric inflation. *Astroparticle Physics*, *10*(4), 387–395.

Kirzhnits, D. A., & Linde, A. D. (1972). Macroscopic consequences of the weinberg model. *Physics Letters B*, *42*(4), 471–474.

Knox, L., & Olinto, A. (1993). Initial conditions for natural inflation. *Physical Review D*, *48*(2), 946.

Kodama, H., & Sasaki, M. (1984). Cosmological perturbation theory. *Progress of Theoretical Physics Supplement*, *78*, 1–166.

Kofman, L. (2003). Probing string theory with modulated cosmological fluctuations. *arXiv preprint astro-ph/0303614*.

Kofman, L., & Linde, A. (2002). Problems with tachyon inflation. *Journal of High Energy Physics*, *2002*(07), 004.

Kofman, L., & Pogosyan, D. Y. (1988). Nonflat perturbations in inflationary cosmology. *Physics Letters B*, *214*(4), 508–514.

Kofman, L. A., & Linde, A. D. (1987). Generation of density perturbations in inflationary cosmology. *Nuclear Physics B*, *282*, 555–588.

Kolb, E. W., & Turner, M. S. (2018). *The early universe*. CRC press.

Kragh, H. S., & Lambert, D. (2007). The context of discovery: Lemaître and the origin of the primeval-atom universe. *Annals of Science*, *64*(4), 445–470.

Kujat, J., Scherrer, R. J., & Sen, A. (2006). Phantom dark energy models with negative kinetic term. *Physical Review D*, *74*(8), 083501.

Langlois, D. (1999). Correlated adiabatic and isocurvature perturbations from double inflation. *Physical Review D*, *59*(12), 123512.

Lazarides, G., & Vamvasakis, A. (2007). Standard-smooth hybrid inflation. *Physical Review D*, *76*(12), 123514.

Lee, P., & Swaminathan, R. (2005). An interior point (karmarkar) project for solving the global routing problem. *Linear algebra with numerical application*, *2005*, 4–6.

Lemaître, G. (1927). Un univers homogène de masse constante et de rayon croissant rendant compte de la vitesse radiale des nébuleuses extra-galactiques. In *Annales de la société scientifique de bruxelles* (Vol. 47, pp. 49–59).

Lemaître, G. (1931). The beginning of the world from the point of view of quantum theory. *Nature*, *127*(3210), 706–706.

Lemaitre, G. (2013). Republication of: A homogeneous universe of constant mass and increasing radius accounting for the radial velocity of extra-galactic nebulae. *General Relativity and Gravitation*, *45*(8), 1635–1646.

Lesgourgues, J. (2000). Features in the primordial power spectrum of double d-term inflation. *Nuclear Physics B*, *582*(1-3), 593–626.

Li, M., Li, X.-D., Wang, S., & Wang, Y. (2011). Dark energy. *arXiv preprint arXiv:1103.5870*.

Li, M., Li, X.-D., Wang, S., & Wang, Y. (2013). Dark energy: A brief review. *Frontiers of Physics*, *8*(6), 828–846.

Li, S., & Liddle, A. R. (2012). Observational constraints on k-inflation models. *Journal of Cosmology and Astroparticle Physics*, *2012*(10), 011.

Li, X.-z., Liu, D.-j., & Hao, J.-g. (2002). On the tachyon inflation. *arXiv preprint hep-th/0207146*.

Liddle, A. R., Mazumdar, A., & Schunck, F. E. (1998). Assisted inflation. *Physical Review D*, *58*(6), 061301.

Lieb, E. H., & Yngvason, J. (1999). The physics and mathematics of the second law of thermodynamics. *Physics Reports*, *310*(1), 1–96.

Linde, A. (1982). Coleman-weinberg theory and a new inflationary universe scenario, lebedev phys. *Inst. preprint*(88).

Linde, A. (1991). Axions in inflationary cosmology. *Physics Letters B*, *259*(1-2), 38–47.

Linde, A. (1994). Hybrid inflation. *Physical Review D*, *49*(2), 748.

Linde, A. (2015). *Inflationary cosmology after planck* (Vol. 100). Oxford University Press Oxford, England, UK.

Linde, A., & Mukhanov, V. (1997). Non-gaussian isocurvature perturbations from inflation. *Physical Review D*, *56*(2), R535.

Linde, A. D. (1974). Is the cosmological constant really constant? *Pisma v Zhurnal*

Eksperimentalnoi i Teoreticheskoi Fiziki, *19*, 320–322.

Linde, A. D. (1979). Phase transitions in gauge theories and cosmology. *Reports on Progress in Physics*, *42*(3), 389.

Linde, A. D. (1982a). A new inflationary universe scenario: a possible solution of the horizon, flatness, homogeneity, isotropy and primordial monopole problems. *Physics Letters B*, *108*(6), 389–393.

Linde, A. D. (1982b). Scalar field fluctuations in the expanding universe and the new inflationary universe scenario. *Physics Letters B*, *116*(5), 335–339.

Linde, A. D. (1982c). Temperature dependence of coupling constants and the phase transition in the coleman-weinberg theory. *Physics Letters B*, *116*(5), 340–342.

Linde, A. D. (1984a). Generation of isothermal density perturbations in an inflationary universe. *ZhETF Pisma Redaktsiiu*, *40*, 496–498.

Linde, A. D. (1984b). The inflationary universe. *Reports on Progress in Physics*, *47*(8), 925.

Liu, Z.-G., & Piao, Y.-S. (2013). Galilean islands in eternally inflating background. *Physical Review D*, *88*(4), 043520.

Louko, J., & Ruback, P. J. (1991). Spatially flat quantum cosmology. *Classical and Quantum Gravity*, *8*(1), 91.

Lourakis, M., & Argyros, A. A. (2005). Is levenberg-marquardt the most efficient optimization algorithm for implementing bundle adjustment? In *Tenth ieee international conference on computer vision (iccv'05) volume 1* (Vol. 2, pp. 1526–1531).

Ludwick, K. J. (2017). The viability of phantom dark energy: A review. *Modern Physics Letters A*, *32*(28), 1730025.

Lyth, D. H., & Liddle, A. R. (2009). *The primordial density perturbation: Cosmology, inflation and the origin of structure*. Cambridge University Press.

Lyth, D. H., & Riotto, A. (1999). Particle physics models of inflation and the cosmological density perturbation. *Physics Reports*, *314*(1-2), 1–146.

Lyth, D. H., Ungarelli, C., & Wands, D. (2003). Primordial density perturbation in the curvaton scenario. *Physical Review D*, *67*(2), 023503.

Lyth, D. H., & Wands, D. (2002). Generating the curvature perturbation without an inflaton. *Physics Letters B*, *524*(1-2), 5–14.

Man, P. K. (2018). Slow-roll analysis of double-field axion inflation. *Progress of Theoretical and Experimental Physics*, *2018*(11), 113E04.

Martin, J., Ringeval, C., & Vennin, V. (2014). Encyclopædia inflationaris. *Physics of the Dark Universe*, *5*, 75–235.

Martins, C., & Moucherek, F. (2016). Cosmological and astrophysical constraints on tachyon dark energy models. *Physical Review D*, *93*(12), 123524.

Massó, E. (2012). The accelerated universe. on the nobel prize in physics 2011 awarded to saul perlmutter, brian p. schmidt, and adam g. riess. *Contributions to science*, 69–75.

Mayer, A. B., & Schmidt, H.-J. (1993). The de sitter spacetime as attractor solution in eighth-order gravity. *Classical and Quantum Gravity*, *10*(11), 2441.

Mazumdar, A., Mohanty, S., & Parashari, P. (2021). Evidence of dark energy in different cosmological observations. *The European Physical Journal Special Topics*, 1–12.

Mazumdar, A., Panda, S., & Perez-Lorenzana, A. (2001). Assisted inflation via tachyon condensation. *Nuclear Physics B*, *614*(1-2), 101–116.

Mielnik, B., & Reyes, M. A. (1996). The classical schrödinger equation. *Journal of Physics A: Mathematical and General*, *29*(18), 6009.

Minkowski, H. (2013). *Space and time: Minkowski's papers on relativity*. Minkowski Institute Press.

Mishra, S., & Chakraborty, S. (2018). Dynamical system analysis of quintom dark energy model. *The European Physical Journal C*, *78*(11), 1–9.

Misner, C. W. (1969). Quantum cosmology. i. *Physical Review*, *186*(5), 1319.

Mohayaee, R., Rameez, M., & Sarkar, S. (2021). Do supernovae indicate an accelerating universe? *The European Physical Journal Special Topics*, 1–10.

Monerat, G., Silva, E. C., Oliveira-Neto, G., Ferreira Filho, L., & Lemos, N. (2006). Quantization of friedmann-robertson-walker spacetimes in the presence of a negative cosmological constant and radiation. *Physical Review D*, *73*(4), 044022.

Moroi, T., & Takahashi, T. (2001). Effects of cosmological moduli fields on cosmic microwave background. *Physics Letters B*, *522*(3-4), 215–221.

Moss, I., & Wright, W. (1984). Wave function of the inflationary universe. *Physical Review D*, *29*(6), 1067.

Mughal, M. Z., & Ahmad, I. (2021). A multi-field tachyon-quintom model of dark energy and fate of the universe. *The European Physical Journal Plus*, *136*(5), 1–20.

Mughal, M. Z., Ahmad, I., & García Guirao, J. L. (2021). Relativistic cosmology with an introduction to inflation. *Universe*, *7*(8), 276.

Mukhanov, V. (2005). *Physical foundations of cosmology*. Cambridge university press.

Mukhanov, V. F., & Chibisov, G. (1981). Quantum fluctuations and a nonsingular universe. *ZhETF Pisma Redaktsiiu*, *33*, 549–553.

Müller, D., Ricciardone, A., Starobinsky, A. A., & Toporensky, A. (2018). Anisotropic cosmological solutions in $r+R^2$ gravity. *The European Physical Journal C*, *78*(4), 1–10.

Myung, Y. S. (2007). Instability of holographic dark energy models. *Physics Letters B*, *652*(5-6), 223–227.

Newton, I., & Huygens, C. (1987). *Mathematical principles of natural philosophy*. Encyclopaedia Britannica.

Nojiri, S., Odintsov, S., & Oikonomou, V. (2017a). Constant-roll inflation in f (r) gravity. *Classical and Quantum Gravity*, *34*(24), 245012.

Nojiri, S., Odintsov, S., & Oikonomou, V. (2017b). Modified gravity theories on a nutshell: inflation, bounce and late-time evolution. *Physics Reports*, *692*, 1–104.

Nojiri, S., & Odintsov, S. D. (2003). Modified gravity with negative and positive powers of curvature: Unification of inflation and cosmic acceleration. *physical Review D*, *68*(12), 123512.

Nojiri, S., & Odintsov, S. D. (2006). Modified f (r) gravity consistent with realistic cosmology: From a matter dominated epoch to a dark energy universe. *Physical Review D*, *74*(8), 086005.

Nojiri, S., & Odintsov, S. D. (2007). Introduction to modified gravity and gravitational alternative for dark energy. *International Journal of Geometric Methods in Modern Physics*, *4*(01), 115–145.

Nojiri, S., & Odintsov, S. D. (2011). Unified cosmic history in modified gravity: from f (r) theory to lorentz non-invariant models. *Physics Reports*, *505*(2-4), 59–144.

Novosyadlyj, B. (2013). Tachyonic fields in cosmology. *arXiv preprint arXiv:1311.0227*.

Novosyadlyj, B., Pelykh, V., Shtanov, Y., & Zhuk, A. (2015). Dark energy: observational evidence and theoretical models. *arXiv preprint arXiv:1502.04177*.

Ochiai, H., & Sato, K. (2000). Numerical analysis of the wave function of the multidimensional universe. *Progress of Theoretical Physics*, *104*(2), 483–488.

Odintsov, S., & Oikonomou, V. (2018). Reconstruction of slow-roll f (r) gravity inflation from the observational indices. *Annals of Physics*, *388*, 267–275.

Odintsov, S., & Oikonomou, V. (2019). Effects of spatial curvature on the f (r) gravity phase space: no inflationary attractor? *Classical and Quantum Gravity*, *36*(6), 065008.

Odintsov, S. D., & Oikonomou, V. (2019). Constant-roll k-inflation dynamics. *Classical and Quantum Gravity*, *37*(2), 025003.

Odintsov, S. D., & Oikonomou, V. (2020). Aspects of axion f (r) gravity. *EPL (Europhysics Letters)*, *129*(4), 40001.

Oks, E. (2021). Brief review of recent advances in understanding dark matter and dark energy. *New Astronomy Reviews*, 101632.

Oliveira-Neto, G. (1998). No-boundary wave function of the anti–de sitter space-time and the quantization of λ. *Physical Review D*, *58*(10), 107501.

Olsson, M. E. (2007). Inflation assisted by heterotic axions. *Journal of Cosmology and Astroparticle Physics*, *2007*(04), 019.

Padmanabhan, T. (2002). Accelerated expansion of the universe driven by tachyonic matter. *Physical Review D*, *66*(2), 021301.

Padmanabhan, T. (2003). Cosmological constant—the weight of the vacuum. *Physics Reports*, *380*(5-6), 235–320.

Palani, A. M. (2010). Dr. n. ganesan dr. k. venkatesh dr. ma rama.

Pan, S., de Haro, J., Yang, W., & Amorós, J. (2020). Understanding the phenomenology of interacting dark energy scenarios and their theoretical bounds. *Physical Review D*, *101*(12), 123506.

Panpanich, S., Burikham, P., Ponglertsakul, S., & Tannukij, L. (2021). Resolving hubble tension with quintom dark energy model. *Chinese Physics C*, *45*(1), 015108.

Peebles, P., & Ratra, B. (1988). Cosmology with a time-variable cosmological'constant'. *The Astrophysical Journal*, *325*, L17–L20.

Peebles, P. J. E., & Peebles, P. J. (1993). *Principles of physical cosmology* (Vol. 27). Princeton university press.

Peebles, P. J. E., & Ratra, B. (2003). The cosmological constant and dark energy. *Reviews of modern physics*, *75*(2), 559.

Perivolaropoulos, L., & Skara, F. (2021). Challenges for λcdm: An update. *arXiv preprint arXiv:2105.05208*.

Perlmutter, S., Aldering, G., Goldhaber, G., Knop, R., Nugent, P., Castro, P. G., ... others (1999). Measurements of ω and λ from 42 high-redshift supernovae. *The Astrophysical Journal*, *517*(2), 565.

Perlmutter, S., Schmidt, B. P., & Riess, A. G. (2011). The nobel prize in physics 2011. *AG Riess, My Path to the Accelerating Universe, Nobel Lecture*.

Perlmutter, S., Turner, M. S., & White, M. (1999). Constraining dark energy with type ia supernovae and large-scale structure. *Physical Review Letters*, *83*(4), 670.

Piao, Y.-S. (2006). Perturbation spectra of "n-flation". *Physical Review D*, *74*(4), 047302.

Piao, Y.-S. (2009). Primordial density perturbation and decaying speed of sound. *Physical Review D*, *79*(6), 067301.

Piao, Y.-S., Cai, R.-G., Zhang, X., & Zhang, Y.-Z. (2002). Assisted tachyonic inflation. *Physical Review D*, *66*(12), 121301.

Polarski, D., & Starobinsky, A. A. (1994). Isocurvature perturbations in multiple inflationary models. *Physical Review D*, *50*(10), 6123.

Qi, J.-Z., Zhang, M.-J., & Liu, W.-B. (2016). Dynamical evolution of quintessence cosmology in a physical phase space. *International Journal of Theoretical Physics*, *55*(8), 3672–3681.

Raja, M. A. Z. (2014). Solution of the one-dimensional bratu equation arising in the fuel ignition model using ann optimised with pso and sqp. *Connection Science*, *26*(3), 195–214.

Ratra, B., & Peebles, P. J. (1988). Cosmological consequences of a rolling homogeneous scalar field. *Physical Review D*, *37*(12), 3406.

Rendall, A. D. (2006). Dynamics of k-essence. *Classical and Quantum Gravity*, *23*(5),

1557.

Riess, A. G. (2020). The expansion of the universe is faster than expected. *Nature Reviews Physics*, *2*(1), 10–12.

Riess, A. G., Filippenko, A. V., Challis, P., Clocchiatti, A., Diercks, A., Garnavich, P. M., ... others (1998). Observational evidence from supernovae for an accelerating universe and a cosmological constant. *The Astronomical Journal*, *116*(3), 1009.

Riess, A. G., Nugent, P. E., Gilliland, R. L., Schmidt, B. P., Tonry, J., Dickinson, M., ... others (2001). The farthest known supernova: support for an accelerating universe and a glimpse of the epoch of deceleration. *The Astrophysical Journal*, *560*(1), 49.

Riess, A. G., Strolger, L.-G., Tonry, J., Casertano, S., Ferguson, H. C., Mobasher, B., ... others (2004). Type ia supernova discoveries at z¿ 1 from the hubble space telescope: Evidence for past deceleration and constraints on dark energy evolution. *The Astrophysical Journal*, *607*(2), 665.

Riotto, A. (2002). Inflation and the theory of cosmological perturbations. *arXiv preprint hep-ph/0210162*.

Rong-Gen, C. (2007). On theoretical models of dark energy. *Chinese Physics C*, *31*(9), 827–834.

Rong-Jia, Y., & Xiang-Ting, G. (2009). Observational constraints on purely kinetic k-essence dark energy models. *Chinese Physics Letters*, *26*(8), 089501.

Rubin, D., & Heitlauf, J. (2020). Is the expansion of the universe accelerating? all signs still point to yes: a local dipole anisotropy cannot explain dark energy. *The Astrophysical Journal*, *894*(1), 68.

Rüger, A. (1988). Atomism from cosmology: Erwin schrödinger's work on wave mechanics and space-time structure. *Historical studies in the physical and biological sciences*, *18*(2), 377–401.

Ruiz-Lapuente, P. (2010). *Dark energy: observational and theoretical approaches*. Cambridge University Press.

Ruzmaikina, T., & Ruzmaikin, A. (1970). Quadratic corrections to the lagrangian density of the gravitational field and the singularity. *Sov. Phys. JETP*, *30*, 372.

Sahni, V., & Starobinsky, A. (2000). The case for a positive cosmological λ-term. *International Journal of Modern Physics D*, *9*(04), 373–443.

Sahni, V., & Starobinsky, A. (2006). Reconstructing dark energy. *International Journal of Modern Physics D*, *15*(12), 2105–2132.

Sami, M. (2007). Models of dark energy. In *The invisible universe: Dark matter and dark energy* (pp. 219–256). Springer.

SAMI, M. (2009). A primer on problems and prospects of dark energy. *Current science*, *97*(6), 887–910.

Sami, M., Chingangbam, P., & Qureshi, T. (2002). Aspects of tachyonic inflation with an exponential potential. *Physical Review D*, *66*(4), 043530.

Sami, M., Chingangbam, P., & Qureshi, T. (2004). Cosmology with rolling tachyon. *Pramana*, *62*(3), 765–770.

Sami, M., & Toporensky, A. (2004). Phantom field and the fate of the universe. *Modern Physics Letters A*, *19*(20), 1509–1517.

Sami, M., Toporensky, A., Tretjakov, P. V., & Tsujikawa, S. (2005). The fate of (phantom) dark energy universe with string curvature corrections. *Physics Letters B*, *619*(3-4), 193–200.

Sandvik, H. B., Tegmark, M., Zaldarriaga, M., & Waga, I. (2004). The end of unified dark matter? *Physical Review D*, *69*(12), 123524.

Sasaki, M., & Stewart, E. D. (1996). A general analytic formula for the spectral index of the density perturbations produced during inflation. *Progress of Theoretical Physics*, *95*(1), 71–78.

Sasaki, M., & Tanaka, T. (1998). Super-horizon scale dynamics of multi-scalar inflation. *Progress of Theoretical Physics*, *99*(5), 763–781.

Sato, K. (1981). First-order phase transition of a vacuum and the expansion of the universe. *Monthly Notices of the Royal Astronomical Society*, *195*(3), 467–479.

Scannapieco, C., White, S. D., Springel, V., & Tissera, P. B. (2009). The formation and survival of discs in a λcdm universe. *Monthly Notices of the Royal Astronomical Society*, *396*(2), 696–708.

Scherrer, R. J. (2004). Purely kinetic k essence as unified dark matter. *Physical review letters*, *93*(1), 011301.

Scherrer, R. J. (2005). Phantom dark energy, cosmic doomsday, and the coincidence problem. *Physical Review D*, *71*(6), 063519.

Schmidt, H. (1990). Class. quantum grav. 7 1023; schmidt hj 1996. *Phys. Rev. D*, *54*(7906), 1996Il.

Scholz, E. (2001). *Hermann weyl's raum-zeit-materie and a general introduction to his scientific work* (Vol. 30). Springer Science & Business Media.

Schrodinger, E. (1926). Quantization as an eigenvalue problem. In *Annales de physique* (Vol. 79, pp. 361–376).

Schrödinger, E. (1926). Quantization as a problem of proper values (part i). *Annalen der Physik*.

Schrödinger, E. (1985). *Space-time structure*. Cambridge University Press.

Sen, A. (2005). Remarks on tachyon driven cosmology. In *String theory and cosmology* (pp. 70–75). World Scientific.

Shah, P., & Samanta, G. C. (2019). Stability analysis for cosmological models in f (r) gravity using dynamical system analysis. *The European Physical Journal C*, *79*(5), 1–9.

Shao, Y., & Gui, Y. (2008). Statefinder parameters for tachyon dark energy model. *Modern Physics Letters A*, *23*(01), 65–71.

Shao, Y., Gui, Y.-X., & Wang, W. (2007). Parametrization of tachyon field. *Modern Physics Letters A*, *22*(16), 1175–1181.

Shawagfeh, N. (1993). Nonperturbative approximate solution for lane–emden equation. *Journal of Mathematical Physics*, *34*(9), 4364–4369.

Sherwin, B. D., Dunkley, J., Das, S., Appel, J. W., Bond, J. R., Carvalho, C. S., ... others (2011). Evidence for dark energy from the cosmic microwave background alone using the atacama cosmology telescope lensing measurements. *Physical review letters*, *107*(2), 021302.

Sheykhi, A., Movahed, M. S., & Ebrahimi, E. (2012). Tachyon reconstruction of ghost dark energy. *Astrophysics and Space Science*, *339*(1), 93–99.

Shi, S.-G., Piao, Y.-S., & Qiao, C.-F. (2009). Cosmological evolution of a tachyon-quintom model of dark energy. *Journal of Cosmology and Astroparticle Physics*, *2009*(04), 027.

Silk, J., & Turner, M. S. (1987). Double inflation. *Physical Review D*, *35*(2), 419.

Singh, A., Sangwan, A., & Jassal, H. (2019). Low redshift observational constraints on tachyon models of dark energy. *Journal of Cosmology and Astroparticle Physics*, *2019*(04), 047.

Smeenk, C. (2005). False vacuum: Early universe cosmology and the development of inflation. In *The universe of general relativity* (pp. 223–257). Springer.

Smith, S. W., et al. (1997). *The scientist and engineer's guide to digital signal processing* (Vol. 14). California Technical Pub. San Diego.

Sola, J. (2013). Cosmological constant and vacuum energy: old and new ideas. In *Journal of physics: Conference series* (Vol. 453, p. 012015).

Sola, J. (2016). Cosmological constant vis-à-vis dynamical vacuum: Bold challenging the λcdm. *International Journal of Modern Physics A*, *31*(23), 1630035.

Sotiriou, T. P. (2006). Constraining f (r) gravity in the palatini formalism. *Classical and Quantum Gravity*, *23*(4), 1253.

Sotiriou, T. P., & Faraoni, V. (2010). f (r) theories of gravity. *Reviews of Modern Physics*, *82*(1), 451.

Sotiriou, T. P., & Liberati, S. (2007). Metric-affine f (r) theories of gravity. *Annals of Physics*, *322*(4), 935–966.

Spaans, M. (2013). a topological extension of general relativity to explore the nature of quantum spacetime, dark energy and inflation. *International Journal of Modern Physics D*, *22*(10), 1330022.

Starobinskii, A. (1979). Spectrum of relict gravitational radiation and the early state of the universe. *JETP Letters*, *30*(11), 682–685.

Starobinsky, A. A. (1980). A new type of isotropic cosmological models without singularity. *Physics Letters B*, *91*(1), 99–102.

Starobinsky, A. A. (1982). Dynamics of phase transition in the new inflationary universe scenario and generation of perturbations. *Physics Letters B*, *117*(3-4), 175–178.

Starobinsky, A. A. (2007). Disappearing cosmological constant in f (r) gravity. *JETP letters*, *86*(3), 157–163.

Štefančić, H. (2005). Dark energy transition between quintessence and phantom regimes: an equation of state analysis. *Physical Review D*, *71*(12), 124036.

Steinhardt, P. J. (2003). A quintessential introduction to dark energy. *Philosophical Transactions of the Royal Society of London. Series A: Mathematical, Physical and Engineering Sciences*, *361*(1812), 2497–2513.

Stewart, E. D., & Lyth, D. H. (1993). A more accurate analytic calculation of the spectrum of cosmological perturbations produced during inflation. *Physics Letters B*, *302*(2-3), 171–175.

Straumann, N., & Zürich, U. (2012). The 2011 nobel prize in physics. *SPG Mitteilungen*(36).

Sur, S., & Das, S. (2009). Multiple kinetic k-essence, phantom barrier crossing and stability. *Journal of Cosmology and Astroparticle Physics*, *2009*(01), 007.

Tan, M. M. A., Mat, F., Abd Rahim, I., Lile, N. T., & Yaacob, S. (2011). Classification of materials by modal analysis and neural network. In *Icimu 2011: Proceedings of the 5th international conference on information technology & multimedia* (pp. 1–5).

Taylor, A., & Berera, A. (2000). Perturbation spectra in the warm inflationary scenario. *Physical Review D*, *62*(8), 083517.

Tegmark, M., Strauss, M. A., Blanton, M. R., Abazajian, K., Dodelson, S., Sandvik, H., ... others (2004). Cosmological parameters from sdss and wmap. *Physical review D*, *69*(10), 103501.

Thomas, S., & Ward, J. (2007). Ir inflation from multiple branes. *Physical Review D*, *76*(2), 023509.

Thorne, K. S., Misner, C. W., & Wheeler, J. A. (2000). *Gravitation*. Freeman San Francisco.

To, C., Krause, E., Rozo, E., Wu, H., Gruen, D., Wechsler, R., ... others (2021). Dark energy survey year 1 results: Cosmological constraints from cluster abundances, weak lensing, and galaxy correlations. *Physical review letters*, *126*(14), 141301.

Tonry, J. L., Schmidt, B. P., Barris, B., Candia, P., Challis, P., Clocchiatti, A., ... others (2003). Cosmological results from high-z supernovae. *The Astrophysical Journal*, *594*(1), 1.

Trzaska, J., & Dobrzański, L. (2006). Application of neural networks for selection of steel with the assumed hardness after cooling from the austenitising temperature. *Journal of Achievements in Materials and Manufacturing Engineering*, *16*(2), 145–150.

Tu, Z., Hu, J., & Wang, F. (2019). Probing cosmic acceleration by strong gravitational lensing systems. *Monthly Notices of the Royal Astronomical Society*, *484*(3), 4337–4346.

Turner, M. S. (2018). λ, λcdm: Much more than we expected, but now less than what we want. *Foundations of Physics*, *48*(10), 1261–1278.

Tzirakis, K., & Kinney, W. H. (2007). Inflation over a local maximum of a potential. *Physical Review D*, *75*(12), 123510.

Urakawa, Y., & Tanaka, T. (2009). Influence on observation from ir divergence during inflation. i: single field inflation. *Progress of Theoretical Physics*, *122*(3), 779–803.

Vakili, B. (2012). Scalar field quantum cosmology: a schrödinger picture. *Physics Letters B*, *718*(1), 34–42.

Valentini, A., et al. (1992). On the pilot-wave theory of classical, quantum and subquantum physics.

Vasilev, T. B., Bouhmadi-López, M., & Martín-Moruno, P. (2021). Little rip in classical and quantum f (r) cosmology. *Physical Review D*, *103*(12), 124049.

Vikman, A. (2005). Can dark energy evolve to the phantom? *Physical Review D*, *71*(2), 023515.

Vilenkin, A. (1982). Creation of universes from nothing. *Physics Letters B*, *117*(1-2), 25–28.

Vilenkin, A. (1983). Birth of inflationary universes. *Physical Review D*, *27*(12), 2848.

Vilenkin, A. (1984). Quantum creation of universes. *Physical Review D*, *30*(2), 509.

Vilenkin, A. (1986). Boundary conditions in quantum cosmology. *Physical Review D*, *33*(12), 3560.

Vilenkin, A. (1988). Quantum cosmology and the initial state of the universe. *Physical Review D*, *37*(4), 888.

Vilenkin, A. (1994). Approaches to quantum cosmology. *Physical Review D*, *50*(4), 2581.

Volovik, G. E. (2005). Cosmological constant and vacuum energy. *Annalen der Physik*, *14*(1-3), 165–176.

Wei, H., & Zhang, S. N. (2008). How to distinguish dark energy and modified gravity? *Physical Review D*, *78*(2), 023011.

Weinberg, S. (1972). Gravitation and cosmology: principles and applications of the general theory of relativity.

Weinberg, S. (2001). The cosmological constant problems. In *Sources and detection of dark matter and dark energy in the universe* (pp. 18–26). Springer.

Wen-Fu, W., Zheng-Wei, S., & Bin, T. (2010). Exact solution of phantom dark energy model. *Chinese Physics B*, *19*(11), 119801.

Wheeler, J. A. (1957). On the nature of quantum geometrodynamics. *Annals of Physics*, *2*(6), 604–614.

Wheeler, J. A., & Zurek, W. H. (1983). *Quantum theory and measurement*. Princeton university press.

Widrow, L. M., & Kaiser, N. (1993). Using the schrödinger equation to simulate collisionless matter. *The Astrophysical Journal*, *416*, L71.

Wolfson, I., & Brustein, R. (2018). Small field models with gravitational wave signature supported by cmb data. *Plos one*, *13*(5), e0197735.

Xia, J.-Q., Cai, Y.-F., Qiu, T.-T., Zhao, G.-B., & Zhang, X. (2008). Constraints on the sound speed of dynamical dark energy. *International Journal of Modern Physics D*, *17*(08), 1229–1243.

Yalcin, Y., & Pekcan, O. (2020). Nuclear fission–nuclear fusion algorithm for global optimization: a modified big bang–big crunch algorithm. *Neural Computing and Applications*, *32*(7), 2751–2783.

Yang, Y., & Gong, Y. (2020). The evidence of cosmic acceleration and observational constraints. *Journal of Cosmology and Astroparticle Physics*, *2020*(06), 059.

Ye, G., & Piao, Y.-S. (2019). Bounce in general relativity and higher-order derivative operators. *Physical Review D*, *99*(8), 084019.

Yoo, J., & Watanabe, Y. (2012). Theoretical models of dark energy. *International Journal of Modern Physics D*, *21*(12), 1230002.

Zajkowski, K. (2014). The method of solution of equations with coefficients that contain measurement errors, using artificial neural network. *Neural computing and applications*, *24*(2), 431–439.

Zeldovich, Y. B. (1965). Survey of modern cosmology. In *Advances in astronomy and astrophysics* (Vol. 3, pp. 241–379). Elsevier.

Zhang, J.-J., Lee, C.-C., & Geng, C.-Q. (2019). Observational constraints on running vacuum model. *Chinese Physics C*, *43*(2), 025102.

Zhang, X.-F., Li, H., Piao, Y.-S., & Zhang, X. (2006). Two-field models of dark energy with equation of state across-1. *Modern Physics Letters A*, *21*(03), 231–241.

Zhang, Y.-C., Zhang, H.-Y., Wang, D.-D., Qi, Y.-H., Wang, Y.-T., & Zhao, G.-B. (2017). Probing dynamics of dark energy with latest observations. *Research in Astronomy and Astrophysics*, *17*(6), 050.

Zhao, G.-B., Raveri, M., Pogosian, L., Wang, Y., Crittenden, R. G., Handley, W. J., ... others (2017). Dynamical dark energy in light of the latest observations. *Nature Astronomy*, *1*(9), 627–632.

Zhao, G.-B., Xia, J.-Q., Li, H., Tao, C., Virey, J.-M., Zhu, Z.-H., & Zhang, X. (2007). Probing for dynamics of dark energy and curvature of universe with latest cosmological observations. *Physics Letters B*, *648*(1), 8–13.

Zlatev, I., Wang, L., & Steinhardt, P. J. (1999). Quintessence, cosmic coincidence, and the cosmological constant. *Physical Review Letters*, *82*(5), 896.

LIST OF PUBLICATIONS

Published Papers

1. Mughal, M. Z., Ahmad, I., & García Guirao, J. L. (2021). Relativistic Cosmology with an Introduction to Inflation. Universe, 7(8), 276.

2. Mughal, M. Z., & Ahmad, I. (2021). Investigation on an Nflation phase diagram with multifield polynomial potential. Modern Physics Letters A, 2150119.

3. Mughal, M. Z., & Ahmad, I. (2021). A multi-field tachyon-quintom model of dark energy and fate of the universe. The European Physical Journal Plus, 136(5), 1-20.

4. Mughal, M. Z., & Ahmad, I. (2021). A study of the accelerating Universe in $f(R)$ modified gravity using dynamical system approach. Gravitation and Cosmology, 1(28), 37-55.

5. Tapia, T., Mughal, M. Z., & Rojas, C. (2020). Semiclassical analysis of the Starobinsky inflationary model. Physics of the Dark Universe, 30, 100650.

6. Meza, S., Altamirano, D., Mughal, M. Z., & Rojas, C. (2021). Numerical analysis of the generalized Starobinsky inflationary model. International Journal of Modern Physics D, 2150062.

7. Ahmad, S., Jami, A. R., & Mughal, M. Z. (2018). Stability of anisotropic self-gravitating fluids. Modern Physics Letters A, 33(17), 1850095.

Submitted Papers

1. Mughal, M. Z., Ahmad, I., & García Guirao, J. L. (2022). Probing the effect of spectral index and e-fold number on multifield inflationary universe and spectrum of curvature perturbation. (under revision in the journal International Journal of Modern Physics D (IJMPD)).

2. Mughal, M. Z., & Ahmad, I. (2022). The dynamical system approach to understand the cosmic dynamics of late time accelerated expansion in perspective of $f(R)$ gravity. (under revision in the journal General Relativity and Gravitation (GRG))

3. Mughal, M. Z., et al. (2022) Integrated Intelligent Computing Paradigm on Schrodinger Equation for the Evolution of Early Universe.(preprint submitted to a Journal).

4. Mughal, M. Z., & Ahmad, I. (2022). A new $f(R)$ model of modified gravity for a given cosmic expansion history. (preprint submitted to a Journal)

APPENDIX-01

Abbreviations Used in the Thesis

S#	Item	Abbreviation
1	Ricci Scalar	R
2	Fundamental tenssor	$g_{\mu\nu}$
3	Lagrangian	$\mathcal{L}$
4	Scale factor characterizing cosmic expansion	$a\,(t)$
5	Cosmological constant	Λ
6	Energy-momentum tensor	$T_{\mu\nu}$
7	Einstein Tensor	$G_{\mu\nu}$
8	Ricci tensor	$R_{\mu\nu}$
9	Affine connection-Christoffel symbols of second kinds	$\Gamma^{\lambda}_{\mu\nu}$
10	Cosmic energy density	ρ
11	Cosmic pressure	p
12	Hubble parameter describing rate of cosmic expansion	H
13	Parameter used to describe various forms of density	Ω
14	Geometric curvature of spacetime	k
15	Deceleration parameter	q
16	Giga year	Gyr (10^9yr)
17	Megaparsec	Mpc

S#	Item	Abbreviation
18	Particle horizon	$d_H(t)$
19	Scalar field (inflaton)	ϕ
20	Potential and Hubble slow roll parameters	ε_V,η_V,ε_H,η_H
21	e-folding number	N
22	Planck mass	M_p
23	An arbitrary function of Ricci scalar	$f(R)$
24	Spectral index	n_s
25	Wave function of the observable universe	$\Psi(a)$
26	Derivative of $f(R)$ with respect to R	F
27	Entropy during Nflation	dS
28	Speed of sound	c_s^2

APPENDIX-02

Space, Time and Spacetime

A background arena woven with space and time fabric is necessarily required for all the physical phenomena to play over it. We actually keep on seeking the compatibility of the physical laws known so far with the structure of space and time. This is because space, time, and motion are concomitant ingredients cohered to matter and can never be disengaged from each other. The universe exists in space and evolves in time so that the universe, space, and time are inseparable from each other and are coherently related to each other. This is what was presented in relativity theories. Space is understood as possessing three dimensions, whereas time is speculated to have only one dimension. Therefore, Newtonian Mechanics has been formulated in such a way as to consider the spatial dimensions existing independently from the dimension of time. Euclidean geometry provides a necessary mechanism in dealing with such notions of space and time. In this regard, Euclidean space becomes important which proposes three independent perpendicular dimensions of space with time dimension being unaffected by it. The spatiotemporal dimensions are envisaged as independent and absolute entities which are not affected by each other at all. The Euclidean structure of space is flat and distances are measured by using the standard Pythagoras theorem for geometry of three dimensions as

$$ds^2 = x^2 + y^2 + z^2, \tag{0.0.1}$$

and in the differential of the distances

$$ds^2 = dx^2 + dy^2 + dz^2, \tag{0.0.2}$$

here $ds = (x, y, z)$ or $ds = (dx, dy, dz)$, respectively. More compactly, it is written as

$$ds^2 = \delta_{\mu\nu} dx^\mu dx^\nu \tag{0.0.3}$$

where

$$\delta_{\mu\nu} = \begin{pmatrix} 1 & 0 & 0 \\ 0 & 1 & 0 \\ 0 & 0 & 1 \end{pmatrix} \tag{0.0.4}$$

and signature of $\delta_{\mu\nu} = (+1, +1, +1)$ The time coordinate does appear anywhere in this distance-measuring formula which means in the geometry of space, the dimension of time will be dealt with separately. Newton's notions of space and time as described in "Principia Mathematica" are defined (Newton & Huygens, 1987) as follows "Absolute space, in its own nature, without regard to anything external, remains always similar and immovable. Relative space is some movable dimension or measure of the absolute spaces which our senses determine by its position to bodies: and which is vulgarly taken for immovable space. Absolute motion is the translation of a body from one absolute place into another: and relative motion, the translation from one relative place into another" where absolute time is defined in the following words "Absolute, true and mathematical time, of itself, and from its own nature flows equably without regard to anything external, and by another name is called duration. Relative, apparent, and common time, is some sensible and external (whether accurate or inequable) measure of duration by the means of motion, which is commonly used instead of true-time".
In 1905, Einstein's paper entitled "On the electrodynamics of moving bodies" put forth on the base of two postulates that time might be dealt on equal footing with space as one of the dimensions of space. Herman Minkowski (1864–1909) translated the mixing of space and time coordinates as requiring a four-dimensional scenario where physical phenomena take place and the geometry of such four dimensional spacetime, where

time is one dimension, is described by spacetime interval which is the generalized form of Pythagoras theorem

$$ds^2 = -dt^2 + dx^2 + dy^2 + dz^2 \tag{0.0.5}$$

or

$$ds^2 = \eta_{\mu\nu} dx^\mu dx^\nu \tag{0.0.6}$$

where

$$\eta_{\mu\nu} = \begin{pmatrix} \eta_{00} & \eta_{01} & \eta_{02} & \eta_{03} \\ \eta_{10} & \eta_{11} & \eta_{12} & \eta_{13} \\ \eta_{20} & \eta_{21} & \eta_{22} & \eta_{23} \\ \eta_{30} & \eta_{31} & \eta_{32} & \eta_{33} \end{pmatrix} = \begin{pmatrix} -1 & 0 & 0 & 0 \\ 0 & 1 & 0 & 0 \\ 0 & 0 & 1 & 0 \\ 0 & 0 & 0 & 1 \end{pmatrix} \tag{0.0.7}$$

and it has the signatures $\eta_{\mu\nu} = (-1, +1, +1, +1)$.
Minkowski first understood that the spacetime interval as given in Eq. (0.0.5) remains invariant for all the observers and carries the similar meaning for all the inertial observers in uniform relative motion, however, Einstein considered in the beginning that either with respect to time or with respect to space, the spacetime interval does not remain identical for all relative observers moving with constant velocity with respect to each other. Minkowski avowedly said in a conference addressing to the German scientists that "Ladies and gentlemen! the views of space and time which I wish to lay before you have sprung from the soil of experimental physics, therein lies their strength, they are radical. Henceforth space by itself and time by itself are doomed to fade away into mere shadows and only a union of the two will preserve an independent reality" (Minkowski, 2013). This marked the point for the emergence of the geometry of the four-dimensional spacetime continuum and the reformulation of the special theory of relativity in its context. It works pseudo-Euclidean due to incorporating the time dimension, however remains flat. However, it was Einstein's ingenuity to carve it before anyone else. General relativity was formulated on the base of four dimensional spacetime continuum as Minkowski has laid it, however in order to incorporate the gravity into it Einstein utilized the power of tensors and modeled the curved geometry of spacetime describing its curvature as gravity. The geometry of curved spacetime is encoded into a two rank symmetric tensor known as fundamental tensor and is given by the spacetime metric or line element as

$$ds^2 = g_{\mu\nu} dx^\mu dx^\nu \tag{0.0.8}$$

where the fundamental tensor $g_{\mu\nu}$ is given by

$$g_{\mu\nu} = \begin{pmatrix} g_{00} & g_{01} & g_{02} & g_{03} \\ g_{10} & g_{11} & g_{12} & g_{13} \\ g_{20} & g_{21} & g_{22} & g_{23} \\ g_{30} & g_{31} & g_{32} & g_{33} \end{pmatrix} = \begin{pmatrix} g_{00} & 0 & 0 & 0 \\ 0 & g_{11} & 0 & 0 \\ 0 & 0 & g_{22} & 0 \\ 0 & 0 & 0 & g_{33} \end{pmatrix} \tag{0.0.9}$$

If a diagonal metric has to represent the curved geometry, its spatial components in the diagonal g_{11}, g_{22} and g_{33} must show a shift from unity. The diagonal metric necessarily implies cosmological principle which portrays a universe that is invariant to translation and rotation on the cosmological scales of extragalactic distances. In the absence of matter-energy content, the curvature of spacetime vanishes, and the geometry of spacetime becomes flat, i.e., $g_{\mu\nu} = \mu_{\mu\nu}$, yet non-Euclidean that is required by the special relativity. The philosophical impact of spacetime, in the vista of independent space and time, is more complicated to apprehend, however describes nature more naturally.

Spectrum of the Black Body

A blackbody can absorb hypothetically radiation of all wavelengths falling on it and reflecting nothing at all. How at the different wavelengths distribution of radiation occurs in a blackbody is given below in Figure 1:

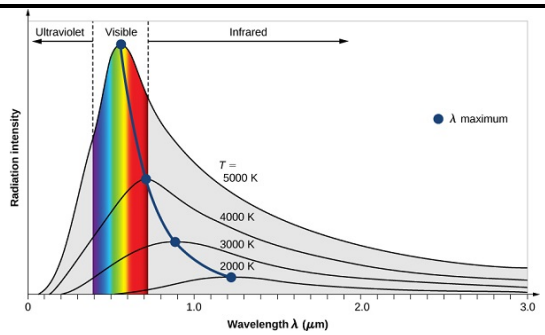

Figure– 1: The figure above shows how the distribution of radiation occurs at different corresponding wavelengths for a perfect blackbody

In the early universe when matter and radiation decoupled from each other, the so-called decoupling, instantly primordial radiation was produced and were given off proving a snapshot of the universe at that time and is known as cosmic microwave background radiation (CMBR) observed accidentally in the 60 s. The recent observations conducted on cosmic microwave background radiation reveals the fact that this is the perfect black body radiation with a temperature of 2.7255 Kelvin on average. We know that the wavelength distribution of a black body is given by

$$u\left(\lambda,T\right)d\lambda=\frac{8\pi hc}{\lambda^{5}}\left(\frac{1}{e^{\frac{hc}{\lambda k_{B}T}}-1}\right)d\lambda \tag{0.0.10}$$

where $u\left(\lambda,T\right)d\lambda$ is the energy per unit volume of the radiation with wavelength between λ and $\lambda+d\lambda$ emitted by a blackbody at temperature T. We consider now a black body radiation from the big bang when the universe first became transparent to photons after 400,000 years after big bang to this time about 4,000,000,000 years. The wavelength of the primordial photons λ is Doppler shifted to λ' due to expansion of universe ,certainly $\lambda'>\lambda$. Let $f\left(\lambda',T'\right)d\lambda'$ be the current per unit volume of the residual big bang radiation as measured from the earth. As the shell of charged particles that emitted the radiation is moving away from the Earth at extremely relativistic speed so we should use the relativistic Doppler shift for light from a receding source to relate λ' to λ that is

$$\lambda'=\frac{\sqrt{1+v/c}}{\sqrt{1-v/c}}\lambda=B\lambda \tag{0.0.11}$$

where we put $B=\frac{\sqrt{1+v/c}}{\sqrt{1-v/c}}$, and v is the speed of recession of the charged shell. As $v<c$, clearly $\lambda'>\lambda$ by a factor

$$\frac{\sqrt{1+v/c}}{\sqrt{1-v/c}} \tag{0.0.12}$$

Eq. (0.0.12) can be interpreted by generalization that all the distances have grown since first radiation emitted. In order to have a relation between currently observed spectrum $f(\lambda', T')\, d\lambda'$ and original black body radiation distribution

$$u(\lambda, T)\, d\lambda \tag{0.0.13}$$

we put from Eq. (0.0.11) $\lambda = \frac{\lambda'}{B}$ into Eq. (0.0.10)

$$u(\lambda, T)\, d\lambda = \frac{8\pi hc}{\left(\frac{\lambda'}{B}\right)^5} \left(\frac{1}{e^{\frac{hc}{\frac{\lambda'}{B} k_B T}} - 1} \right) \frac{d\lambda'}{B} \tag{0.0.14}$$

$$\frac{u(\lambda, T)\, d\lambda}{B^4} = \frac{8\pi hc}{{\lambda'}^5} \left(\frac{1}{e^{\frac{hc}{\lambda' k_B T'}} - 1} \right) d\lambda' \tag{0.0.15}$$

where $T' = \frac{T}{B}$ and right hand side of Eq. (0.0.15) can be identified with current black body spectrum $f(\lambda', T')\, d\lambda'$ which has standard functional form of a blackbody spectrum with wavelength λ' and temperature T'. Eq. (0.0.13) becomes

$$\frac{u(\lambda, T)\, d\lambda}{B^4} = f(\lambda', T')\, d\lambda' \tag{0.0.16}$$

Eq. (0.0.16) says that the radiation from a receding blackbody has same spectral distribution as yet but its temperature T' and energy

$$u(\lambda, T)\, d\lambda \tag{0.0.17}$$

dropped by factors of B and B^4 respectively.

APPENDIX-04

Turnitin Originality Report

Tested on 24 February, 2022, by Turnitin Anti Plagiarism Software Provided by Higher Education Commission, Pakistan to the Instructors of the University of Gujrat, Pakistan.

Thesis Title: A MATHEMATICAL STUDY FOR THE DYNAMICS OF SPACE-TIME, INFLATION AND ACCELERATING UNIVERSE

Author's Name: Muhammad Zahid Mughal

Institution: Department of Mathematics, University of Gujrat, Pakistan

PRIMARY SOURCES

SIMILARITY INDEX	INTERNET SOURCES	PUBLICATIONS	STUDENT PAPERS
15%	12%	6%	3%

INTERNET SOURCE — **12%**

1. arxiv-export-lb.library.cornell.edu (Internet Source)

2. epdf.tips (Internet Source)

3. www.sciencegate.app (Internet Source)

4. arxiv.org (Internet Source)

6. www.coursehero.com (Internet Source)

PUBLICATION — **6%**

7. Iftikhar Ahmad. "The spectrum of curvature perturbation for multi-field inflation with a small-field potential", Journal of Cosmology and Astroparticle Physics, 02/04/2008 (Publication)

23. Iftikhar Ahmad. "On the number of Nflation fields", Journal of Cosmology and Astroparticle Physics, 06/20/2008 (Publication)

30. Luca Amendola, Radouane Gannouji, David Polarski, Shinji Tsujikawa."Conditions for the cosmological viability of dark energy models", Physical Review D, 2007 (Publication)

STUDENT PAPER — **3%**

5. Submitted to AUT University (Student Paper)

8. Submitted to Higher Education Commission of Pakistan (Student Paper)

26. Submitted to University of Exeter (Student Paper)